Chemo- and Bio-Catalysis for the Synthesis of Chiral Amines in Continuous Flow Reactors

Lisa Alice Thompson

Submitted in accordance with the requirements for the degree of Doctor of Philosophy

University of Leeds

School of Chemistry

June 2017

The candidate confirms that the work submitted is his/her own and that appropriate credit has been given where reference has been made to the work of others.

This copy has been supplied on the understanding that it is copyright material and that no quotation from the thesis may be published without proper acknowledgement.

Acknowledgements

In the Turner group I would specifically like to thank Scott France and Shahed Hussain for their assistance during my brief visit there to learn about protein production. They were very welcoming and patient with me working in an area that was completely out of my comfort zone.

During my studies I was fortunate to work on a number of collaborations that served to re-inforce my knowledge and skills and I would particularly like to thank Julia Pitzer (Graz), Katharina Hugentobler (Manchester) and Simon Doherty (Newcastle) for giving me interesting side-projects to work on.

I would like to thank my family and friends for their support over many years of studying and stressing. Amy and Michelle provided me with many fun and happy weekends away from work, for which I am so grateful.

Finally and most importantly, to Nick. You have given me so much support throughout my PhD, both in the lab and emotionally, plus you have taught me everything that I know about pumps! I could not have got through this without you; you're the reason that I work so hard to acheive my goals.

Abstract

The prevalence of chiral amines in pharmaceutical compounds means that efficient synthetic methods are highly desirable. Asymmetric catalysis offers the opportunity for enantioselective synthesis of chiral amines under milder reaction conditions. Chemical and biological catalysts both offer specific advantages and disadvantages that are different to the other catalyst type. Therefore, the combination of catalysts would allow for the advantages of each to be exploited, whilst overcoming the associated disadvantages.

This research investigates the combination of chemical and biological catalysts for the production of chiral amines and essential medicines using continuous reactors. Continuous reactors are increasingly seen as a method to improve synthesis routes due to their improved productivity and safety compared to batch reactors. In addition to continuous reactors, immobilised catalysts and design of experiments (DoE) strategies were employed for the development of optimised procedures.

Firstly, the enzymatic kinetic resolution of a chiral primary amine was studied in a continuous packed bed reactor (PBR) using an immobilised lipase enzyme. Optimum reaction conditions were determined using a one variable at a time (OVAT) approach to give the maximum 50% conversion with high product *ee* in only a 6 min residence time (tRes). The PBR system was then applied to an expanded substrate set, including chiral amines and alcohols, to act as a comparison to the standard amine.

Secondly, metal catalysed racemisation was investigated as a method to utilise the waste enantiomer from the enzymatic resolution in a dynamic kinetic resolution process (DKR). Homogeneous and heterogeneous Ir, Ru and Pd catalysts were tested for the amine racemisation step. However, the amount of racemisation observed was not sufficient and uncontrolled dimerisation primarily occurred.

Next, the enzymatic PBR was applied to the production of essential medicines *via* enzymatic ammoniolysis. The development of cheaper more efficient methods to produce essential medicines is vital to make them more affordable and accessible to the developing world. In this instance, the reaction conditions were optimised using DoE with the objective being to maximise conversion. Nicotinamide and pyrazinamide were produced in 94% and 100% yields with a tRes of 60 min and 20 min, respectively. The ammoniolysis of a chiral substrate was also tested; however, this was not successful using the experimental conditions described.

Finally, metal catalysed *N*-alkylation using Ir was investigated for the *N*-alkylation of the chiral primary amine as an alternative method to utilise the waste enantiomer from the continuous resolution. DoE and microwave heating techniques were employed to optimise the reaction conditions and reduce the amount of waste associated with development. In this example, the formation of un-desired dimeric products was problematic and so the optimisation objectives were both maximum conversion and maximum selectivity for the desired product.

Overall, the transferal of processes into continuous PBR and optimisation techniques allowed for the intensification of reaction conditions, which led to more productive, efficient routes. However, the difficulties in combining chemical and biological catalysts were also highlighted when the combination of reactions was attempted.

Table of Contents

List of Figures

List of Schemes

List of Tables

19

List of Abbreviations

AAO	Amine acid oxidase
Ac	Acyl
AmDH	Amine dehydrogenase
API	Active pharmaceutical ingredient
Ar	Aryl
Asp	Aspartic acid
ATH	Asymmetric transfer hydrogenation
ATHase	Artificial transfer hydrogenase
atm	Atmospheres
BINAP	1,1'-Binaphthalene-2,2'-diyl*bis*(diphenylphosphine)
Bn	Benzyl
BPR	Back pressure regulator
Bu	Butyl
CalA	*Candida Antarctica* lipase A
CalB	*Candida Antarctica* lipase B
CCF	Central composite face-centred
Conc	Concentration
Conv	Conversion
Cp	Cyclopentadiene
Cp*	Pentamethylcyclopentadiene
CSTR	Continuous stirred tank reactor
de	Diastereomeric excess
DCM	Dichloromethane
Det	Detector
DKR	Dynamic kinetic resolution
DMSO	Dimethyl sulfoxide
DoE	Design of experiments
DIPEA	*N,N*-Diisopropylethylamine

ee	Enantiomeric excess
E. coli	*Escherichia coli.*
Eq	Equivalents
ESI	Electrospray ionisation
Et	Ethyl
FAD	Flavin adenine dinucleotide
FBR	Fluidised bed reactor
FDA	Food and Drug Administration
FID	Flame ionisation detector
GC	Gas chromatography
GCMS	Gas chromatography – mass spectrometry
H-acceptor	Hydrogen acceptor
H-donor	Hydrogen donor
His	Histidine
HIV	Human immunodeficiency virus
HPLC	High performance liquid chromatography
HRMS	High resolution mass spectrometry
ICP	Inductively coupled plasma
ID	Inner diameter
Inj	Injector
*i*Pr	*Iso*-propyl
IR	Infrared red spectroscopy
IRED	Imine reductase
LCMS	Liquid chromatography – mass spectrometry
LeuDH	Leucine dehydrogenase
MAO	Monoamine oxidase
MCF	Mesocellular foam
Me	Methyl
MLR	Multiple linear regression
MS	Mass spectrometry

m/z	mass to charge ratio
N435	Novozym 435
NADH	Nicotine adenine dinucleotide
NADPH	Nicotine adenine dinucleotide phosphate
NMR	Nuclear magnetic resonance
Nu	Nucleophile
OD	Outer diameter
OVAT	One variable at a time
PBR	Packed bed reactor
PE	Petroleum ether
Ph	Phenyl
PMI	Process mass intensity
ppm	Parts per million
Pr	Propyl
psi	Pounds per square inch
PTFE	Polytetrafluoroethylene
rac	Racemic
RaNi	Raney Nickel
RSM	Response surface methodology
RTD	Residence time distribution
RV	Reactor volume
Ser	Serine
SM	Starting material
STY	Space time yield
TB	Tuberculosis
TBME	*tert*-butylmethyl ether
*t*Bu	Tertiary butyl
TEAF	Triethylamine/formic acid mixture
tert	Tertiary
TFA	Trifluoroacetic acid

TLL	*Thermomyces lanuginosus* lipase
TLC	Thin layer chromatography
TMS	Tetramethylsilyl
TON	Turnover number
tRes	Residence time
TsDPEN	*N*-Tosyl-1,2-diphenylethylenediamine
vs.	*versus*
WHO	World Health Organisation

1 Introduction

Chiral amines are prevalent moieties in pharmaceutical molecules, with over 40% of active pharmaceutical ingredients (API) containing chiral amines within their structures (Figure 1).[1]
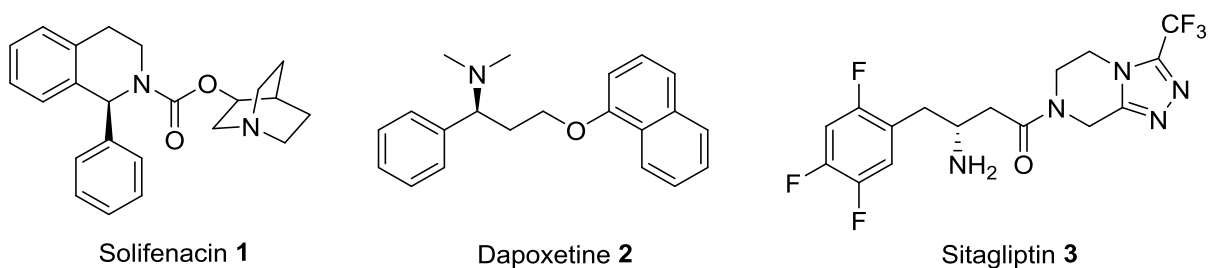
Figure 1. APIs containing chiral amine moieties.

The two enantiomers of a chiral molecule can have different modes of action within the body due to the interaction with proteins and enzyme active sites. Enzyme active sites also have chiral structures and so each enantiomer of a chiral molecule will bind to the active site in a different orientation which can lead to different responses within the body. This difference in biological activity means that strict requirements from regulatory bodies are in place to fully characterise the mode of action of both enantiomers and to produce single enantiomer drugs of very high enantiopurity.[2] Despite this high demand for single enantiomer chiral amines, industrially viable methods for the production of chiral amines are still limited.

The development of a novel pharmaceutical molecule is usually unrestricted by the cost of each synthetic step due to the high return provided by a patent protected monopoly of the product. However drugs that are no longer protected by a patent do not generate as high a

revenue because of the loss of exclusivity to generic suppliers. Therefore, processes to make generic drugs must be stream-lined and cost-effective. Novel processes, intensification of reaction conditions, reactor design and optimisation methods present an opportunity to develop efficient cost-effective pharmaceutical manufacturing processes in both novel and generic pharmaceutical development.

Catalysis is one of the 12 principles of green chemistry, used as a method to reduce the amount of waste associated with chemical manufacturing processes.[3, 4] Catalysts improve the efficiency of reactions, allow less harsh reaction conditions to be used, and reduce the amount of waste by removing the need for stoichiometric reagents. Catalysts can be used to produce chiral amines *via* asymmetric synthesis or resolution methodologies.[2] In asymmetric synthesis, chirality is introduced into a prochiral centre using chiral catalysts and auxiliaries. Resolution methods involve the separation of the individual enantiomers from a racemic mixture and can be carried out by diastereomeric crystallisation or enzymatically. Chemical and biological methods for the production of chiral amines will now be discussed.

1.1   Asymmetric Synthesis of Chiral Amines

Primary, secondary and tertiary amines can be produced using chemical catalysis by asymmetric reduction, hydrogenation or transfer hydrogenation of imines or reductive amination of ketones. Asymmetric reduction methods using borane, silanes or other stoichiometric hydrides are not used in industry due to their cost, reactivity and associated waste, so will not be considered here further.[5]

1.1.1   Asymmetric Hydrogenation of Imines and Enamines

Asymmetric hydrogenation involves the addition of H_2 to an unsaturated system to generate a saturated chiral product. A chiral catalyst is employed to induce stereoselectivity in the reaction. The first examples of catalytic asymmetric hydrogenation were developed independently by Noyori and Knowles. Noyori developed Ru catalysts with BINAP and diamine ligands for the asymmetric hydrogenation of ketones to produce chiral alcohols (Scheme 1).[6] Initially the reaction using BINAP ligands required functionalised ketone substrates to act as directing groups. This was later improved upon by using BINAP and diamine ligands, which allowed for the reaction of ketones without directing groups.
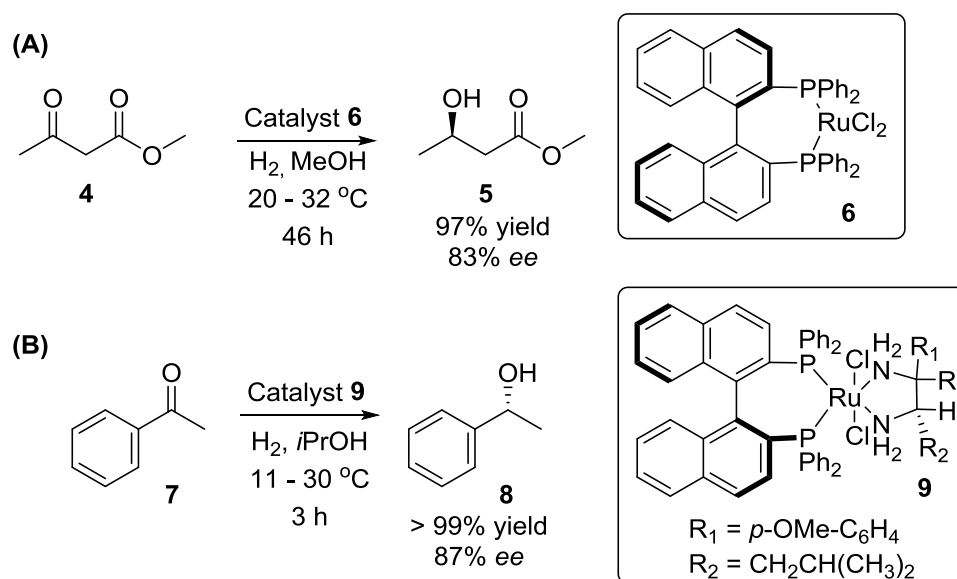
Scheme 1. Noyori's Ru catalysed asymmetric hydrogenation of ketones. (A): Ru-BINAP catalyst for the hydrogenation of functionalised ketones; (B): Ru-BINAP-diamine catalyst for the hydrogenation of non-functionalised ketones.[7, 8]

Knowles developed the asymmetric hydrogenation of an enamide for the production of *L*-DOPA **12**, a treatment for Parkinson's disease (Scheme 2).[9, 10] In this reaction enamide **10**

was hydrogenated using a Rh catalyst to give the chiral amide product **11** in 95% *ee*, cleavage of the amide then yielded the *L*-DOPA target **12**. In 2001, Noyori and Knowles shared the Nobel Prize for their early contributions to asymmetric hydrogenation.[11, 12]
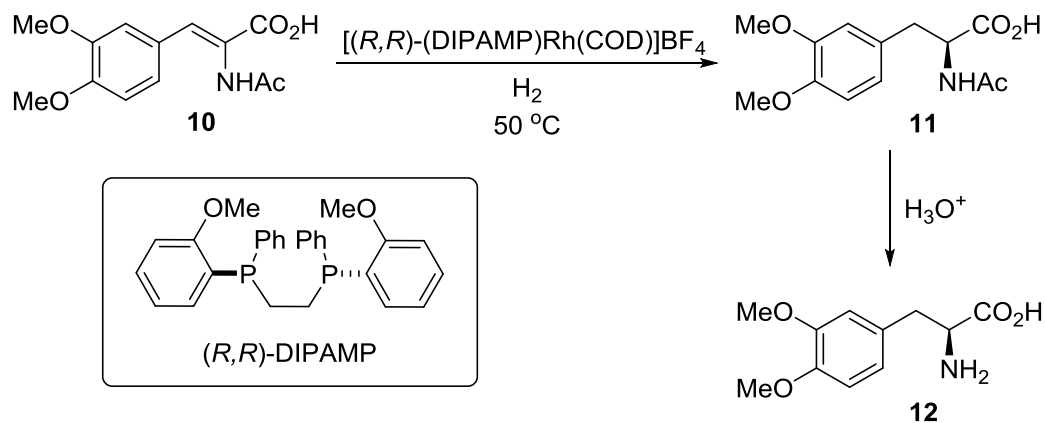
Scheme 2. Asymmetric hydrogenation process for the production of *L*-DOPA **12**.[9, 10]

More recently examples of the catalytic asymmetric hydrogenation of imines,[13] enamines[13] and oximes[14] to produce chiral amines have been developed, primarily using Ir, Ru or Rh catalysts (Scheme 3).
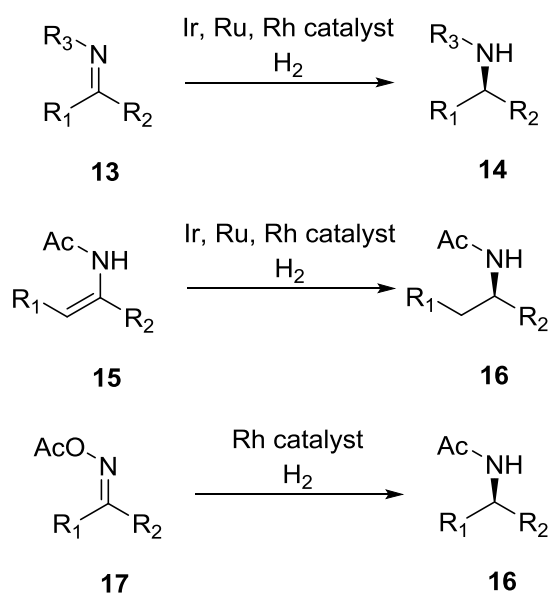
Scheme 3. General reaction scheme for the asymmetric hydrogenation of imines, enamines and oximes to produce chiral amines.

Using H_2 gas in this approach can be considered as a green route to chiral amines because there are no by-products. However, there are significant hazards and costs associated with the use of H_2 gas due to its explosive nature and the need for pressure reactors.

1.1.2 Asymmetric Transfer Hydrogenation

Asymmetric transfer hydrogenation (ATH)[15] was later developed in which a hydrogen donor molecule (*H*-donor) is used as the hydrogen source, removing the need for potentially explosive H_2 gas and expensive pressure reactors. In this case, the hydrogen is transferred from the *H*-donor to the substrate *via* the chiral catalyst. A major development in the area was the use of *N*-tosyl-1,2-diphenylethylenediamine (TsDPEN) ligands by Noyori and Ikariya, which were used for the ATH of ketones.[16, 17] The Noyori catalyst structures are based on a Ru centre with an arene ligand and bidentate diamine ligands (Scheme 4). Catalysts of this type with Ir and Rh centres have also been developed.[18, 19]
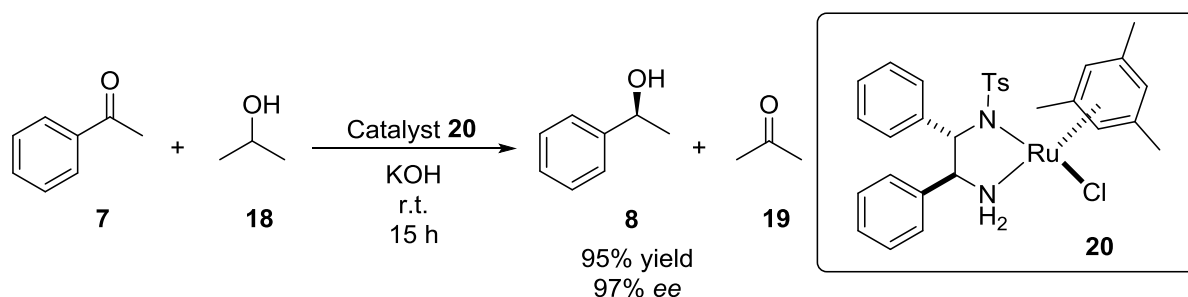
Scheme 4. ATH of acetophenone **7** to produce (*S*)-1-phenylethanol **8** using Noyori's (*S*,*S*)-[TsDPEN-RuCl(η^6-arene)] catalyst **20**.[16]

Isopropanol (*i*PrOH, **18**) is often used as the as the *H*-donor, however, the reaction is reversible due to the acetone by-product. In the reverse reaction acetone can accept hydrogen from the amine, re-forming the imine (Scheme 5). The equilibrium can be shifted

in favour of product formation by using *i*PrOH as the reaction solvent or by removing the acetone as it is formed. In the latter case, removing acetone efficiently requires high mass transfer rates that can be achieved by applying vacuum distillation to a batch reactor,[20] or using specialised continuous reactors.[21, 22]
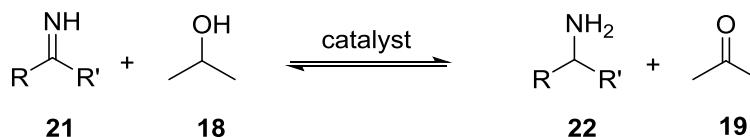
Scheme 5. Reversibility of imine reduction in the presence of *i*PrOH **18**.

To overcome the problems associated with using *i*PrOH, a triethylamine/formic acid (TEAF) mixture has also been used as *H*-donor.[23, 24] A 5:2 (formic acid:triethylamine) molar, single phase, azeotropic mixture is frequently used along with a suitable organic solvent. In this case the reaction is irreversible due to the loss of CO_2 (Scheme 6).
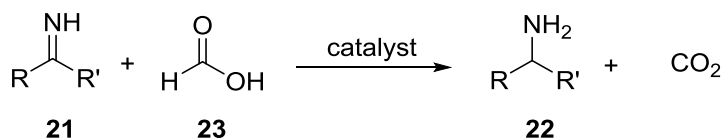
Scheme 6. Irreversibility of imine reduction in the presence of formic acid.

The majority of examples are for the ATH of ketones, although some examples of imine ATH to produce chiral amines have been reported. The ATH of imines has mainly been applied to cyclic substrates, as this infers greater stability on the imine. Noyori *et al.* reported on the ATH of imines with the [TsDPEN-RuCl(η^6-arene)] catalysts using TEAF.[24] Reduction of the imine **24** to salsolidine **25** was found to be most efficient using a 5:2 TEAF mixture in MeCN with (*S,S*)-[TsDPEN-RuCl(*p*-cymene)] **26** at 28 °C, providing > 99% yield and 95% *ee* after 3h (Scheme 7).
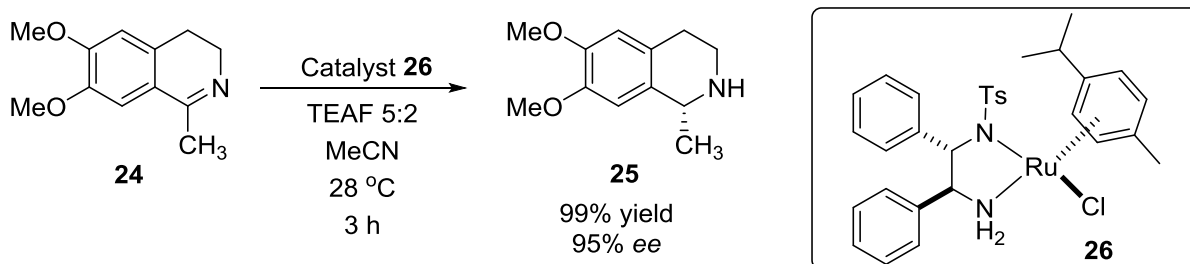
Scheme 7. Asymmetric reduction of 6,7-dimethoxy-1-methyl-3,4-dihydroisoquinoline **24** with (*S,S*)-[TsDPEN-RuCl(*p*-cymene)] **26**, 5:2 TEAF in MeCN at 28 °C.[24]

In this study, the hydrogenation of acyclic imines was also carried out (Scheme 8). However, the reactions were lower yielding and showed lower selectivity than the reactions using cyclic substrates.[24]
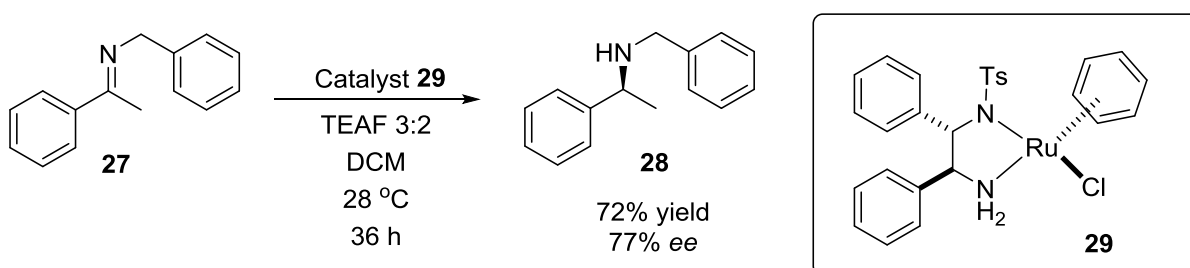
Scheme 8. ATH of an acyclic imine using (*S,S*)-[TsDPEN-RuCl(η^6-benzene)] **29**, TEAF 3:2 in DCM at 28 °C.[24]

ATH of imines has been employed for the synthesis of the tetrahydroisoquinoline core unit of almorexant **32** (Scheme 9), an orexin receptor antagonist.[25] Screening of reactions conditions led to a reaction system using the Noyori (*R,R*)-[TsDPEN-RuCl(*p*-cymene)]

catalyst **26**, TEAF 1:1 in DCM. On a 9 g scale, these conditions gave 99% conversion and 89% *ee* after 20 h, Scheme 9.
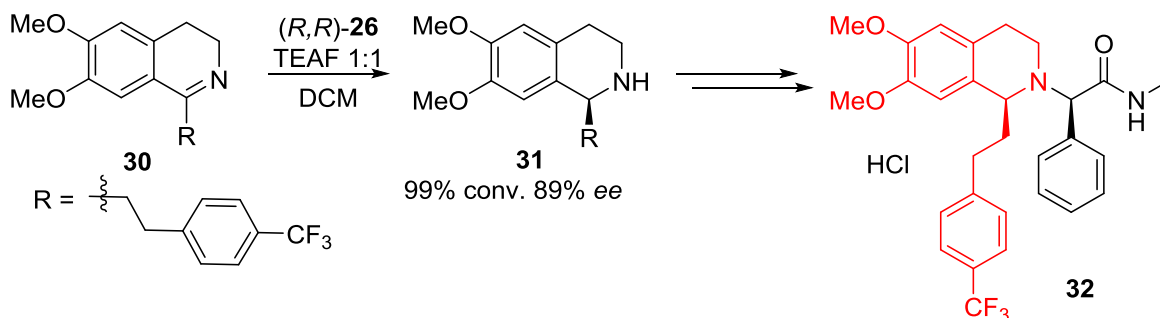
Scheme 9. ATH route for the production of the tetrahydroisoquinoline core unit of almorexant **32**.[25]

The reaction was scaled up to 18 and 12 kg batches and compared to an initial hydrogenation route using an Ir/TaniaPhos catalyst.[25] The fixed costs for the two routes were the same because the ATH can be run at a higher concentration, despite having a longer reaction time. Less waste was produced for the hydrogenation route compared to ATH. However, the ATH route had an overall lower cost due to the catalyst prices and had greater flexibility because the reaction could be carried out in any standard reactor whereas the hydrogenation required a pressure reactor.

ATH reactions have also been carried out under aqueous conditions, using HCOONa /H_2O as the *H*-donor system.[19, 26, 27] The ability of these catalysts to work in the presence of water was a significant step forward in the drive towards greener and cheaper chemistry.

1.1.3   Hydrogen Borrowing

The *N*-alkylation of amines *via* metal catalysed hydrogen borrowing has recently been developed as a method for the production of secondary and tertiary amines. Hydrogen borrowing involves the transfer of H_2 from the substrate to the metal catalyst and then the

H_2 is given back to the reagent to form the product. Unlike ATH, where H_2 is transferred from a *H*-donor to the substrate *via* the metal catalyst, hydrogen borrowing does not require an additional *H*-donor. Hydrogen borrowing can be employed for the coupling of an amine and an alcohol or the coupling of two amines (Scheme 10). Each process results in an *N*-alkylated amine product of a higher order than the substrate. This method has the advantage that the only by-product is H_2O when using alcohols or NH_3 when coupling amines.
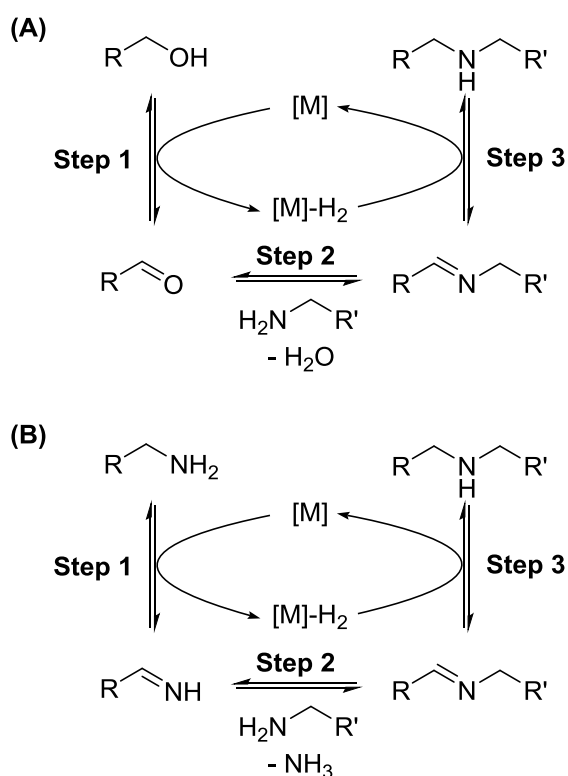
Scheme 10. Hydrogen borrowing mechanism for the *N*-alkylation of amines: (A) coupling of amines and alcohols,[28] (B) coupling of two amines.[29]

Fujita *et al.* reported the *N*-alkylation of primary amines with alcohols using the [Cp*IrCl$_2$]$_2$ catalyst (Scheme 11).[30] The reaction of aniline with benzyl alcohol gave a yield of 88% of only the *mono*-alkylated product. A range of Ir catalysts were tested, all of which had lower activity than [Cp*IrCl$_2$]$_2$. The system was applied to a range of amines

and primary and secondary alcohols, with good yields for all and high selectivity for the *mono*-alkylated product.
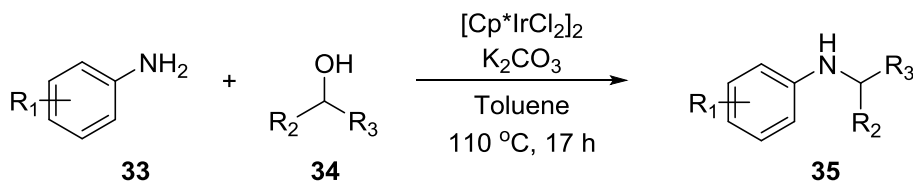
Scheme 11. *N*-alkylation of anilines with primary and secondary alcohols.[30]

Saidi *et al*. employed the [Cp*IrI$_2$]$_2$ catalyst for the *N*-alkylation of amines using alcohols in H$_2$O by the hydrogen borrowing approach.[28] The reaction of 1-phenylethylamine **36** with propan-1-ol using 1 mol% catalyst in water gave the secondary amine, with 96% conversion in 6 h (Scheme 12). When the reaction was carried out in H$_2$O, additives were not required to activate the catalyst and the addition of K$_2$CO$_3$, which is typically used to activate the catalyst, actually caused a reduction in the conversion. Also, no product formation was observed when using the analogous [Ru(*p*-cymene)Cl$_2$]$_2$ catalyst.
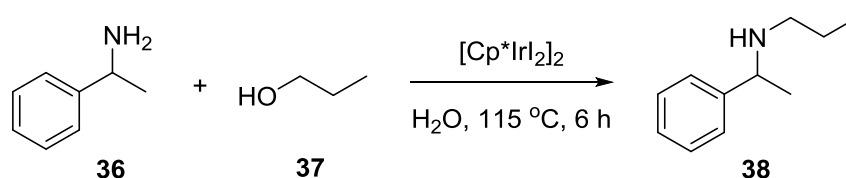
Scheme 12. Reaction of 1-phenylethylamine **36** with propan-1-ol by [Cp*IrI$_2$]$_2$ in H$_2$O.[28]

The transition metal catalysed coupling of two amines has often been shown to lead to a mixture of products due to the ability of both of the amines to undergo oxidation and so coupling can occur between two molecules of the same type of amine. Bähn *et al*. presented the first selective *N*-alkylation of amines using the Ru Shvö catalyst **42** for the coupling of aliphatic amines with *tert*-alkylamines to give the desired *mono*-alkylated

products (Scheme 13).[31] The reaction was selective for one product because only the aliphatic amine was able to undergo oxidation, which limits the breadth of its application.
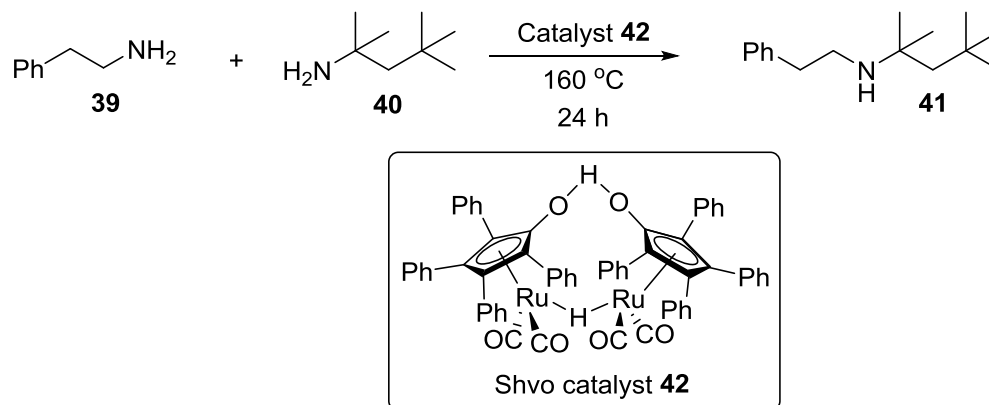
Scheme 13. *N*-alkylation of *tert*-octylamine **40** with 2-phenethylamine **39** using the Shvö catalyst **42** at 160 °C for 24 h.[31]

Saidi *et al*. reported on the first examples of selective cross-coupling of amines *via* the hydrogen borrowing mechanism using the [Cp*IrI$_2$]$_2$ catalyst when both of the amines were able to undergo oxidation.[29] The *N*-alkylation of 4-methoxyaniline **43** was used to screen the amines that could act as alkyl donors, with 1 mol% [Cp*IrI$_2$]$_2$ in xylene at 155 °C for 10 h (Scheme 14).
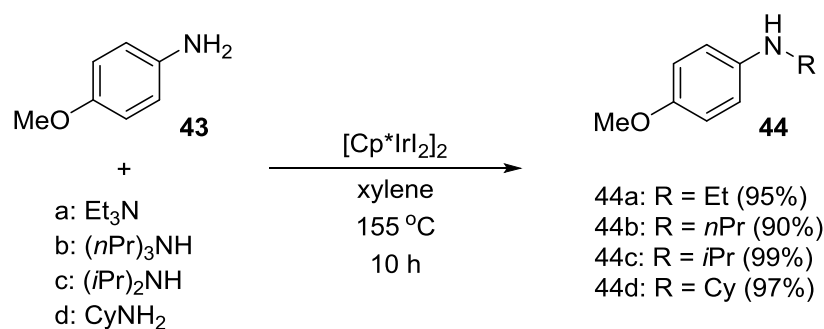
Scheme 14. *N*-alkylation of 4-methoxyaniline **43** with a range of amine donors using the [Cp*IrI$_2$]$_2$ catalyst at 155 °C for 10 h (Yields are shown in brackets).[29]

Whilst the dehydrogenation step to produce the imine intermediate would result in a loss of chirality, Zhang *et al.* reported a method to introduce enantiopurity into the product by using an asymmetric hydrogenation catalyst with the addition of chiral phosphoric acids (Scheme 15).[32] Using this approach, they were able to couple racemic alcohols with non-chiral primary amines to generate chiral secondary amines with moderate to high enantioselectivities (70-97% *ee*).
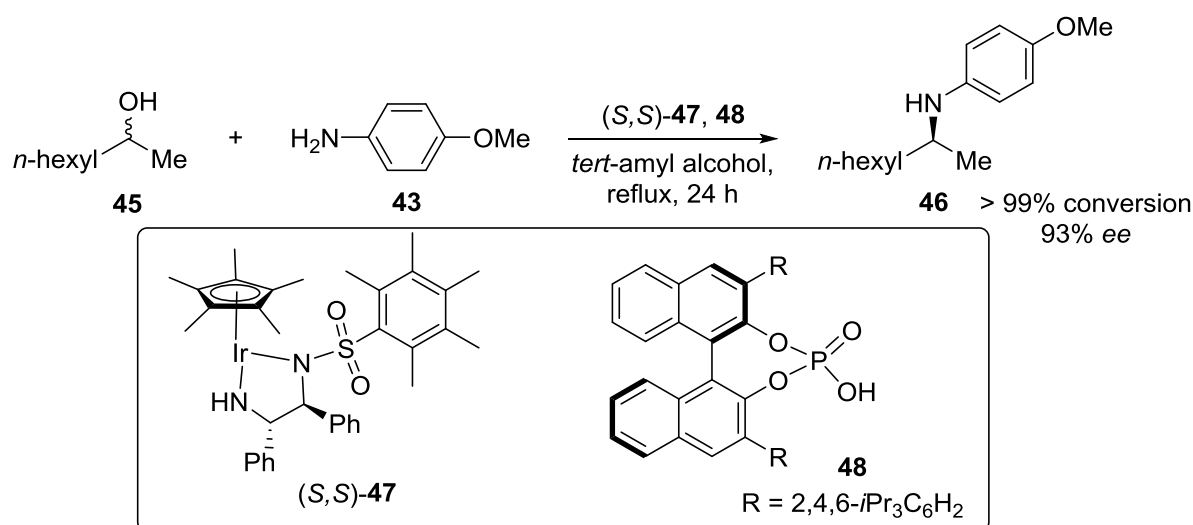
Scheme 15. Enantioselective hydrogen borrowing procedure developed by Zhang *et al.*[32]

These hydrogen borrowing procedures have thus far been carried out at high temperatures over long reaction times with high catalyst loadings, making them energy intensive and costly. Whilst high temperatures are required for activity, optimisation of the reaction conditions may allow the reaction times to be shortened, making a more efficient process.

1.1.4   Bio-Catalysis

The biocatalytic synthesis of chiral amines can be achieved using imine reductase, monoamine oxidase, amine dehydrogenase and transaminase enzymes.[1] The uniquely high

selectivity of enzymes under mild reaction conditions makes them a very attractive option for industrial asymmetric synthesis. Enzymes are also seen as a greener alternative to traditional chemical synthesis because there is no demand for precious metals. Conversely, enzymes can be sensitive to reaction conditions and have a narrow substrate scope. This can be improved through directed mutation and as such there are examples of commercial enzymes that can tolerate organic solvents and higher temperatures. In addition, some enzymes are cofactor dependent and so require either stoichiometric addition of expensive cofactors or additional reagents to be able to recycle the cofactor *in situ*, such as glucose or formate, which generates a significant amount of waste.

1.1.4.1 Enzymatic Asymmetric Reduction of Imines using Imine Reductase

Imine reductase (IRED) enzymes provide a biologically catalysed route for the synthesis of enantiopure amines *via* the asymmetric reduction of imines (Scheme 16).
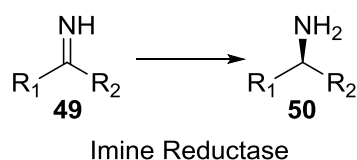
Scheme 16. General reaction scheme for imine reductase catalysed chiral amine production.

Leipold *et al.* reported the asymmetric reduction of imines using (*S*)-IRED from *Streptomyces sp.* GF3546.[33] The isolated (*S*)-IRED enzyme was used to convert 2-methyl-1-pyrroline **51** into 2-methylpyrrolidine **52** (55% conversion and > 95% *ee* after 18 h), using NADPH as the cofactor (Scheme 17). This system was applied to cyclic imine and iminium substrates with 5-, 6- and 7-membered rings. The catalytic activity was found to be higher for 6-membered rings compared to 5- or 7-membered rings.
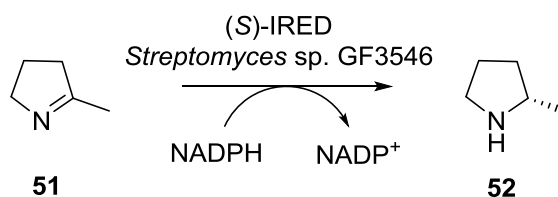
Scheme 17. Asymmetric reduction of 2-methyl-1-pyrroline **51** using (*S*)-IRED.[33]

A whole cell system was then developed, in which resting *E. coli* cells overexpressing (*S*)-IRED were used to catalyse the reaction (Scheme 18).[33] The whole cell system allowed for the addition of glucose to recycle the cofactor, without the need for the addition of a second enzyme to recycle the glucose. The whole cell system was applied to substituted dihydroisoquinolines and substituted dihydro-*β*-carbolines. The system was able to reduce 5-, 6- and 7-membered cyclic imines as well as iminium ions with 50 – 98% conversion and >98% *ee* for all substrates.
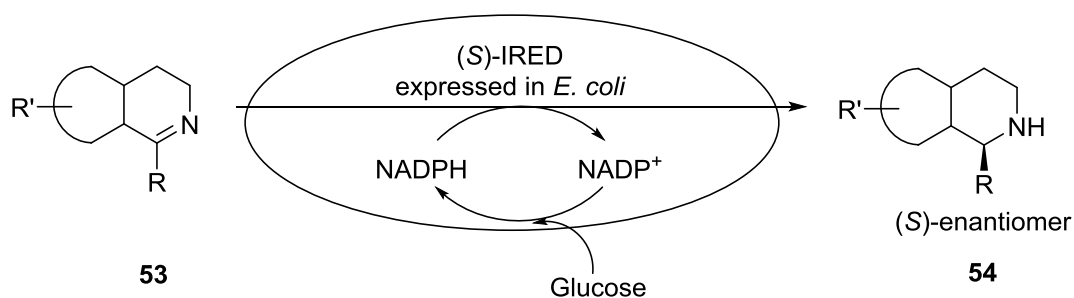
Scheme 18. Whole-cell reduction of cyclic imine substrates using (*S*)-IRED in *E. coli*.[33]

The IRED system requires a stable imine substrate. The production of the imines is problematic as only cyclic imines are stable enough to resist hydrolysis for reasonable lengths of time.

1.1.4.2 Enzymatic Asymmetric Oxidation of Amines using Monoamine Oxidase

Monoamine oxidase (MAO) enzymes catalyse the oxidation of amines to imines under mild conditions (Scheme 19A) and they have also been employed for the deracemisation of chiral amines to obtain single enantiomer products (Scheme 19B)[1].
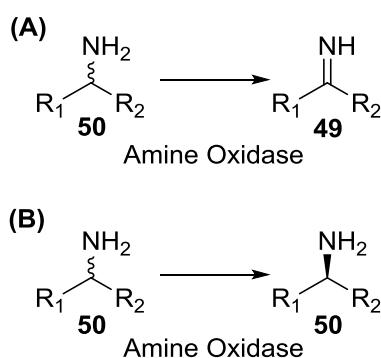
Scheme 19. General reaction scheme for monoamine oxidase catalysed reactions: (A) Amine oxidation for imine production; (B) Deracemisation for single enantiomer amine production.

Turner *et al*. subjected monoamine oxidase from *Aspergillus niger* (MAO-*N*) to directed evolution to create libraries of mutant strains to increase the substrate scope as the wild type enzyme had high activity but was only active for a narrow range of achiral substrates.[34, 35] This led to the D5 mutant strain that exhibited activity towards a broad range of chiral substrates, with (*S*)-selectivity. The same group then reported a method for the oxidation of substituted pyrrolidines using this MAO-*N* D5 variant (Scheme 20A).[36] The oxidation of the prochiral pyrrolidine **55** (20 mM) was carried out using *E. coli* cells expressing MAO-*N* in aqueous phosphate buffer (100 mM). The product imine **56** was obtained in 77% yield and 94% *ee*. The imine **56** was then reacted with TMS-CN to make a secondary amino nitrile, with a diastereomeric ratio of 97:3 (Scheme 20B). Hydrolysis of the amino nitrile **57** in aqueous HCl gave the free amino acid **58** in 40% yield and 98% *ee*.

(A)

(B)
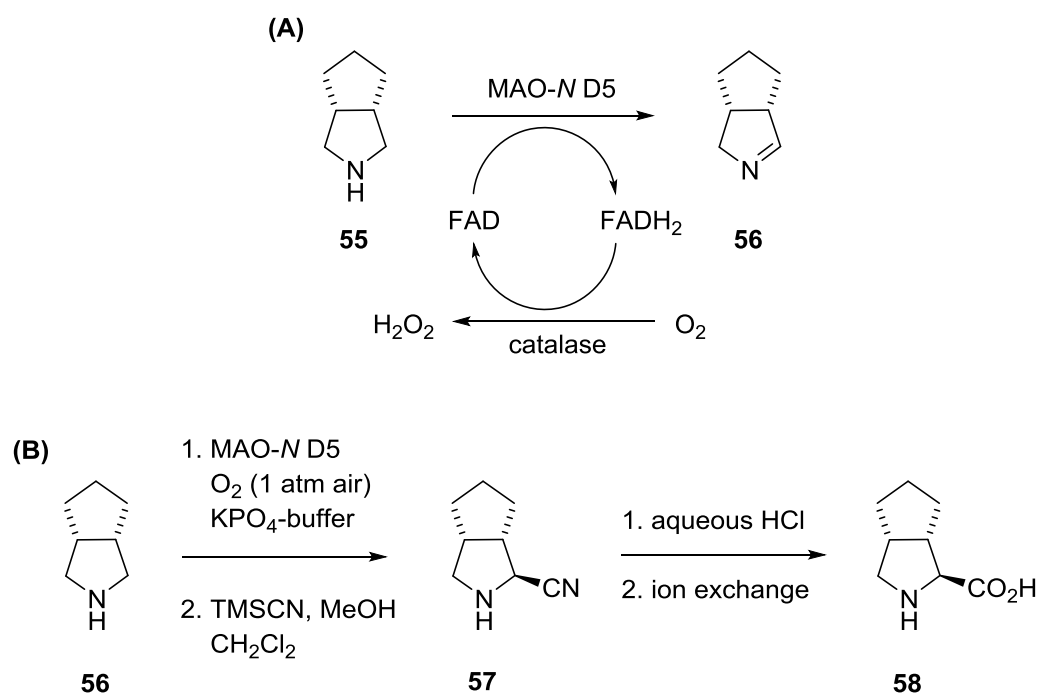
Scheme 20. (A) Oxidation of pyrrolidine using MAO-N D5 variant, cofactor recycling using O_2; (B) Asymmetric synthesis of amino acid *via* oxidation with MAO-N D5 and desymmetrisation with TMS-CN/MeOH, followed by acid hydrolysis.[36]

MAO-*N* derivatives have been used in manufacturing processes. Merck utilised MAO-*N* for the production of the bicyclic [3.1.0]proline intermediate of the hepatitis C drug Boceprevir **59** (Figure 2).[37]
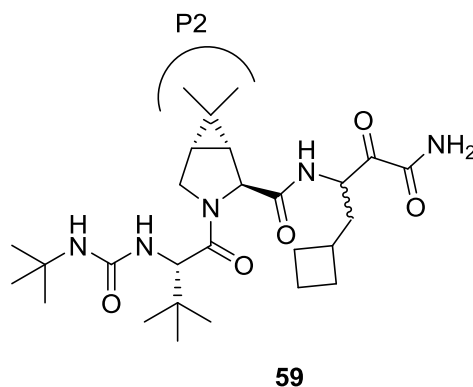
Figure 2. Structure of boceprevir **59**, showing the P2 subunit.[37]

A process was sought by which the imine **61** could be prepared directly from dimethylcyclopropylproline **60** *via* desymmetrisation. A MAO-*N* catalysed desymmetrisation was developed (Scheme 21). Enzyme optimisation was carried out on MAO-*N* through mutation to provide increased activity and thermal stability in comparison to the wild type enzyme. Downstream imine trapping reactions gave the desired salt of the P2 subunit in 56% yield and > 99% *ee*. The specific activity of the enzyme was 17.7 μmol min^{-1} mg^{-1} however the concentration of the process was quite low (65 g L^{-1}).
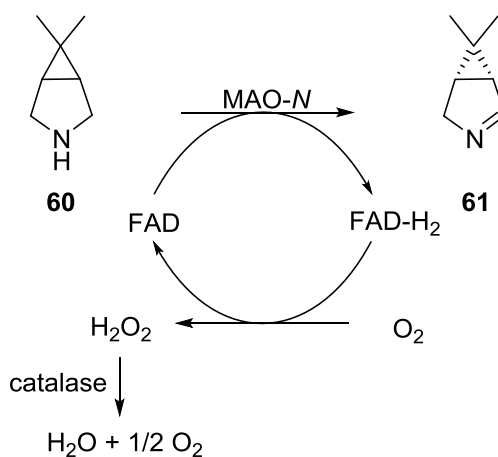
Scheme 21. Desymmetrisation of dimethylcyclopropylproline **60** using the enzymatic method.[37]

As mentioned above, MAO can also be used to obtain single enantiomer chiral amines through deracemisation. Ghislieri *et al*. reported the deracemisation of tetrahydro-*β*-carbolines, important bioactive alkaloids, using MAO-*N* variants (Scheme 22 A).[38] The MAO-*N* enzyme catalysed the enantioselective oxidation of chiral amines to convert one enantiomer into an imine, whilst leaving the opposite enantiomer untouched (Scheme 22B). The nonselective reducing agent ammonia-borane was used to regenerate the

racemic amine by reduction of the imine. The opposite amine enantiomer accumulates through multiple cycles, leading to deracemisation of the amine sample and so an increase in the amine *ee*.

(A)

62 → **63** (R) or (S)

1. MAO-*N* D9/11
   O_2 (1 atm air)
2. BH_3-NH_3
   phosphate buffer

(B)

Accumulates

64 → **65** + **64**

1. MAO-*N*
   O_2 (1 atm air)
   phosphate buffer

2. BH_3-NH_3
   phosphate buffer
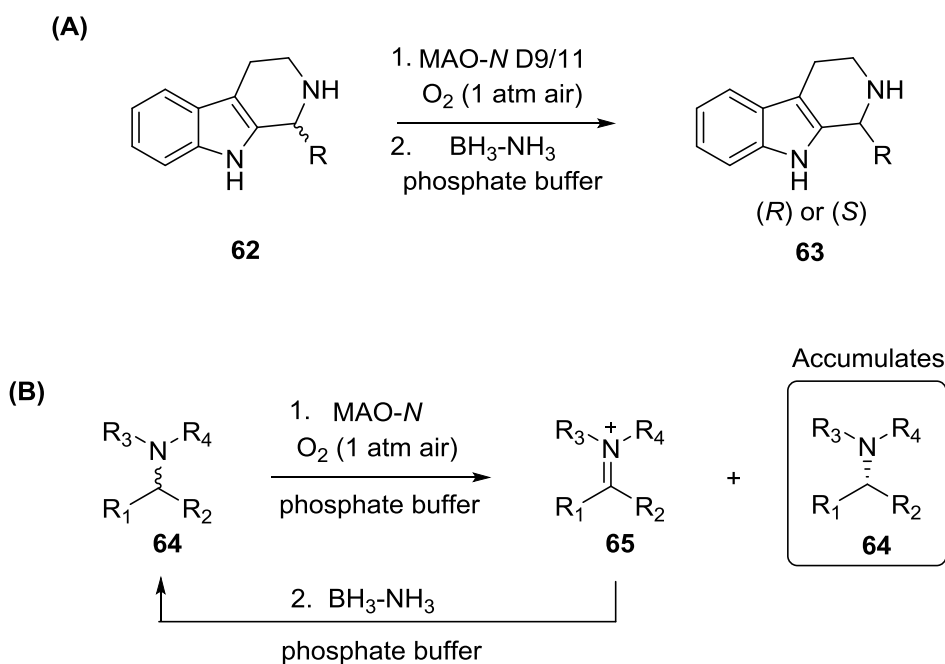
Scheme 22. (A) MAO-*N* D9 and D11 mediated deracemisation of *β*-carbolines; (B) Catalytic cycle for the deracemisation of chiral amines *via* the combination of enantioselective MAO-*N* and a non-selective reducing agent.[38]

This method employed borane as the chemical reductant, which is air and moisture sensitive, highly toxic, potentially explosive, and atom inefficient. Therefore, this method would not be desirable for use on-scale in industry.

1.1.4.3 Enzymatic Reductive Amination of Ketones using Amine Dehydrogenase

Amine dehydrogenase (AmDH) enzymes present a route to chiral amines through the reductive amination of ketones (Scheme 23).
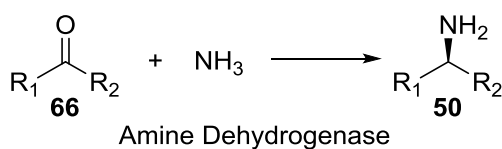
Scheme 23. General reaction scheme for amine dehydrogenase (AmDH) catalysed chiral amine production.

Abrahamson *et al.* produced an AmDH from an amino acid dehydrogenase *via* protein engineering for use in the synthesis of chiral amines.[39] The substrate for the wild-type leucine dehydrogenase (LeuDH) was the α-keto acid, which reacted to give leucine. The AmDH that was developed accepted the related methyl *iso*butyl ketone, to give the corresponding chiral amine (Scheme 24).
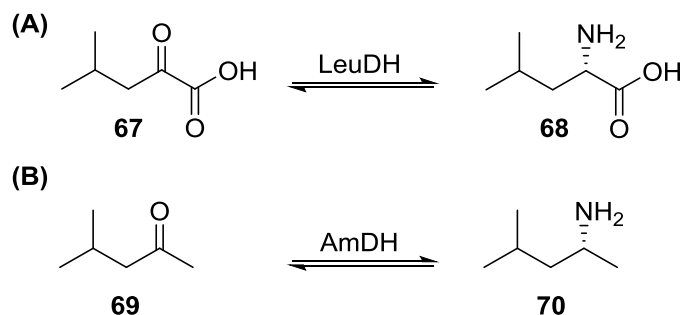
Scheme 24. (A): Wild-type leucine dehydrogenase (LeuDH) reaction; (B): Amine dehydrogenase (AmDH) reaction.[39]

AmDH are NADH dependent enzymes and so it was coupled to a glucose dehydrogenase enzyme for cofactor recycling (Scheme 25). The deamination of (*R*)- and (*S*)-1-phenylethylamine was used to determine the enantioselectivity of the AmDH, which was found to maintain the (*S*)-selectivity of the wild-type enzyme. The engineered AmDH was found to be active against a range of substrates.
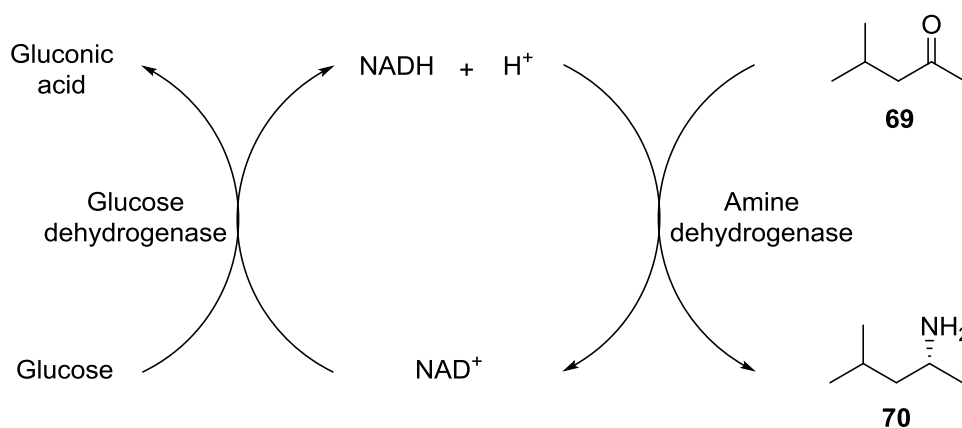
Scheme 25. Asymmetric synthesis of amines *via* amine dehydrogenase, coupled to glucose dehydrogenase for cofactor recycling.[39]

1.1.4.4 Enzymatic Chiral Amine Synthesis using Transaminases

Transaminase enzymes can be used for the asymmetric synthesis of chiral amines from ketones, *via* the transfer of an amino group from a donor molecule (Scheme 26).
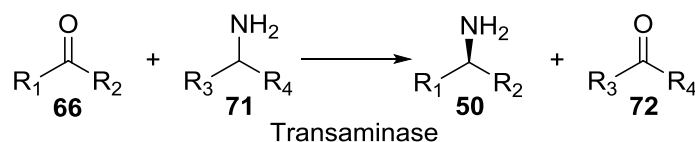
Scheme 26. General reaction scheme for transaminase catalysed chiral amine production.

Most notably, Merck employed a transaminase in the penultimate step towards the synthesis of the anti-diabetic drug sitagliptin **3** (Januvia, Scheme 27).[40] In the original chemical synthesis route, ketone **73** was first converted to an enamine, followed by Rh catalysed asymmetric hydrogenation to give **3**. In the biocatalytic route, the chiral amine could be produced directly from ketone **73** using the transaminase. The implementation of a biocatalytic approach reduced the number of steps in the synthesis but also improved the

stereoselectivity and reduced the amount of purification that was required because there was no longer any Rh in the process waste.
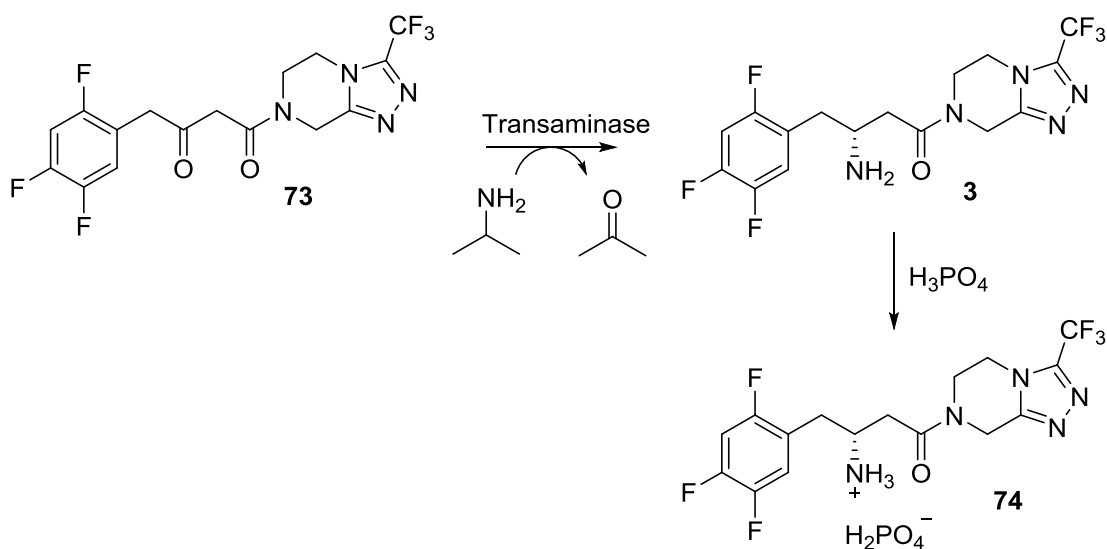
Scheme 27. Merck synthesis of sitagliptin **3**, employing a transaminase to install the desired chiral amine unit.[40]

Transaminase enzymes can also be used for the kinetic resolution of racemic amines, which requires an amine acceptor, typically pyruvate. Pyruvate is required in a stoichiometric amount, which is expensive and can also lead to inhibition of the reaction.[41] To overcome this, Truppo *et al*. reported the kinetic resolution of racemic amines *via* a transaminase coupled to an amino acid oxidase (AAO) (Scheme 28A).[41] The combination with an AAO allowed for a catalytic amount of pyruvate to be used as the AAO catalysed the regeneration of pyruvate from alanine. The kinetic resolution of 1-phenylethylamine was carried out using both the (*R*)- and (*S*)-selective transaminases to yield > 99% *ee* at 50% conversion in both cases. The system was applied to a range of amine substrates, all with the same efficiency. The (*S*)-selective transaminase was also shown to be able to prepare both the (*R*)- and (*S*)-enantiomers in > 99% *ee*, by kinetic resolution and

asymmetric synthesis, respectively. The (*S*)-enantiomers were prepared by the combination

of the transaminase with lactate dehydrogenase, using *L*-alanine as the amine donor

(Scheme 28B). The driving force for the reaction was the reduction of the pyruvate by-

product to lactate by the lactate dehydrogenase. The NADH cofactor required for this

reaction was recycled by glucose dehydrogenase.
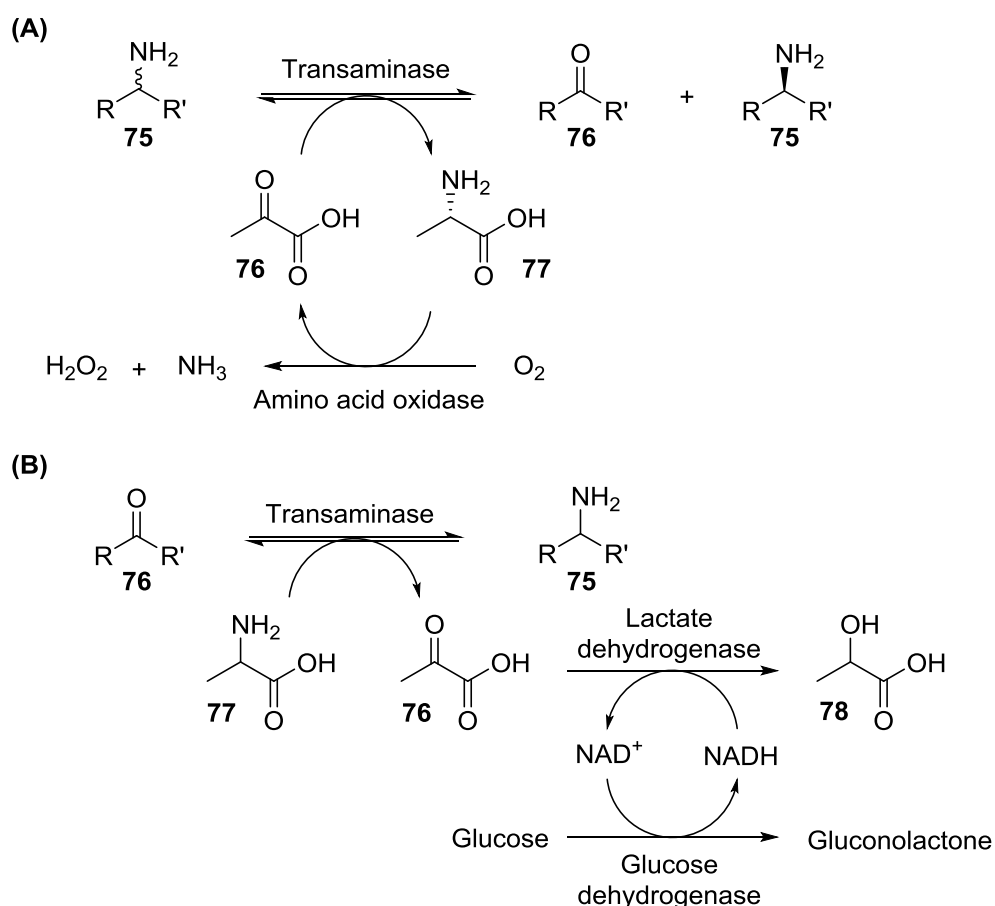
Scheme 28. (A) Kinetic resolution of racemic amines using a transaminase coupled to an amino acid oxidase; (B) Asymmetric synthesis of amines using a transaminase coupled to lactate dehydrogenase.[41]

1.2   Resolution

The production of chiral amines using resolution methodologies involves the separation of

enantiomers from a racemic mixture that has been created by traditional non-asymmetric

synthesis. Resolution can be carried out by diastereomeric crystallisation or enzymatically.

Chiral chromatography can be used to separate enantiomers, but is generally a laboratory analytical technique so will not be discussed further.

1.2.1 Diastereomeric Crystallisation

In diastereomeric crystallisation enantiomers are separated by the formation of a diastereomeric salt between the chiral amine and a chiral carboxylic acid (Scheme 29).[2, 42] One of the diastereomeric salts will then crystallise out of solution, whilst the other remains in solution. This difference in solubility allows the two amine enantiomers to be separated from each other.
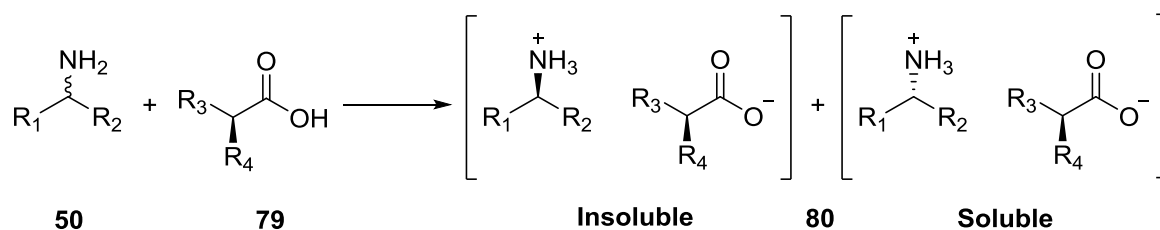
Scheme 29. General reaction scheme for diastereomeric crystallisation of chiral amines.

Diastereomeric crystallisation of a pharmaceutically relevant amine molecule was reported by Blacker *et al.* for the production of single-isomer Sertraline **81**, an API for the treatment of depression (Scheme 30).[43, 44] The (1*S*,4*S*)-isomer was selected for from a mixture of four isomers using (*R*)-mandelic acid **82** (99% *ee*). The crystallisation was coupled to a racemisation step to recycle the undesired enantiomer and increase the yield.
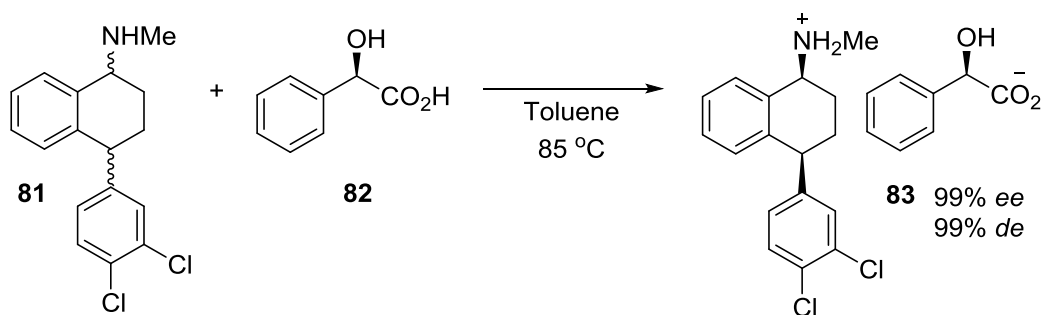
Scheme 30. Separation of the isomers of Sertraline **81** *via* diastereomeric crystallisation, reported by Blacker *et al.*[43]

Resolution by diastereomeric crystallisation allows for the separation of enantiomers by the simple formation of salts, which also means that after the separation the single enantiomer amine can be readily obtained from the salt by extraction methods. However, it can be difficult to predict which chiral acid and solvent system will be required for a particular amine and so a degree of trial and error has to be employed, which can be time and resource consuming. Also, the crystallisation process alone is highly wasteful because of the leftover undesired enantiomer. This can be improved by coupling to recycling procedures as in the sertraline example.[43] Further procedures for recycling the remaining enantiomers from resolution procedures will be discussed later.

1.2.2 Enzymatic Kinetic Resolution

Enzymatic kinetic resolution uses an enzyme to selectively modify one of the enantiomers in a racemic mixture, allowing them to be separated. The most common type of enzymes used for this strategy are lipases.[45, 46] The lipase uses an acyl donor to acylate amine and as only one enantiomer is accepted into the enzyme active site, only one product enantiomer is formed (Scheme 31). In order for the method to succeed a highly selective enzyme must be used to ensure that the rate of acylation of one enantiomer (k_1) is much greater than the other (k_2), meaning that $k_1 \gg k_2$.
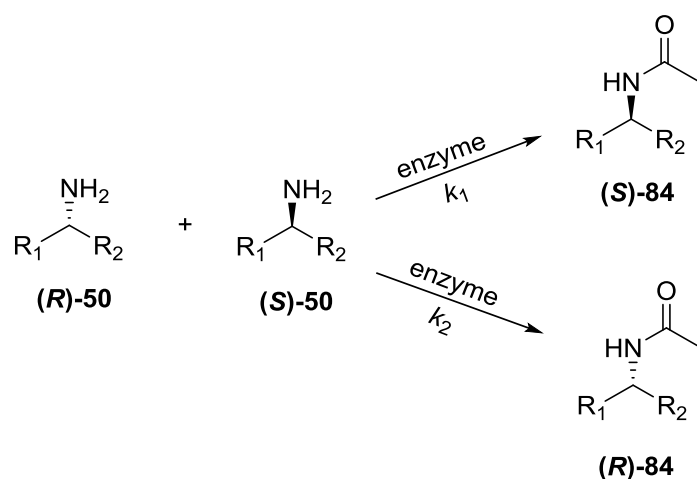
Scheme 31. General reaction scheme for enzymatic kinetic resolution.

The lipase catalysed resolution of chiral amines was first studied by Kitaguchi *et al.*, employing the enzyme Subtilisin.[47] More recently, lipase B from *Candida antarctica* (CalB) has been widely employed for kinetic resolution due to its broad substrate specificity and tolerance of temperature and organic solvents. The most common primary amine studied for enzymatic resolution is 1-phenylethylamine **36**, due to its value in asymmetric synthesis.[48, 49] The development of a commercially available immobilised version of the CalB lipase (Novozyme 435, N435)[50] has led to an increased popularity due improved stability and ease of re-use. The first example of the resolution of primary amines using N435 with EtOAc as the acyl donor was developed by Reetz (Scheme 32).[51] However, conversions were variable and reaction times were long (7 – 60 h).
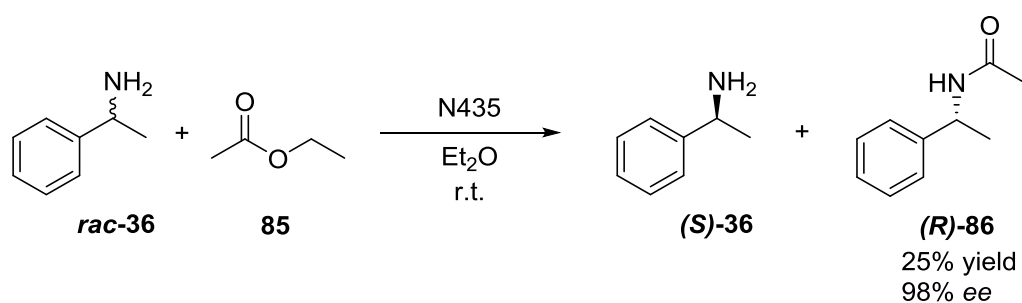
Scheme 32. Enzymatic resolution of 1-phenylethylamine **36** catalysed by immobilised lipase N435, first reported by Reetz.[51]

For the kinetic resolution of alcohols, acyl donors such as vinyl acetate are often used. However, these donors could not be used for amines due to their higher reactivity that leads to un-catalysed background reaction, EtOAc is often used instead.[52] The reactions using EtOAc are highly enantioselective, however the products of these reactions are amides, which require harsh conditions to cleave the bond and regenerate the single enantiomer amine.[53] Hoben *et al.* improved on this by using dibenzyl carbonate **87** as the acyl donor, which could be removed under much milder conditions (Scheme 33).[54]
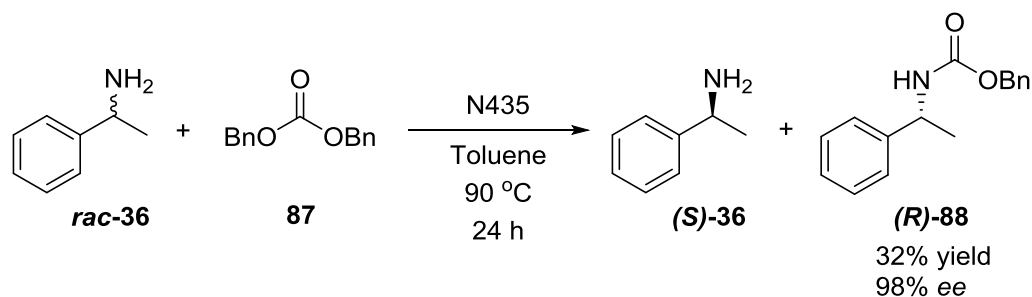
Scheme 33. Lipase catalysed resolution of 1-phenylethylamine **36** using dibenzyl carbonate **87** as the acyl donor.[54]

There are far fewer examples of lipase catalysed resolution of secondary amines due to the lower number of enzymes that will accept these substrates. This is because the extra steric bulk on the amine makes it more difficult to fit into the active site.[53] Breen developed a process for the resolution of secondary amines using a carbonate donor and lipase from *Candida rugosa* (Scheme 34).[55] After 8 h, 47% yield of carbamate **91** was produced, with 98% *ee*.

Scheme 34. Resolution of secondary amines developed by Breen.[55]

Enzymatic resolution is a well-documented method to obtain chiral amines with high enantiopurity and the development of robust enzymes, with increased stability and good tolerance of organic solvents, has led to the use of enzymatic resolution in the pharmaceutical industry.[2] However, the resolution approach is inherently wasteful as only one enantiomer is generally desired for the API. This means that the maximum possible yield is 50% for a resolution process, with the remaining undesired enantiomer being waste, unless the resolution can be coupled to another reaction to use the waste enantiomer, which will be discussed in the following sections.

1.3 Racemisation

The racemisation of amines provides an opportunity to recycle the waste enantiomer leftover from the resolution process. A classical method employed is base catalysed racemisation, in which the substrate is deprotonated at the chiral centre by the base. Transfer of the proton back to the substrate gives the racemic molecule. This method suffers from a limited substrate scope due to the requirement for a labile proton and as such most amines are not suitable for this approach.[56, 57]

An increasingly popular method is metal catalysed racemisation. In this approach the enantiopure amine is first dehydrogenated by the metal catalyst to generate an imine intermediate (Scheme 35); this imine can then be re-hydrogenated to regenerate the amine.

The catalysts used are not chiral, so do not favour a particular prochiral face of the imine for the re-hydrogenation step, and therefore produce a racemic amine.
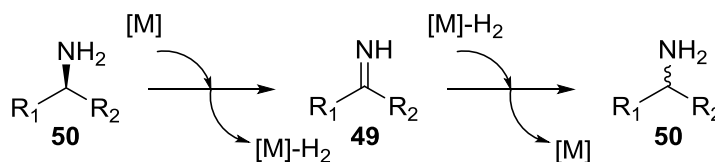
Scheme 35. Generic reaction scheme for metal catalysed racemisation of amines.

Murahashi *et al*. first showed that Pd black could be used to racemise amines.[58] Reetz *et al*. then built upon this by using Pd/C to racemise 1-phenylethylamine.[59] Using heterogeneous Pd catalysts for the racemisation of amines led to the formation of impurities, namely ethylbenzene and dimeric impurities. The proposed mechanism for their production is shown in Scheme 36.[60] First, H_2 is removed from the single enantiomer substrate to generate the imine **92**. This imine can then either be re-hydrogenated to give the racemic amine or condense with a second amine molecule, producing an imine dimer **93**. Hydrogenation of the imine dimer then leads to the amine dimer **94**. The ethylbenzene impurity **95** was formed by hydrogenation and cleavage of the amine dimer, to regenerate the amine monomer.
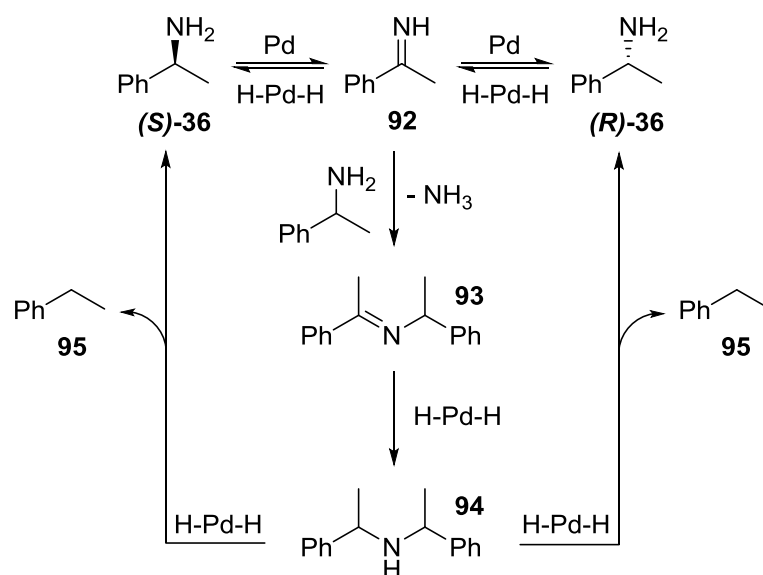
Scheme 36. Pd catalysed amine racemisation showing proposed mechanism for impurity formation.[60]

Parvulescu *et al.* found that Pd on alkaline-earth supports such as $BaSO_4$ and $CaCO_3$ suppressed by-product formation, owing to the basic nature of the support.[60] This group also employed microwave heating to enhance the racemisation of chiral amines and increase the selectivity for the desired product using these heterogeneous Pd catalysts.[61] However, a drawback of this Pd catalysed racemisation is that it is only suitable for benzylic substrates. Parvulescu *et al.* then developed a process to racemise both benzylic and aliphatic amines using heterogeneous Raney Ni (RaNi) as a cheaper alternative to precious metal catalysts.[62] These Pd and RaNi catalysts all required H_2 gas to be able to perform the racemisation and so would require pressure vessels, which can be problematic on a laboratory scale.

The Bäckvall group established a process for the racemisation of chiral alcohols using the Ru Shvö catalyst **42**,[63, 64] and then developed modified versions of this catalyst for the racemisation of chiral amines as well as an expanded substrate scope for alcohols (Scheme

37).[65-67] Whilst high selectivity for the racemisation of the amine monomer was achieved *vs.* the dimer formation, long reaction times were typically required (24 h).
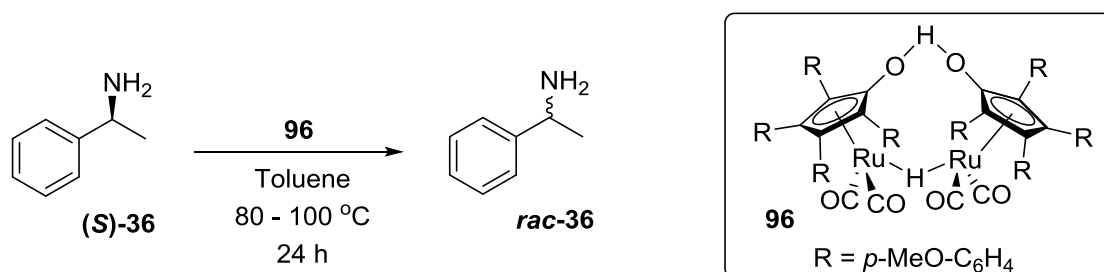
Scheme 37. Ru catalysed primary amine racemisation using modified Shvö catalyst **96**, developed by Bäckvall *et al.*[66]

Blacker *et al.* utilised the $[Cp^*IrI_2]_2$ catalyst for the racemisation of 6,7-dimethoxy-1-methyl-1,2,3,4-tetrahydroisoquinoline **25** (Scheme 38).[57] This catalyst provided much shorter reaction times and milder reaction conditions, with **25** being racemised after only 2 h at 40 °C.
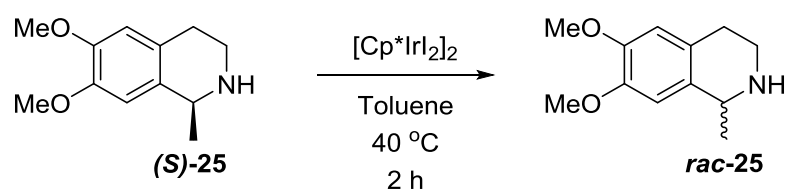
Scheme 38. Ir catalysed racemisation of 6,7-dimethoxy-1-methyl-1,2,3,4-tetrahydroisoquinoline **25**, reported by Blacker *et al.*[57]

In the same study, a range of other chiral amines were shown to racemise with the $[Cp^*IrI_2]_2$ catalyst. It was found that this catalyst was particularly useful for the racemisation of secondary amines, whilst primary amines were again shown to form

dimeric products due to the reactivity of the intermediate imine species **92** (Scheme 39). Higher temperatures and catalyst loadings were also required for the majority of substrates.
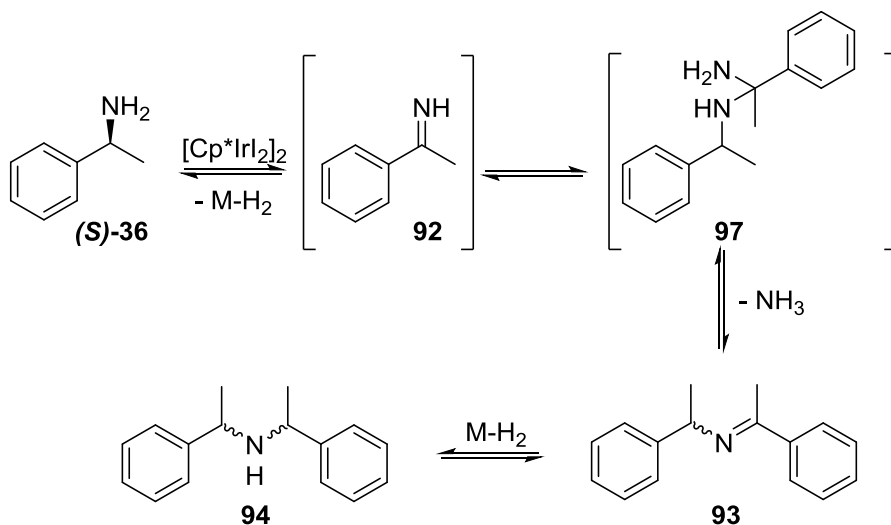
Scheme 39. Formation of dimeric impurities in the $[Cp*IrI_2]_2$ racemisation of a primary amine.[57]

1.4   Dynamic Kinetic Resolution

Chemical and biological catalysts both have advantages and disadvantages. Metal catalysts tend to have a wide substrate scope and high activity but are not always as highly enantio- and regioselective as enzymes due to coordination of species within the reaction system. As discussed above, biological catalysts have high enantio- and regioselectivities and function under milder aqueous conditions however, the substrate scope is often very narrow and the stability in organic solvents and at high temperatures can be poor. The combination of catalysts would allow for the advantages of each catalyst to be exploited. Tandem processes in which multiple catalytic steps occur in one-pot are an attractive route for synthesis as the number of purification steps would be reduced, the selectivity and substrate scope would be improved and the reactivity enhanced, all of which would lead to increased conversion and efficiency.[68]

One of the most common techniques for the combination of enzymes and metal catalysts is dynamic kinetic resolution (DKR),[46] in which enzymatic resolution is coupled to an *in situ* racemisation (Scheme 40). This is an improvement on the classical method of resolution described above, which has a theoretical maximum yield of 50% and so is highly wasteful. DKR increases the maximum theoretical yield to 100% as the undesired enantiomer is converted back to the racemic compound to undergo further enzymatic resolution. As previously discussed, to obtain the (*S*)-Ac product the rate of reaction of the (*S*)-amine with the enzyme must be faster than for the (*R*)-amine ($k_1 > k_2$). For DKR to be successful, the rate of racemisation must also be faster, to rapidly convert the (*R*)-amine to the (*S*)-amine; $k_{rac} > k_2$.
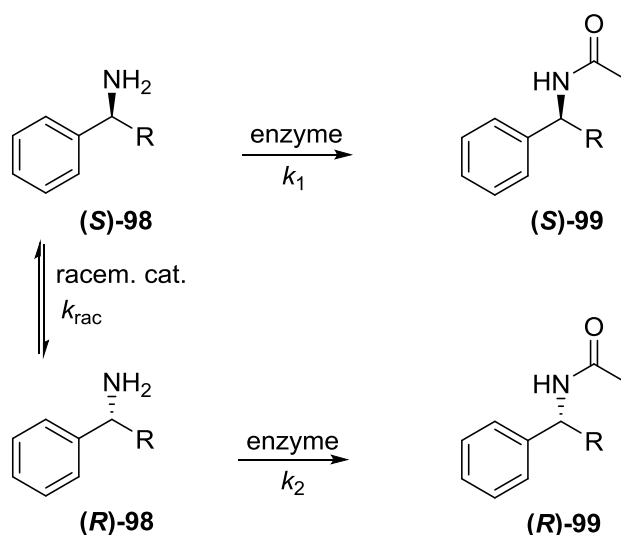
Scheme 40. DKR process for obtaining enantiomerically pure amines.

A recent review by Verho *et al*. highlights the DKR process for both alcohol and amines and describes the greater difficulties associated with amine substrates compared to alcohols.[53] Specifically, fewer examples of efficient racemisation methodologies exist for amines due to the ability of the amines themselves to act as ligands for the catalysts, leading to catalyst deactivation or the need for higher temperatures to break this

coordination and re-activate the catalyst. However, amine racemisation in DKR has been successfully carried out using Pd, Ru and Ir catalysts and selected examples are described below.

The first example of amine DKR was reported by Reetz, which employed CalB for the resolution combined with Pd/C for the racemisation of 1-phenylethylamine **36**.[59] However, the reaction was very slow, with only 60% conversion obtained after 8 days.
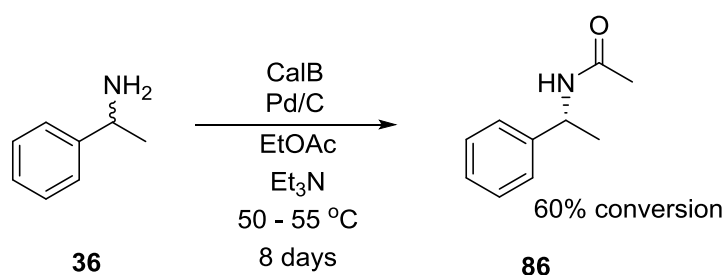
Scheme 41. The first example of an amine DKR from Reetz.[59]

Parvulescu *et al*. further developed the use of Pd for the DKR of primary amines, utilising Pd/BaSO$_4$ as the racemisation catalyst.[60] Using this method 91% conversion of 1-phenylethylamine **36** was achieved after 24 h, with > 99% *ee* for the product.

Pd nanoparticles were utilised for amine racemisation by Engström *et al*. in the development of an artificial metalloenzyme for the DKR of *rac*-1-phenylethylamine **36** (Scheme 42).[69] Pd nanoparticles and CalB were immobilised within the same pore of a siliceous mesocellular foam (MCF). The metalloenzyme was produced from a previously developed Pd(0)-aminopropyl MCF,[70] where the Pd nanoparticles were immobilised in an aminopropyl functionalised MCF, the remaining free aminopropyl groups were then reacted with glutaraldehyde to form a Schiff base and then CalB was immobilised by a second Schiff base forming reaction.
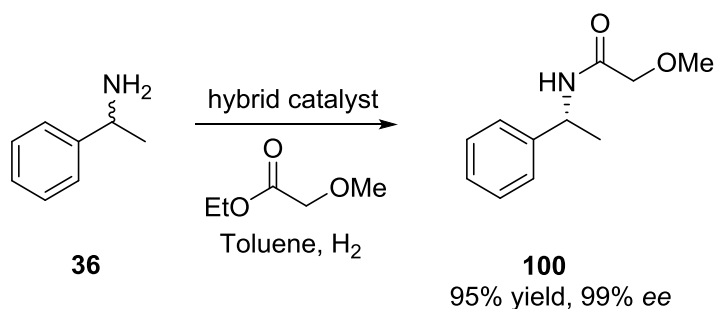
Scheme 42. DKR of 1-phenylethylamine **36** using the Pd-CalB hybrid catalyst.[69]

The DKR of **36** using the Pd-CalB metalloenzyme gave a 95% yield and a 99% *ee* after reacting for 16 h at 70 °C. This resultant yield was much higher than for the reaction at 80 °C and the separate component system, indicating that the close proximity of the two catalysts within the same cavity of the MCF resulted in enhanced efficiency. The tandem catalysis mechanism (Scheme 43) proceeded by the entrance of the racemic amine into the cavity, which is selectively acylated on the (*R*)-enantiomer by the enzyme. The (*R*)-enantiomer exits the cavity and the (*S*)-enantiomer is then racemised by the Pd nanoparticles. The racemic amine can then undergo an enzymatic resolution and so a cyclic process is set-up. Denaturation of the CalB enzyme was observed due to the polar surface of the MCF, which limited the lifetime and turnover of the system. Whilst this method is elegant, the use of Pd nanoparticles limits the type of amine that can be racemised to benzylic amines.
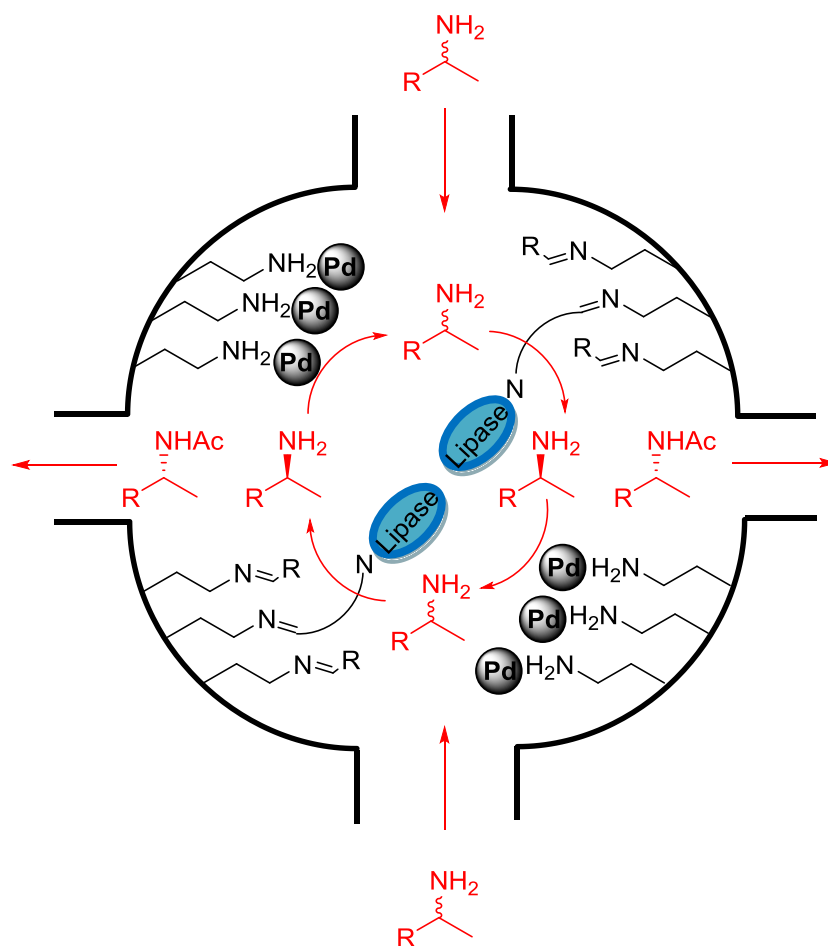
Scheme 43. DKR of 1-phenylethylamine catalysed by the Pd-CalB hybrid catalyst. A: Reaction scheme; B: Pd nanoparticles and CalB immobilised in an MCF pore with tandem catalysis mechanism.[69]

The Bäckvall group also reported the combination of CalB with their modified version of the Ru Shvö catalyst for the DKR of *rac*-1-phenylethylamine **36** (Scheme 44).[71] A range of alkyl methoxyacetates were screened as acyl donors alongside the *H*-donor, *i*PrOH. The acyl donors chosen for the scale up were alkylmethoxy acetates **101a** and **101b**. The DKR was scaled up from 1 mmol to 45 mmol scale using the acyl donor **101a** with R = OMe. The acyl donor and CalB were added in three portions to give the amide product in 98% *ee* and 68% yield after 48 h.
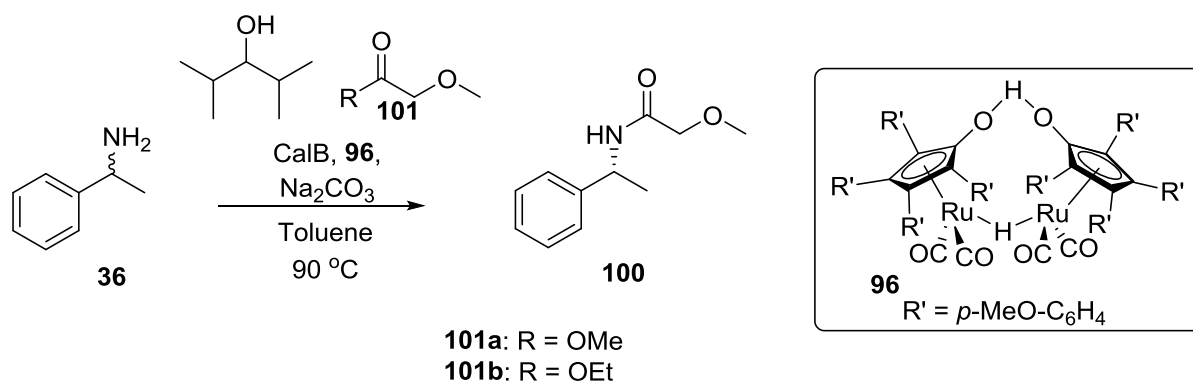
Scheme 44. Combination of Bäckvall's Ru catalyst **96** with CalB for the DKR of 1-phenylethylamine **36**.[71]

Blacker *et al*. reported the DKR of secondary amine *rac*-6,7-dimethoxy-1-methyl-1,2,3,4-tetrahydroisoquinoline **25**, combining their [Cp*IrI$_2$]$_2$ catalysed racemisation with *Candida rugosa* lipase[57, 72] and the allyl carbonate acyl donor **102** system developed by Breen[55] (Scheme 45). An isolated yield of 82% and 96% *ee* of **103** was obtained after 48 h on a 3 g scale. This enzyme was not particularly active and so 50 wt% loading was required initially, followed by an additional 20 wt% after 24 h.
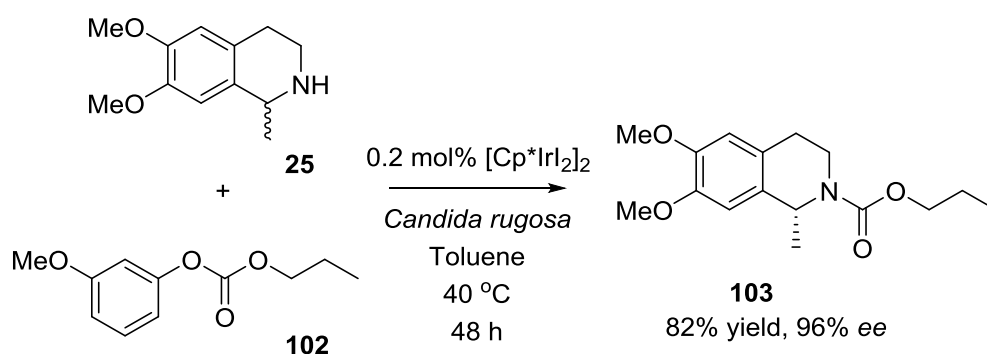
Scheme 45. Combination of the [Cp*IrI$_2$]$_2$ catalyst with *Candida rugosa* lipase for the DKR of *rac*-**25**.[57, 72]

Another potential way to utilise the waste enantiomer from the resolution step could be to perform a second reaction to modify that enantiomer to give a higher value product. The metal catalysed hydrogen borrowing approach discussed above could be used to *N*-alkylate the waste enantiomer to provide a chiral secondary amine (Scheme 46). If the reaction conditions can be adjusted to maintain the enantiopurity, then this would present a viable method to obtain single enantiomer secondary amines. This is difficult to achieve *via* enzymatic resolution as few lipases exist that will accept these substrates. Coupling these two procedures would create two different single enantiomer chiral amine products and so would be more productive and less wasteful than a resolution alone.
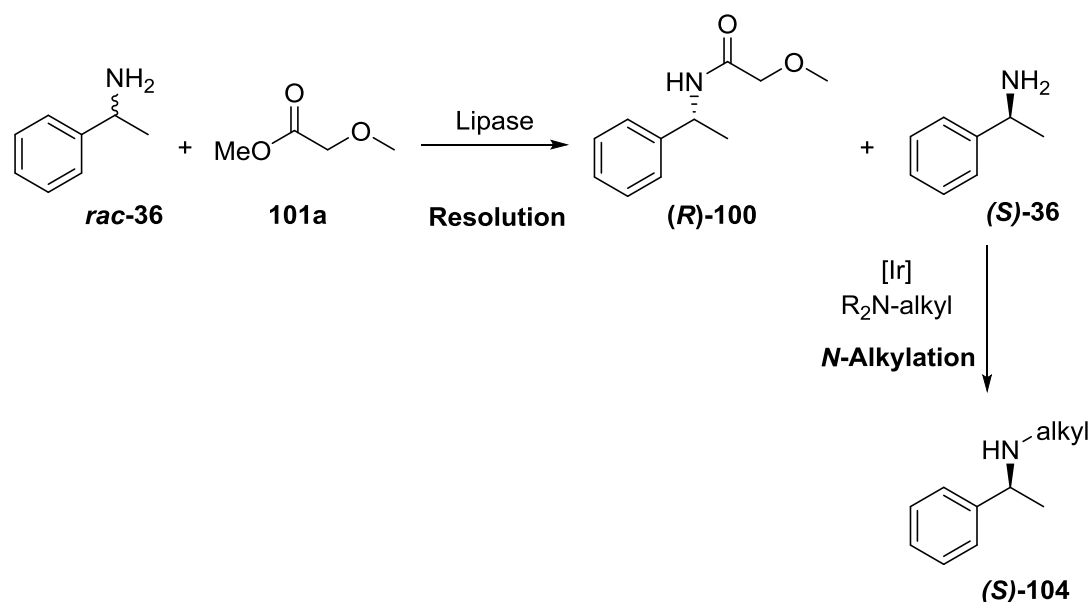
Scheme 46. Potential enzymatic resolution – *N*-alkylation coupled process.

The combination of metal catalysts with enzymes faces problems in the incompatibility of the optimal working conditions of the two individual catalysts such as: solvent preferences, differing solubilities, reaction rates and optimum temperatures. As a result, the combination of the catalysts may lead to mutual inactivation. Combined processes are often carried out with both the metal catalyst and the enzyme in one pot, meaning that a compromise on reaction conditions is often required to avoid deactivation. This can result

in long reaction times and poor efficiency. The ability to physically isolate the two catalysts and operate the two steps under different reaction conditions would potentially avoid this compromise and allow the catalysts to operate at their optimum. Continuous flow chemistry presents an attractive strategy for isolation of catalytic steps whilst passing the reaction solution between them.

1.5 Continuous Flow Chemistry

In a continuous flow system the reactants are continuously pumped into and the products are continuously pumped out of the reactor.[73] Unlike batch reactors, in which the composition of the reaction mixture varies with time, the composition in flow reactors varies with distance along the reactor tube. When operating at steady state, the concentration of reactants and products at a fixed position within the tube does not vary, and so the conversion achieved at the reactor outlet is constant during the entire steady state operation. Due to the small reactor volumes and narrow reactor diameters, only small amounts of reagents are present in continuous reactors at any one time and heat is dissipated readily. This means that continuous reactors are a safer method for using hazardous materials or highly exothermic reactions. Flow reactors are able to operate at increased temperatures and pressures compared to batch reactors and this intensification of reaction conditions can be utilised to reduce reaction times and increase productivity.[74] Flow reactors also lend themselves to coupling to sequential procedures, including multi-step synthesis,[75] downstream processing[76, 77] and online analysis methods.[78, 79] Using a flow system for the isolation of catalysts, with the reagents flowing directly between the two vessels, means that no extraction or separation has to be performed between the steps. This would not be the case for the analogous procedure carried out in batch with the

catalysts isolated in two different vessels, as some form of filtration or extraction would have to be carried out.

1.5.1 Immobilised Catalysts in Continuous Reactors

Immobilisation of enzymes provides many advantages for industrial synthesis, including increased stability and the potential to re-use, and are ideally suited for use in flow reactors. The main continuous reactor types for using immobilised catalysts are packed bed reactors (PBR) and fluidised bed reactors (FBR) (Figure 3).[80] In PBR, the immobilised catalyst is packed within a reactor chamber and the reagents are pumped through. In FBR, the immobilised catalyst is suspended within a fluid in the reactor chamber.
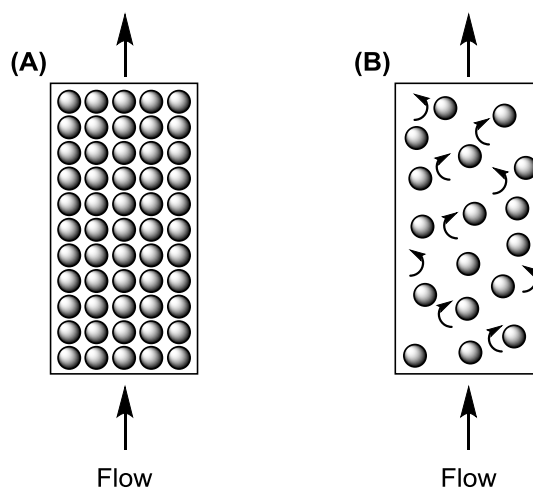
Figure 3. Schematic of packed bed reactor (A) and fluidised bed reactor (B). (Grey circle = catalyst particle)

There are both advantages and disadvantages associated with using either PBRs or FBRs, which are described by Levenspiel.[81] PBRs approximate plug flow behaviour, meaning that the reaction solution moves through the reactor bed as a uniform plug of material,

giving a narrower residence time distribution (RTD) and so better control and consistency. In contrast, FBRs have a more complicated flow pattern that is not well understood and can lead to inconsistencies in conversion. In addition, the fluid nature of FBRs means that reagent molecules have a lower chance of contact with a catalyst particle than in PBRs and so a higher catalyst loading would be required to achieve the same conversion. When using large PBRs, the temperature can be difficult to control due to the requirement of conducting the heat to the centre of the bed. This can lead to non-uniformity across the bed and the generation of hot spots. The FBR has mixing of the solid particles within the fluid bed and so the heat is more easily distributed. In terms of particle size, very small particles cannot be used in PBRs due to high pressure drop. This is a drop in pressure across the reactor bed, which is induced by the friction involved with the fluid passing over the catalyst particles. This is not a concern when using FBRs.

A direct comparison of the two reactor types was presented in recent work by Matte *et al*. which found that PBRs produced the highest conversions compared to a batch reactor and a FBR for the production of butyl butyrate using immobilised *Thermomyces lanuginosus* lipase (TLL).[80] The most common choice of reactor for immobilised catalysts is the PBR. Overall, PBRs are much easier to set-up and operate and so this research will focus on the use of PBRs when immobilised catalysts are studied under continuous conditions. In comparison to batch reactors, PBRs allow for much higher effective catalyst loadings to be achieved, which leads to significant reductions in reaction times and concurrent increases in productivity. The physical isolation of the catalyst within the reactor bed makes for easy separation and re-use of the catalyst, making the process more cost effective and industrially viable. In addition, in PBRs the catalyst is not exposed to the high shearing conditions of stirred batch reactors and so catalyst breakdown is reduced and lifetime is increased. Selected examples of the use of PBRs for amine production include: the chemically catalysed *N*-alkylation of morpholine with benzyl alcohol *via* hydrogen

borrowing using an immobilised Ru catalyst,[82] the *N*-alkylation of a range of amines with alcohols using a heterogeneous Au/TiO$_2$ catalyst,[83] and the use of immobilised whole cell transaminase enzymes for the biologically catalysed synthesis of chiral amines.[84]

The availability of immobilised lipase enzymes has led to an increasing number of examples of lipase catalysed reactions being carried out in PBR, including esterifications, kinetic resolutions, hydrolysis and transesterifications.[85] For kinetic resolution, the main substrates studied have been 1-phenylethanol[86-88] and ibuprofen.[89, 90] In one example, the Poppe group reported the continuous resolution of 1-phenylethanol **8** and other secondary alcohols in a PBR,[87] using the commercial X-cube reactor from ThalesNano.[91] The product was obtained in 48% yield, 99% *ee* with a residence time (tRes) of 8.2 min at 25 °C and 0.082 M (Scheme 47).
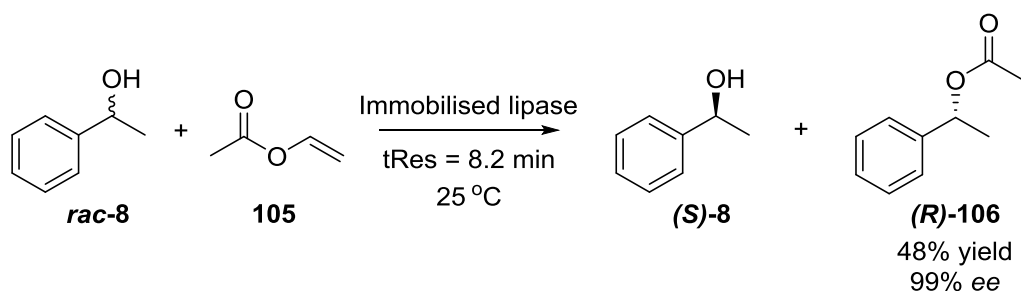
Scheme 47. Continuous kinetic resolution of 1-phenylethanol **8** from Poppe and co-workers.[87]

Sánchez *et al.* employed a continuous PBR for the kinetic resolution of ibuprofen **107** using immobilised *Rhizomucor miehei* lipase (Scheme 48).[89] Optimisation of the reaction variables (temperature, concentration and molar ratio) was first carried out in batch using an experimental design approach to provide 50% conversion and 94% *ee* and then the

process was transferred to the continuous reactor. Conversion and enantioselectivity were maintained at 46% and 94% in the PBR for 100 h (~100 x tRes).
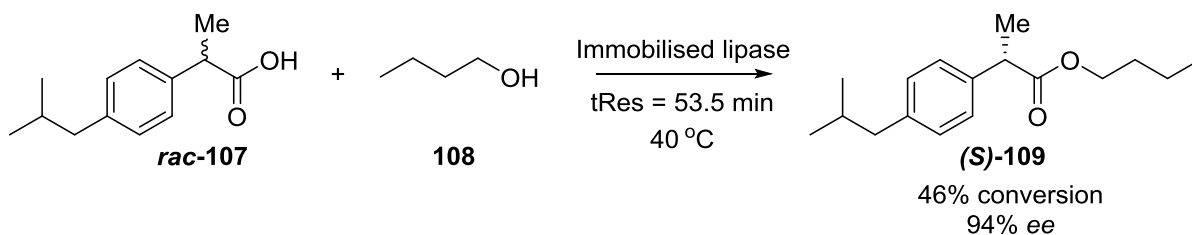
Scheme 48. Continuous kinetic resolution of ibuprofen **107** developed by Sánchez *et al.*[89]

The group of De Souza carried out the continuous resolution 1-phenylethylamine **36** using EtOAc as the acyl donor using a PBR (Scheme 49).[92] The reactor was packed with the commercially available immobilised N435 and the substrate and acyl donor pumped through at varying temperatures and concentrations. Optimum conditions were determined as 40 min, 70 °C and 0.08 M with 4 equivalents of acyl donor, which provided 48% conversion.
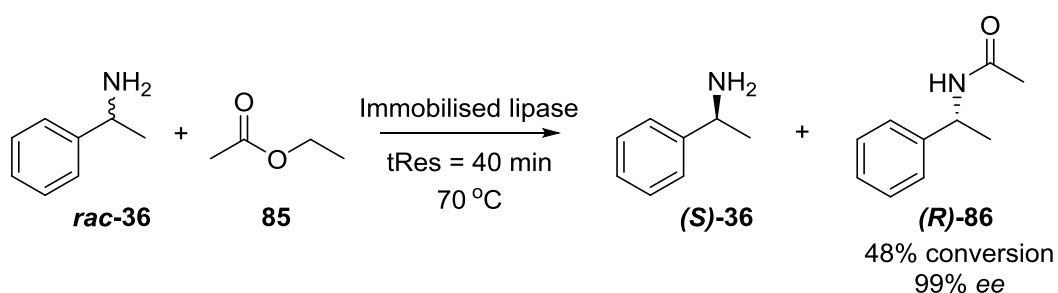
Scheme 49. Continuous kinetic resolution of 1-phenylethylamine **36** reported by De Souza *et al.*[92]

1.5.2 Dynamic Kinetic Resolution in Continuous Reactors

PBRs present an opportunity to couple immobilised enzymes and chemical catalysts in separate reactors that are operated at different temperatures. For a DKR process,

continuous flow allows for facile multiple re-circulations of the reaction mixture through the two separate catalysts, each time increasing the yield of desired product. Using a flow reactor for the DKR of primary amines may also reduce dimer formation due to the low local concentration of amine.

Roengpithya *et al*. combined the Ru Shvo catalyst **42** with CalB for the continuous DKR of 1-phenylethylamine **36** wherein the enzyme was retained within a membrane reactor and the reaction solution containing the racemisation catalyst was flowed through it.[93] A second reaction vessel was included in the system that was heated to 100 °C for the racemisation to occur within. After 72 h 99% *ee* was achieved but isolated yields were poor and the mass balance was only 55%.

De Miranda *et al*. combined Pd/BaSO$_4$ and CalB for a semi-continuous DKR of 1-phenylethylamine **36**, using ammonium formate as the hydrogen source for the Pd catalysed racemisation (Scheme 50).[94] The lipase was contained within a PBR and Pd/BaSO$_4$ was contained within a separate heated reservoir. The reaction solution was pumped out of this reservoir into the PBR flow system and then collected back into the reservoir. A filter was fitted to ensure that the Pd/BaSO$_4$ ammonium formate mixture remained in the reservoir. The solution was re-circulated for 10 h, after which 77% conversion and 95% product *ee* was observed.
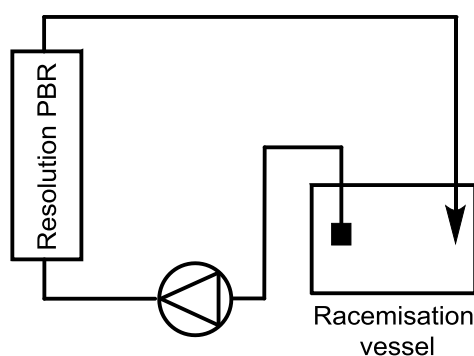
Scheme 50. Semi-continuous reactor set-up for the DKR of 1-phenylethylamine **36** reported by De Miranda *et al*.[94]

A recent notable example of DKR in a PBR was also reported by De Miranda *et al*. for the resolution of 1-phenylethanol **8**, employing immobilised CalB and VOSO$_4$ as the heterogeneous racemisation catalyst (Scheme 51).[95] The two catalysts were constrained within the same reactor bed in individual segments separated by cotton segments, so that the catalysts were isolated from one another to avoid deactivation. By using vinyl acetate **105** as the acyl donor, 92% conversion with 99% product *ee* was achieved with a tRes of 5.2 min at 70 °C, although selectivity for the desired product was only 68% under these conditions. This exemplified how the use of a flow system can overcome the incompatibility issues observed under batch conditions.[96]
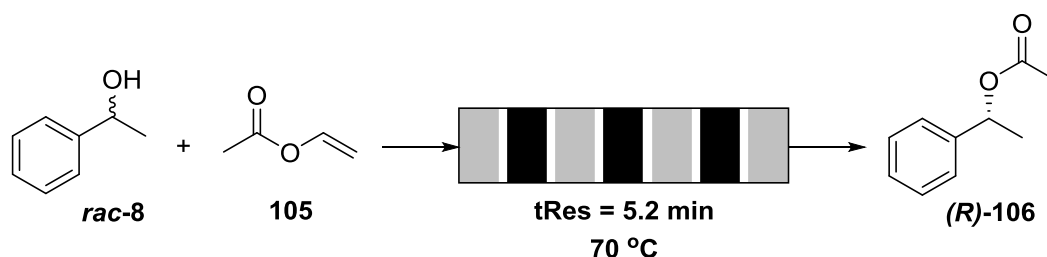
Scheme 51. Continuous DKR system developed by De Miranda *et al*., combining a lipase and VOSO$_4$ in a single PBR. (Grey = lipase, Black = VOSO$_4$, White = cotton).[95]

1.5.3 Flow Reactors for Efficient Manufacture

The intensification of reaction conditions achievable in flow reactors leads to increased yields and productivity and a reduction in the cost of the process. When applied to the manufacture of essential medicines,[97] this reduction in cost increases the affordability and availability of these drugs to the developing world, where the demand for these essential medicines is often at its highest.[98-100]

In one such example Watts and co-workers employed continuous reactors towards the synthesis of lamivudine **110** (Figure 4), an anti-retroviral drug for the treatment of HIV and

hepatitis B that is on the World Health Organisation's (WHO) essential medicines list.[97, 98] The continuous process presented reduced reaction times and temperatures to achieve increased yields compared to batch synthesis methods. The research was carried out in South Africa, with a view to developing cheaper large scale manufacture local to the areas where the drug is in high demand.
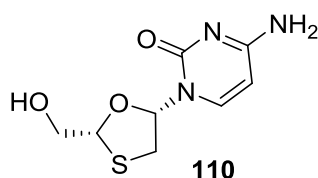
Figure 4. Structure of lamivudine **110**, an essential medicine for the treatment of HIV and hepatitis B.

1.6   Research Objectives

The importance of chiral amines in pharmaceutical molecules has led to an increasing demand for efficient, cost-effective methods to obtain enantiopure amines. Both chemical and biological catalysts have found applications in this field, however there are disadvantages to using each type of catalyst. The combination of catalysts allows for the favourable characteristics of each catalyst to be exploited whilst compensating for the un-favourable characteristics.

The overall aims of the research were to combine chemical and biological catalysts for the production of chiral amines, combining the strengths of the individual catalysts in asymmetric synthesis to develop efficient, industrially relevant processes. The use of continuous reactors was considered as a way to isolate the two catalysts to avoid deactivation and to be able to use more forcing reaction conditions to increase productivity.

The combination of an enzyme and metal catalyst in continuous reactors for the DKR of chiral amines was studied initially. The two steps were investigated independently, with a

view to optimising each reaction before combining as a DKR process. The development and optimisation of a continuous enzymatic resolution is presented in Chapter 2 and the metal catalysed racemisation of this substrate is discussed in Chapter 3. In Chapter 4, the continuous enzyme catalysed coupling of NH_3 with esters for the production of pharmaceutically relevant amides is presented. This Chapter introduces a design of experiments approach to optimisation of the process. Finally in Chapter 5, the metal catalysed cross coupling of amines for *N*-alkylation *via* the hydrogen borrowing approach is investigated as a method to utilise the un-derivitised enantiomer from the enzymatic resolution step.

2   Enzymatic Resolution of a Chiral Primary Amine

2.1   Introduction

Enzymatic resolution of chiral amines has been studied extensively in batch,[46] and increasingly in continuous flow.[85, 92] Immobilised catalysts present an advantage over homogeneous or slurry-type catalytic systems due to ease of separation and the potential for re-use. The use of a continuous packed bed reactor (PBR) allows for the reagents to be exposed to high amounts of catalyst, and easy separation of the catalyst from the solution, as the catalyst remains within the reactor whilst the reagents are introduced and the products removed from the system.[101]

In this chapter, the lipase catalysed resolution of the chiral primary amine 1-phenylethylamine **2.1** was investigated (Scheme 52). Reactions were initially screened under batch conditions and then transferred to a continuous system for further reaction optimisation. The continuous system was then applied to a range of chiral amines and alcohols.
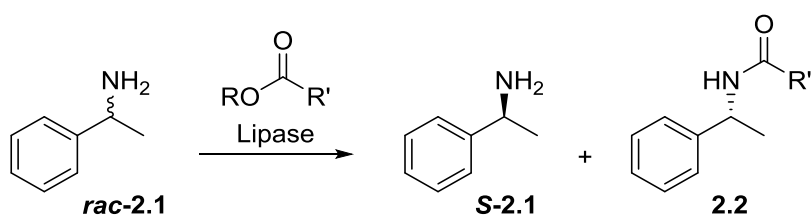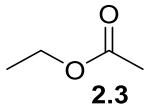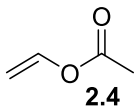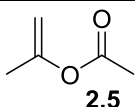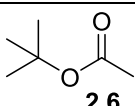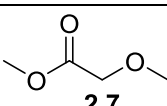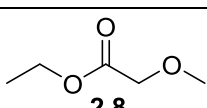
Scheme 52. Enzymatic resolution of racemic 1-phenylethylamine **2.1**.

2.2   Batch Resolution Screening

Initial screening to determine the effect of the type of the acyl donor and the number of equivalents was carried out, using esters **2.3 – 2.8**, under batch conditions (Table 1). All reactions were carried out using commercially available lipase B from *Candida antarctica*

immelled on a polyacrylic resin (Novozym 435, N435). Control reactions were also carried out for all conditions tested, in which N435 was omitted from the reaction mixture.

Table 1. Screening of acyl donors for resolution of *rac*-**2.1** under batch conditions.[a]

Entry	Acyl donor	Time / h	Amide ee[b] / %	Amine ee[c] / %	Conversion[d] / %	E[e]
1	**2.3**	24	99	42	30	150
2	**2.4**	3.5	43	10	19	3
3	**2.5**	30	86	53	38	23
4	**2.6**	24	X	0	0	X
5	**2.7**	24	99	99	50	> 200
6	**2.8**	24	99	97	49	> 200

[a]Reaction conditions: 0.07 mmol *rac*-**2.1**, 1 Eq acyl donor, 10 mg N435, 10 mL toluene, 60 °C; [b]Determined by chiral GC analysis; [c]Determined by chiral GC analysis after derivatisation using trifluoroacetic anhydride; [d]Determined using Conversion = [ee_{amine} / (ee_{amine} + ee_{amide})]*100; [e]Determined using E = {ln[1 − C)*(1 − ee_{amine})]}/{ln[(1 − C)*(1 + ee_{amine})]}, where C = conversion;

Enantiomeric excess (*ee*) for the substrate and product was calculated from gas chromatography (GC) peak areas according to:

$$ee\ (\%) = \left[\frac{(Area\ 1) - (Area\ 2)}{(Area\ 1) + (Area\ 2)} \right] \times 100 \qquad (2.1)$$

where Area 1 corresponds to the enantiomer with the major peak area and Area 2 corresponds to the enantiomer with the minor peak area. Conversion of the amine substrate to the amide product was calculated according to:

$$Conversion\ (\%) = \left[\frac{ee_{Amine}}{(ee_{Amine} + ee_{Amide})}\right] \times 100 \qquad (2.2)^{92}$$

This method for calculation of conversion was only used when no other products were observed and when the enzyme was completely selective for one enantiomer, generating only one product enantiomer. Conversion can be calculated using this method because it is in a direct relationship with substrate and product *ee*, but is only possible when there is baseline separation between enantiomer peaks in a chromatogram. In following chapters, conversion was calculated from calibration curves that were recorded relative to an internal standard. The calibration data was used retrospectively to confirm the conversions calculated in this chapter and when a significant discrepancy was determined the experiment was repeated. For any reactions that were not selective or had side reactions, conversion was determined by comparison of peak integrals in ^{1}H NMR.

Assuming a completely selective reaction, the amine *ee* will increase as the conversion of amine to amide increases (Figure 5). At the start of the reaction there is a racemic mixture of amine and so the amine *ee* starts at zero. As the reaction progresses, one enantiomer of the amine is converted preferentially to the amide and so the amine *ee* increases. At 50% conversion, one enantiomer has been completely converted to the amide and so the amine is enantiopure and the *ee* is 100%. As only one enantiomer is being converted to the amide then the *ee* of the amide produced is 100%.

If the reaction is not completely selective, and some of the other amine enantiomer is also converted to the amide, the amide *ee* will be less than 100%. If both enantiomers are completely converted to the amide then the amide *ee* will become zero, as a racemic

mixture of amide has been produced (above 50% conversion on Figure 5). The amine *ee* will not increase if both enantiomers are being converted at the same rate, as a racemic mixture is maintained. So for a resolution, the maximum desired conversion is 50% as all of one enantiomer will have been converted (Scheme 53).
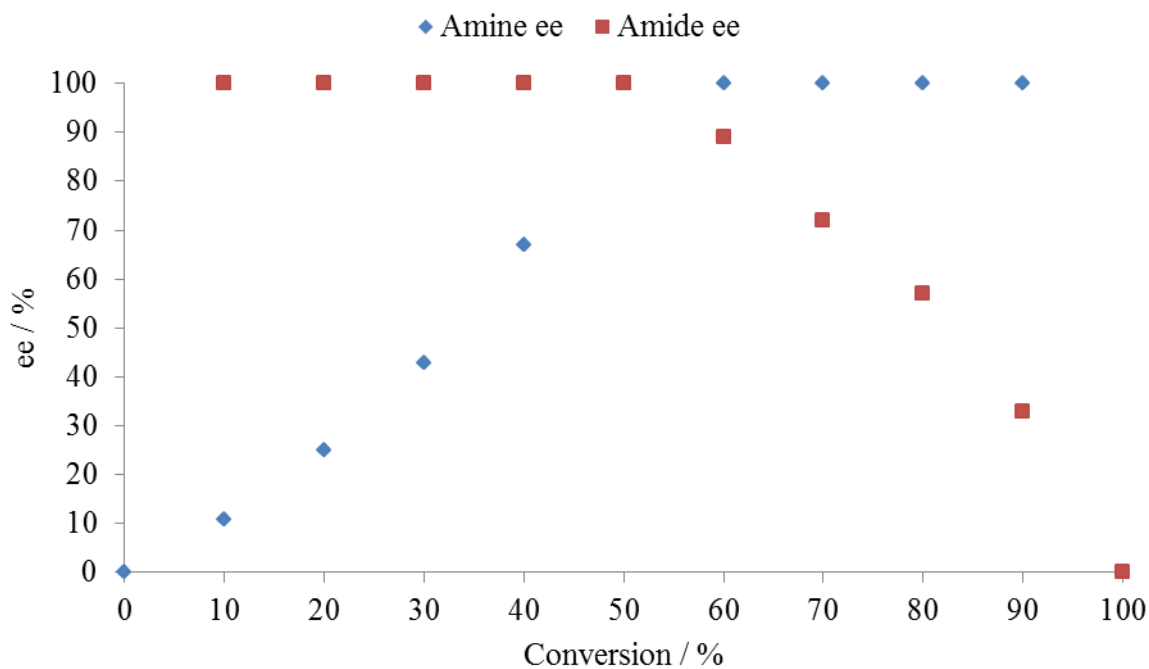
Figure 5. Change in amine *ee* and amide *ee* with increasing conversion for a completely selective reaction.
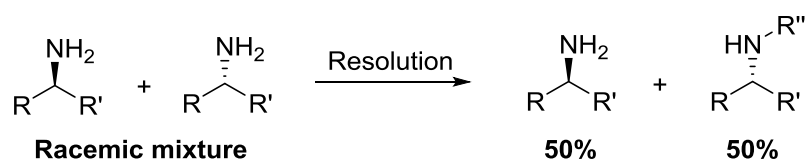
Scheme 53. Ideal resolution reaction, showing 50% conversion.

Selectivity values (E) are also shown in Table 1, which give a ratio of the relative rates for the two enenatiomers reacting with the catalyst. Larger numbers denote an enzyme that is highly selective for one enantiomer and so will give a highly enantiopure product.[102, 103]

Esters **2.4** and **2.5** showed significant uncatalysed background reaction which resulted in low *ee* for the product amide. In the case of ester **2.4**, the reaction was stopped after 3.5 h due to the production of by-products that prevented accurate analysis of conversion to the desired amide product. The reaction using ester **2.5** showed the formation of a by-product during monitoring of the reaction. Gas chromatography – mass spectrometry (GCMS) analysis of these samples indicated that this was imine **2.10**, formed by reaction of the amine with the acetone by-product (Scheme 54). This was not isolated as the imine was hydrolysed during the work-up.
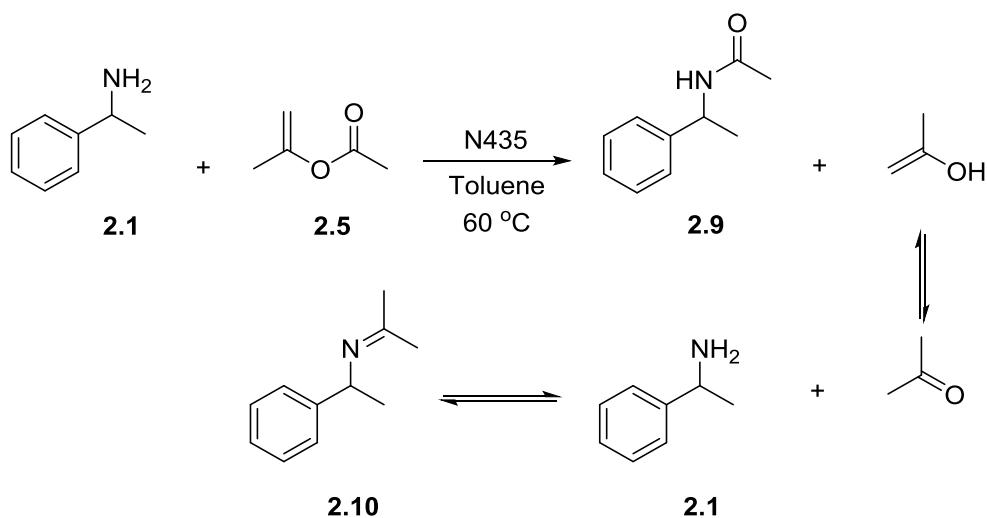
Scheme 54. Proposed mechanism for formation of imine by-product **2.10** in the resolution of **2.1** using acyl donor **2.5**.

Esters **2.3**, **2.7** and **2.8** all showed high selectivity for the amide product, with only one amide enantiomer being observed in all cases. The reactions using esters **2.7** and **2.8** were considerably faster than using ester **2.3**, as 50% conversion was observed after 24 h, compared to 30%. The initial rate was also faster for esters **2.7** and **2.8**, as well as the final

conversion being higher. Molecular modelling carried out by Cammenberg *et al.* indicated that the reaction rate was enhanced when using alkyl methoxyacetates as the acyl donor due to the presence of a hydrogen bonding interaction between the amine proton and the *β*–oxygen of the ester in the active site (Figure 6).[104] For these types of acyl donors, Bäckvall *et al.* reported that the amide *ee* increased and yield decreased with decreasing leaving group size for methyl-, ethyl- and isopropyl-methoxy acetate.[71] The leaving group for the larger esters would be more stabilised and so more labile, leading to a higher yield. This higher reactivity may cause uncatalysed background reaction, which would lead to the reduction in the amide *ee*.
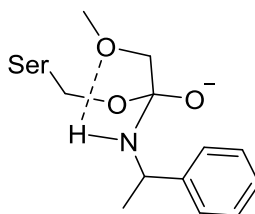
Figure 6. Active site hydrogen bonding interaction proposed by Cammenberg *et al.* (Ser = Serine).[104]

The resolution of **2.1** was tested using 1, 2 and 4 equivalents (Eq) of ester **2.7**, relative to the total racemic amine present. Increasing the number of Eq of **2.7** increased the initial rate of the reaction, with higher conversions observed after 2 h using 2 and 4 Eq (Table 2, Entries 3 and 5). However, background reaction was then observed using higher Eq, leading to a reduction in amide *ee* after 24 h. (Table 2, Entries 4 and 6). Due to this, 1 Eq of ester **2.7** was used for all further reactions, to maintain amide *ee* and reduce the waste associated with the process.

Table 2. Screening of ester **2.7** Eq under batch conditions.[a]

Entry	Eq	Time / h	Amide ee^b / %	Amine ee^c / %	Conversion[d] / %
1	1	2	99	27	21
2	1	24	99	99	50
3	2	2	99	46	32
4	2	24	96	99	54
5	4	2	99	47	32
6	4	24	91	99	58

[a]Reaction conditions: 0.07 mmol **rac-2.1**, 10 mg N435, 10 mL toluene, 60 °C; [b]Determined by chiral GC analysis; [c]Determined by chiral GC analysis after derivatisation using trifluoroacetic anhydride; [d]Determined using Conversion = [ee_{amine} / (ee_{amine} + ee_{amide})]*100; Eq = equivalents of **2.7**.

2.3   Continuous Resolution Screening

The reaction was then transferred to a continuous PBR system for further screening and optimisation. It was envisaged that the process could be improved in a PBR as the reactor could be filled with a much higher amount of catalyst than would be feasible in batch, resulting in a greatly reduced reaction time. Employing a continuous reactor creates a more productive system, as the reagents are constantly being pumped into the reactor and the products are constantly being pumped out of the reactor, for as long as the catalyst remains active. The lifetime of the immobilised catalyst is often longer than in batch because it is not exposed to mechanical mixing, which breaks down the support.

2.3.1   Reactor Design

The continuous reactor set up consisted of a 316 stainless steel tubular reactor (1/4" OD, 1/8" ID, 3.0 mL), fitted with Supelco stainless steel frits (1/4" diameter). The reactor was contained within an aluminium block, heated by aluminium cartridges powered by a custom manufactured Eurotherm temperature controller (Figure 7). Temperature monitoring was achieved using Green K-type thermocouples. Reagent feeds were

introduced into the system using Jasco PU-980 or PU-2085 dual piston pumps. PTFE

tubing (1/16" OD, 1/32" ID) was used to connect the piston pump to the reactor and at the

outlet of the reactor. All tee-pieces and unions used were Swagelock 316 stainless steel.
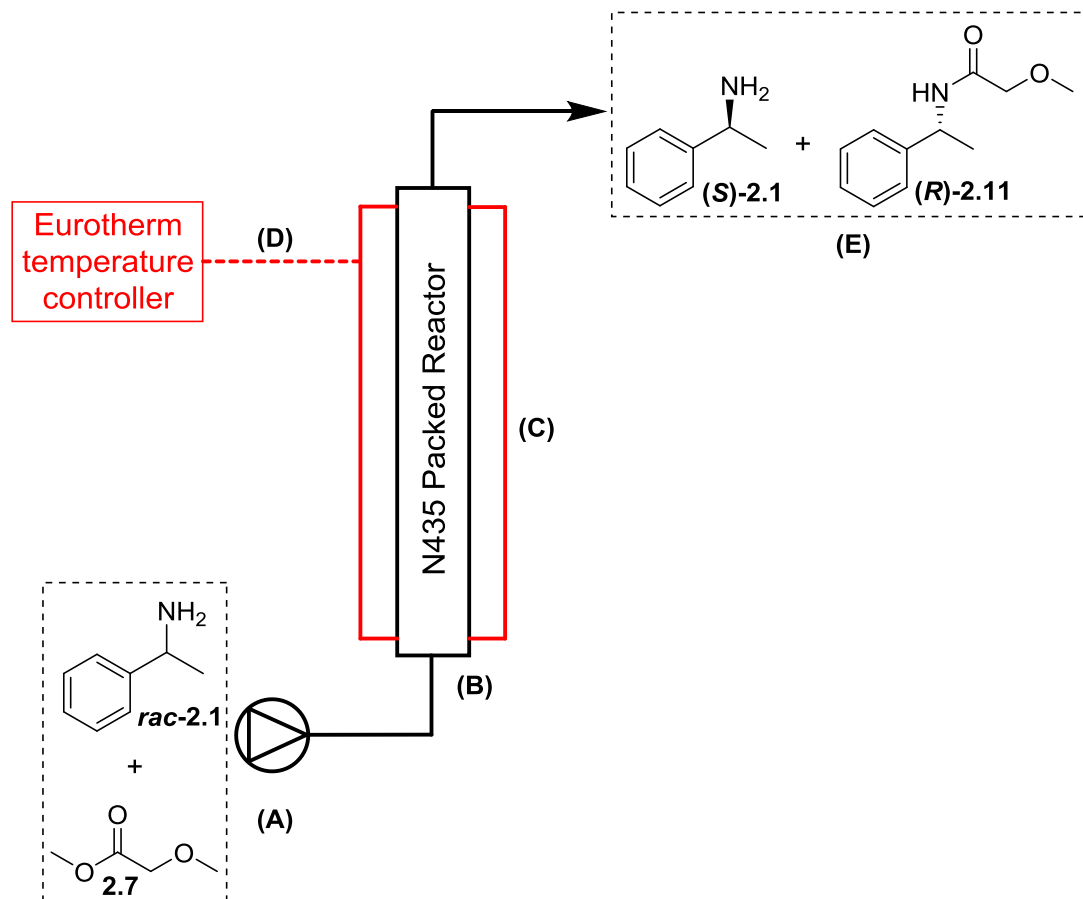
Figure 7. Continuous resolution PBR design. (A) Piston pump; (B) Tubular reactor packed with N435; (C) Aluminium heating block; (D) Eurotherm temperature controller; (E) Product outlet and collection.

General procedure followed for all further flow reactions: 1 g of N435 was measured out

and transferred into the stainless steel tube. The tube was then installed within the heating

block and toluene pumped through the reactor, to purge any air from the system, and then

the reactor was set to the desired temperature. The reagent stock solutions were made-up

individually in volumetric flasks, for both amine **2.1** and ester **2.7**, using toluene to make-

up the solution to the graduated mark. Equal volumes of the individual amine and ester

stock solutions were then combined for the reaction mixture. This provided a reaction

mixture at half the concentration of the individual stock solutions. Once the reactor reached the desired temperature, the reaction mixture was pumped through the reactor at the specified flow rate. The flow rate required was determined using the 3 mL volume of the reactor and the desired residence time (tRes), according to:

$$Flow\ rate\ (mL\ min^{-1}) = \frac{Reactor\ volume\ (mL)}{Residence\ time\ (min)} \qquad (2.3)$$

The reactor volume (RV) was assigned as the volume of the stainless steel tube packed with N435, as control reactions showed that the reaction was only occurring in the presence of N435 and so no reaction was occurring in the PTFE tubing that connected the reactor to the pump and connected the outlet of the reactor to the collection vessel. The reaction mixture was collected at the outlet of the reactor in individual RV samples and analysed by chiral GC.

2.3.2   Residence Time Screen

The tRes within the reactor was varied between 30 – 1.5 min, by adjusting the flow rates accordingly (Table 3). Increasing conversion and amine *ee* was observed with increasing tRes, up to the maximum of 50% conversion. Selectivity for **(R)-2.11** was maintained at all tRes, with only one enantiomer being observed. Steady state was observed after 4 RV and maintained throughout operation. Steady state is achieved when the product composition at the outlet of the reactor is constant. The optimum tRes was determined to be 6 min, producing 99% amide *ee*, 96% amine *ee* and 49% conversion to amide (Figure 8). This tRes was used for all further reactions as it produced the highest conversion in the least amount of time.

Table 3. Screening of tRes in the continuous resolution of *rac*-**2.1**.[a]

Entry	tRes / min	Flow rate / mL min^{-1}	Amide ee[b] / %	Amine ee[c] / %	Conversion[d] / %
1	30	0.1	99	99	50
2	6	0.5	99	96	49
3	3	1	99	71	42
4	1.5	2	99	47	32

[a]Reaction conditions: 0.07 M *rac*-**2.1**, 1 Eq **2.7**, 60 °C, 3 mL reactor volume; [b]Determined by chiral GC analysis; [c]Determined by chiral GC analysis after derivatisation with trifluoroacetic anhydride; [d]Determined using Conversion = [ee_{amine} / (ee_{amine} + ee_{amide})]*100;
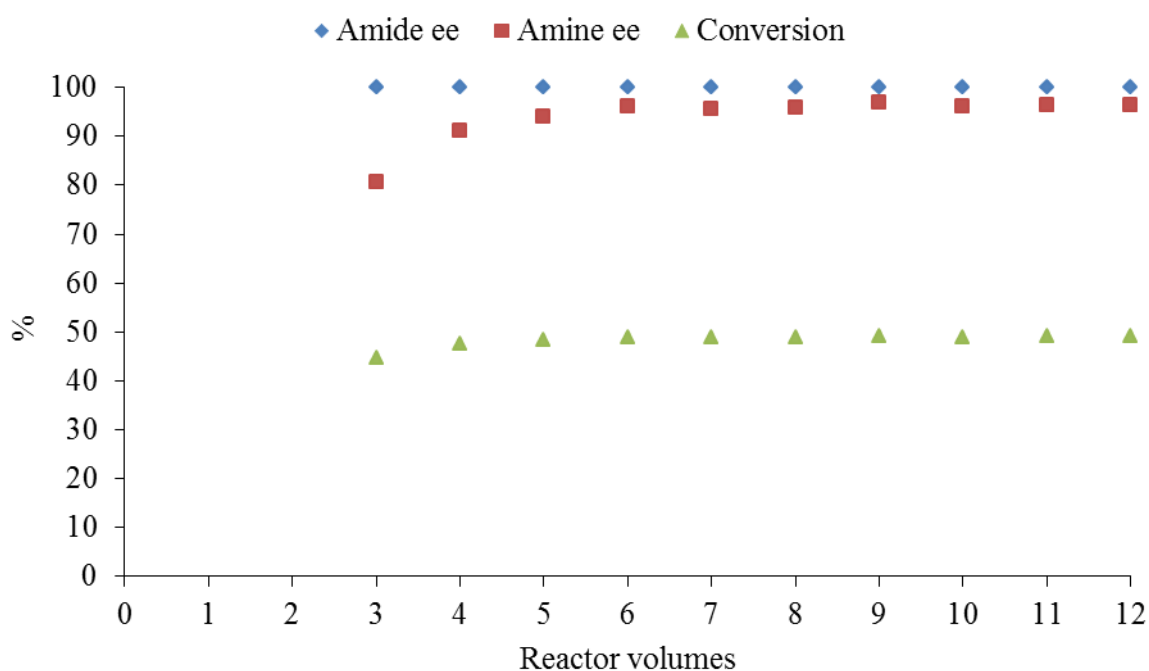
Figure 8. Continuous resolution of *rac*-**2.1** with tRes = 6 min at 60 °C.

2.3.3 Temperature Screen

The temperature of the reactor was then varied between 30 − 100 °C for the continuous resolution with a tRes of 6 min (Figure 9). At temperatures of 60 °C and above, maximum conversion of 50% was consistently observed. At temperatures up to 50 °C, an initiation period was observed wherein steady state was not achieved until 8 RV.
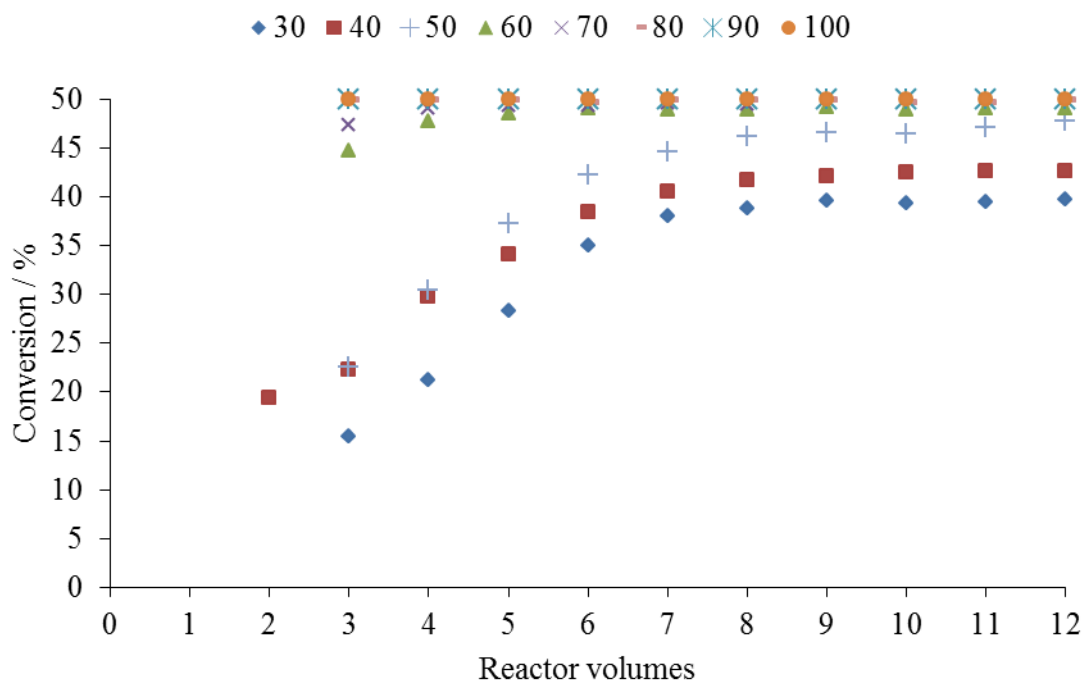
Figure 9. Temperature profile for the continuous resolution of *rac*-**2.1**.

Further investigation was carried out to determine the cause of this initiation period and whether it could be prevented. Firstly, the reaction at 30 °C was repeated with a tRes of 30 min to see if the maximum conversion could be achieved at the lowest temperature. The conversion to amide (**R**)-**2.11** did increase from 40% to 49% after the 30 min tRes. The ability to achieve maximum conversion showed that the enzyme was not deactivated at lower temperatures but unsurprisingly required a longer reaction time. However, this did not overcome the initiation period as steady state was still not reached until after 8 RV.

It was next postulated that the initiation period may have resulted from a reduced amount of coordination of the acyl donor to the active site at lower temperatures. The initial step of the catalytic mechanism involves the coordination of the acyl donor to the serine (Ser) residue in the active site to form an acyl-enzyme intermediate (Scheme 55).[105] This intermediate undergoes nucleophilic attack by the amine to give the amide product and re-generate the active site residues.
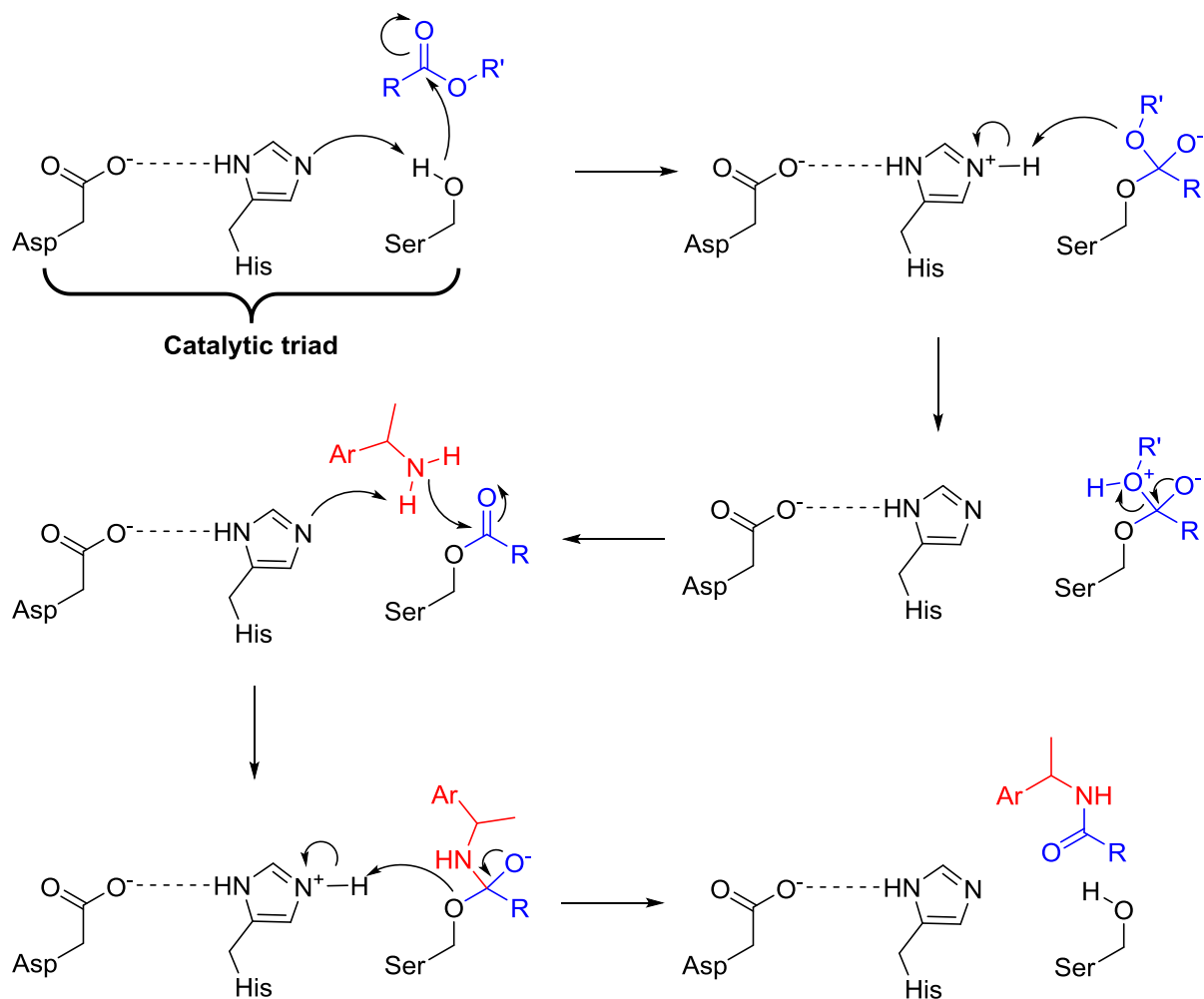
Scheme 55. Lipase active site mechanism (Asp = Aspartic acid, His = Histidine, Ser = Serine).[105] Step 1: Coordination of the acyl donor to the Ser residue of the three key residues (catalytic triad) within the active site; Step 2: Proton transfer; Step 3: Formation of acyl-enzyme intermediate on Ser and loss of alcohol by-product; Step 4: Nucleophilic attack of amine at the ester carbonyl; Step 5: De-coordination of amide from Ser and proton transfer to recycle the active site residues.

To investigate whether the coordination of the acyl donor to the Ser in the active site is inhibited at lower temperatures, the reaction at 30 °C was repeated with an initial feed of only ester **2.7** up to 4 RV followed by the introduction of the amine/ester reaction mixture (Figure 10). If the initiation was caused by a reduction in the coordination of the acyl donor, then exposing the enzyme to only the acyl donor for a period before the reaction would have allowed for some of the acyl donor to coordinate to the enzyme prior to the introduction of the amine substrate. For this reaction, the tRes was again reduced to 6 min

for speed of analysis and because the absolute value for conversion was not important for this experiment. Again steady state was not reached until 7-8 RV, indicating that the initiation period at 30 °C was not caused by slower coordination of the acyl donor to the enzyme.
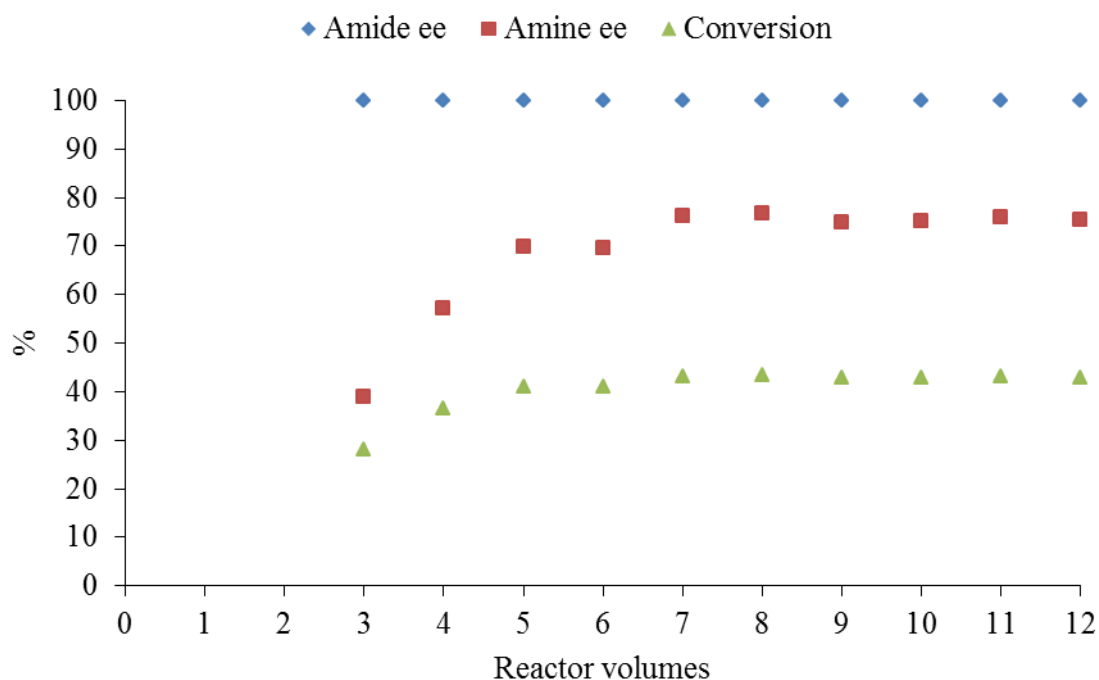
Figure 10. Continuous resolution of *rac*-**2.1** at 30 °C, with only ester **2.7** in the reagent feed for 4 RV prior to starting the reaction (tRes = 6 min).

Finally, it was investigated if the initiation period was due to physical properties of the resin at different temperatures and whether pre-heating the reactor would reduce the initiation period. To do this, the reactor was heated to 60 °C and flushed with solvent for 10 RV prior to pumping the reaction mixture at 30 °C (Figure 11). Under these conditions steady state was reached after 5 RV, which was much closer to the 3-4 RV required to reach steady state at higher temperatures. This finding suggests that the immobilised catalyst undergoes physical changes when exposed to higher temperatures, swelling of the

resin may occur, which increases the accessibility of the enzyme. Therefore, pre-heating of the reactor and a longer tRes would be recommended if lower temperatures were to be used in this system.
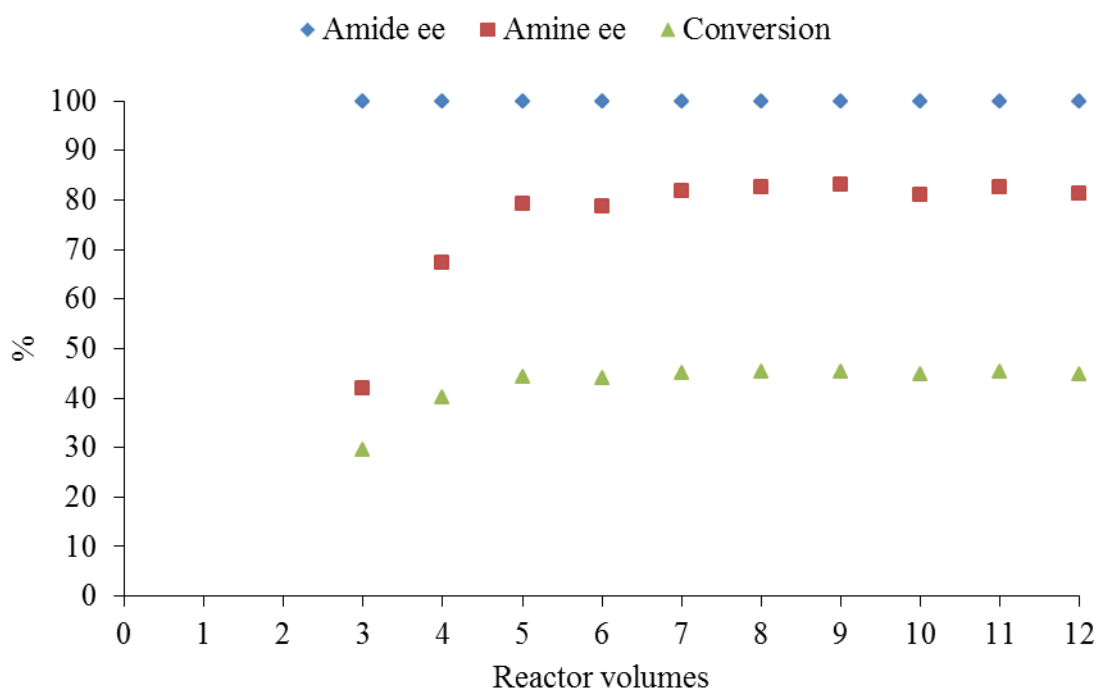
Figure 11. Continuous resolution of *rac*-**2.1** at 30 °C, with only solvent at 60 °C for 10 RV prior to starting the reaction (tRes = 6 min).

From the temperature studies, it was decided that 60 °C would be taken as the optimum operating temperature because the maximum conversion was achieved within the 6 min tRes, there would be a lower energy demand for the process compared to using the temperatures above 60 °C, for which the conversion achieved was the same, and there was no initiation period at 60 °C and so no pre-heating of the reactor would be required.

2.3.4 Concentration Screen

The concentration of reagents was then varied between 0.07 M and 0.70 M for the continuous resolution with a tRes of 6 min at 60 °C (Table 4). A significant reduction in the conversion was observed for concentrations of 0.28 M and above. At these higher concentrations the amine *ee* observed was lower (< 90%) because the (*R*)-amine was not completely converted. Whilst the amine *ee* was lower at higher concentrations, the amide *ee* observed remained at >99% for all concentrations as the selectivity for one amine enantiomer to be converted to the amide remained the same. This also showed that the increased reagent concentration did not cause any un-catalysed background reaction to occur.

Table 4. Screening of concentration in continuous resolution of *rac*-**2.1**.

Entry	Concentration / M	Amide *ee*[b] / %	Amine *ee*[c] / %	Conversion[d] / %
1	0.07	99	96	49
2	0.14	99	93	48
3	0.28	99	86	46
4	0.42	99	71	41
5	0.56	99	70	41
6	0.70	99	73	42

[a]Reaction conditions: 1 Eq **2.7**, 60 °C, 3 mL reactor volume, 0.5 mL min^{-1}, 6 min tRes; [b]Determined by chiral GC analysis; [c]Determined by chiral GC analysis after derivatisation with trifluoroacetic anhydride; [d]Determined using Conversion = [ee_{amine} / (ee_{amine} + ee_{amide})]*100;

The reduction in conversion occurs at higher concentrations as the amount of enzyme remains constant throughout the reactions and so the number of active sites available for the reaction to take place remains constant. An increased number of reagent molecules within the system causes saturation of the enzyme active sites, as the number of active sites has not increased with the reagent. According to Michaelis-Menten kinetics,[106, 107] the rate equation for enzymatic reactions takes the form:

$$\nu = \frac{V_{max}\,[S]}{K_M + [S]} \qquad (2.4)$$

where ν is the rate of reaction, V_{max} is the maximum rate, $[S]$ is substrate concentration and K_M is the Michaelis constant, which denotes the $[S]$ at which the rate is half of V_{max}. The rate increases with increasing $[S]$ up to V_{max}, where all enzyme is bound in the enzyme-substrate complex. Once V_{max} has been reached, the rate will no longer be affected by a further increase in $[S]$ as the enzyme is saturated.

Therefore, a longer tRes would be required to enhance the conversion at higher reagent concentrations, to allow the reaction mixture to be exposed to the enzyme for a sufficient amount of time for all the reagent molecules to react. A larger catalyst loading could also be used, meaning that the ratio of active sites to substrate molecules would be larger and so V_{max} would not be reached for the concentrations studied.

2.3.5 Catalyst Recyclability

The longevity of the continuous process developed was then investigated through catalyst studies. Deactivation of the catalyst was monitored over 30 h of operation at 60 °C (Figure 12). No drop in activity was observed within this time scale, with the conversion to amide (*R*)-2.11 remaining at 49% throughout the study. The stability of the catalyst after treatment for storage and re-use was also investigated. A batch of catalyst was used in the continuous resolution of *rac*-2.1 and then exposed to ether, as a highly volatile solvent to aid in drying out the catalyst. The ether solution was filtered and the dry catalyst stored in the fridge. On re-use of the catalyst, no drop in activity was observed as conversion was maintained at 49%.
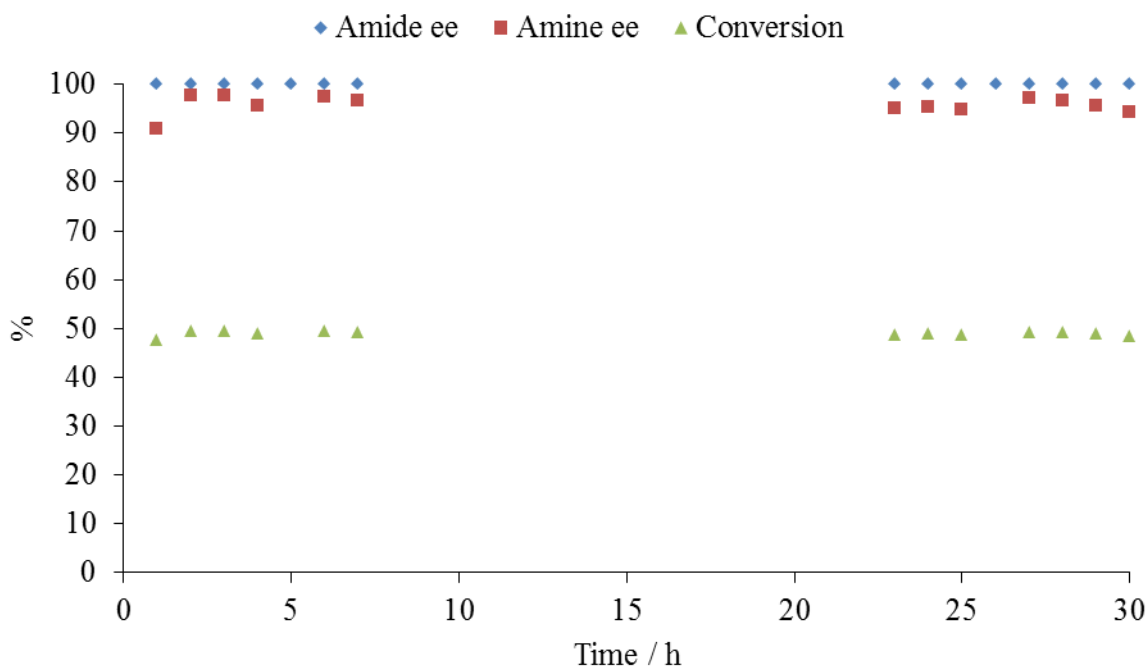
Figure 12. Catalyst deactivation for continuous resolution of *rac*-**2.1** using tRes = 6 min, 60 °C and 0.07 M.

2.3.6   Reaction Metrics

Optimum reaction conditions were determined to be 6 min tRes, 60 °C and 0.07 M, because this gave the highest conversion in the shortest amount of time. These conditions were used for all further continuous resolution studies. De Souza *et al*. developed an analogous continuous system for the resolution of **2.1**.[92] This literature process utilised 4 Eq of EtOAc as the acyl donor, had a tRes of 40 min and was operated at 70 °C and 0.08 M, to achieve conversions of 48%. The process developed herein, provided a reduction in waste due to the use of 1 Eq of acyl donor **2.7** and a reduction in tRes. Space time yield (STY) for the process was calculated according to:

$$STY\ (kg\ m^{-3}\ h^{-1}) = \frac{Moles\ of\ Product\ (mol)\ x\ MW\ (kg\ mol^{-1})}{tRes\ (h)\ x\ Reactor\ Volume\ (m^3)} \qquad (2.5)$$

where MW is the molecular weight of the product.[108] The optimum reaction conditions determined in terms of conversion to product (0.07 M) provided a STY of 66.3 kg m^{-3} h^{-1}. However, an even greater STY of 568 kg m^{-3} h^{-1} was obtained for the process carried out at higher reaction concentration (0.7 M), indicating that this would be the optimised reaction conditions in terms of productivity. The process developed exhibited a greater productivity than the existing literature process, for which a STY of 0.25 kg m^{-3} h^{-1} was reported.[92] STY could be further optimised by increasing the reactor size to allow for a larger amount of catalyst to be used, which would be expected to shorten the reaction time and so increase the STY. To compare the waste associated with the process at 0.07 and 0.7 M, E factors[109] were determined according to:
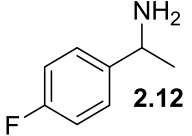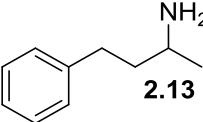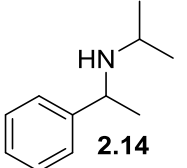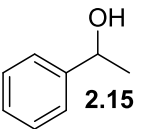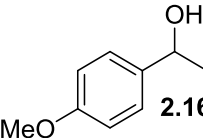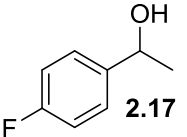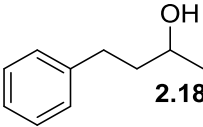
$$E\ factor = \frac{Mass\ of\ Amine + Mass\ of\ Ester - Mass\ of\ Amide}{Mass\ of\ Amide} \quad (2.6)$$

The E factors were calculated as 1.34 and 1.74 for the reactions at 0.07 M and 0.7 M, respectively. Therefore the process at 0.07 M had less associated waste. It should be noted that solvent and catalyst were not included in the calculation of E factors as it was assumed that these could be recycled.

2.3.7   Substrate Scope

The optimised conditions for conversion for the continuous resolution of *rac*-**2.1** were then applied to an expanded substrate set, including chiral amines and alcohols (Table 5). All reactions were tested using the same conditions to give a direct comparison.

Table 5. Expanded substrate scope for continuous resolution.[a]

Entry	Substrate	Product ee[b] / %	Substrate ee[c] / %	Conversion[d] / %	E[g]
1	NH$_2$ (4-F-phenyl) **2.12**	100	100	50	> 200
2	NH$_2$ **2.13**	100	95	47[e]	110
3	HN(iPr) **2.14**	-	0	0	X
4	OH **2.15**	100	17	15	4
5	OH (4-MeO-phenyl) **2.16**	38	7	15[f]	2
6	OH (4-F-phenyl) **2.17**	80	16	22[e]	4
7	OH **2.18**	94	25	20	

[a]Reaction conditions: 0.07 M substrate, 1 eq **2.7**, 60 °C, 3 mL reactor volume, 0.5 mL min^{-1}, tRes = 6 min; [b]Determined by chiral GC analysis; [c]Determined by chiral GC analysis after derivatisation with trifluoroacetic anhydride; [d]Determined using Conversion = [$ee_{substrate}$ / ($ee_{substrate} + ee_{product}$)]*100; [e]Determined by online achiral HPLC analysis; [f]Determined by ^{1}H NMR; [g]Determined using E = {ln[1 − C)*(1 − $ee_{substrate}$)]}/{ln[(1 − C)*(1 + $ee_{substrate}$)]};

For amine substrates, the 4-fluoro electron withdrawing substituent (**2.12**) did not affect the reaction rate and full conversion was observed within the 6 min tRes (Entry 1). Extending the carbon chain between the amine functionality and the aryl group (**2.13**) only marginally reduced the conversion (Entry 2). The enzyme used was not able to resolve secondary

amines (Entry 3). 1-Phenylethanol **2.15** showed reduced activity within the continuous resolution system (Entry 4), producing 15% conversion compared to 49% conversion for **2.1**. This reflected a lower rate of reaction for alcohols, compared to amines. It would be expected that the lower nucleophilicity of alcohols would cause the attack at the Ser-bound carbonyl to be slower, and so a longer tRes would be required for alcohols. In general, the enzyme also showed a reduced stereospecifity when using alcohol substrates, indicating that the enzyme was not able to distinguish between the two enantiomers as efficiently as it did for amines. There are literature examples in which high selectivity has been achieved for the resolution of **2.15** also using N435,[63, 64] this indicates that different reaction conditions are required to achieve the optimum for this substrate, including different solvent, acyl donor and temperature.

2.4   Conclusions

A robust process was developed for the continuous resolution of a primary chiral amine using an immobilised lipase enzyme within a PBR. The type of acyl donor and the number of Eq was investigated under batch conditions and then the process was transferred to a continuous PBR. The reaction parameters of tRes, temperature and concentration were varied within the continuous system using a one variable at a time (OVAT) approach to obtain an optimised set of reaction conditions in terms of the highest conversion obtained in the shortest tRes (6 min, 60 °C, 0.07 M). During the temperature studies it was found that the system suffered from a slow initiation period when operated at lower temperatures due to physical changes of the resin. This provided a lower limit for the system operating temperature, above which no special treatment of the reactor was required. By transferring the reaction from batch into the packed bed reactor the reaction time was significantly reduced and the productivity increased due to the ability to greatly increase the catalyst

loading. The productivity could have been increased further by using a higher concentration of substrate but this would have required a longer tRes.

The stability of the catalyst within the continuous system was investigated, with no drop in activity being observed over 30 h of reaction, showing that the process could be operated over the long timescales required for industrial applications. The ability to use the same batch of catalyst over long periods or over multiple different reaction runs reduces the catalyst contribution to the total cost of the process and so is desirable for commercial processes. The process developed also presented improvements on the existing literature procedures, with reduced reaction times and increased productivity.

The optimised continuous resolution conditions obtained were then applied to a range of chiral amines and alcohols. It was found that alcohols displayed a lower rate of reaction, and a lower selectivity was achieved, using these conditions. Variation in the amine substrates had little effect on the outcome of the reaction, however, the enzyme was not active for secondary amines.

This continuous resolution system presents an opportunity for the efficient production of single enantiomer chiral amines on a rapid timescale. The coupling of this procedure to a racemisation step for the recycling of the undesired enantiomer to develop a more productive system will be discussed in the following chapter.

3 Metal Catalysed Racemisation of a Chiral Primary Amine

3.1 Introduction

As discussed in Chapter 2 (page 74), the maximum theoretical yield achievable for a kinetic resolution is 50% when only one enantiomer is desired. This maximum yield can be improved by recycling of the undesired enantiomer through racemisation (Scheme 56 A). Racemisation creates a mixture of enantiomers, and so more of the desired enantiomer can be re-introduced into the resolution, setting up a re-circulation process termed dynamic kinetic resolution (DKR). As the desired enantiomer is constantly being formed in the racemisation, the overall yield increases above 50%.
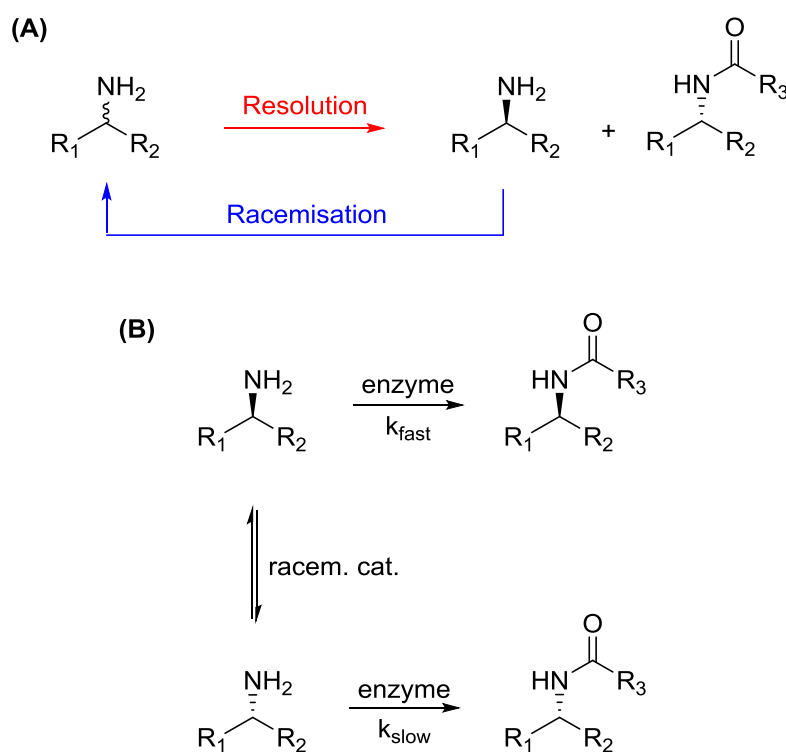
Scheme 56. Dynamic kinetic resolution. (A): Re-circulation process showing recycling of undesired enantiomer by racemisation; (B): Relatives rates of the two reaction types.

The DKR process relies on the rate of racemisation being fast, and that the enzyme reacts with one enantiomer much more quickly than the other (Scheme 56B). Racemisation keeps

the ratio of amine enantiomers constant, so that the enzyme selectivity remains the same. In a kinetic resolution the enzyme selectivity can decrease as the ratio of amine enantiomers changes over the course of the reaction; the higher proportion of undesired enantiomer in the reaction, the more likely it becomes that the enzyme will select for the undesired enantiomer. Figure 13 exemplifies this for a perfectly selective enzyme, wherein the product *ee* is 100% up to 50% conversion as only one enantiomer is being converted, but the *ee* drops at higher conversions as the other enantiomer begins to be converted to the product. For a less selective enzyme, the product *ee* would begin to drop before the 50% conversion is reached, as the enzyme cannot distinguish between the substrate enantiomers as efficiently. The selectivity value (described in Chapter 2, page 75) gives a measure of the relative rates for the reaction of the two enantiomers of a particular substrate with the enzyme. A lower selectivity value would mean that the product *ee* begins to fall at lower conversion values. This would be exacerbated by the change in the ratio of the enantiomers during the resolution.
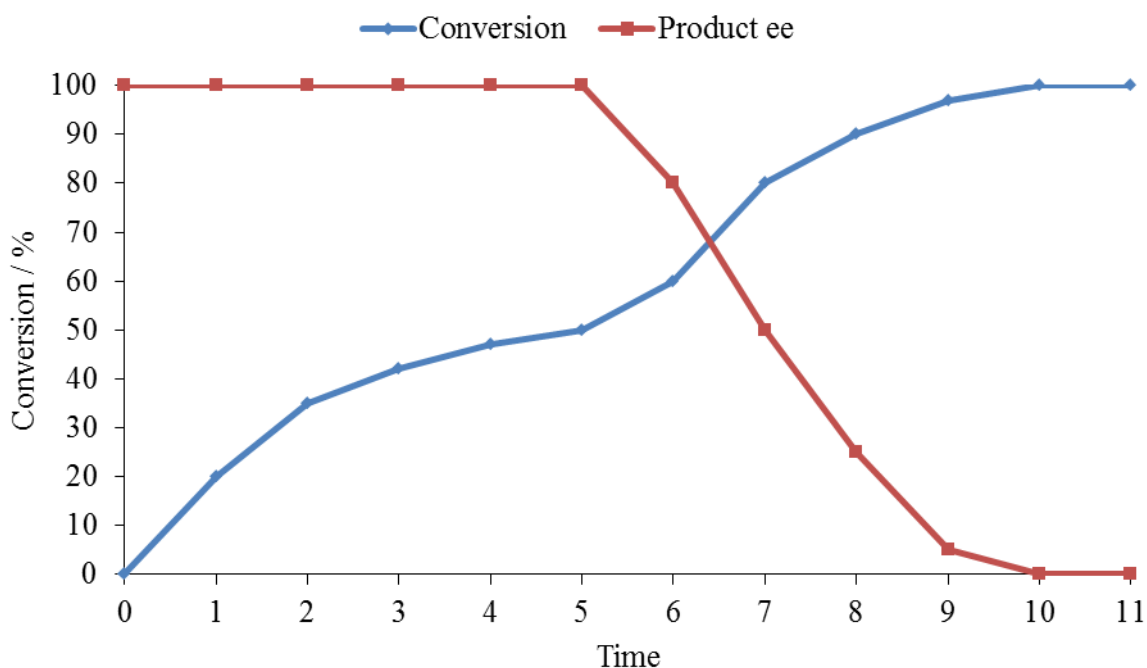
Figure 13. Conversion and product *ee* for a perfectly selective enzyme, showing a decrease in the product *ee* above 50% conversion.

The process also requires that the reaction conditions for the two steps are compatible, for one-pot reactions. As already discussed, there are many examples in the literature for the DKR of amines employing a lipase enzyme for the resolution and a metal catalyst for the racemisation,[53] typically Pd,[59, 60, 110, 111] Ru[66, 71, 112] or Ir.[57, 72] The majority of processes are carried out as a one-pot procedure under batch conditions and as the two catalysts typically have different optimum operating conditions a compromise often has to be reached between the conditions. For example, the optimum temperature for enzymes tends to be lower (~40 °C) than the temperature required for the metal catalysts (~100 °C). Exposing the enzymes to higher temperatures can lead to denaturation of the enzyme. If lower temperatures are used, then the metal catalysed reactions are slower or may not occur at all, especially if activation requires high temperatures. This can result in a less efficient process; consequently many of the examples require the reaction to be carried out over a number of days.[59, 112]

In a recent review, Bäckvall highlights the challenges associated with the DKR of amines compared to the more facile DKR of alcohols.[53] There are few amine racemisation catalysts: Shvö,[112] [Cp*IrI$_2$]$_2$,[57] (modified) Pd/C,[59, 60] and amino acid racemases.[113] The homogeneous catalysts often require high temperatures to be activated, the heterogeneous catalysts are unselective and the enzymes of narrow scope. Since amines can act as ligands or surface modifiers, they can also cause inhibition of the catalysts. The high temperatures needed to overcome this inhibition are incompatible with the majority of enzymes. Also, the reactivity of primary imine intermediates formed during the catalytic cycle generates significant dimeric products, which is exacerbated at higher temperatures.

The objective of this work was to investigate the coupling of the continuous chiral amine resolution developed in Chapter 2 with continuous metal catalysed racemisation. Ideally, a

heterogeneous catalyst would be used, so that the two catalysts could be isolated in separate packed bed reactors (PBRs) operated at different temperatures, to avoid compromising on reaction conditions, and thus and develop a more efficient DKR (Scheme 57).
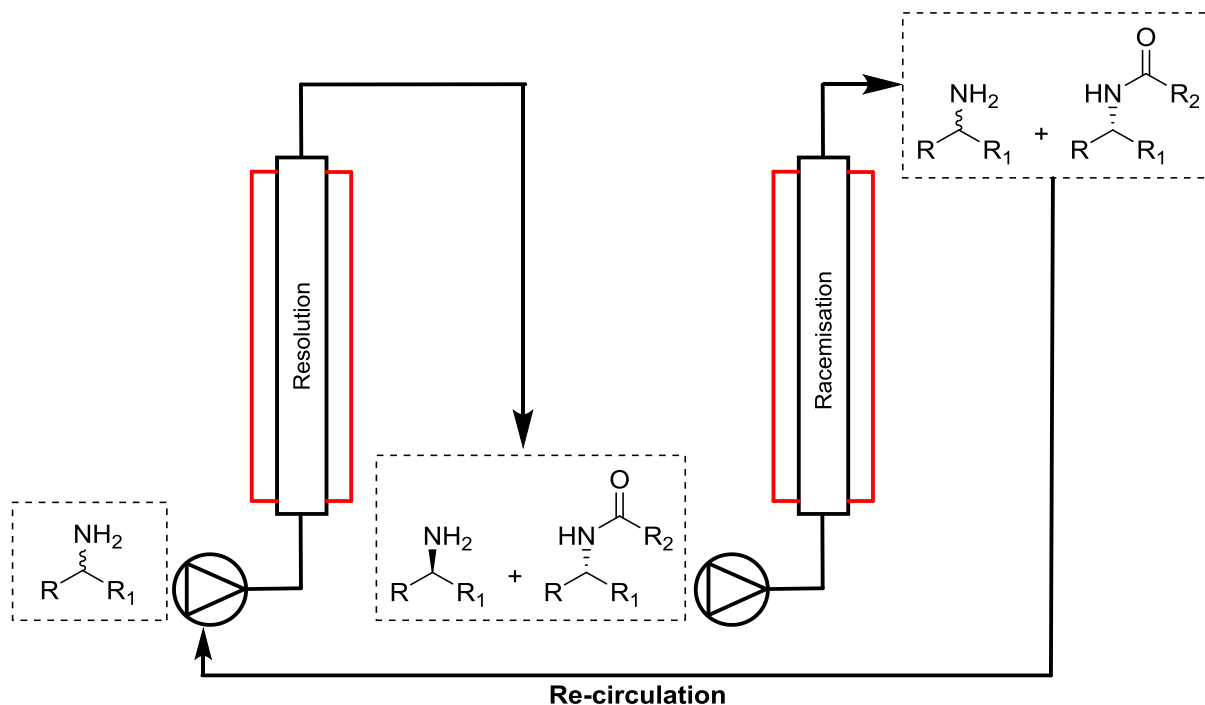
Scheme 57. Proposed continuous reactor set-up for DKR using PBRs in series.

In this chapter, the metal catalysed racemisation of (*S*)-1-phenylethylamine **(S)-3.1** was investigated using heterogeneous and homogeneous Ir, Ru and Pd catalysts.

3.2 Racemisation using Iridium Catalysts

3.2.1 Heterogeneous Iridium Catalyst

The racemisation of **(S)-3.1** was first studied using a heterogeneous Cp*Ir catalyst **3.2** (Scheme 58). The catalyst was produced from the [Cp*IrI$_2$]$_2$ dimer by immobilisation on

the Wang resin through a 5-carbon chain (supplied by Yorkshire Process Technologies).[43, 114]
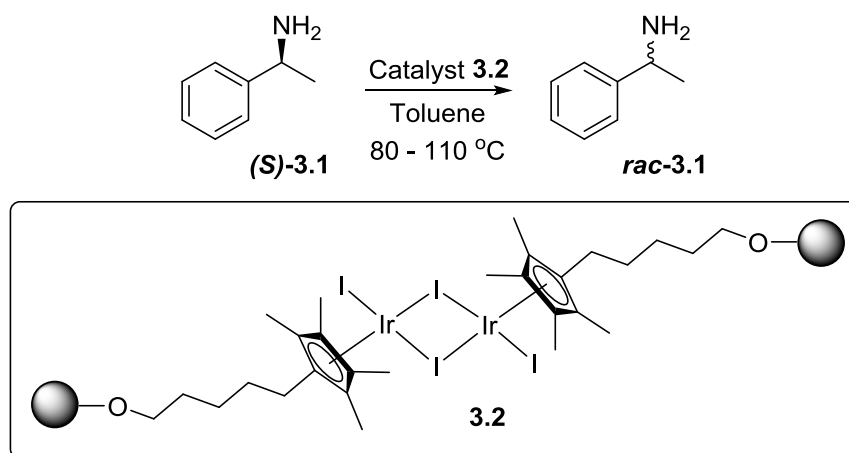
Scheme 58. Racemisation of **(S)-3.1** using heterogeneous Cp*Ir catalyst **3.2**.

The experiments using heterogeneous catalyst **3.2** were only carried out under continuous reaction conditions, using either of the set-ups shown in Figure 14, with a view to developing the coupled reactor system. For the first reactor type, catalyst **3.2** was manually packed into a stainless steel tubular reactor (4.0 mm ID, 25 cm, 3.1 mL), which was installed within a heating jacket set on top of a hot-plate. The reaction stock solution (**(S)-3.1** in toluene) was pumped through the reactor using a Harvard 11 syringe pump, set to the desired flow rate. For the second reactor type, catalyst **3.2** was again manually packed into a stainless steel tubular reactor (1/4" OD, 1/8" ID, 3 mL), which was installed within an aluminium heating block under Eurotherm temperature control. In this case the reaction stock solution was pumped through the reactor using a Harvard 2000 dual syringe pump.
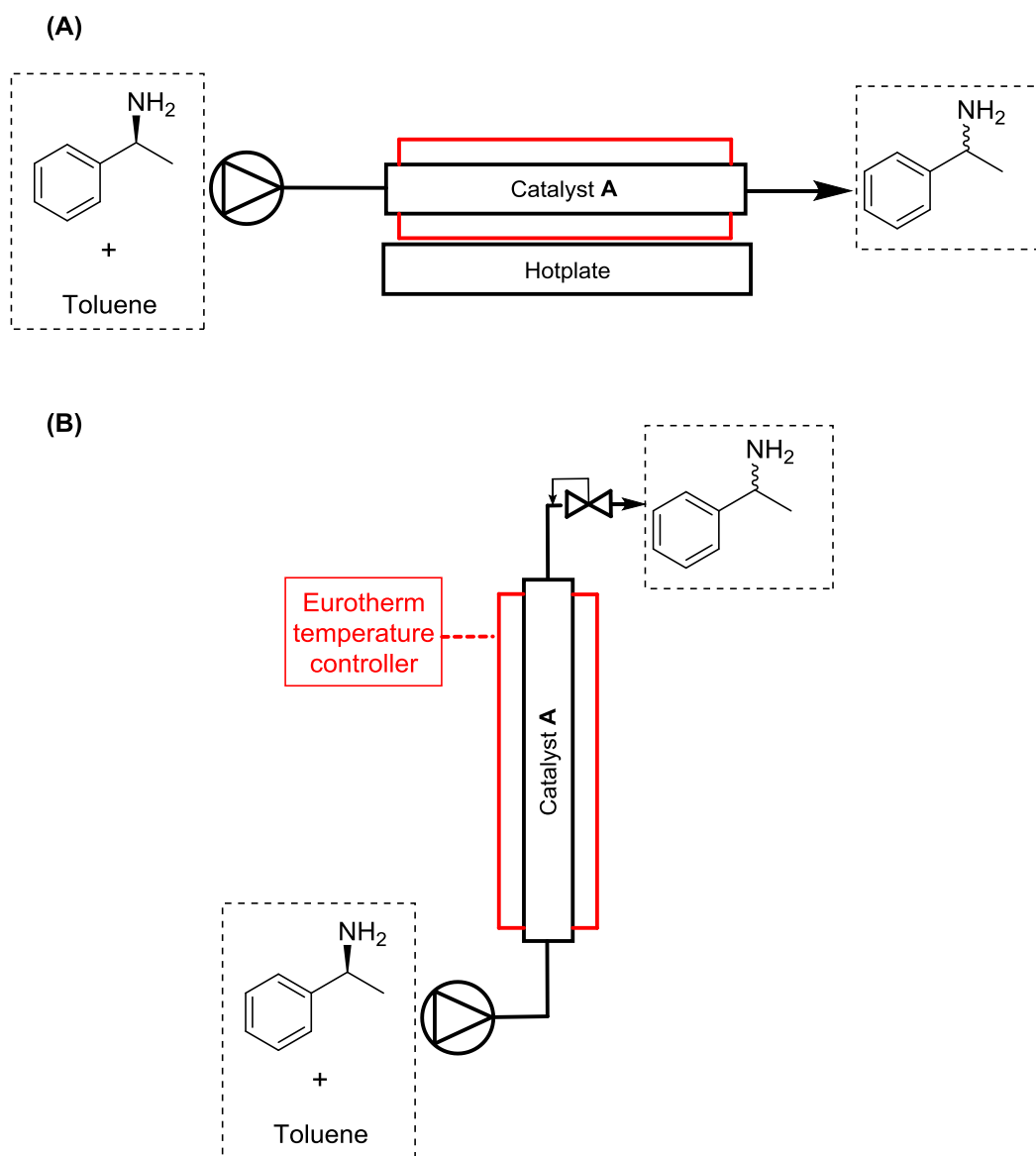
Figure 14. First (A) and second (B) continuous reactor set-ups for the racemisation of (*S*)-**3.1**, using catalyst **3.2**.

The catalyst loading, temperature and residence time (tRes) were varied within the continuous reactors and the results are presented in Table 6. For all Entries, the entire reaction stock solution was pumped through the reactor, collected and a sample taken for GC analysis. The solution was then re-circulated through the reactor, up to 4 cycles, so as to increase the exposure of the substrate to the catalyst, with the aim of increasing the amount of racemisation with each cycle. The reactions were analysed for the change in

amine *ee* using chiral GC, after derivatisation using trifluoroacetic anhydride, as described in Chapter 2.

Table 6. Continuous racemisation of (*S*)-**3.1**, using heterogeneous catalyst **3.2**.[a]

Entry	Catalyst loading[c] / mol%	Temperature / °C	tRes / min	Conversion of **3.1**[d] / %	*ee*[e] / % of **3.1**
1	2.5	80	6	0	> 99
2	2.5	100	6	6	> 99
3	5	100	6	12	> 99
4[b]	2.5	110	6	1	> 99
5[b]	2.5	110	12	1	> 99
6[b]	2.5	110	30	3	> 99

[a]Reaction conditions: heterogeneous catalyst **3.2**, 0.07 M (*S*)-**3.1**, toluene, reactor volume = 3.1 mL; [b]Second reactor type, reactor volume = 3.0 mL; [c]Calculated relative to the entire solution flowed through the reactor over multiple cycles; [d]Determined by achiral GC analysis; [e]Determined by chiral GC analysis after derivatisation with trifluoroacetic anhydride; Data values shown were obtained after 4 cycles through the reactor.

Initially a short tRes of 6 min was tested so as to match the optimum tRes for the continuous resolution of *rac*-**3.1** from Chapter 2. The *ee* of amine **3.1** did not decrease over the course of the cycles and so no racemisation was occurring for reaction temperatures between 80 – 110 °C with 2.5 mol% catalyst loading (Entries 1,2 and 4). Increasing the catalyst loading to 5 mol% did not encourage any racemisation (Entry 3). The tRes was then increased to 12 min (Entry 5) and 30 min (Entry 6), however, no racemisation was observed. For all of the conditions tested, amine **3.1** was observed to form dimeric products (Scheme 59).
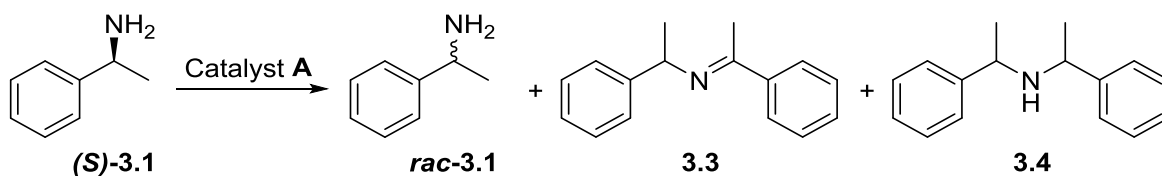
Scheme 59. Attempted racemisation of (*S*)-**3.1** using heterogeneous Cp*Ir catalyst **3.2**, showing dimer products.

The dimer products are formed by the reaction between two of the amine molecules, according to the proposed catalytic cycle (Scheme 60).[57, 115] In the catalytic cycle, the amine first coordinates to the catalyst and is de-hydrogenated to form an imine. For racemisation to occur, the imine must then be re-hydrogenated to re-form the amine, with scrambling of the stereochemistry. For dimer formation to occur, a second amine molecule reacts with the imine intermediate to form an imine dimer that can be hydrogenated to give the amine dimer. The formation of dimers observed therefore indicated that the de-hydrogenation step was occurring, but that the nucleophilic attack by the second amine molecule then occurred preferentially over the re-hydrogenation. Recent work carried out by Stirling *et al*. studying the kinetics and mechanism of the homogeneous [Cp*IrI$_2$]$_2$ catalyst **3.5** for the racemisation of amines, indicated that the imine dissociates from the Ir complex into solution and then re-associates for hydrogenation to occur.[115] Therefore, the dimer formation would occur in solution rather than bound to the catalyst. However, unpublished work carried out within the research group suggests that primary imines remain bound to the catalyst and dimerisation occurs on the catalyst, as when the imine and amine were mixed without catalyst, no dimer was formed.[116]
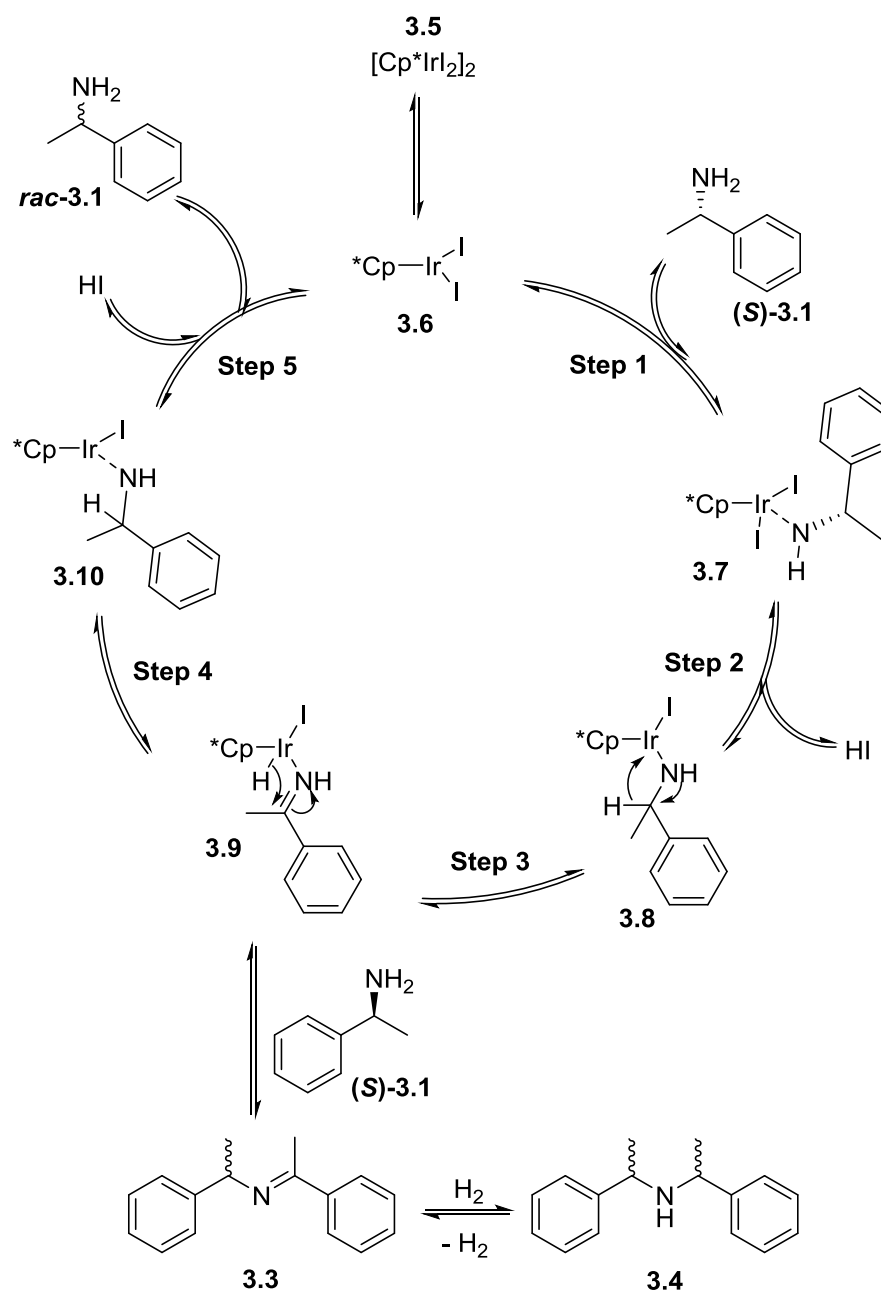
Scheme 60. Proposed catalytic cycle for racemisation and dimer formation.

The temperatures used for the reactions with catalyst **3.2** were chosen based on previous studies carried out within the research group, which showed that the supported catalyst was active for longer and could be recycled more times when operated at 80 °C, mainly due to decomposition of the Wang resin.[117] Therefore, reactions were carried out around this temperature and not above 110 °C. The catalyst loading was not increased above 5 mol%,

relative to the entire solution over the multiple cycles, so as not to increase the cost associated with the process. A short tRes would have been favourable for coupling to the existing continuous resolution process but increasing the tRes to 30 min did not encourage the racemisation. Racemisation may have been achieved with more forcing reaction conditions, such as higher temperature, however due to the reasons described, this could not be further investigated for catalyst **3.2**.

Initially, the goal was to use the heterogeneous catalyst **3.2** to racemise the amine so as to be able to couple this reaction to the continuous resolution described in Chapter 2, using continuous PBRs in series. However, testing of the heterogeneous catalyst within the required operating conditions: short reaction time required for flow and temperature required to maintain catalyst stability; showed that this was not an appropriate set-up.

3.2.2 Homogeneous Iridium Catalyst

The racemisation of (*S*)-**3.1** was next investigated using the homogeneous $[Cp*IrI_2]_2$ catalyst **3.5** (Scheme 61). This catalyst was employed by Stirling *et al*. for the DKR of secondary amines[72] and was then applied to the racemisation of a range of primary and secondary amines.[57] Whilst the catalyst was able to racemise secondary amines effectively, attempts using primary amines led to mainly the formation of dimers, as observed for the heterogeneous Ir catalyst described above. Nevertheless, catalyst **3.5** was tested to determine if racemisation of (*S*)-**3.1** could be achieved preferentially over the dimer formation by varying the reaction conditions. Using the homogeneous catalyst provided the ability to operate at higher temperatures than could be achieved with the heterogeneous catalyst, as there were no concerns over the stability.
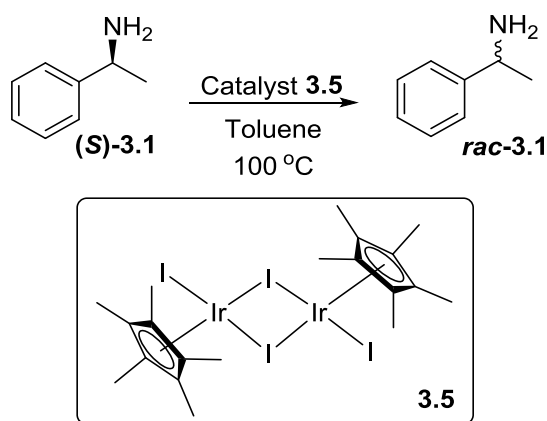
Scheme 61. Racemisation of **(S)-3.1** using [Cp*IrI₂]₂ catalyst **3.5**.

The reactions were carried out under batch conditions, using 0.23 M amine, 2 mol% homogeneous [Cp*IrI₂]₂ catalyst **3.5** in toluene at 100 °C. The *ee* of **(S)-3.1** was unchanged over the course of the reaction, indicating that it was not being racemised (Figure 15). However, dimers were again formed until no more monomer remained in the reaction solution after 7 h.
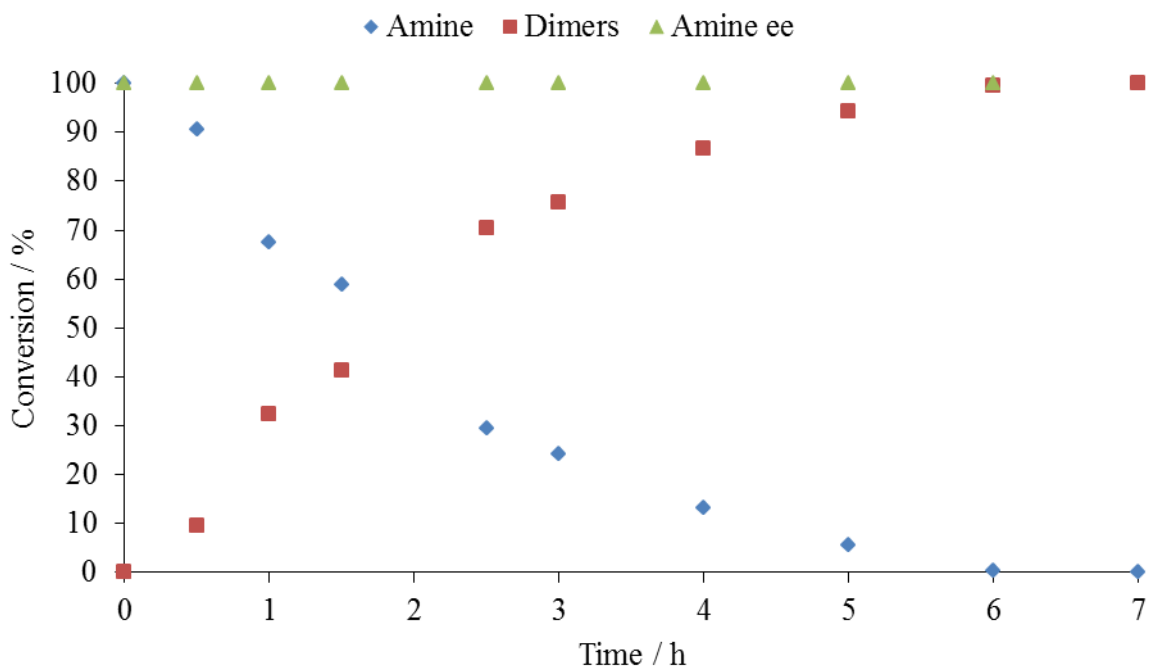
Figure 15. Racemisation of **(S)-3.1** using [Cp*IrI₂]₂ catalyst **3.5**. (Dimers corresponds to a mixture of imine dimer and diastereomeric amine dimers).

Previous work carried out within the research group showed that the combination of amine and imine without any $[Cp*IrI_2]_2$ catalyst did not produce dimers.[116] This showed that coordination to the catalyst is required to form dimers. The formation of dimers indicated that coordination to the catalyst and de-hydrogenation was occurring but that the reaction with a second amine molecule was favoured over the re-hydrogenation of the imine. As no racemisation was observed, the H_2 produced on de-hydrogenation was not being used to re-hydrogenate the monomer imine and so was presumably being used to hydrogenate the dimer imine, as no gas evolution was observed.

Based on these findings and other work using catalyst **3.5** (discussed in Chapter 5), reaction testing was then carried out using the homogeneous $[Cp*IrI_2]_2$ catalyst **3.5** at higher temperatures. Reactions were carried out using 0.5 mol% catalyst **3.5** and 1 M (*S*)-**3.1** in anisole under microwave heating at the specified temperature for 30 min. The shorter reaction times were desirable for coupling to the continuous resolution process. The results are displayed in Figure 16.
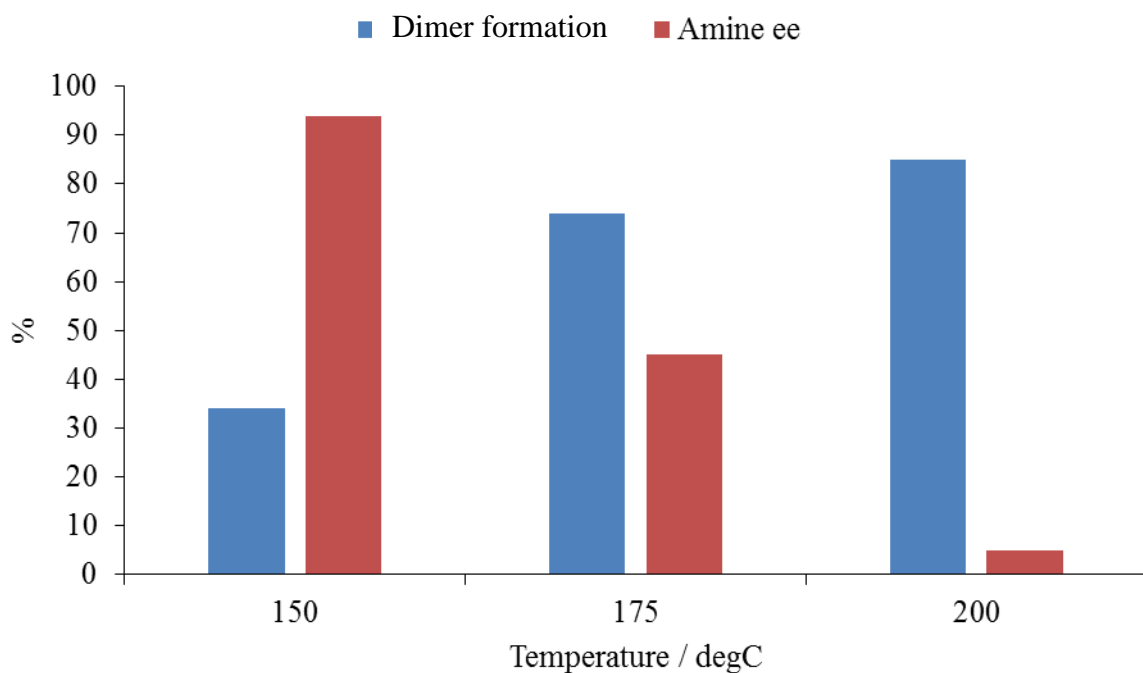
Figure 16. High temperature testing for **3.5** catalysed racemisation of (*S*)-**3.1** using microwave heating.

At higher temperatures, the amine was found to racemise from 96% *ee* at 150 °C to 5% *ee* at 200 °C. However, the production of dimers also increased, up to 85% conversion of amine at 200 °C. Since racemisation was only achieved when the reaction temperature was > 150 °C, this was inappropriate for the heterogeneous catalyst, due to the stability of the polymer support. If the racemisation using catalyst **3.5** at 200 °C was coupled to the enzymatic resolution, there would be virtually no amine monomer remaining after one cycle of resolution-racemisation-resolution. This prevented the possibility of coupling both the racemisation and resolution catalysts in separate packed bed reactors. As the conversion of the amine monomer to form dimers was so high, the maximum theoretical yield of 100% for a DKR could not be achieved. Indeed, for these conditions only around 54% yield would be possible when combining the resolution-racemisation-resolution steps (Scheme 62).

None of the conditions tested allowed for racemisation to be preferred over dimer formation and so this substrate/catalyst system was deemed inappropriate for the desired DKR process.

100% racemic amine
     ↓ Resolution ⟶ 50% (*R*)-amine
50% (*S*)-amine
     ↓ Racemisation
7.5% racemic amine
     ↓ Resolution ⟶ 3.75% (*R*)-amine
3.75% (*S*)-amine
     54% Total yield of desired enantiomer
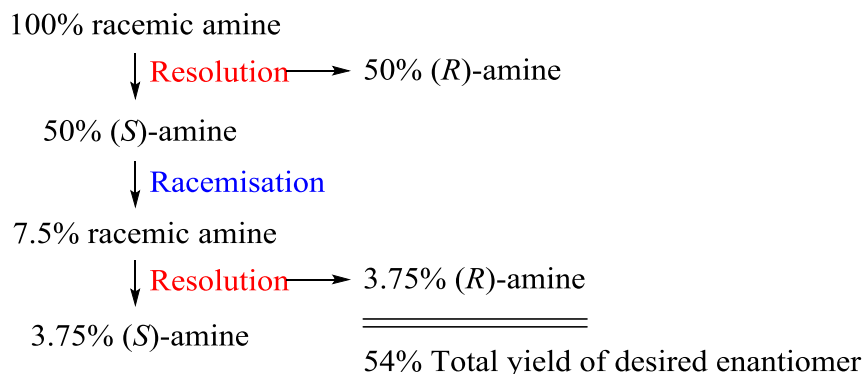
Scheme 62. Theoretical combination of enzymatic resolution with $[Cp^*IrI_2]_2$ racemisation at 200 °C, showing maximum possible yield due to percentage decrease in amine monomer in solution.

3.3 Racemisation using Ruthenium Catalyst

The racemisation of **(*S*)-3.1** was then tested using the Ru Shvö catalyst **3.11** (Scheme 63). This catalyst was used by Paetzold *et al*. for the DKR of primary amines, including **(*S*)-3.1**.[112] Catalyst **3.11** has been used more widely for the DKR of alcohols,[53, 63, 64] and has only been used for a limited scope of amines due to the high temperature required for activation of the catalyst, which led to poor selectivity and was not compatible with the enzyme.[65] Bäckvall *et al*. developed modified versions of the catalyst by substitution of the phenyl groups on the Cp ring with *para*-substituted aryl groups, and was able to achieve the DKR of amines with higher selectivity for the racemisation.[67, 112]
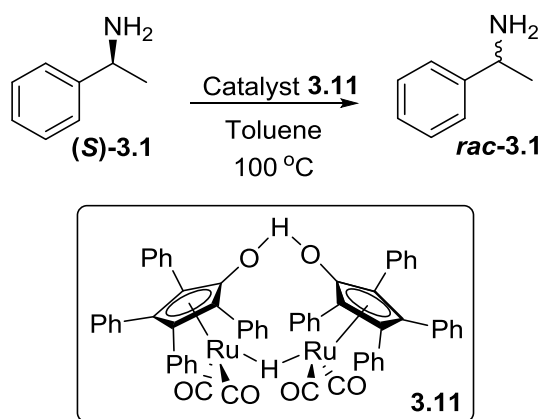
Scheme 63. Racemisation of (*S*)-**3.1** using the Shvö catalyst **3.11**.

A batch reaction was carried out at 100 °C, using 0.23 M (*S*)-**3.1** and 2 mol% loading of catalyst **3.11**. For this catalyst, a reduction in amine *ee* was observed over the course of the reaction to 2% after 53 h (Figure 17). However, significant formation of dimers was also observed, with all of the amine being consumed as dimers after 72 h.

Whilst the racemisation of (*S*)-**3.1** occurred to a greater extent when using the Ru catalyst compared to the Ir catalyst, the formation of dimers was so significant that the amine had been almost completely converted by the time the *ee* had dropped to a sufficiently low level. The reaction with the Ru catalyst was also much slower, taking several days to racemise. This meant that the reaction was too slow to be able to couple to the continuous enzymatic resolution (tRes = 6 min) and to set-up a re-circulating DKR process. For these reasons, catalyst **3.11** was not suitable for the racemisation of this substrate and was not investigated further. Im *et al*. reported an immobilised version of the Shvö catalyst, using a modified γ-alumina support, for the DKR of 1-phenylethanol.[118] And so this may be an area of further research, although the modified Shvö-type catalysts developed by Bäckvall showed better properties for amine substrates.[112]
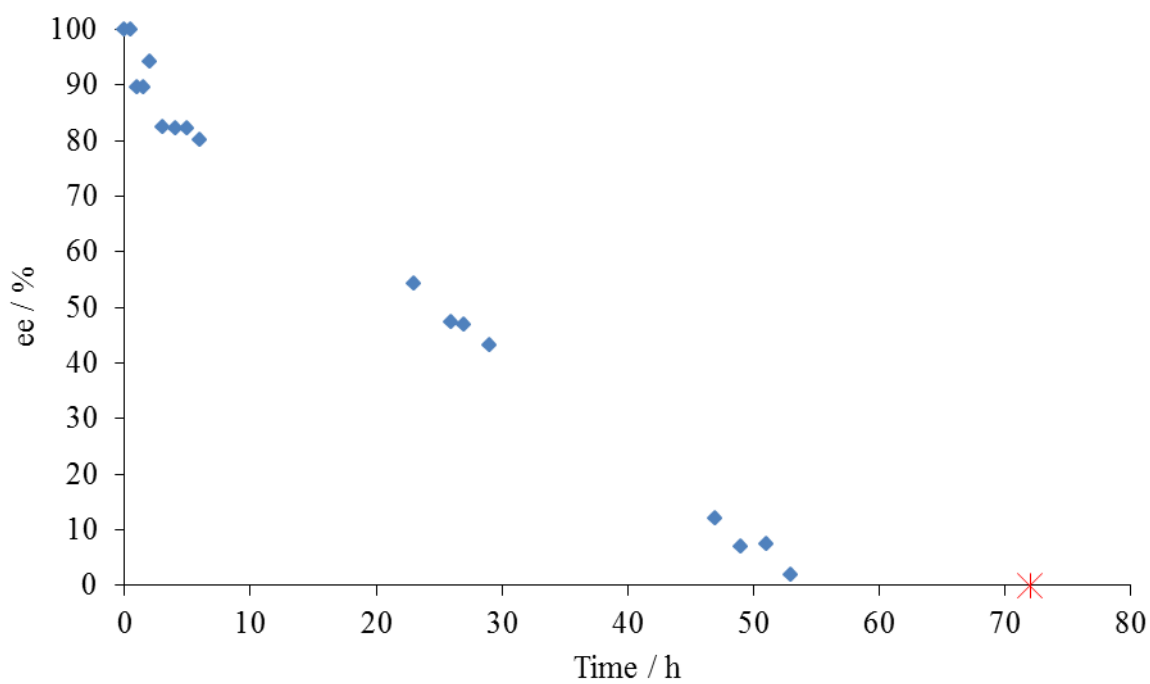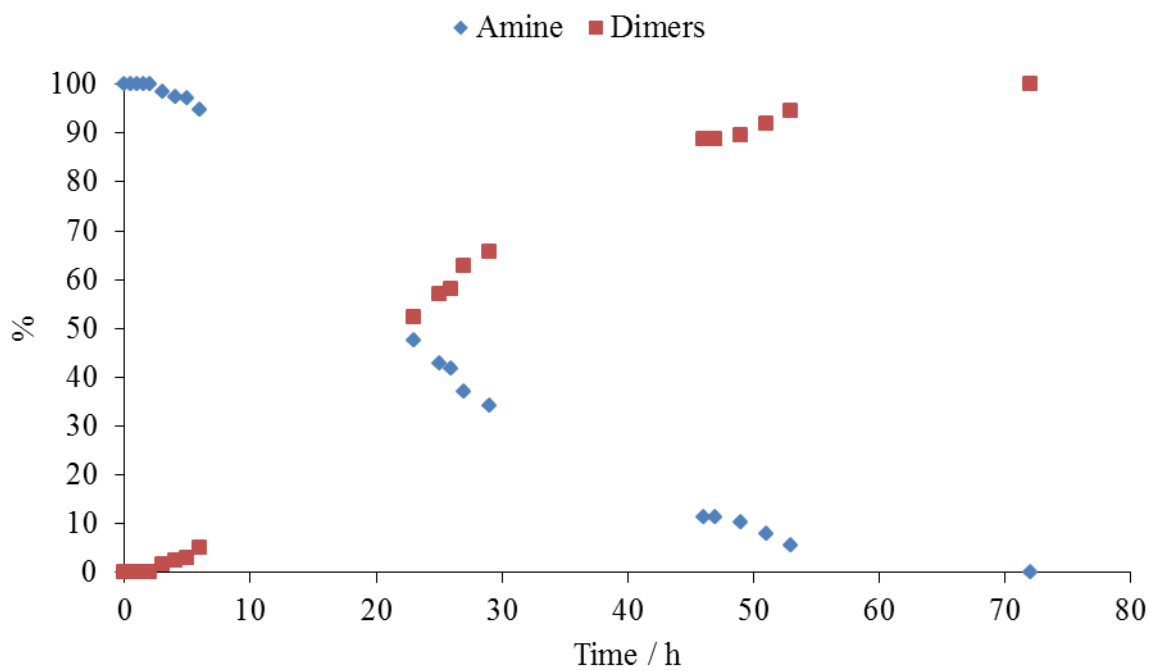
Figure 17. Racemisation of (*S*)-**3.1** using catalyst **3.11** (top panel = area ratio as percentage; bottom panel = amine *ee*, red star denotes no amine present).[a]

3.4 Racemisation using Palladium Catalyst

Pd/C heterogeneous catalyst was then tested for the racemisation of (*S*)-**3.1** (Scheme 64). The use of Pd/C in a DKR of (*S*)-**3.1** was first described by Reetz,[59] for which a yield of 64% was achieved after 8 days. Parvulescu *et al*. showed that using Pd on alkaline-earth supports (BaSO₄) gave higher selectivities in the DKR of primary benzylic amines, again with reaction times of several days.[60] In both cases significant hydrogenolysis of the benzylamine took place forming ethylbenzene as a by-product. Pd/C is non-selective, so limits the types of substrate that can be used. Nevertheless the simplicity of the system makes it attractive to evaluate in continuous flow DKR.
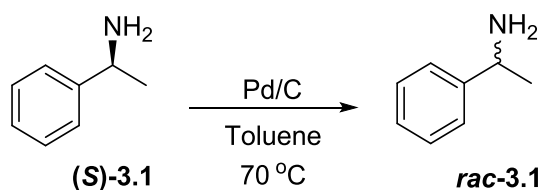
Scheme 64. Racemisation of (*S*)-**3.1** using Pd/C

3.4.1 Batch Reactions

The racemisation was studied initially under batch conditions, with variation of temperature, catalyst loading and the percentage of Pd in the catalyst (Table 7). All of the reactions using Pd/C showed dimer formation but no racemisation of amine **3.1**. Increasing the percentage of Pd in the catalyst from 5% to 10% did not appear to affect the degree of dimer formation (Entries 1 and 3). However, increasing the temperature from 70 to 100 °C did increase the conversion of **3.1** to 50% (Entry 2). Pd/BaSO₄ was also tested as the racemisation catalyst as the literature suggested that alkaline-earth metal supports favour the racemisation reaction over any by-product formation.[60] No racemisation or dimer formation occurred when using Pd/BaSO₄ (Entry 4).

Table 7. Racemisation of (*S*)-**3.1** using Pd/C catalyst, under batch conditions.[a]

Entry	Catalyst type	Catalyst loading / mol%	Temperature / °C	Time / h	Amine **3.1** ee^c/ %	Conversion of **3.1**[e] / %
1	5% Pd/C	5.7	70	24	99	16
2	5% Pd/C	6.4	100	23	99	50
3	10% Pd/C	8.5	70	23	99	10
4[b]	Pd/BaSO$_4$	3.0	70	50	99[d]	0

[a]Reaction conditions: 0.33 mmol (*S*)-**3.1**, 4.0 mL toluene, 200 μL decane as internal standard; [b]Reaction conditions: 0.35 mmol (*S*)-**3.1**, 5.0 mL toluene, 5% Pd/ BaSO$_4$ catalyst, 70 °C; [c]Determined by chiral GC after derivatisation with trifluoroacetic anhydride; [d]Determined by chiral HPLC after derivatisation with acetic anhydride; [e]Determined by achiral GC.

3.4.2   Continuous Reactions

It was envisaged that transferring the reaction to the continuous PBR would allow for the catalyst loading to be increased relative to amine (*S*)-**3.1**, and these more forcing conditions may enhance the reaction. The second reactor set-up (Figure 14, B) was used with the reactor packed with 5% Pd/C catalyst. The reactor was heated to 70 ºC and the reaction solution (0.07 M (*S*)-**3.1** in toluene) was pumped through the reactor using a Jasco PU-980 dual piston pump, set to a flow rate of 0.1 mL min^{-1} (tRes = 30 min). The catalyst loading within the reactor was 24 mol% relative to the total amount of reaction solution passed through (24 mL). Each RV was collected separately at the reactor outlet and analysed for *ee* and conversion. No racemisation or dimer formation was observed using the continuous system.

These results indicated that the catalyst loading was not a significant variable for this reaction, as increasing the catalyst loading did not enhance the reaction. Based on the studies in the literature,[53, 60] it would also be expected that the reaction of Pd/C would require H$_2$ to proceed with the desired racemisation reaction, as the H$_2$ would be available to re-hydrogenate the imine and out-compete the dimer formation. The PBR used in these

experiments was not designed to allow simultaneous flow of H_2 gas. To do this an alternative reactor design would be required, such as the Thales Nano H-Cube®[119] or multi-stage continuous stirred tank reactors (CSTRs) that allow triphasic flow with good mixing, as being developed in the iPRD lab.[120] The lack of racemisation using Pd/C under any conditions tested meant that this catalyst was not investigated any further.

3.5   Conclusions

The metal catalysed racemisation of (*S*)-**3.1** was investigated using Ir, Ru and Pd catalysts for the potential use in DKR. Heterogeneous Ir catalyst **3.2** was tested using a continuous PBR, with a view to coupling to the enzymatic resolution continuous PBR for a DKR process. No racemisation occurred but conversion of amine **3.1** to dimer products was observed. The formation of dimers in flow was an example of *N*-alkylation in flow *via* hydrogen borrowing,[29] which will be investigated further (Chapter 5). Racemisation was achieved using homogeneous Ir catalyst **3.5** when high temperatures were used (200 °C). Unfortunately, the amount of dimer formation (85%) was prohibitive at this temperature for these conditions to be used for the DKR process.

Using the homogeneous Ru catalyst **3.11** the amine *ee* did reduce over time to 2% after 53 h, however, the amount of amine monomer remaining at that time was only 6%, and then dropped to 0%. The reaction using this catalyst was very slow and the dimer formation still dominated and so this catalyst was not studied any further. The use of the modified Ru catalysts developed by Bäckvall may have been beneficial to this process as they displayed higher selectivity for the racemisation over the dimer formation.[112] However, the reported DKR using these catalysts required a reaction time of 3 days and so would not have been an improvement on the long reaction time for catalyst **3.11** and would still not have been suitable for this reactor set-up.

Finally, Pd/C was tested under batch conditions and using the continuous PBR. No racemisation was observed for any of the reactions and dimer formation was again prevalent. Increasing the temperature did not encourage racemisation and caused an increase in dimer formation. Increasing the catalyst loading within the PBR did not encourage the racemisation. The Pd/C catalyst may require gaseous H_2 to achieve racemisation, which was not feasible within the current reactor set-up.

For all conditions tested, dimer formation occurred preferentially over racemisation. The presence of dimers indicated that the amine was being de-hydrogenated but that the coupling of a second amine molecule was occurring in favour of re-hydrogenation. For the reactions in which a drop in amine *ee* was observed, the formation of dimers was too significant and meant that there was little amine monomer remaining in solution by the time the *ee* had dropped to a suitable level. Therefore these catalysts were not suitable for the racemisation of (*S*)-**3.1** to be used in the desired continuous DKR system.

Reducing the concentration of the amine could also be investigated as a method to reduce the dimer formation. A lower concentration of amine would reduce the rate of reaction as the amine is present in the rate determining step. This may allow re-hydrogenation of the monomer imine to occur before dimer formation. Slow addition of the amine into the reaction solution is one technique that could be tested in future to probe this.

4 Continuous Ammoniolysis for the Production of Amides

4.1 Introduction

In Chapter 2 the lipase catalysed reaction of amines with esters for the production of single enantiomer amines and amides was studied. In that reaction the amine reacts with the acyl-intermediate formed in the active site between the ester and the serine residue (Scheme 65). Many examples exist that employ different nucleophiles[105] to interact with this intermediate, including hydrazine[121, 122] and hydrogen peroxide.[123-125]
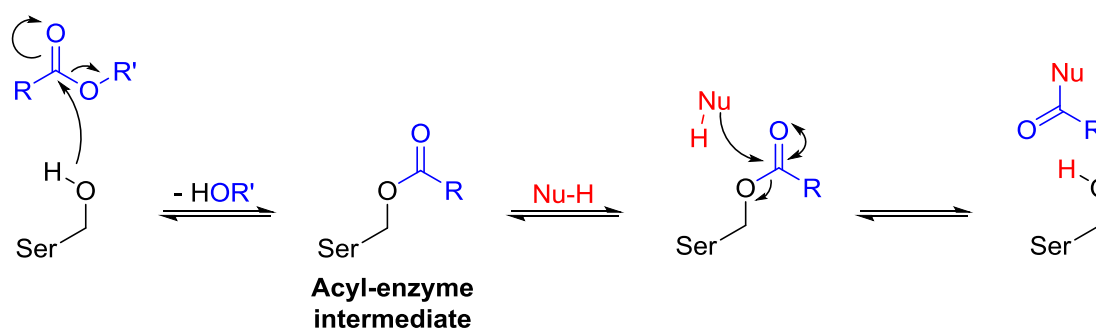
Scheme 65. Reaction of a nucleophile (Nu) with the acyl-enzyme intermediate within the lipase active site. (Full active site mechanism shown in Chapter 2).

The reaction of ammonia with the acyl-enzyme intermediate to produce amides, termed ammoniolysis, was first described by Sheldon *et al.* for the production of octanamide **4.2** from ethyl octanoate **4.1** (Scheme 66).[126]
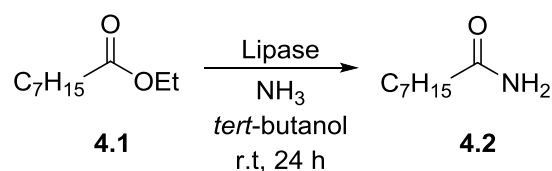
Scheme 66. Ammoniolysis of ethyl octanoate **4.1** to produce octanamide **4.2**.[126]

The reaction was further developed for the reaction of carboxylic acids, *via* lipase catalysed esterification followed by ammoniolysis,[127] and amino acid esters.[128, 129] Although high conversions and high enantioselectivities were observed, the reactions suffered from long reaction times, even up to several days for the carboxylic acid substrates.[127]

It was envisaged that the use of a continuous PBR, using an immobilised lipase, would reduce the reaction time and improve the productivity. The packed bed allows for the reaction mixture to be exposed to a much higher amount of catalyst than is possible in a batch reaction.[101] The lifetime of the catalyst may also be increased using the packed reactor compared to a stirred vessel, as mechanical stirring can lead to increased breakdown of the immobilised catalyst.[85] Also, the use of an immobilised catalyst allows for easy separation and re-use and the constant removal of the reaction stream under flow conditions should prevent any hydrolysis of the starting ester to the carboxylic acid that could occur in the presence of H_2O.

Slotema *et al*. reported a continuous procedure for the lipase catalysed ammoniolysis of oleic acid **4.3** with NH_3 for the synthesis of oleamide **4.4** (Scheme 67).[130] A PBR was employed filled with lipase B from *Candida antartica* (CalB) and ammonium carbonate was used as the NH_3 source, with 2-methyl-2-butanol as the solvent. The highest conversion achieved was 97% for a 90 min residence time (tRes).
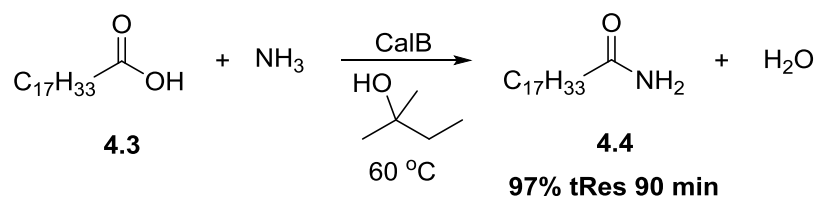
Scheme 67. Ammoniolysis of oleic acid **4.3** for the production of oleamide **4.4**.[130]

Luque *et al.* described a continuous procedure for the lipase catalysed ammoniolysis of ethyl octanoate **4.1**, using a gas-liquid membrane reactor in which the enzyme was immobilised onto a membrane.[131] A liquid substrate feed and a gaseous NH_3 feed were combined in the enzyme membrane reactor and a re-circulation loop set-up. No information regarding flow rates and tRes within the reactor were provided, however an octanamide **4.2** yield of 95% after 10 h of operation was reported. As a re-circulation process was used it can be inferred that a single pass through the enzyme membrane reactor was not sufficient to convert all of the substrate. Re-circulation of the reaction solution once the substrate has partially converted can lead to inconsistencies in the conversion for subsequent cycles. As the substrate concentration is reduced with each cycle, the likelihood of contact between the substrate and enzyme is reduced. In addition, the system has a finite amount of substrate within the re-circulating mixture. In a truly continuous system the substrate solution would be constantly replenished and so the throughput of the system would be much higher.

This chapter describes the development of a lipase catalysed ammoniolysis process using a continuous PBR for the production of two generic pharmaceutical compounds: nicotinamide and pyrazinamide. The reaction conditions were optimised for conversion using a design of experiments (DoE) approach and then further green metrics were calculated for the process to determine productivity and efficiency. This technique was applied to the resolution of a chiral substrate.

4.2   Ammoniolysis for the Production of Nicotinamide

Nicotinamide **4.5** (Figure 18) is on the World Health Organisation (WHO) essential medicines list, as a member of the vitamin B family.[97] As these types of essential

medicines are particularly required in the developing world, it is important that generic

pharmaceuticals such as nicotinamide can be produced using cheap and efficient methods.
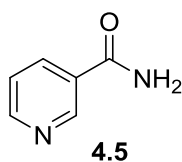
Figure 18. Structure of nicotinamide **4.5.**

In 2005, Chuck presented a review of the developments in nicotinate production, including

nicotinamide and nicotinic acid, from starting material synthesis to reaction development

and work-up procedures.[132] The most widely used chemical synthesis of nicotinamide

starts from 3-picoline **4.6**, which is subjected to ammoxidation conditions to produce 3-

cyanopyridine **4.7** (Scheme 68A). The nitrile is then hydrolysed by exposure to strongly

basic conditions to produce nicotinamide **4.5**. This chemical synthesis method generally

suffers from the production of large amounts of nicotinic acid **4.8** as a by-product, due to

over-hydrolysis in the presence of base (Scheme 68B).
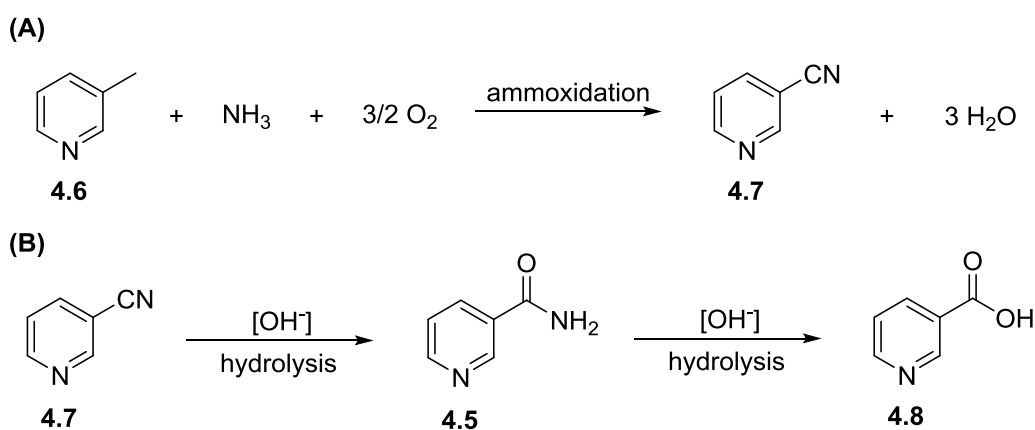
Scheme 68. Chemical synthesis of nicotinamide: (A) Ammoxidation of 3-picoline **4.6** to produce 3-cyanopyridine **4.7**; (B) Hydrolysis of 3-cyanopyridine **4.7** to produce nicotinamide **4.5**, also showing over-hydrolysis to nicotinic acid **4.8**.[132]

An enzymatic process using nitrile hydratase from *Rhodococcus* to form amides *via* the hydrolysis of nitriles was identified by Nagasawa *et al.*[133] and patented along with Nitto Chemical Industry Co (Scheme 69).[134] Nitrile hydratase enzymes catalyse the hydrolysis of nitriles with H_2O to produce amides, unlike nitrilase enzymes which catalyse the conversion of nitriles to the corresponding carboxylic acids and NH_3.[133] The enzymatic reaction was found to be much more selective than the chemical synthesis methods, as no nicotinic acid by-product was formed.
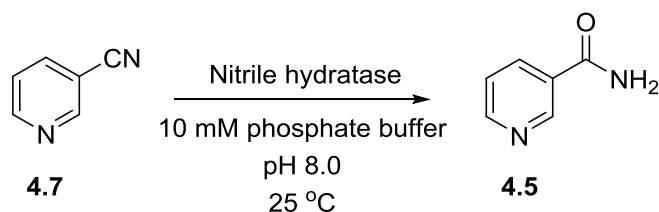
Scheme 69. Enzymatic hydrolysis of nitriles to form amides using nitrile hydratase.

This was further developed by Lonza,[135] who have implemented the process in their China plant to produce over 3500 tonnes of nicotinamide per year.[136] The Lonza process involved four continuous catalytic reactions, with the final step being the enzymatic hydrolysis in which the substrate solution was pumped continuously into a reactor containing the nitrile hydratase immobilised in polyacrylamide (Scheme 70). As this is a patented process, broad ranges of operating conditions were presented for each step.
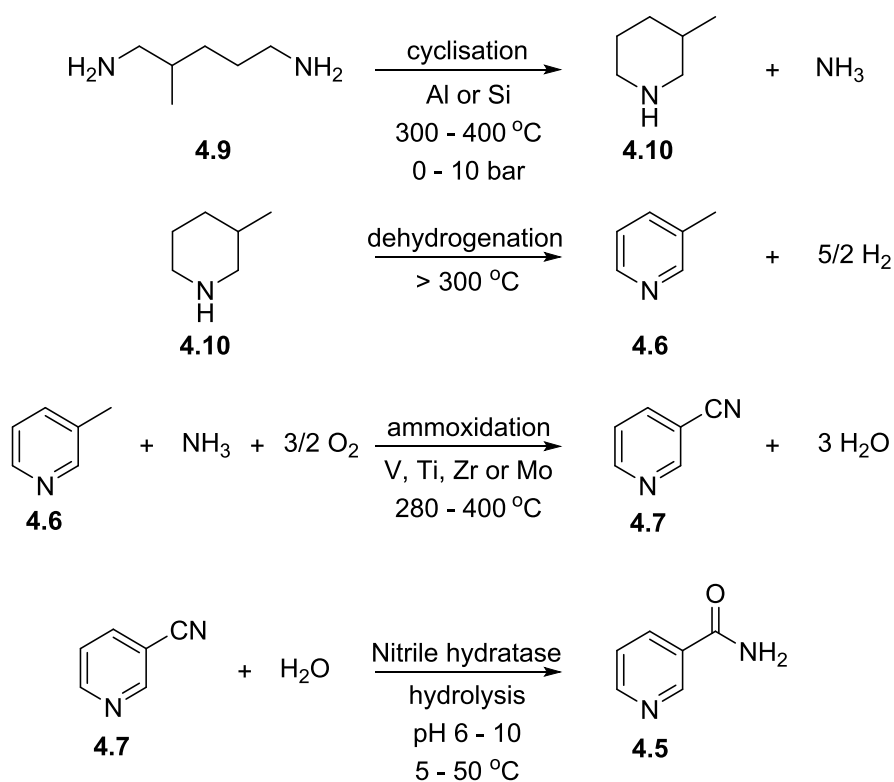
Scheme 70. Lonza four step nicotinamide process.[136]

In the following sections the production of nicotinamide *via* lipase catalysed ammoniolysis of the corresponding carboxylic acid and methyl ester was investigated. The aim was to develop the reaction in a continuous system to be able to expose the substrate to more forcing reaction conditions and to be able to reduce the reaction time whilst achieving high conversion to product.

4.2.1 Batch Ammoniolysis

The reaction of nicotinic acid **4.8** to form nicotinamide **4.5** was initially investigated (Scheme 71).
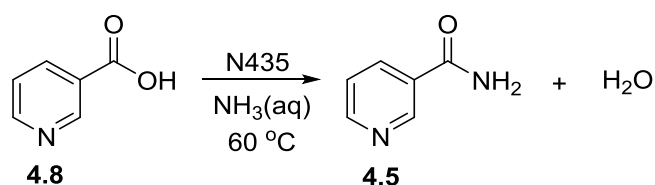
Scheme 71. Nicotinamide **4.5** synthesis from nicotinic acid **4.8** (N435 = Novozyme 435).

The solubility of nicotinic acid **4.8** was tested in a 3 of commercially available NH_3 solutions: aqueous (30-33% NH_3), 1,4-dioxane (0.5 M) and MeOH (0.46 M and 1.79 M, prepared from a 7 N commercial solution). Nicotinic acid **4.8** was found to be poorly soluble in organic solvents, but was soluble in an aqueous NH_3 solution at 0.07 M substrate concentration. This substrate concentration was used based on the concentration screening results carried out in Chapter 2. Using this result, the reaction to form nicotinamide was carried out in an aqueous NH_3 solution (0.5 M) using commercially available immobilised lipase B from *Candida Antarctica* (Novozyme 435, N435) at 60 °C (Scheme 71), however no product was observed after 24 h. Due to the poor solubility and un-reactivity of nicotinic acid, the substrate was changed to methyl nicotinate **4.11**. The reaction of methyl nicotinate **4.11** to form nicotinamide **4.5** was carried out under batch conditions using NH_3 solution (0.5 M in 1,4-dioxane) and N435 at 60 °C (Scheme 72).
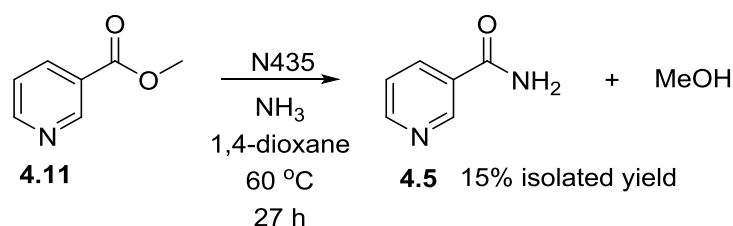
Scheme 72. Nicotinamide **4.5** production from methyl nicotinate **4.11**.

The choice of NH_3 solution was determined by three factors: availability, solubility and reactivity. The three commercially available NH_3 solutions considered were aqueous,

MeOH and 1,4-dioxane. Aqueous solution was not used due to concerns over the potential for hydrolysis to produce the carboxylic acid. MeOH solution would have been preferred over 1,4-dioxane in terms of greener solvents,[137] however no reaction was observed when using MeOH solutions (see solvent comparison section). Therefore, NH_3 in 1,4-dioxane was used as it was commercially available, both the substrate and product showed good solubility and the reaction was shown to proceed.

Under these conditions, nicotinamide **4.5** was obtained in 15% isolated yield after 27 h, using an enzyme loading of 14 mg catalyst per mmol of substrate (121 mg substrate, 12 wt%). A control reaction, carried out in the absence of N435, showed no formation of nicotinamide **4.5** after 27 h and so no background reaction was taking place.

4.2.2 Continuous Ammoniolysis

4.2.2.1 Reactor Design

The reaction of methyl nicotinate **4.11** to form nicotinamide **4.5** was then transferred to a continuous PBR system (Figure 19), described in detail in Chapter 2. The stainless steel tubular reactor (1/4" OD, 1/8" ID, 2.8 mL) was manually packed with N435 and a 75 psi back-pressure regulator (BPR) was fitted to the outlet of the reactor. The reactor was installed within the aluminium heating block and the desired temperature set using the Eurotherm temperature controller. A stock solution of methyl nicotinate **4.11** (0.07 M) dissolved in NH_3 solution (0.5 M in 1,4-dioxane), with biphenyl added as internal standard, was pumped through the reactor as one feed using a Jasco PU-2085 dual piston pump. Each reactor volume (RV) was collected as a separate sample at the reactor outlet and analysed by HPLC, which was calibrated for methyl nicotinate and nicotinamide against the internal standard, to determine a percentage conversion for each reactor volume (for details and calibration plots see Experimental Chapter).
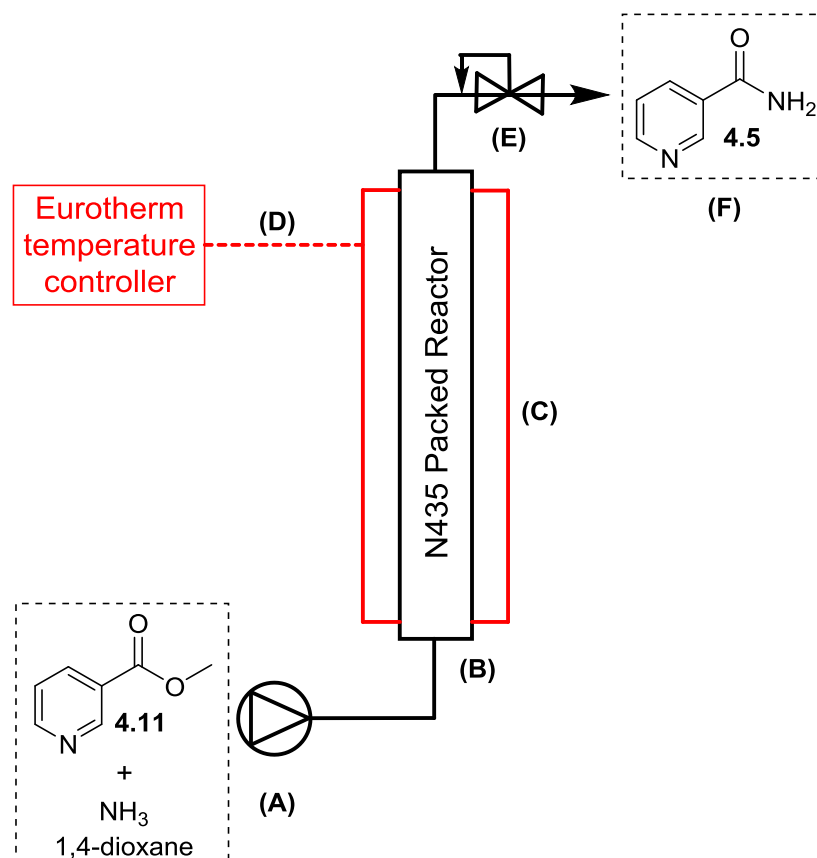
Figure 19. Continuous ammoniolysis PBR design. (A) Piston pump; (B) Tubular reactor packed with N435; (C) Aluminium heating block; (D) Eurotherm temperature controller; (E) BPR; (F) Product outlet and collection.

4.2.2.2 Scoping Reactions

A DoE approach was applied to determine the optimum operating conditions for the continuous ammoniolysis of methyl nicotinate **4.11**. The most common method employed for optimisation of reaction conditions is the one variable at a time approach (OVAT) in which one reaction parameter (*e.g* temperature) is varied until the highest yield is achieved and then the temperature is maintained at that optimum value whilst another reaction parameter is varied until the highest yield is found. This method requires a large number of experiments when many variables are being considered and does not account for any interaction between the variables, meaning that the true optimum of the system may be

missed.[138] DoE is a statistical method to be able to determine significant variables and interactions and to generate optimum conditions for a given process. The nature of experimental design defines the specific experiments that are required before any lab work is started, allowing for fewer experiments to be carried out. This method is able to account for interactions between variables unlike the OVAT approach and can fit a model within the design space to predict the outcome for reactions that have not yet been carried out experimentally. The type of experimental design will vary depending on the number of variables and the objective of the design (screening or optimisation) and is chosen to obtain the maximum amount of information about the process.

The general procedure for optimisation by DoE follows Figure 20. First scoping reactions are carried out to determine the design space to be explored, which is defined by the upper and lower limits for each of the variables being investigated. Once the appropriate design space has been chosen, screening reactions are carried out. These reactions are typically employed to determine the variables that have a significant effect on the process and those which do not, allowing for the variables to be narrowed down. The optimisation stage involves further experimentation within the design space using the significant variables, resulting in a response surface across the whole design space and allowing for prediction of the optimum conditions. The final stage is robustness testing, in which reactions are carried out to verify the predicted optimum. The design space is reduced around the predicted optimum and reactions carried out to determine how far from the predicted optimum the conditions can be varied without a drop in yield or conversion.
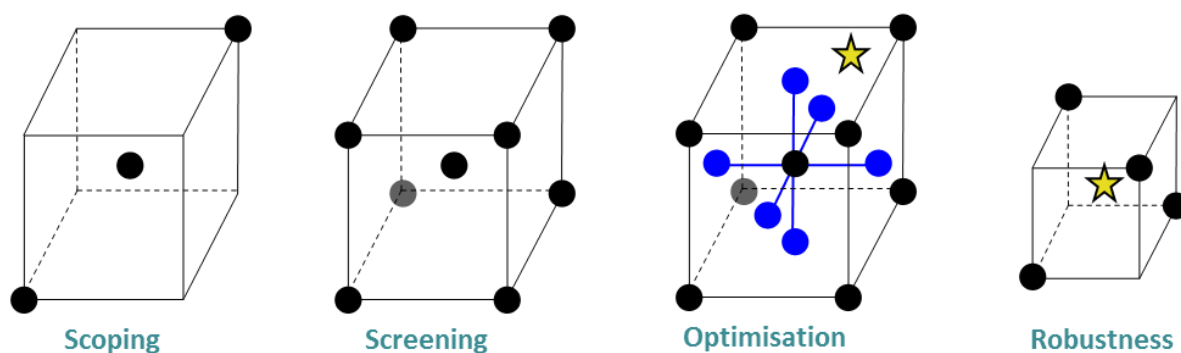
Figure 20. Stages followed for process optimisation by design of experiments (DoE).

As with all techniques, there are limitations and assumptions made when using DoE. For example it is assumed that there are no other unknown competing pathways that could occur during the experiment and so the variables and responses chosen can only be those that are foreseen by the experimenter and selected for using prior chemical knowledge or experimentation. As in traditional OVAT approaches to optimisation, if an important variable is omitted from the list of variables tested in a DoE then it will not be included in the model. However, statistical tests that can be carried out with DoE data can indicate whether there is lack of fit in the model and if a variable is missing. However, it cannot give information as to what that variable is, or what the contribution of that variable is to the overall reaction outcome. Therefore it is crucial to have some understanding of the process before carrying out an experimental design, and the amount of prior knowledge will dictate the starting point for the design: scoping, screening or optimisation.

In this work, scoping reactions were first carried out to determine upper and lower limits for the three variables being considered: tRes, temperature and catalyst loading (Table 8). Catalyst loading was determined as the total mass of immobilised catalyst packed into the reactor, 1.0 g catalyst represented a completely filled reactor and so for the lower catalyst

loadings, glass beads were mixed with the catalyst before packing into the reactor. This ensured the same total reactor volume for all reactions studied.

Table 8. Conversion of methyl nicotinate **4.11** obtained in scoping reactions.[a]

Reaction Level	tRes / min	Temperature / °C	Catalyst loading / g	Conversion[c] / %
Low	20	40	0.5[b]	29
Mid	40	60	0.75[b]	78
Mid	40	60	0.75[b]	76
High	60	80	1.0	89

[a]Reaction solution = 1.75 mmol methyl nicotinate **4.11** in 25 mL NH_3 solution (0.5 M in 1,4-dioxane), biphenyl added as internal standard. Reactor volume = 2.8 mL; [b]Glass beads added to fill the reactor; [c]Determined by HPLC analysis, after calibration against internal standard.

The results obtained were plotted in Figure 21 with the lower limit set to -1, the mid-point set to zero and the upper limit set to +1. Scoping reactions are used to determine whether it is likely that a good model fit will be achievable, and therefore that the limits chosen for the variables are appropriate. The results of the scoping reactions showed that the design space chosen was appropriate and so these limits were used for optimisation reactions. As there were only three variables being considered, it was deemed unnecessary to carry out a screening design prior to the optimisation experiments.
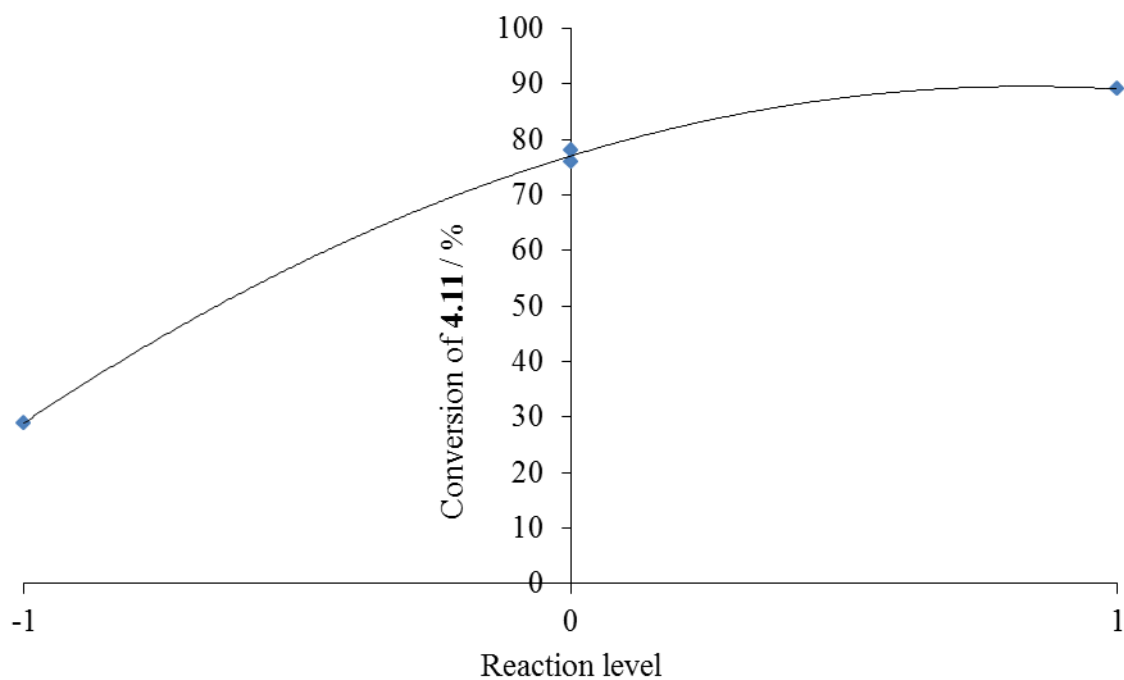
Figure 21. Results of scoping reactions, plotted as lower limit = -1, mid-point = 0 and upper limit = +1.

4.2.2.3 Optimisation Reactions

A response surface methodology (RSM) was then employed to carry out a three-level central composite face-centred (CCF) design for three variables.[139] Three-level designs are used for optimisation reactions because a quadratic model is generated, which allows a surface to be fitted across the design space. In a CCF design (Figure 22), experiments are carried out for the corner points, the centre point and the points in the centre of each face ('star points') of a cube that has been composed from the three variables attributed to the three axes (x, y, z).
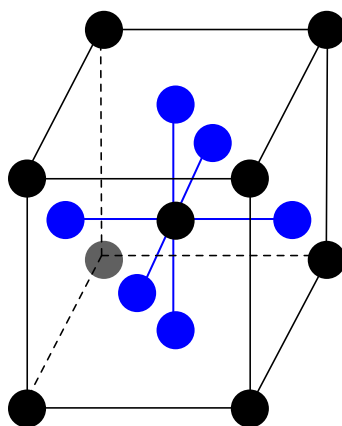
Figure 22. CCF experimental design. (Black spheres indicate corner point and centre point experiments, blue spheres indicate star point experiments).

In total 17 experiments were carried out, including 3 replicates of the mid-point experiment (Data shown in Appendix A). Statistical design software (MODDE) was used to fit a response surface to the data using multiple linear regression (MLR). The summary of fit plots (Figure 23) for both conversion of methyl nicotinate **4.11** (left) and conversion to nicotinamide **4.5** (right) showed a good model fitting, with high values for R^2, Q^2, model validity and reproducibility. The R^2 value shows how well the model fits the data, the Q^2 value is a measure of how well the model predicts new data and the model validity shows if there is 'lack of fit' in the model, a value greater than 0.25 shows that there is no lack of fit. Reproducibility shows the degree of variation in the data obtained from the replicates of the centre point experiments.[140] As only conversion of methyl nicotinate **4.11** to nicotinamide **4.5** was observed the data and model produced would be expected to be the same, which can be seen in the summary of fit plots. There was only a slight difference in the values for model validity and reproducibility, with the reproducibility being marginally higher and the model validity being marginally lower for the conversion to amide plot. The variation between the data for the two responses (conversion of methyl nicotinate and nicotinamide yield) was small and could be attributed to error in the analysis method.
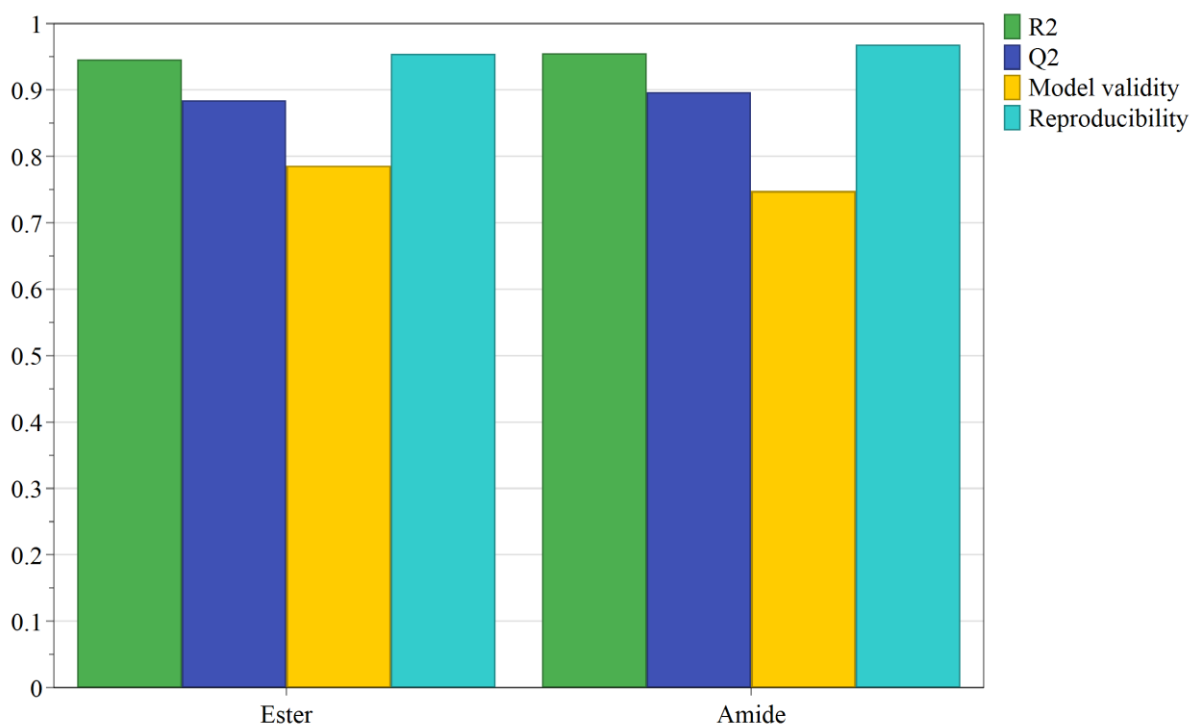
Figure 23. Summary of fit plots for conversion of methyl nicotinate **4.11** (left) and nicotinamide yield **5** (right).

The model generated was then used to predict optimum conditions, *via* the optimizer function in MODDE. Figure 24 shows the contour plot for the conversion of methyl nicotinate model, with the predicted optimum conditions denoted by the black cross. The predicted optimum was 99% conversion at 60 min tRes, 67 °C and 1.0 g catalyst loading. The contour plots showed that the highest conversions would be achieved at the highest tRes and catalyst loadings, but at intermediate temperatures. This would be expected as the longer tRes and higher catalyst loadings would mean that the substrate was exposed to more catalyst and for a longer period, leading to a higher conversion. The temperature effect would also be expected in terms of the recommended operating conditions for N435, for which the stated optimum temperature range is 30 – 60 °C.[50]
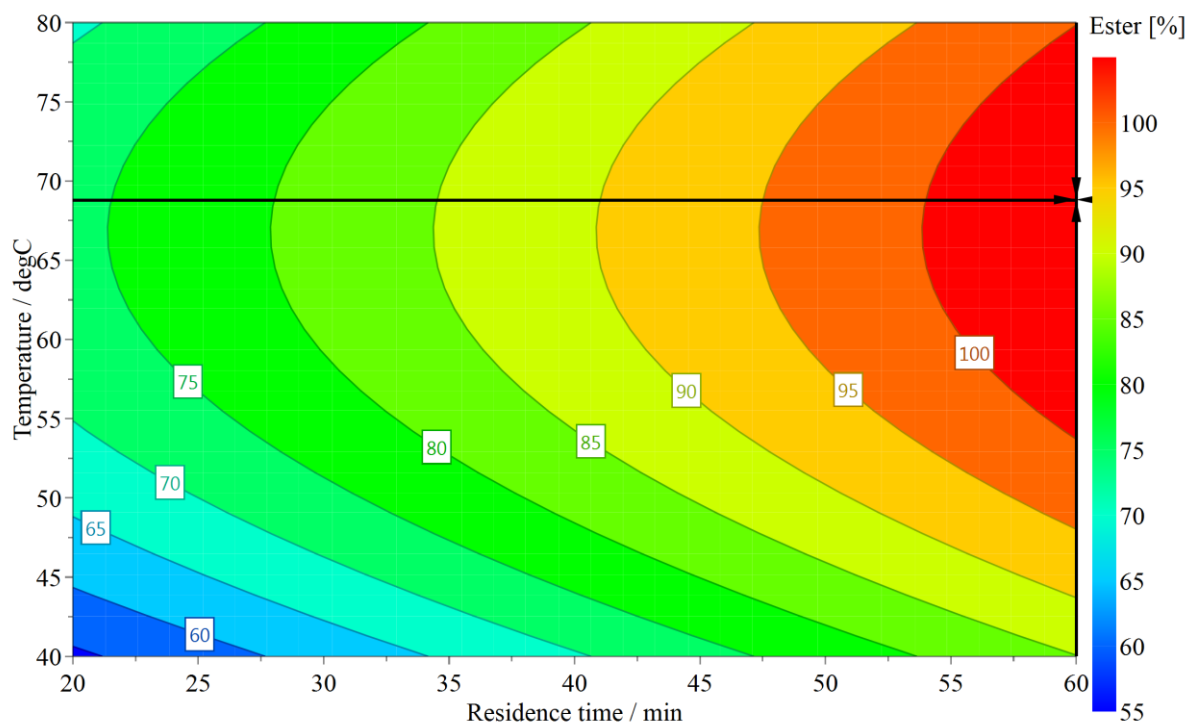
Figure 24. Contour plot showing conversion of **4.11** for tRes *vs*. temperature. Percentage conversion shown by the contour lines and colour: blue = low conversion, red = high conversion. Catalyst loading is not shown on the plot and is set to 1.0 g. Predicted optimum conditions denoted by the black cross.

4.2.2.4 Testing of Optimum Conditions

A reaction was carried out in the continuous reactor using the predicted optimum conditions, which gave 94% conversion of ester **4.11**. This was the same conversion as was achieved for the most forcing conditions, which was unsurprising as a large area of the contour plot showed 95 – 100% conversion (red). This also indicated that even less forcing conditions could still be used to achieve the optimum conversion, as the temperature was reduced from 80 °C to 67 °C without a drop in conversion. The model predicted a large area of the design space where the optimum conversion could be achieved, and so further reactions could be carried out to determine how far from the predicted optimum conditions reactions can be carried out without observing a decrease in conversion. The conversion obtained with the predicted optimum conditions was slightly lower than the predicted conversion. Solid formation was observed within the PTFE tubing between the reactor

outlet and the BPR inlet, which had been previously observed for some reactions with high conversions, and so the difference in conversion between the predicted and experimental could be attributed to the build-up of material within the tubing when high amounts of product were being formed. A control reaction was also carried out under these conditions, wherein the reactor was packed with glass beads only. No conversion was observed in this control reaction.

4.2.2.5 Comparison of 1,4-Dioxane and Methanol NH$_3$ solutions

To confirm that 1,4-dioxane was the best choice of solvent, the continuous reaction was tested using NH$_3$ solutions in MeOH at two different concentrations. The solutions were prepared by dilution of a commercially available 7 N NH$_3$ in MeOH solution and the concentration verified by titration with a standardised HCl solution. The two solutions (0.46 and 1.79 M) were tested in the continuous system. The concentration of methyl nicotinate **4.11** was 0.07 M so as to be consistent with the amount of substrate used in the 1,4-dioxane reaction and allow for a comparison in the results. Both of the reactions showed no conversion of methyl nicotinate **4.11** to nicotinamide **4.5**. It was proposed that this was due to the MeOH stripping water molecules (Figure 25) from the enzyme surface, leading to disruption of the catalyst structure and consequent deactivation.[141, 142] The enzyme surface forms interactions with water molecules that are integral to maintaining the 3D shape of the enzyme. If these water molecules are removed the 3D shape will be able to change, affecting the ability to accept substrates into the active site. The lack of conversion could also be a result of the MeOH being able to compete with the NH$_3$ to react at the acyl-enzyme intermediate, which would result in regeneration of the methyl ester substrate.

To probe this, the continuous reactor was packed with N435, primed with the NH$_3$ in MeOH solution (0.46 M) and heated to 67 °C. The flow rate was set to 0.047 mL min^{-1} and

the NH$_3$ in MeOH solution flowed through the reactor for 2 RV (tRes = 60 min). After this, the reactor was primed with NH$_3$ in 1,4-dioxane solution (0.5 M) and then a reaction stock solution of methyl nicotinate **4.11** was flowed through the reactor for 5 RV (tRes = 60 min). HPLC analysis of the samples obtained whilst flowing the reaction stock solution showed no conversion, indicating that the NH$_3$ in MeOH solution was deactivating the enzyme.
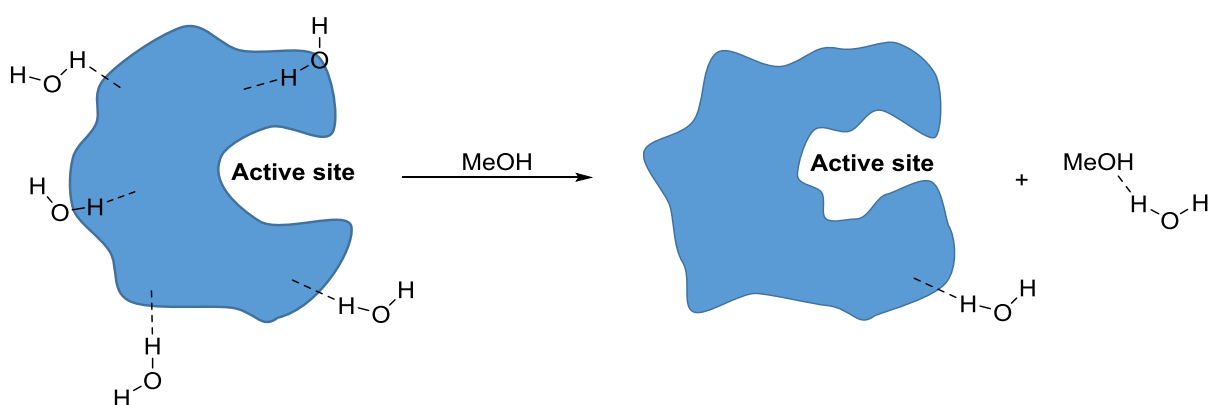
Figure 25. Proposed stripping of water molecules from enzyme structure in the presence of MeOH, showing loss of defined 3D structure.

These results confirmed that 1,4-dioxane was the most appropriate solvent of those investigated for this system, as the desired reaction occurred with high conversion and the solution is commercially available.

The dioxane solution was the most appropriate for the process of the solutions tested. However, the solvents tested in this study were by no means an exhaustive list and so a more favourable solvent in terms of green solvents[137] could be found with access to more resources and more time to increase the screen. Dioxane is not a preferred solvent as it is a suspected carcinogen, and so susbstitution is recommended according to the green solvent guide. Industrial processes have to meet specific targets in terms of green chemistry

approaches and so ensuring that green reagents and solvents are selected early in the process development would save time and money.

4.2.2.6 Reaction Metrics

Transfer of the process from batch to the continuous PBR and subsequent optimisation by DoE led to an improvement in conversion and a much reduced reaction time: 94% in 1 h compared to 15% in 27 h under batch conditions. The use of an experimental design allowed for reaction optimisation to be achieved faster and with fewer experiments than would be required in an OVAT. The catalyst loadings for the initial batch reaction and the optimised continuous procedure (per RV) were 14 mg and 5 g of catalyst per mmol of substrate, respectively. The high exposure of the substrate to catalyst achievable in the PBR resulted in high conversions in shorter tRes, which was not feasible in batch. The loading of the catalyst was high in the continuous reactor, which may seem unfavourable compared to batch, but the longevity study described in Chapter 2 showed that the catalyst was capable of operating for at least 30 h without any reduction in activity. If it could be assumed that the catalyst would have the same longevity in this case the catalyst loading would actually be much lower relative to the entire amount of reaction solution over time. Additionally, the tRes in the resolution study was 6 min and so the catalyst would have turned over more times in the 30 h than in the 60 min process developed in this Chapter. The turnover numbers (TON) for the resolution and ammoniolysis processes were, 1.05 and 0.196 mmol of substrate h^{-1} g of catalyst^{-1}, respectively. This means that 31.5 mmol of substrate was converted in 30 h in the continuous resolution but only 5.88 mmol of substrate would be converted in 30 h for the continuous ammoniolysis. The reduced number of turnovers per unit time may lead to the catalyst being active for an even longer period. A theoretical calculation of the catalyst loading relative to the entire solution that

would be flowed through the reactor during 30 h of operation would give 0.17 g of catalyst per mmol of substrate.

Additional reaction metrics were next calculated to assess the productivity and efficiency of the optimised continuous process. Space time yield (STY)[108] is a measure of productivity of the process in terms of amount of material produced per volume per time and is calculated according to Equation 2.5. The optimised continuous process for the production of nicotinamide **4.5** had an STY of 8.0 kg m^{-3} h^{-1}. This was quite low due to the long tRes and low substrate concentration, which both led to a reasonably low amount of product being produced per hour. Although the initial batch reaction carried out before optimisation of reaction conditions had an STY of 0.046 kg m^{-3} h^{-1}, which was considerably lower than the continuous process and due to the lengthy reaction time and low conversion observed when using un-optimised conditions. The nitrile hydratase process described by Nagasawa operated at a much higher substrate concentration of 12 M, giving a higher productivity.[133] However, the reaction time was 9 h and whole cell catalysts were used, which could not be recovered and re-used.

Process mass intensity (PMI) is a measure of the efficiency of the process and the associated waste.[143] It describes how much of the total reaction mass (including solvents and catalysts) is incorporated into the final product and is calculated according to:

$$Process\ mass\ intensity\ (PMI) = \frac{total\ mass\ in\ the\ process\ (kg)}{mass\ of\ product\ (kg)} \qquad (4.1)$$

The PMI for the optimised process was 177, this was high because the reaction concentration was quite low and so a higher proportion of the reaction mass was made up of solvent compared to the substrate and so a higher proportion of the reaction mass was not incorporated in the final product. Solvents are routinely recycled on an industrial scale and so the PMI for this process could be reduced by recycling the solvent. Also, for a

catalytic process to be industrially viable the catalyst needs to be re-used multiple times and so the catalyst is often omitted from calculations of waste and efficiency, which would lead to a more preferable PMI.

Both the STY and PMI may be improved by increasing the substrate concentration within the reactor. This variable was not investigated in the experimental design as it was desired to keep a low complexity in the design, with a low number of variables. If a fourth variable was introduced into the CCF design, 30 experiments would have been required (including 3 centre point repeats). Additionally, concentration screening carried out in Chapter 2 showed that higher concentrations would have required a longer tRes for this fully packed reactor bed. As the optimum tRes developed for nicotinamide production was already quite lengthy for flow (60 min), this would not have been preferable.

4.2.3   Discussion

The lipase catalysed ammoniolysis of methyl nicotinate **4.11** for the production of pharmaceutically relevant nicotinamide **4.5** was carried out using an immobilised enzyme within a continuous PBR. After initial testing in batch, the process was transferred to the continuous reactor and optimised using DoE.

The aim was to develop an efficient process for the synthesis of a generic pharmaceutical and synthetic building block. By transferring the process into a packed bed reactor, the substrate could be exposed to a much higher amount of catalyst than was feasible in a batch reactor, leading to a higher conversion in a shorter amount of time. When reactions were carried out in batch using the same amount of reaction solution and catalyst loading as in the continuous reaction it was difficult to mix the catalyst throughout the whole solution without increasing the stirrer speed to a point where high attrition of the particles was observed. The use of a PBR also allowed for the catalyst to be constrained within the

reactor bed and so isolated from the solution, which would allow for easier separation and re-use than in batch.

The immobilised catalyst used was commercially available and widely used in industry. The NH_3 solution was also commercially available and, whilst the solvent was not preferred in terms of green solvents,[137] a comparison against a MeOH solution confirmed that the 1,4-dioxane solution was the most appropriate for this system. In this case, the vast difference in reactivity between the two solvents meant that productivity outweighed greenness.

The reaction conditions were optimised *via* DoE using a CCF design for three variables: temperature, tRes and catalyst loading. Using this design, 17 experiments were carried out and the data modelled to be able to predict optimum reaction conditions. Using these predicted optimum conditions (67 °C, 60 min, 1 g catalyst) 94% conversion was achieved.

STY and PMI metrics were calculated to determine the productivity and efficiency of the process developed. This showed a significant improvement on the initial batch reactions due to the large reduction in reaction time. However, the substrate concentration was quite low in the reaction and so this led to lower values for STY and PMI than would be desired. This may be improved by further experimentation into the effect of concentration on the process.

Compared to existing ammoniolysis reactions in batch the procedure developed herein had a vastly reduced reaction time and so a much greater productivity. For example, the batch production of octanamide first described by Sheldon had a STY of 2.6 kg m^{-3} h^{-1},[126] compared to 8.0 kg m^{-3} h^{-1} for this process. The tRes was also shorter than for the continuous PBR employed by Slotema *et al.*[130] and the high conversion was achieved with a single pass through the reactor unlike the re-circulation required for the continuous

membrane reactor developed by Luque *et al*, for which a 95% yield after 10 h of operation was reported.[131]

No nicotinic acid by-product was observed in this system which is an advantage over the traditional chemical synthesis[132] of nicotinamide **4.5** and is analogous with the nitrile hydratase procedure.[136] As specific reaction conditions for the nitrile hydratase procedure used for manufacture by Lonza were not available, a more detailed comparison could not be made. Whilst the nicotinamide product itself is a generic pharmaceutical the nitrile hydratase procedure is not and is protected under patent and so the process is not widely applicable. The immobilised nitrile hydratase is protected and so is not commercially available, meaning that a direct price comparison could not be carried out between the nitrile hydratase and lipase. However, because N435 is commercially available and has been widely used in academia and industry and there are more examples of commercially available lipases than nitrile hydratase, it can be reasonably inferred that the lipase would be cheaper than the nitrile hydratase and so the contribution of cost from the enzyme to the whole process would be lower for the lipase catalysed process.

The reaction was not investigated any further as high conversions were obtained within a much shorter time frame than in batch. Ideally, a further reduction in the tRes for the process would be desired. However, further increasing the temperature would be unfavourable due to the effect on the long term stability of the enzyme, and the amount of catalyst could not easily be increased as this would require a larger reactor and heating block to be able to pack more into it. Therefore it would have been difficult to force this process to go any faster within these process constraints.

4.3 Ammoniolysis for the Production of Pyrazinamide

Pyrazinamide **4.12** (Figure 26) is a treatment for tuberculosis (TB) that is also on the WHO essential medicines list.[97] In 2005, 1.8 million people died from TB, with 95% of these deaths occurring in developing countries.[144] The higher occurrence of TB cases in developing countries reaffirms the need for cheap and efficient routes for pyrazinamide synthesis to ensure it is affordable and accessible.
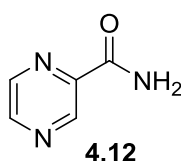
Figure 26. Structure of pyrazinamide **4.12**.

Pyrazinamide was synthesised by Hall and Spoerri in 1940 from pyrazine-2,3-dicarboxylic acid **4.13** (Scheme 73).[145] The first step involves decarboxylation at 210 °C to give pyrazine-2-carboxylic acid **4.14**, followed by esterification with MeOH to give methyl pyrazine-carboxylate **4.15**. The final step was the chemical ammoniolysis step for the reaction of NH_3 with methyl ester **4.15** to produce pyrazinamide **4.12**, which required reaction overnight to give a 92% yield. Pyrazinamide can also be synthesized enzymatically according to the nitrile hydratase process described above for the production of nicotinamide.[134]
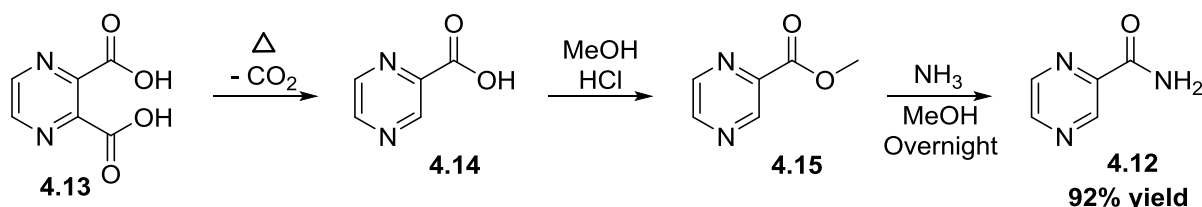
Scheme 73. Pyrazinamide synthesis developed by Hall and Spoerri.[145]

Suresh *et al.* reported the Pd-catalysed aminocarbonylation of hetero-aryl halides to produce primary amides, and applied this to the production of pyrazinamide **4.12** to achieve 76% yield on 10 mmol scale after 3 h (Scheme 74).[146] The use of expensive metal catalysts, ligands and a high number of reaction components would lead to a high reaction cost if this were to be carried out on larger scale. In addition, in pharmaceutical synthesis it is unfavourable to have a metal catalysed reaction as the final step in the synthesis of an active pharmaceutical ingredient (API). The United States Food and Drug Administration (FDA) guidelines for impurities in APIs requires Pd levels to be < 10 ppm and so stringent purification must be carried out to ensure the removal of the metal, leading to increased cost and processing time.[147] The continuous lipase procedure in this work uses far fewer reaction components and does not use metal catalysts and so circumvents these process issues.
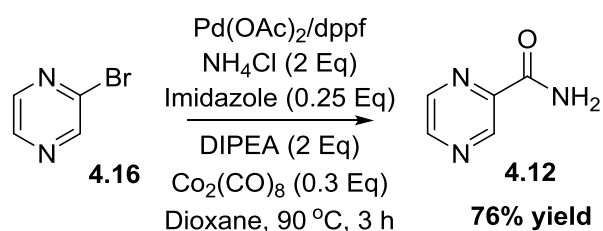
Scheme 74. Pd-catalysed aminocarbonylation to produce pyrazinamide **4.12**.[146]

An example of the continuous flow synthesis of pyrazinamide **4.12** was presented by Ingham *et al*. as an intermediate in the automated production of piperazine-2-carboxamide **4.18** (Scheme 75).[148] Pyrazinamide **4.12** was produced by the hydration of pyrazine-2-carbonitrile **4.17** using hydrous zirconia in a PBR in quantitative yields after a 20 min tRes at 100 °C. It was found that without the addition of H_2O to the reagent stream the catalyst activity ceased after 3 h of operation, indicating that all of the zirconia catalyst had been dehydrated.
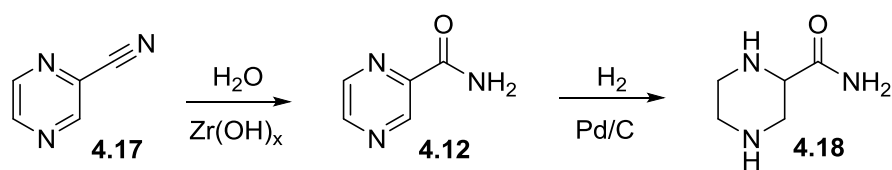
Scheme 75. Literature automated continuous flow synthesis of pyrazinamide **4.12** and subsequent reduction to piperazine-2-carboxamide **4.18**.[148]

In the following sections, the reaction conditions developed in the continuous production of nicotinamide **4.5** was applied to the synthesis of pyrazinamide **4.12** to determine optimum conversion. Green metrics were again calculated to determine productivity and efficiency.

4.3.1 Continuous Ammoniolysis

The optimum conditions determined for nicotinamide **4.5** were applied to the production of pyrazinamide **4.12** from the methyl ester **4.15** in the continuous reactor (Scheme 76).
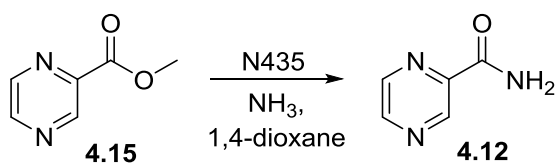
Scheme 76. Lipase catalysed ammoniolysis of methyl ester **4.15** to produce pyrazinamide **4.12**.

The continuous reactor set-up was the same as used for the nicotinamide studies (Figure 19). The continuous reaction using the predicted optimum conditions (60 min tRes, 67 °C, 1.0 g catalyst) gave full conversion of the methyl ester **4.15** to pyrazinamide **4.12** (Table 9,

Entry 1). Due to the complete conversion observed under these conditions the reaction was further investigated using less forcing conditions (Table 9). Complete conversion was observed even at the lower limits of the variables (Entry 3) and so the reaction at the lower limits was repeated with the catalyst further reduced to 0.25 g (Entry 4), for which 98% conversion was observed. A control reaction was carried out using the lower limits of tRes and temperature, with the reactor packed with glass beads (Entry 5). A small amount of pyrazinamide **4.12** product was observed in the HPLC samples, with a conversion of 1.5%. The control reaction was then repeated at the upper limits of tRes and temperature, for which a conversion of 10% was observed (Entry 6). A batch reaction was also carried out using the least forcing conditions, 98% conversion was observed after the 20 min reaction.

Table 9. Lipase catalysed **c**ontinuous ammoniolysis for pyrazinamide **4.12** formation.[a]

Entry	tRes / min	Temperature / °C	Catalyst loading / g	Conversion[c] / %
1	60	67	1.0	100
2	40	60	0.75[b]	100
3	20	40	0.50[b]	100
4	20	40	0.25[b]	98
5	20	40	0	1.5
6	60	80	0	10

[a]Reaction solution = 1.75 mmol methyl ester **4.15** in 25 mL NH_3 solution (0.5 M in 1,4-dioxane), biphenyl added as internal standard. Reactor volume = 2.8 mL; [b]Glass beads added to fill the reactor; [c]Determined by HPLC analysis, after calibration against internal standard.

4.3.1.1 Comparison of 1,4-Dioxane and Methanol NH_3 solutions

From the positive results using NH_3 in 1,4-dioxane described above, the reaction using the lower limit was repeated using the two different NH_3 in MeOH solutions used in the nicotinamide study (0.46 and 1.79 M). Ester **4.15** was not completely soluble in the MeOH solution and so the reactor set-up had to be modified to include a filter on the end of the

tubing that was pumping out of the reaction stock solution to prevent solid from blocking the pump head. The poor solubility meant that inconsistencies were seen in the amount of ester **4.15** observed in the HPLC samples. The reference sample taken from the reaction stock had to be filtered before running the HPLC analysis. Therefore, some of ester **4.15** was removed and a reference from which to calculate the conversion in the reactor *vs.* the stock solution could not be obtained.

However, all HPLC samples showed the presence of pyrazinamide **4.12**, including the reference sample taken from the reaction stock, indicating that the reaction was occurring without the N435 catalyst. A comparison of the concentrations determined from the HPLC data showed that the concentration of pyrazinamide **4.12** in the reaction stock was equal to the concentration in the samples collected at the outlet of the reactor and so no further reaction was occurring in the presence of the lipase. This reflected the deactivation of the enzyme observed when using the MeOH solutions in the nicotinamide study. The poor solubility, inconsistencies in analysis and un-catalysed background reaction showed that an NH_3 solution in MeOH was not appropriate for this continuous lipase system and confirmed that the NH_3 solution in 1,4-dioxane was the most suitable.

4.3.1.2 Reaction Metrics

The reaction metrics were again calculated to determine the productivity and efficiency of the process and to give a comparison of the two substrates. The STY was calculated for the continuous process (20 min, 40 °C, 0.5 g catalyst loading) as 26 kg m^{-3} h^{-1}. This showed a higher productivity than the nicotinamide process as the tRes was shorter for the pyrazinamide process and so more product was produced per hour. The PMI was calculated as 141, which was slightly lower than the nicotinamide PMI, due to the

reduction in catalyst loading. Again these metrics could be improved by investigation of the effect of substrate concentration, requiring further experimentation.

4.3.2 Discussion

Due to the high yield of pyrazinamide **4.12** achieved with the least forcing conditions, further optimisation for this substrate was deemed unnecessary. The pyrazinamide reaction required a shorter tRes to achieve the same high conversions as for the nicotinamide reaction, indicating that the catalyst was more reactive toward the pyrazinamide substrate. This is due to the presence of the second nitrogen atom in the aromatic ring for the pyrazine, which makes the ring more electron deficient and consequently makes the carbonyl carbon more electrophilic. The higher electrophilicity of the carbonyl carbon allows for more facile nucleophilic attack by the serine residue in the active site and by NH_3 and so the reaction progress more readily than for nicotinamide.

The continuous enzymatic process developed in this work achieved the same conversion within the same tRes as in the continuous chemical process described by Ingham *et al*.[148] However, the reaction temperature was significantly reduced for the enzymatic reaction (40 °C) compared to the chemical reaction (100 °C), showing a much lower energy demand for the enzymatic process.

4.4 Ammoniolysis of a Chiral Substrate

Wegman *et al*. described the lipase catalysed ammoniolysis of phenylglycine esters and *in situ* racemisation under batch conditions (Scheme 77, A).[129] Variation of the ester group, solvent and temperature produced phenylglycine amide **4.20** in 85% conversion and 88% *ee* for the DKR process. The coupled reaction had to be carried out at -20 °C to favour

ester racemisation over amide racemisation, which required a 66 h reaction time. The individual ammoniolysis reaction gave 46% conversion to amide **4.20** with 78% *ee* after 4 h at 40 °C (Scheme 77, B). Indicating the reaction was not very selective.
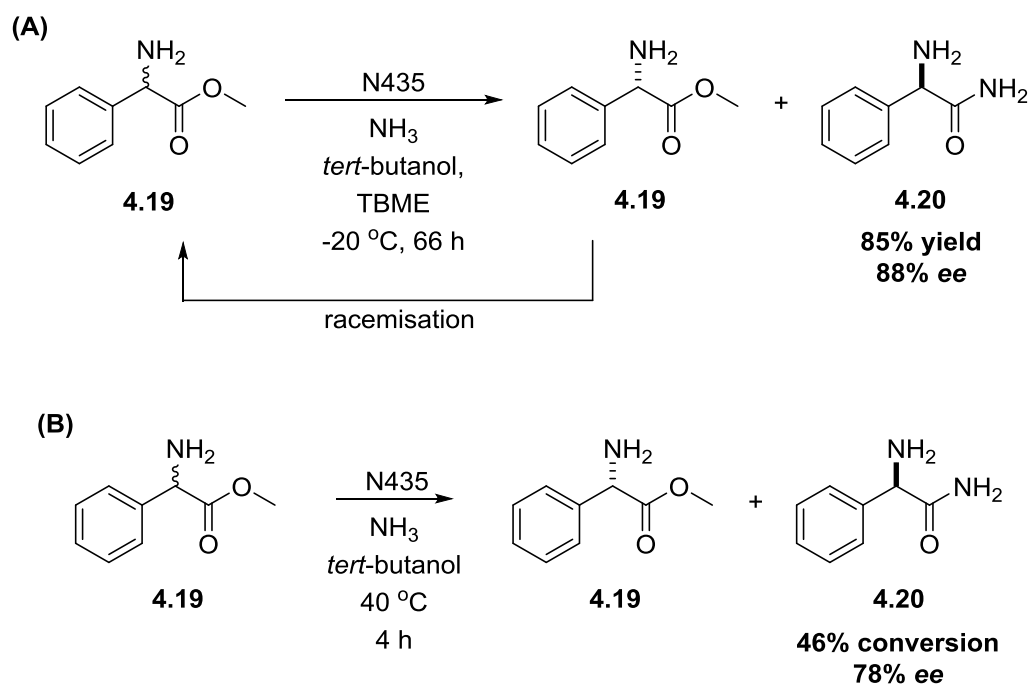
Scheme 77. Ammoniolysis of phenylglycine with *in situ* racemisation. (A): Dynamic kinetic resolution; (B): Individual ammoniolysis reaction.[129]

The use of the continuous process developed herein could reduce these lengthy reaction times. It was desired to test the process developed on a chiral substrate to determine the enzyme selectivity under ammoniolysis conditions and to be able to produce single enantiomers, which would have greater value for the production of pharmaceutical molecules.

4.4.1 Batch Ammoniolysis

The ammoniolysis of *N*-acetyl-*(D/L)*-phenylalanine **4.21** was investigated, to determine the selectivity of the reaction. The predicted optimum conditions in terms of temperature (67 °C) and catalyst loading (scaled down according to reaction volume) from the nicotinamide optimisation were used in batch for the reaction with *N*-acetyl-*(D/L)*-phenylalanine **4.21** (Scheme 78).
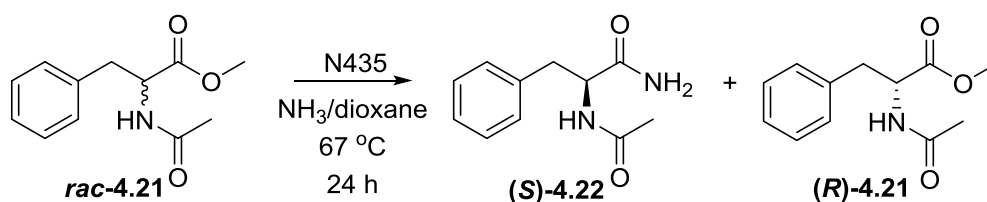
Scheme 78. Batch test of ammoniolysis of *N*-acetyl-*(D/L)*-phenylalanine **4.21**.

The *N*-acetyl protected version was used to prevent any reaction of the unprotected amine with the acyl-enzyme intermediate, formed within the active site, which could have led to dimer by-products. After 24 h, no reaction was observed and the *ee* of ester **4.21** remained at 9% throughout the course of the reaction.

A range of immobilised lipase enzymes were then tested in batch to try to obtain some reactivity. The enzymes used were Lipase A from *Candida antarctica* (CalA), *Candida rugosa* lipase and *Thermomyces lanuginosus* lipase (TLL), all of which were immobilised on Immobead 150. Batch reactions were carried out for each of the enzymes, and for N435 as a comparison, using conditions based on those reported by López-Serrano *et al.*[149] The reactions were carried out at 50 mM substrate concentration, in NH_3 solution (0.5 M in 1,4-dioxane) at 40 °C . Two reactions were carried out using *C. Rugosa* lipase as the activity for this batch of enzyme was much lower than the other enzymes tested and so a second reaction was carried out with 3.5 g lipase to achieve a similar activity to the other enzymes. However, the mass of immobilised *C. Rugosa* lipase required to achieve the higher activity

was so large that the reaction mixture was unable to be stirred properly. Regardless, no conversion was observed using any of the enzymes, under these conditions.

The literature procedures used NH_3 saturated *tert*-butanol and so the 0.5 M NH_3 solution in 1,4-dioxane may not be concentrated enough for this substrate. The literature procedure also required sub-zero temperatures to achieve a reasonable conversion and selectivity, which would not be possible with the continuous reactor set-up described in this work.

4.5 Conclusions

Lipase catalysed ammoniolysis was investigated using the continuous PBR for the production of two essential medicines: nicotinamide **4.5** and pyrazinamide **4.12**. The continuous procedure was first developed for nicotinamide **4.5** production and optimised using a DoE approach to achieve high conversion to product in a short reaction time compared to batch studies.

Whilst this study was being carried out, Andrade *et al*. published a similar system for the production of carboxamide derivatives using immobilised CalB in a PBR.[150] The study demonstrated the coupling of amines and esters to produce carboxamides in generally high yields in a short tRes (10 min). They also employed the reactor for the coupling of NH_3 with a number of methyl esters (Scheme 79).
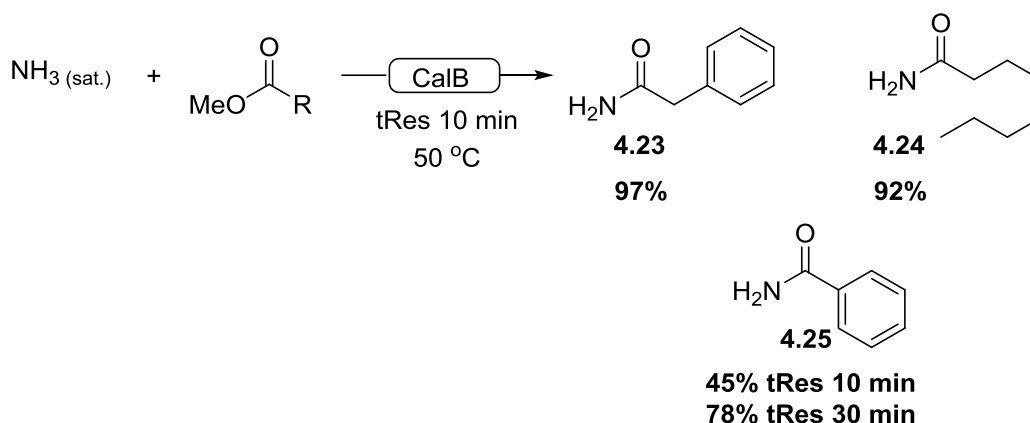
Scheme 79. Literature continuous CalB catalysed ammoniolysis.[150]

The reaction to produce **4.23** and **4.24** gave high conversions for the 10 min tRes however, the tRes had to be increased for product **4.25** to achieve a reasonable conversion. Whilst this literature procedure had shorter tRes than the process developed herein, the substrate scope indicated that the tRes needed to be increased to achieve high conversion for different substrates. Also, the reaction concentration was 3.5-fold more dilute for the literature procedure and used saturated NH_3 solution, which would indicate a lower process efficiency. Interestingly, they also showed continuous operation of the coupling of amines and esters over a 14 h period (84 x tRes) without any loss of CalB activity. This reflects the results described in Chapter 2 for the stability of the enzyme over long periods (30 h) and re-iterates the potential for the long term operation of the continuous ammoniolysis developed herein.

The optimised procedure developed for nicotinamide **4.5** was then applied to the continuous production of pyrazinamide **4.12**. The higher activity observed for this substrate allowed for much less forcing reaction conditions to be used without a loss in conversion.

To determine the selectivity of the lipase under ammoniolysis conditions, a chiral substrate **4.21** was then studied. However, no reactivity was observed using the conditions tested.

The literature precedence for this type of substrate showed low conversions and the requirement for sub-zero temperatures, which was not feasible for this piece of work. Unfortunately, the chiral example could not be studied any further.

The process described herein represents a cheap and efficient route to two generic pharmaceutical molecules, with the potential for high throughput *via* the continuous reactor.

5 Iridium Catalysed *N*-Alkylation of Primary Chiral Amines

5.1 Introduction

The formation of dimers during the attempted racemisation of 1-phenylethylamine **5.1** described in Chapter 3 prompted investigation into the *N*-alkylation reaction of 1-phenylethylamine **5.1** *via* coupling to another amine, using hydrogen borrowing methodology (Scheme 80).[29]
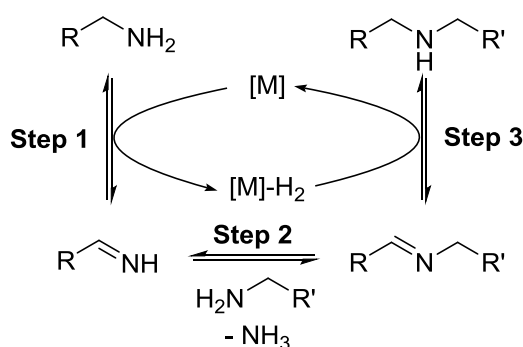
Scheme 80. Hydrogen borrowing methodology for the coupling of amines.

The dimer formation observed was a result of the coupling of two molecules of the same type of amine in Step 2 of Scheme 80. To achieve *N*-alkylation using this method, a second type of amine needs to be coupled to the first amine type in Step 2. This *hetero*-coupling must be favoured over the *homo*-coupling to preferentially form the desired *N*-alkylated product.

The *N*-alkylation reaction could present an opportunity to utilise the remaining amine enantiomer from the enzymatic resolution of 1-phenylethylamine **5.1** described in Chapter 2 (Scheme 81).

145
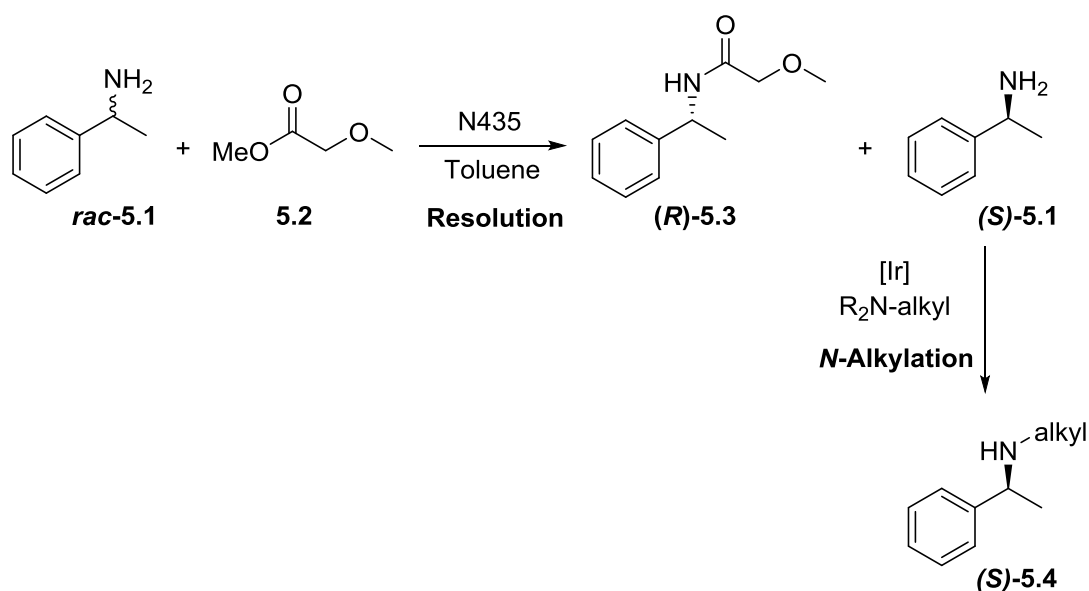
Scheme 81. Proposed coupling of enzymatic resolution and iridium catalysed *N*-alkylation.

In this chapter, the iridium catalysed coupling of two amines for the *N*-alkylation of **5.1** was investigated with a view to coupling the reaction to the continuous resolution process described in Chapter 2. The *N*-alkylation of *rac*-**5.1** was first studied using a heterogeneous and a homogeneous catalyst. DoE was employed to determine significant variables and optimum operating conditions. The *N*-alkylation of single enantiomer **5.1** was then studied for coupling to the enzymatic resolution. The selectivity observed gave some insights into the catalytic mechanism, which are also presented.

5.2 *N*-Alkylation of Racemic 1-Phenylethylamine

5.2.1 Heterogeneous catalyst

5.2.1.1 Batch Reactions

The coupling of *rac*-**5.1** with *di-iso*propylamine **5.5** using an iridium Cp* catalyst was studied (Scheme 82). Initially, the reactions were investigated using a heterogeneous Cp*iridium catalyst **5.9**), which was immobilised on the Wang resin through a 5-carbon

chain (supplied by Yorkshire Process Technologies).[114] The use of an immobilised catalyst would enable the coupling of the *N*-alkylation and enzymatic resolution processes in continuous flow as the separate catalysts could be set-up in packed bed reactors in series. This would allow for isolation of the two catalysts and therefore operation of the individual catalytic reactions under different conditions. *Di-iso*propylamine was chosen for this study as this amine donor performed the best in a literature screen, providing 98% of the desired *N*-isopropyl product after 10 h at 155 °C.[29]
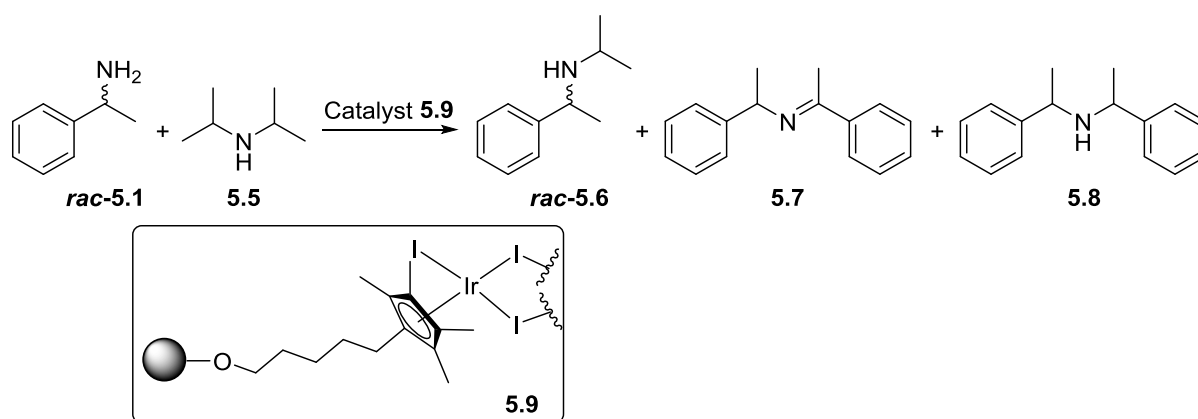
Scheme 82. *N*-alkylation of *rac*-**5.1** using *di-iso*propylamine **5.5** and immobilised Cp*iridium catalyst **5.9**.

The desired product **5.6** may be obtained according to the proposed mechanism, shown below (Scheme 83).
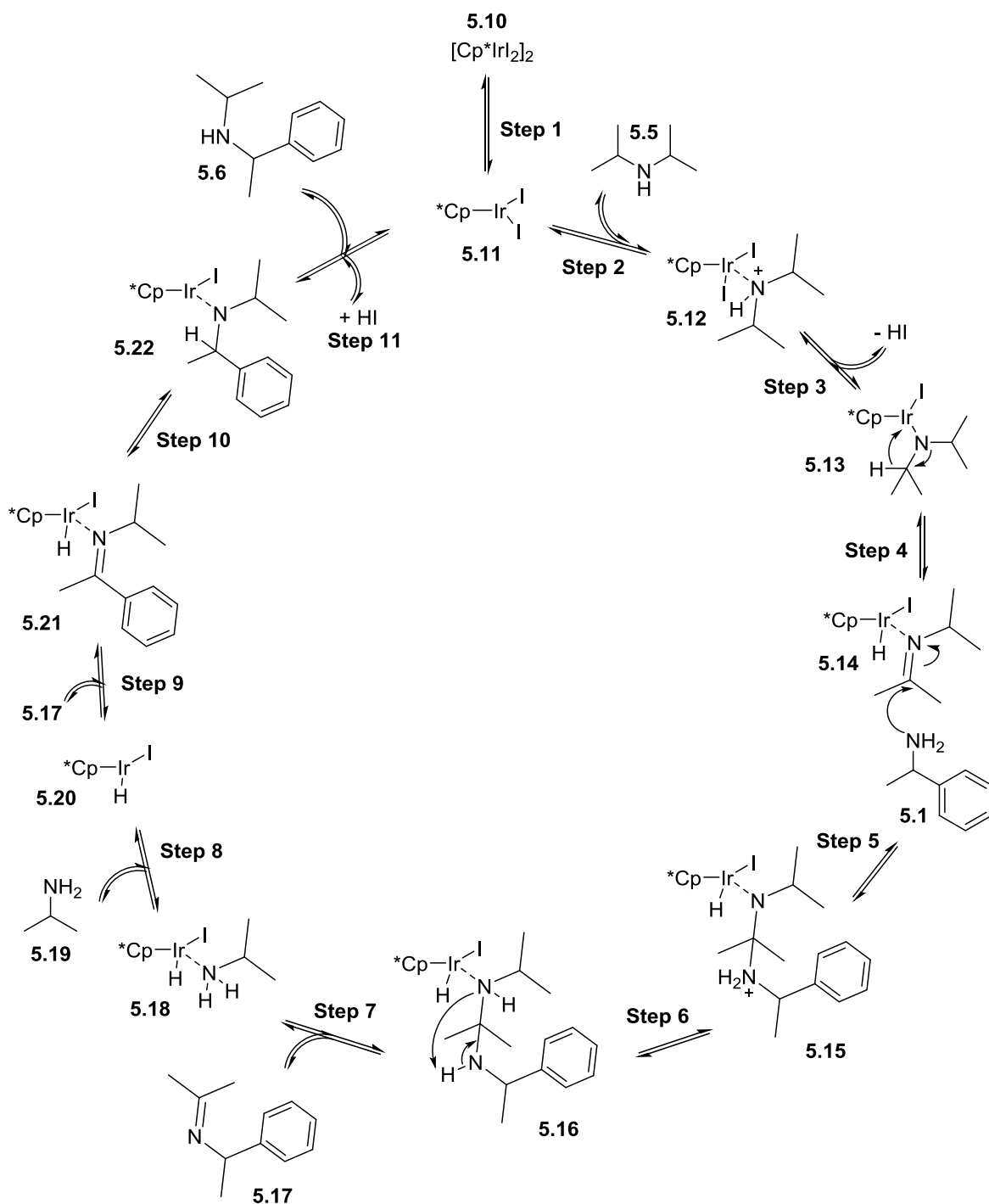
Scheme 83. Proposed catalytic cycle for [Cp*IrI₂]₂ catalysed *N*-alkylation.

In the mechanism shown, the cross-coupled imine **5.17** de-coordinates from the catalyst and then re-coordinates for the hydrogenation step to occur and to re-form the active catalyst. This could be confirmed by labelling studies, wherein deuterated imine **5.17** could be added to the reaction mixture, to see if the deuterium is observed in the final product

5.6. As the steps are reversible, the incorporation of deuterium in the product would mean that **5.17** is released from the catalyst in Step 7. This would allow both **5.17** and the deuterated version to re-coordinate in Step 9, leading to deuterated product. The *homo-coupled* products **5.7** and **5.8** would be formed by the coordination of amine **5.1** to the catalyst in Step 1 of the cycle.
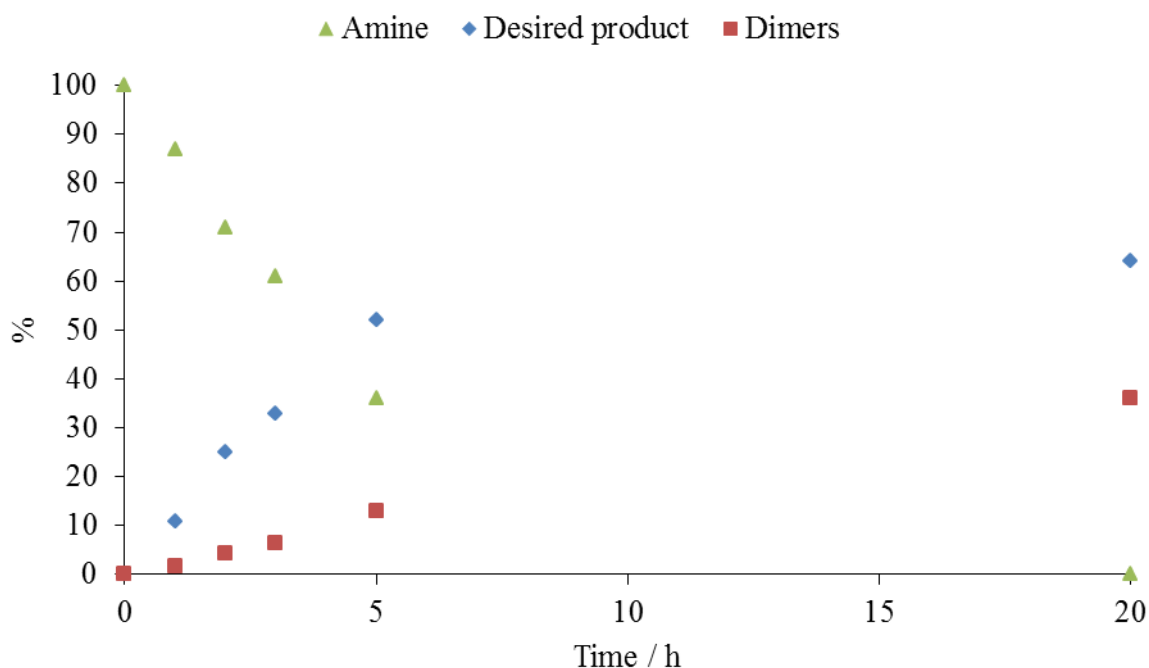
Figure 27. *N*-alkylation of ***rac*-5.1** with **5.5** using immobilised Cp*iridium catalyst **5.9**, under batch conditions. (***rac*-5.1** shown in green, desired product ***rac*-5.6** shown in blue, dimers shown in red).

An initial reaction was carried out under batch conditions, at 130 ℃ in xylene with a catalyst loading of (0.5 mol%) and 3 equivalents (Eq) of **5.5** (Figure 27). The reactions were analysed by GCMS to determine the percentage composition of the substrate and products within the reaction sample. The percentage composition was determined from the area% of each component that was obtained from the auto-integration feature on the GCMS data analysis software (ChemStation). After 20 h, full conversion of amine **5.1** was

observed to the desired *N*-alkylated product **5.6** (63%) and dimers (37%), compared to the reaction using homogeneous [Cp*IrI$_2$]$_2$ reported by Saidi *et al.* to give a 98% yield of **5.6** at 155 ºC in xylene after 10 h.[29]

The full conversion achieved was encouraging, however the reaction time was long and selectivity for desired product was only 63%. It was envisaged that the unfavourably long reaction time could be reduced by the more forcing conditions achievable in the continuous PBR and that the selectivity could be improved through optimisation strategies.

Previous unpublished studies within the research group had shown that the polymer support and immobilised catalyst were stable for longer periods at temperatures lower than 130 ºC,[117] therefore the temperature was reduced to 100 ºC for further reactions to allow for recycling of the catalyst.

5.2.1.2 Continuous Reactions

As the reaction was shown to proceed in batch, the reaction was transferred directly to a continuous system using the immobilised catalyst within a PBR without further investigation in batch. This continuous system would allow for the reaction mixture to be exposed to a much higher amount of catalyst than would be feasible in batch. These more forcing conditions within the flow reactor would reduce the reaction time required to achieve high conversion. The PBR would also allow for easy re-use of the catalyst as the catalyst is retained in the reactor and so separate from the reaction solution.

The continuous reactor set-up (Figure 28) was described in detail in Chapter 2 and consisted of a 2.8 mL stainless steel tubular reactor (1/4" OD, 1/8" ID), which was manually packed with immobilised catalyst **5.9** (ICP > 0.3 mmol/g) to a loading of 4.7 mol%, calculated relative to one reactor volume (RV). The reactor was housed within an

aluminium heating block under Eurotherm temperature control. *rac*-**5.1** (0.5 M) and **5.5** (3 Eq) were dissolved in toluene as a single stock solution. The stock solution was fed into the reactor using a Jasco PU-2085 dual piston pump, with a 60 min residence time (tRes), under 40 psi back pressure.
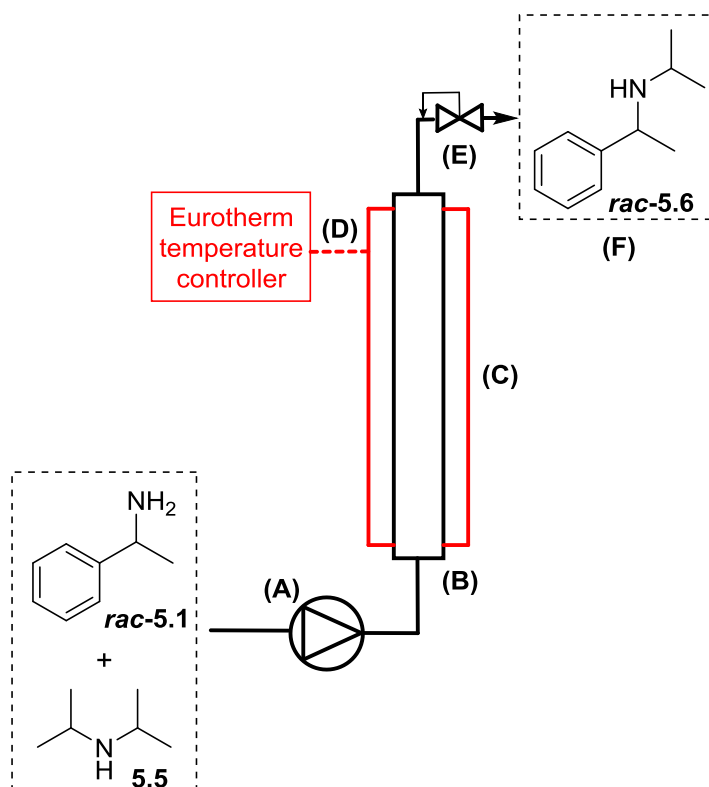
Figure 28. Reactor set-up for continuous *N*-alkylation using immobilised catalyst. (A): Piston pump; (B): Tubular reactor packed with immobilised catalyst; (C): Aluminium heating block; (D) Eurotherm temperature controller; (E) BPR; (F): Product outlet and collection.

For this reaction the conversion observed was very low with the highest value being 24 area% after 3 RV. This also rapidly decreased to 6 area% after 7 RV, which indicated deactivation of the catalyst (Figure 29). It was observed that the eluent from the reactor was highly coloured, suggesting leaching of the iridium from the resin. This was investigated further to determine the reason for the low conversion and to ascertain whether the catalyst had leached off the resin. A microwave batch test using the catalyst

recovered from the continuous reactor showed no conversion after heating to 100 °C for 3 x 60 min periods. A further microwave reaction using a fresh portion of immobilised catalyst, again showed no conversion after heating to 100 °C for 3 x 60 min periods. This further testing indicated that higher temperatures would be required for the reaction to progress in the desired time scale. As previously stated, the heterogeneous catalyst cannot be operated at higher temperatures due to long term stability, therefore all further reactions were carried out using homogeneous catalyst.
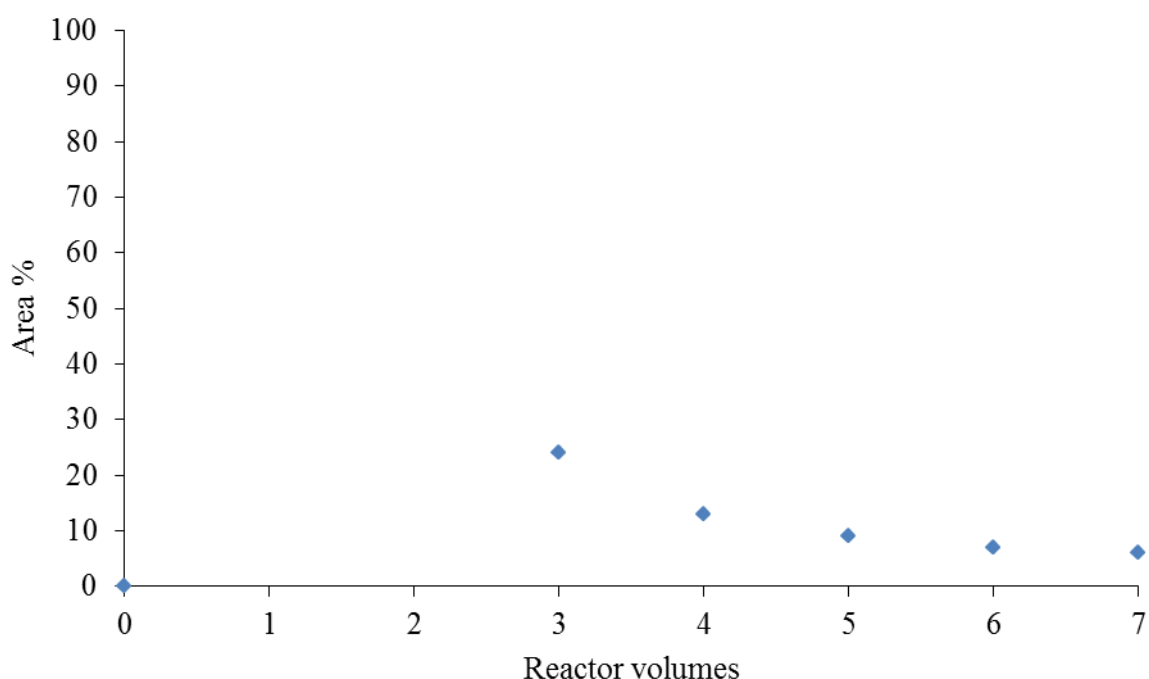
Figure 29. Continuous *N*-alkylation of *rac*-**5.1** using immobilised Cp*iridium catalyst **5.9**. (Area% of desired product **5.6** in each RV sample was determined by GCMS analysis, 1st and 2nd RV were too dilute to carry out GCMS analysis).

The reaction time could not be increased in the continuous reactor due to three main reasons. Firstly, due to the desired coupled process. If one of the reactions is much slower than the other then it would be impractical to combine then as it would be difficult to match the flow rates and tRes. Secondly, long residence times were not feasible with the

current pump capabilities as the flow rates required would be lower than could be reliably achieved. Thirdly, a long tRes and accompanying slow flow rate creates a low fluid velocity within the tube, which leads to a broadening of the residence time distribution (RTD).[151] A broadening of the RTD can lead to variation in the conversion observed as a large number of molecules will have a shorter tRes than desired and so a lower conversion may be observed. It can also cause a reduction in the selectivity of a reaction, when the selectivity for a particular product is dependent on the tRes. The molecules with a longer tRes than desired are exposed to the reaction conditions for a longer period, which may favour a different reaction pathway or cause over-reaction of the desired product. This can lead to an increase in the amount of by-products and so reduction in the selectivity.

5.2.2   Homogenous catalyst

5.2.2.1 Microwave Batch Reactions

Due to the problems with the immobilised catalyst, further studies were carried out using the homogeneous $[Cp*IrI_2]_2$ catalyst (**5.10**). This catalyst was used by Saidi *et al.* for the selective cross coupling of two amines to produce *N*-isopropyl derivatives of anilines and benzylamines.[29] Whilst these reactions were generally high yielding, long reaction times of 10 h were used. The aim of this piece of work was to improve on these reaction conditions through optimisation by DoE, thereby reducing reaction times whilst maintaining high conversion and selectivity.
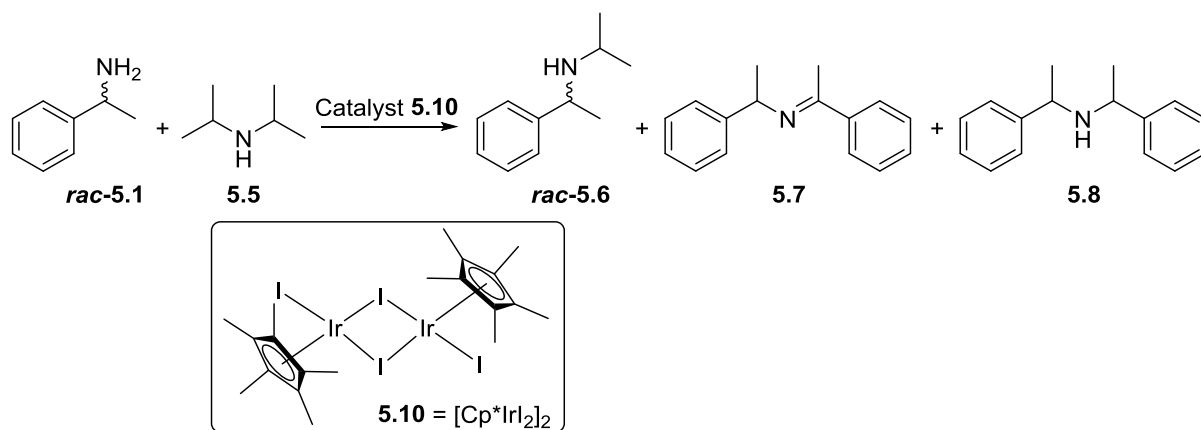
Scheme 84. *N*-alkylation of *rac*-**5.1** using **5.5** and homogeneous [Cp*IrI$_2$]$_2$ catalyst **5.10**.

Reactions were carried out under microwave batch heating using homogeneous [Cp*IrI$_2$]$_2$ catalyst **5.10**, microwave heating was used as it enabled higher temperatures to be reached than conventionally heated batch. As the catalyst was not immobilised on a resin, it could be heated to higher temperatures and so all microwave testing was carried out at temperatures of 100 °C and above, to ensure higher conversions.

Initial experiments using microwave heating (Table 10) confirmed that 100 °C was too low for the reaction to proceed in these short reaction times (Entries 1 and 2). Temperatures of 150 °C and above were sufficient to obtain conversion within the desired time frame, with full conversion being observed after only 10 min at 220 °C (Entries 6 and 7). Interestingly, the selectivity for desired product was greatly increased when using 3 Eq of **5.5**, compared to 1 Eq (Entries 6 and 7). These experiments also showed that the catalyst loading could be reduced to only 0.1 mol% at the highest temperatures and still achieve full conversion (Entry 7).

Table 10. Racemic *N*-alkylation initial microwave reactions.[a]

Entry	Temperature / °C	Time / min	Catalyst loading / mol%	Conc of **5.1** / M	Eq	Amine **5.1**[c] / %	Desired product **5.6**[c] / %	Dimers[c] / %
1	100	10	0.1	0.1	1	100	0	0
2	100	30	0.2	1	3	100	0	0
3	150	10	1.0	0.5	3	28	69	3
4	200	10	1.0	0.5	3	5	84	11
5	200	30	0.5	1	3	0	89	11
6[b]	220	10	0.2	1	1	0	64	36
7[b]	220	10	0.1	1	3	0	93	7

[a]Reaction conditions: **rac-5.1**, *di-iso*propylamine **5.5**, [Cp*IrI$_2$]$_2$ **5.9**, toluene, biphenyl added as internal standard, total reaction volume = 2 mL; [b]Solvent = anisole; [c]Percentage composition determined by GCMS analysis; Eq = equivalents of **5.5**.

The overall aim was to use a continuous reactor for the *N*-alkylation reaction to allow coupling to the continuous resolution, however it was decided to carry out further screening and optimisation experiments using microwave batch heating to allow for smaller reaction volumes to be used so that less catalyst could be used per experiment. The optimum conditions determined from the microwave studies would then be transferred to the continuous reactor for development of the coupled process.

5.2.3 Optimisation of Racemic *N*-Alkylation

5.2.3.1 Screening Design

The reaction was optimised using a DoE approach, with the aim to maximise the yield of *N*-alkylated product and limit the yield of dimers. First, screening experiments were carried out following a fractional factorial Resolution V design, to determine the important variables.[152, 153] A fractional factorial design was chosen as this would reduce the number of experiments to be carried out and so would save time and reagents. For screening purposes a fractional factorial is sufficient to determine the few important variables from a

large group of variables. A full factorial two-level (-1 and +1) design for 5 variables would require 32 experiments. The fractional factorial Resolution V two-level design for 5 variables required 16 experiments (plus 3 mid-point experiments) and so was preferred.

The variables considered were: temperature, reaction time, catalyst loading, concentration of **5.1** and Eq of **5.5** (Table 11). The limits for the variables were chosen based on the results obtained in the initial microwave reactions described above and the desire to have short reaction times ($\leq$ 30 min) and reasonably low catalyst loadings ($\leq$ 0.5 mol%). The upper limit of temperature was set to 200 °C as 220 °C could not be achieved consistently within the microwave.

Table 11. Variables with limits for first racemic *N*-alkylation screening design.

Variable	Low	Mid	High
Temperature / °C	150	175	200
Reaction time / min	10	20	30
Catalyst loading / mol%	0.1	0.3	0.5
Amine **5.1** concentration / M	0.1	0.55	1.0
Eq of **5.5**	1	2	3

All further reactions were analysed by achiral GC and conversions were determined from the analyte peak areas, after calibration against internal standard (for further details and calibration plots see Experimental Chapter).

The responses generated were: conversion of amine **5.1**, desired product yield, dimer yield and selectivity. The results from the screening design are shown in Appendix B and showed a broad range in conversions of amine **5.1** from 0 to 93%. Statistical design software (MODDE) was used to generate models for each response (Figure 30), using multiple linear regression (MLR).
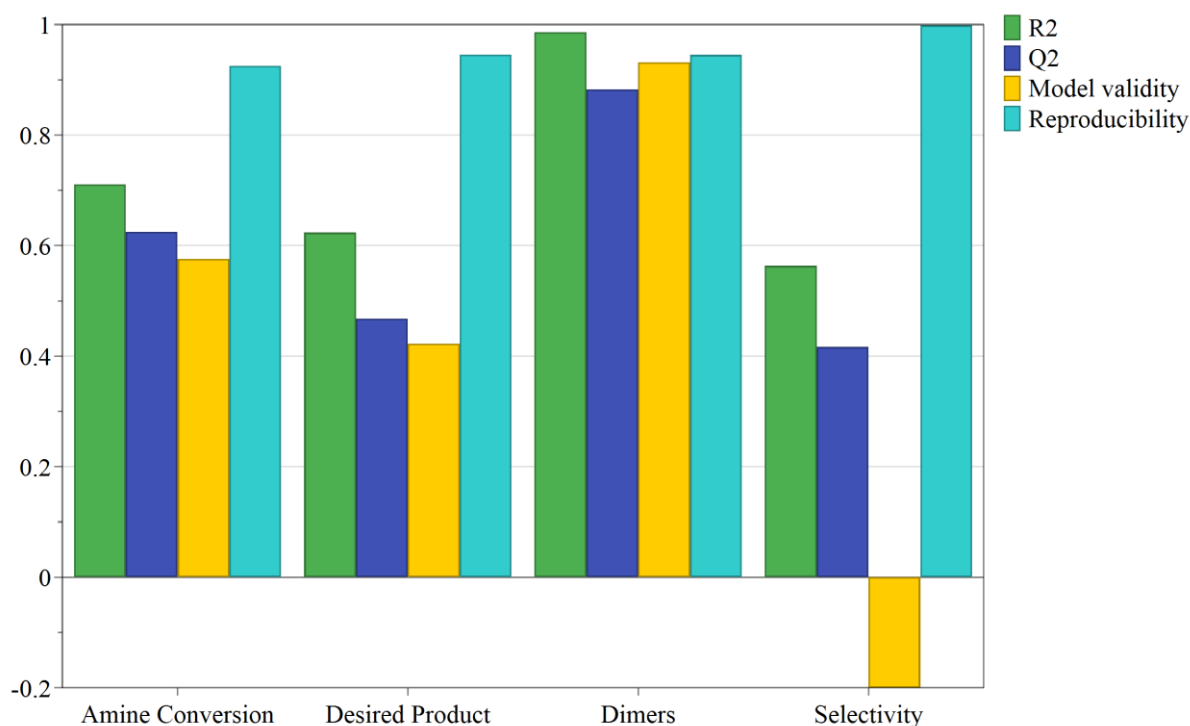
Figure 30. Summary of fit plots for all 4 responses from the first screening design.

From this screening design, a good model fitting with high values for R^2, Q^2 and model validity was only achieved for the dimer yield response. After analysis of the experimental data points, it was determined that the range in the results was too great to obtain a reliable model fitting for the other 3 responses. For example, the data obtained for conversion of amine **5.1** ranged from 0 – 93%. The model works by fitting polynomial curves to the data until it finds the best fit. When the data covers such a large range of responses, as obtained in this screen, the model can struggle to fit the data as exampled by Figure 31. For this theoretical data set, a polynomial curve has been fit to the data over the whole range (A) and over part of the range (B). This shows that the curve can achieve a more reliable fit when a narrower data range is used as the curve cannot take into account any deviations from the curve, as shown in (A). For this same reason data cannot be extrapolated from the curves obtained within the model, as a good fit outside of the limits tested for the variables cannot be assured.
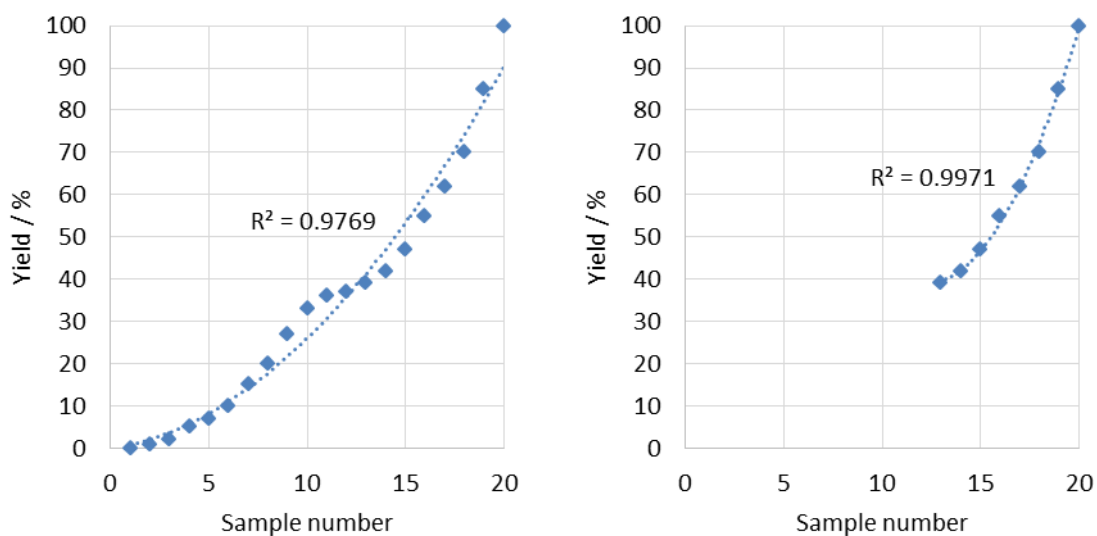
Figure 31. Comparison of polynomial fitting for a theoretical data set over different ranges.

Due to the difficulties with the data fitting, the screening design was repeated with new limits for the variables to narrow the data range. This would be advantageous for the model fitting and would also act as a second step to further hone the reaction conditions to give the best conversions. The selection of new limits for the variables was carried out as follows. The reactions at 150 °C showed the lowest conversions and so the lower limit was increased to 180 °C. The range for the catalyst loading was narrowed as the conversion was lower using 0.1 mol%, however the maximum limit of 0.5 mol% was maintained so as to conserve catalyst and reduce the cost associated with the process. The limits for the reaction time were not changed as a short reaction time was still desired. It was observed that the higher the Eq of **5.5** the greater the selectivity for the desired product and so the number of Eq was increased for the new screen to enhance the selectivity. To check whether the new limits would be appropriate, scoping reactions were first carried out at the upper and lower limits of the variables as well as the mid-points (Table 12).

Table 12. Scoping reactions for second set of racemic *N*-alkylation variable limits.[a]

Reaction Level	Temperature / °C	Reaction time / min	Catalyst loading / mol%	Amine **5.1** concentration / M	Eq	Desired product **5.6**[b] / %
Low	180	10	0.3	0.5	2	50
Mid	190	20	0.4	0.75	3.5	95
High	200	30	0.5	1.0	5	87

[a]Reaction conditions: ***rac*-5.1**, *di-iso*propylamine **5.5**, [Cp*IrI$_2$]$_2$ **5.10**, anisole, biphenyl added as internal standard; [b]Determined by achiral GC analysis, after calibration against internal standard; Eq = equivalents of **5.5**.
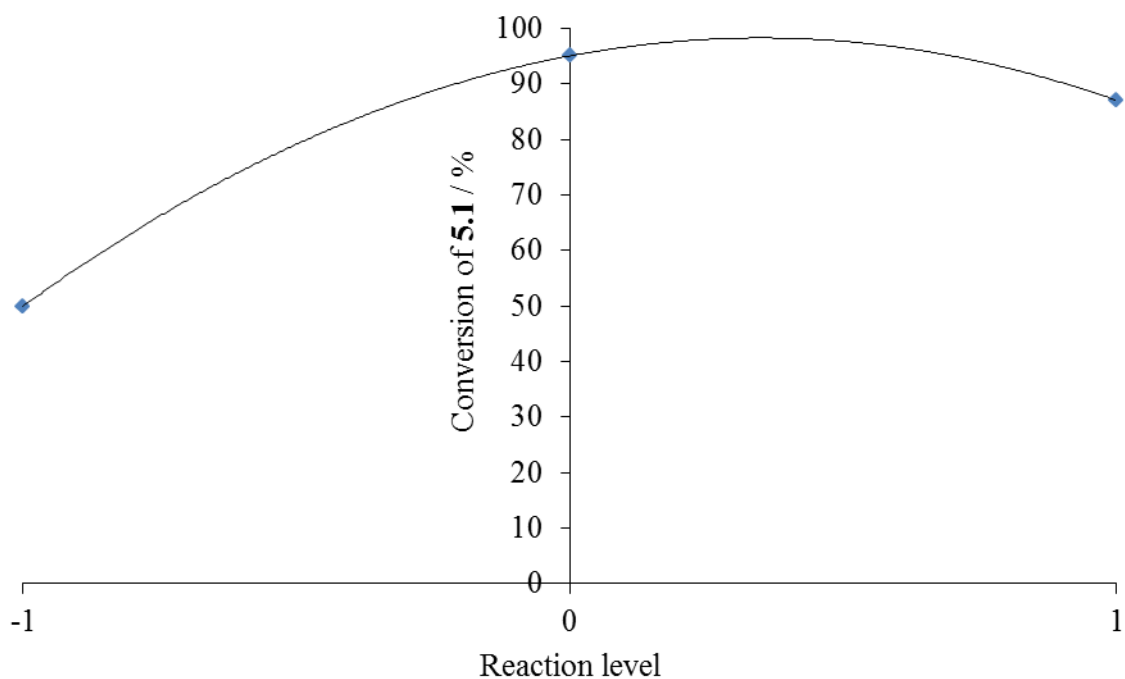
Figure 32. Scoping reactions for the second set of racemic *N*-alkylation of variable limits.

In Figure 32 the results from the scoping reactions were plotted with the reaction level being attributed to -1 for the lower limit, 0 for the mid-point and +1 for the upper limit. The results showed that the limits chosen for the variables were appropriate, and so these conditions were then used for the second screening design (Table 13).

Table 13. Variables with limits for the second racemic *N*-alkylation screening design.

Variable	Low	Mid	High
Temperature / ºC	180	190	200
Reaction time / min	10	20	30
Catalyst loading / mol%	0.3	0.4	0.5
Amine **5.1** concentration / M	0.5	0.75	1.0
Eq of **5.5**	2	3.5	5

Again, 19 experiments were carried out according to the fraction factorial Resolution V screening design (Table 44). The results from the screening design were modelled using statistical design software to identify important variables and determine the optimum reaction conditions. These results showed a much narrower range than the first screen, with conversion of amine **5.1** values between 74 and 97%.

5.2.3.2 Models from Screening Designs[140]

For the second screening design, models were generated for each of the 4 responses (Figure 33) and then analysed for the degree of fitting. The models generated for the conversion of amine **5.1** and desired product yield showed good model fitting in terms of high R^2 and Q^2, however the model validities were low. The models generated for the dimer yield and selectivity showed poor model fitting as the values for R^2, Q^2 and validity were all low. The reproducibility is also shown in Figure 33 and was high for all 4 responses due to very low variation in the data obtained from the replicates of the centre point experiments.
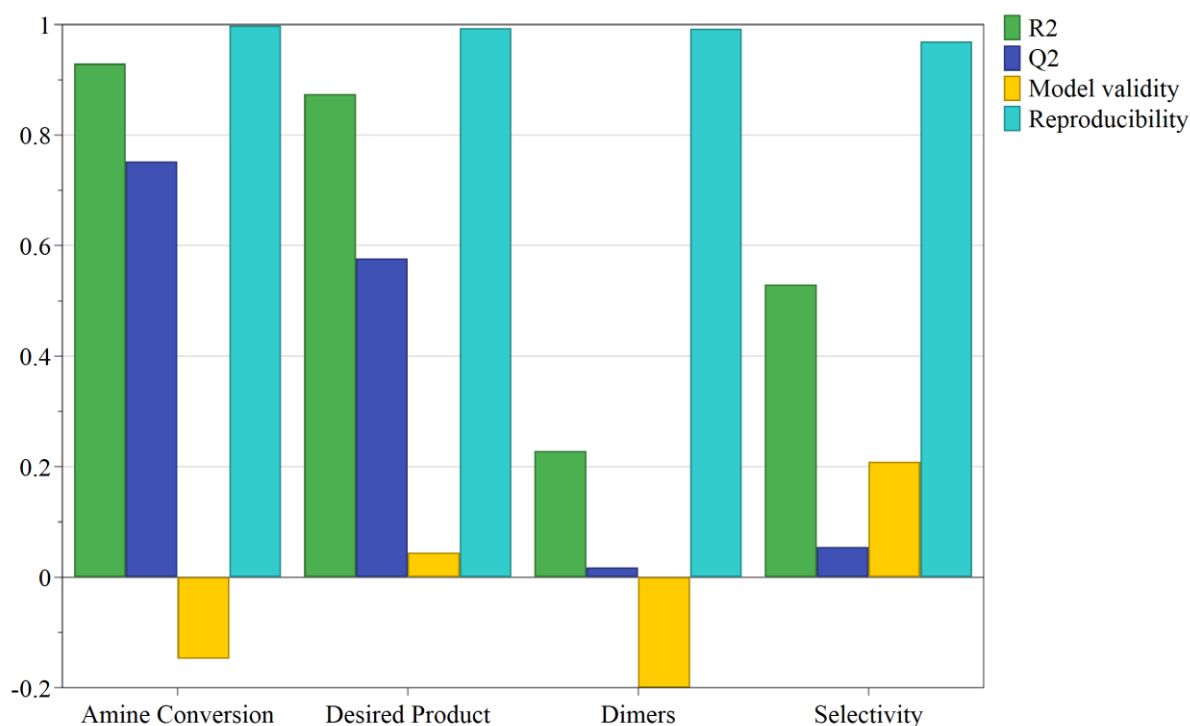
Figure 33. Summary of fit plots for all 4 responses from the second screening design.

The models with overall poor fitting (dimer yield and selectivity) are considered first. The low values for R^2 and Q^2 showed a poor fit to the existing data and poor prediction of new data points, as described in Chapter 4. The low model validities meant that there was a significant lack of fit within the models.

The difficulty with fitting a reliable model in the case of dimer yield and selectivity appeared to be due to the lack of variation in the experimental data within the chosen design space. The experimental data values for dimer yield and selectivity only varied between 5 - 14% and 85 - 96%, respectively (Figure 34). The lack of variation indicated that, within this design space, the change in variables had little effect on the reaction outcome and so the model fitting was unable to determine the significant variables. As shown by the presence of only one term (Equiv) in the dimer model.
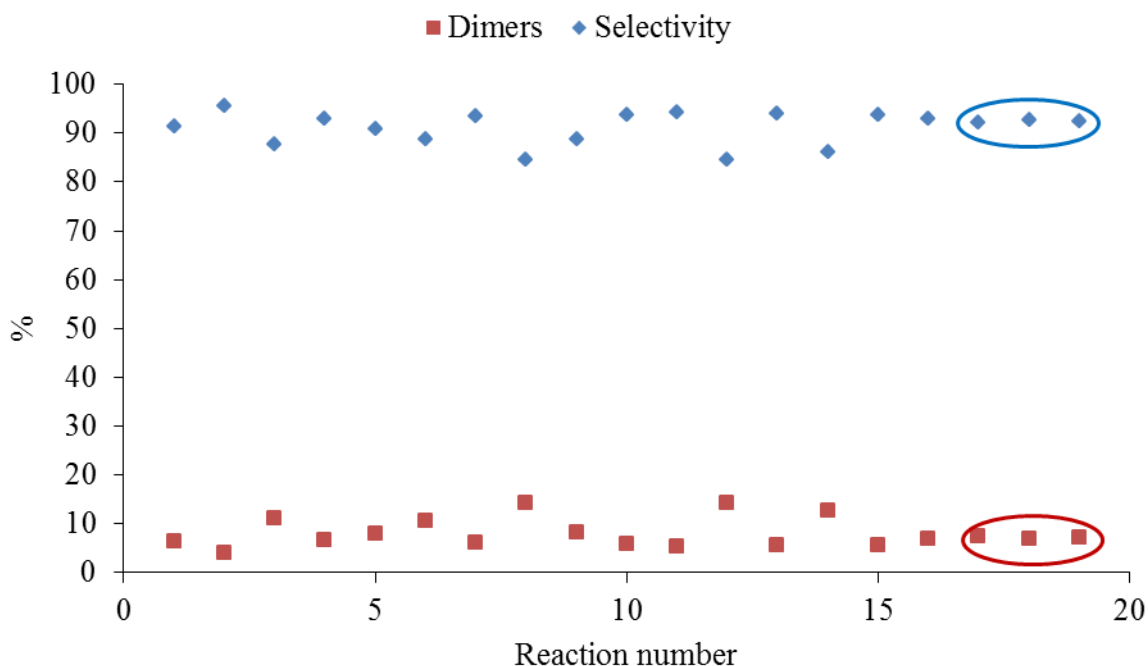
Figure 34. Experimental data points for dimer yield (red) and selectivity (blue) from the second screening design. (Replicate experiments are highlighted within the ovals).

During the first screening design, the model fitting for dimer yield (Figure 30) showed a good model fit as the values for R^2, Q^2, validity and reproducibility were all high. The experimental results varied between 0 - 43% for dimer yield and the data showed more variation (Figure 35) compared to the data from the second screening design discussed above. This further illustrated that a more reliable model was obtained from the data that showed larger variation. This could also indicate that the design space chosen in the first screening design was more appropriate to generate a model and determine the significant variables for this particular response.
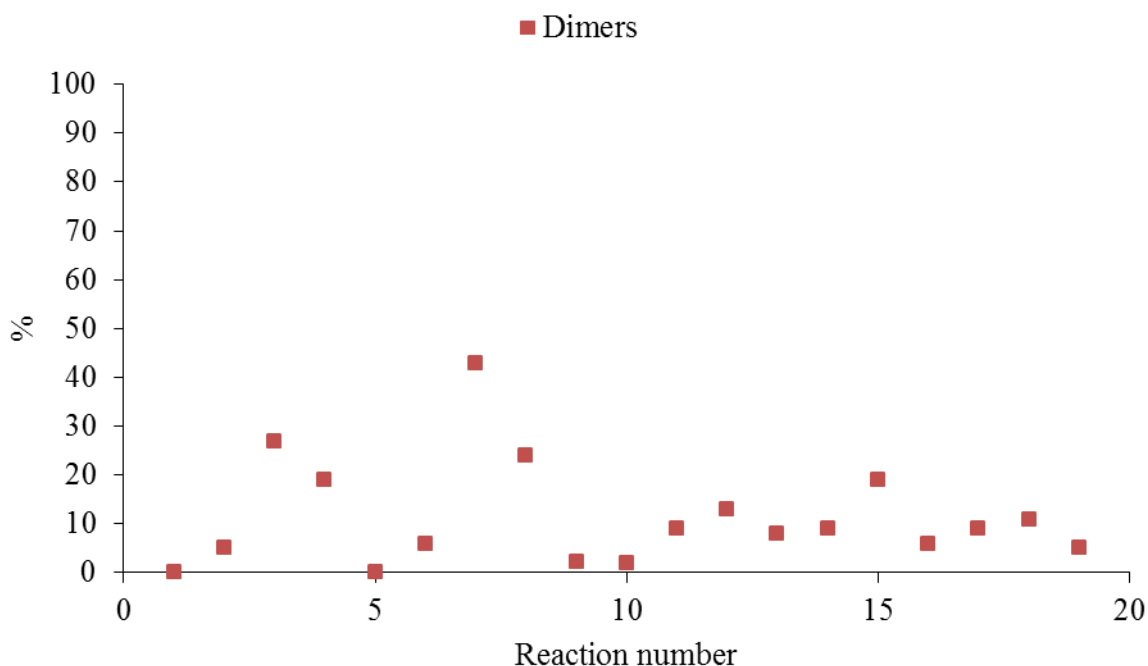
Figure 35. Experimental data points for dimer yield from first screening design.

If the design space chosen is appropriate to determine the significant variables for a particular response, then the variation in the experimental results will be tolerated within the model. However if the design space is not appropriate for a particular response, then variation in the experimental results (either too little variation that generates a straight line or too much variation to be able to pick out a trend) will be detrimental to the model fitting as it cannot determine which variables are having an effect on the outcome of the reaction.

It was decided that it was not appropriate to consider models for all four responses as, whilst the model for each response was developed independently, the design space explored was the same and so was not appropriate to generate a reliable model for each of the four separate responses. Therefore, the responses for dimer yield and selectivity were no longer considered. The aim of the study was to determine the significant variables in order to ensure a high yield of desired product, and so considering only the responses for conversion of amine **5.1** and desired product yield would be sufficient to achieve this.

The models generated for the conversion of amine **5.1** and desired product yield were next considered. From the second screening design a much better model fit was achieved (Figure 33), with reasonably high values for R^2 and Q^2. The reproducibility values were again high due to the centre point replicate experiments. However, the model validity was very low. Low model validity can indicate outliers within the data, that the data requires a transformation (*e.g* logarithmic function) or be caused by missing terms within the model. In this case there were no outliers observed and the use of a transformation did not improve the fit of the models. Further analysis of the model fitting was next carried out to assess the lack of fit and determine if it was due to missing terms within the model.

The data showed more variation than for the dimer yield and selectivity, with values between 74 - 97% for amine **5.1** conversion and 66 - 91% for desired product yield and so a lack of variation in the data was not considered to be responsible for the low model validity.

The lack of fit plots for both conversion of amine **5.1** and desired product yield showed a significant lack of fit (Figure 36). In this plot, the 1st bar is the standard deviation of the lack of fit, the 2nd bar is standard deviation of the pure error and the 3rd bar is the standard deviation of the pure error multiplied by the critical value for the confidence level (95%). If the 3rd bar is smaller than the first bar then there is a lack of fit, which was the case for both of the responses.
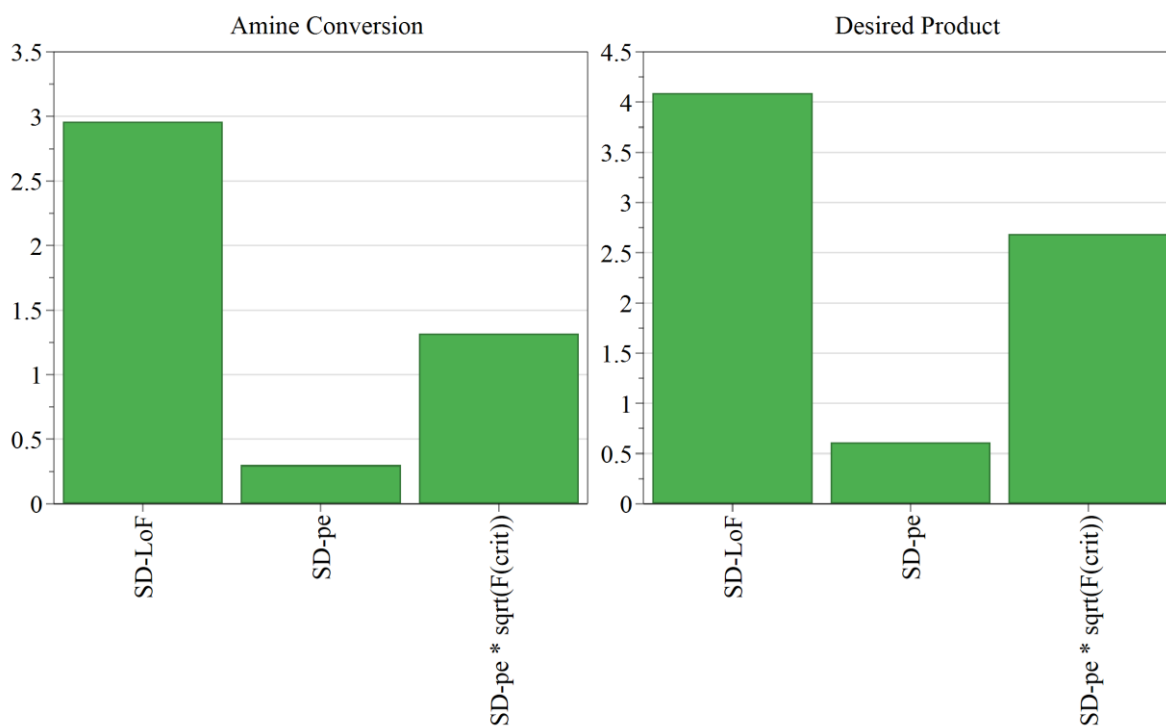
Figure 36. Lack of fit plots for conversion of amine **5.1** (left) and desired product **5.6** yield (right) from the second screening design.

If the lack of fit is caused by missing square terms within the model, then this can be indicated using main effect plots (Figure 37), which show the data points in relation to confidence intervals for each variable. When the data points lie outside the confidence intervals (dashed lines), as in this case, then there is curvature in the model. Curvature in model means that there are missing square terms. This can also be confirmed by the residuals *vs.* variables plot (Figure 38), which shows the trend in the data points for each variable. Ideally the spread of the data points would be random with no apparent trend. In this case the data shows an arched or curved pattern for some of the variables, indicating that there is curvature associated with the particular variable and so a quadratic term relating to this variable is missing from the model. The fractional factorial Resolution V screening design used in this study does not account for square terms as only two-levels are investigated for the variables and so only a linear model can be developed.[139]
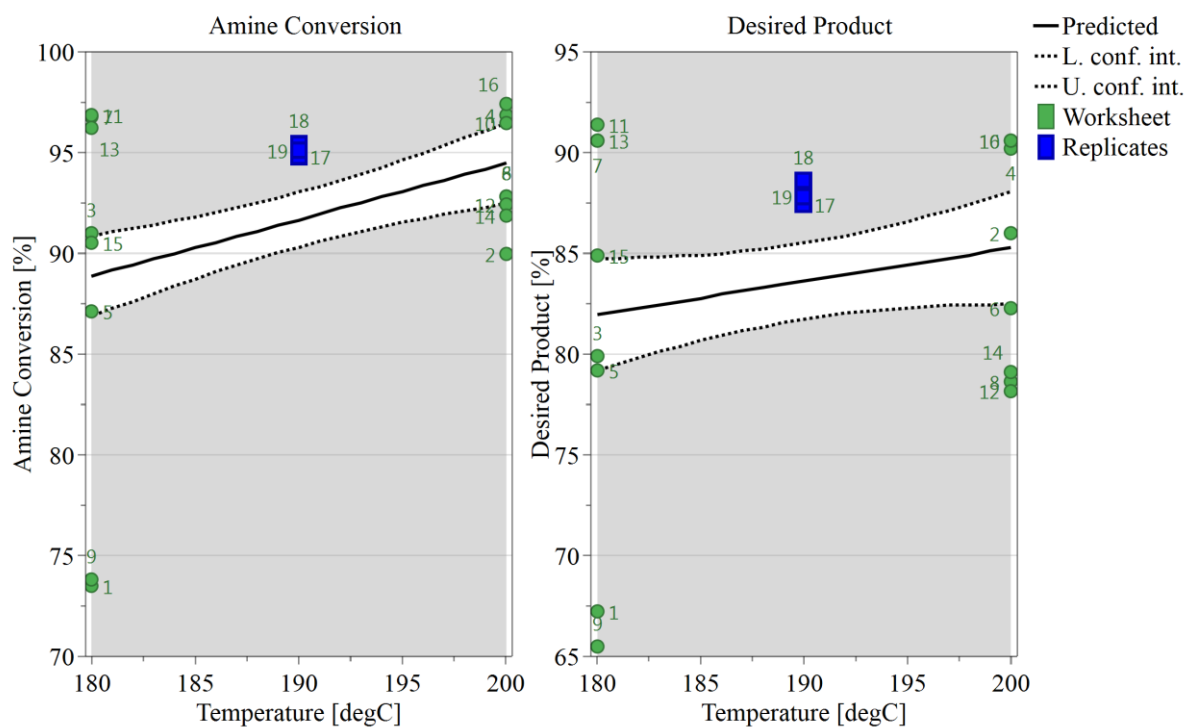
Figure 37. Main effect plots for conversion of amine **5.1** (left) and desired product yield (right) from second the screening design. (Green circles are experimental data points, blue squares are experimental data points for the centre point replicates, dashed lines denote the upper and lower confidence intervals. Variable shown is temperature).

As the models appeared to be missing square terms and showed a significant lack of fit, then the important variables could not be determined empirically using this screening design. This indicated that a different type of design may have been required to obtain a better model for the data and to be able to pick out the significant variables and determine optimum operating conditions. As square terms appeared to be important then a response surface methodology (RSM) approach should be employed as this develops a quadratic model and can describe curvature within the model as it can account for interaction effects and quadratic effects (squared terms).[139] The types of design that could be used include central composite designs such as CCF, which would require 33 experiments for a fractional factorial or 52 experiments for a full factorial. A Box-Behnken design could also be used,[154] which would require 46 experiments. Both of these types of design require

three levels for each of the variables, resulting in a higher number of experiments than the two-level screening designs.
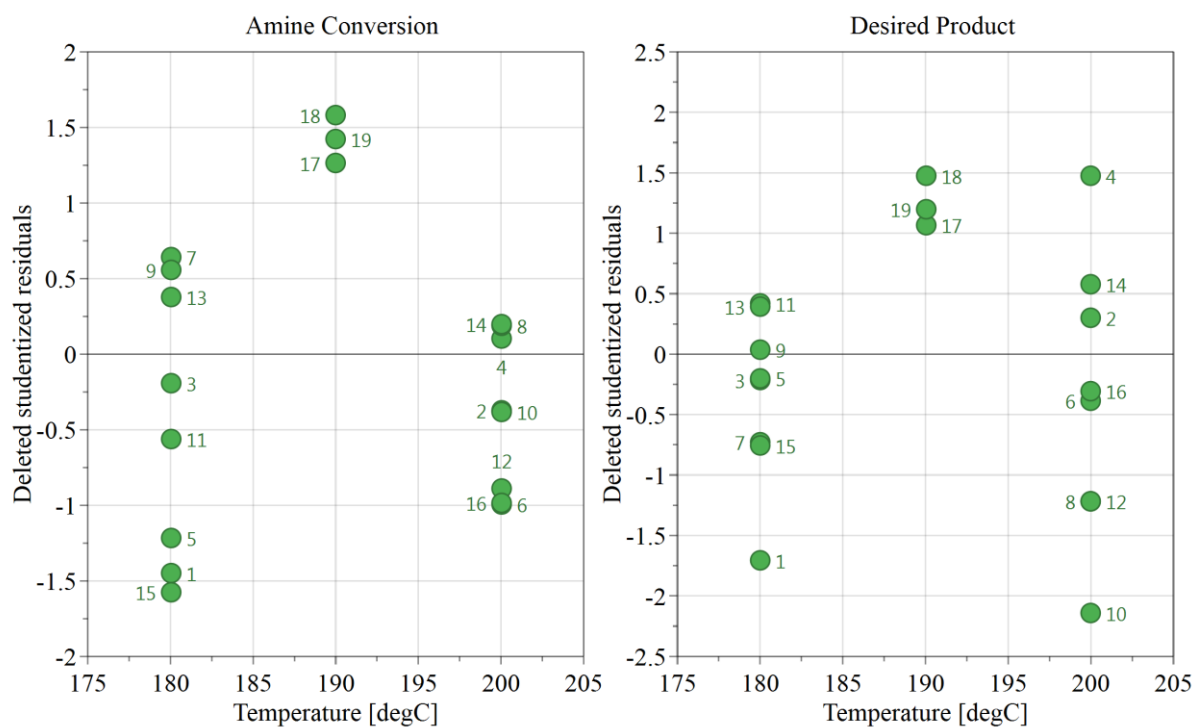
Figure 38. Residuals *vs.* variable plots for conversion of amine **5.1** (left) and desired product yield (right) from the second screening design. (Variable shown is temperature).

At the start of the screening and optimisation process it was not known that square terms would be required and so it would not have been appropriate to start with a design type that would require such a large number of experiments. Also, the choice of experimental design was dependent on the objective: screening designs allow for the important variables to be selected from a large number of un-important variables, whereas RSM designs are generally used once the number of variables has been reduced (either by screening or by existing chemical knowledge) and are used to find optimum conditions and develop a robust process.[138] Therefore a screening design was selected to be able to narrow down the

number of significant variables and to be able to investigate the large number of variables in fewer experiments than would be required for an RSM.

Once it had become apparent that a different type of design would have been more appropriate, the experiments that had already been carried out were sufficient to show experimentally derived optimum conditions (180 °C, 10 min, 0.5 mol%, 1 M and 5 Eq of **5.5**), which gave very high conversions. Therefore it was deemed unnecessary to carry out a new type of design that would require a large number of experiments and would be a waste of material. If the experimental results did not produce such high conversions, then it would have been advisable to do further testing and to try a different type of screening design.

5.2.3.3 Testing of Optimum Conditions

The experimentally observed optimum conditions were determined to be: 180 °C, 10 min, 0.5 mol%, 1 M and 5 Eq of **5.5**, which gave 96% conversion of amine **5.1** and 91% desired product yield. These conditions were then used within a continuous reactor system, to determine if the conditions were completely transferable and to be able to increase the throughput of the reaction, as the microwave reactions would be limited by the batch size.[155] The reactor set-up used was the same as for the heterogeneous catalyst in Section 5.2.1 with some modifications (Figure 39). The stainless steel tubular reactor was used as an empty cartridge and not packed with catalyst in this instance. As higher temperatures were required, a 250 psi BPR was fitted to the outlet of the reactor. Also, screening reactions had shown that the catalyst was poorly soluble at room temperature and so the reagents were combined in a beaker and stirred in a sand bath (40 °C) to encourage dissolution. Due to the potential presence of solid in the stirred reaction solution, a filter

was fitted to the tubing going from the reaction solution into the pump to prevent blockages.
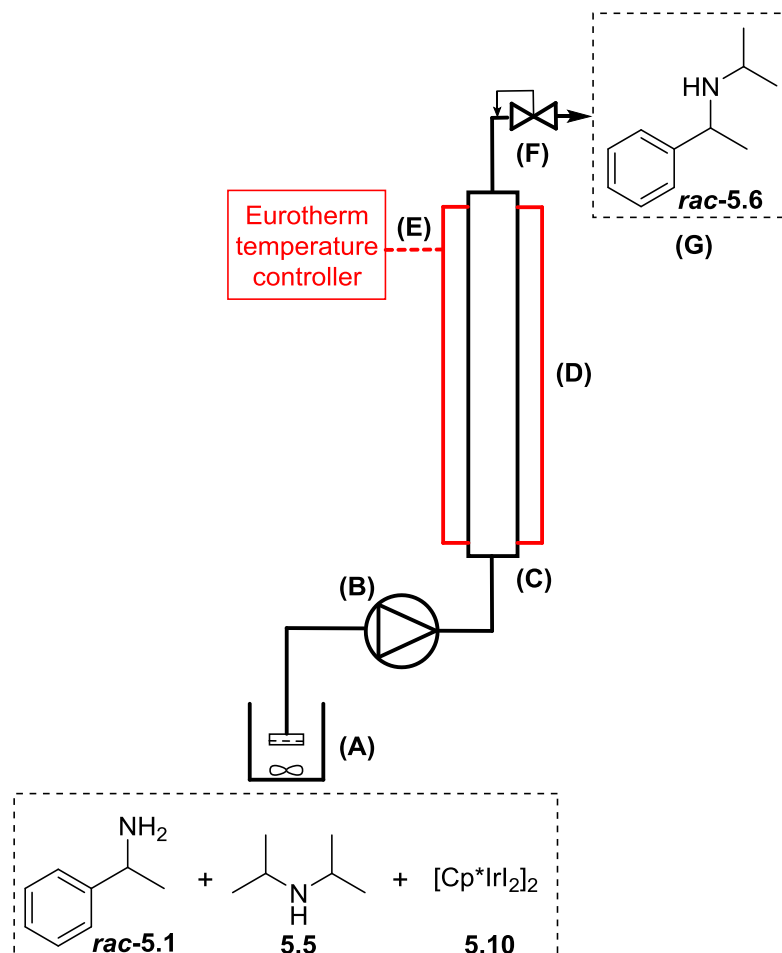
Figure 39. Continuous reactor set-up for *rac*-**5.1** *N*-alkylation. (A): Reaction solution with in-line filter; (B): Piston pump; (C): Tubular reactor; (D): Aluminium heating block; (E) Eurotherm temperature controller; (F) BPR; (G): Product outlet and collection.

For this continuous reaction using 180 °C, 10 min, 0.5 mol% catalyst loading, 1 M of *rac*-**5.1**, 5 Eq of **5.5**, the conversion of amine **5.1** and desired product yield were 27 and 25%, respectively, compared to 96 and 91% under microwave conditions. When the reagents were combined it was observed that a particulate suspension formed when **5.5** was added and large clumps of orange solid were observed in the reaction solution beaker at the end

of the reaction (Figure 40). This indicated that not all of the material was being pumped into the reactor and so the reaction composition and consequently the conversion was lower than expected.
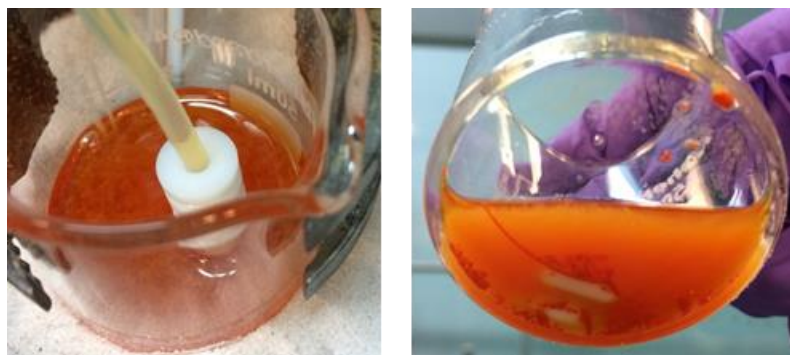
Figure 40. Continuous flow reaction stock solution (1 M). Left: stirred solution during reaction; Right: remaining stock solution at end of reaction.

The same reaction was repeated at half the concentration to see if this prevented the solid formation. The reaction solution was a clear orange solution under these conditions with little solid observed (Figure 41), indicating that all of the desired material was able to enter the reactor system. To confirm this, a sample was taken from the reaction mixture and also from the tubing in between the pump and the reactor and analysed for amine concentration by GC. These samples showed the same amine concentration, meaning that the reactor concentration matched the desired concentration. For this reaction using 180 °C, 10 min, 0.5 mol%, 0.5 M, 5 Eq, the conversion of amine **5.1** and desired product yield were 60 and 59%, respectively. Whilst this was an improvement on the more concentrated continuous reaction, this was still lower than would be expected based on the microwave screening.

Figure 41. Continuous flow reaction stock solution, during 0.5 M reaction.

Next, the set-up was modified to use two pumps, feeding the reagents into a tee-piece prior to entering the heated reactor (Figure 42), to determine if the presence of **5.5** caused the solid formation in the catalyst solution. Pump A contained **5.5** in anisole and Pump B contained *rac*-**5.1** and catalyst **5.10** dissolved in anisole, with internal standard added to both solutions. The same reaction conditions as the one pump set-up were used (180 ºC, tRes = 10 min, 0.5 mol% catalyst loading). When the two feeds met at the tee-piece the reagent concentrations were reduced, as the addition of a second feed diluted the first. For example, if a feed containing a 1 M reagent meets a second feed the reagent concentration will be diluted to 0.5 M, if the two feeds have equal flow rates. Therefore the concentrations of the stock solutions needed to be increased to account for this dilution. In this case the stock concentration for **5.5** was 6.25 M and the stock concentration for *rac*-**5.1** was 5.0 M and the ratio of the pump flow rates was 0.8:0.2, to obtain the desired concentrations and reagent equivalents within the reactor.
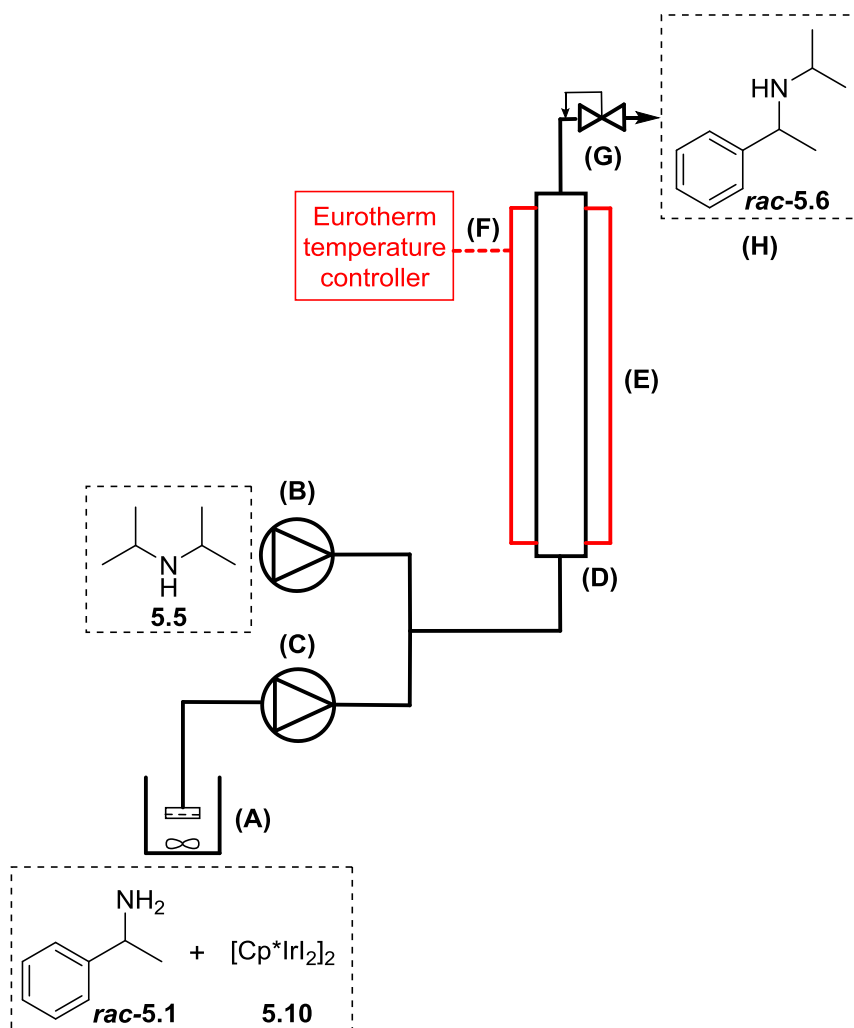
Figure 42. Continuous *N*-alkylation reactor using two pumps. (A): Reaction solution with in-line filter; (B): Piston pump A; (C) Piston pump B; (D): Tubular reactor; (E): Aluminium heating block; (F) Eurotherm temperature controller; (G) BPR; (H): Product outlet and collection.

Samples were collected for each RV up to 7 RV. GC analysis of the samples showed that the amine **5.1** conversion varied between 39 and 57% across the RV (Figure 43). Variation was also observed for the desired product yield, from 8 to 63%. Again, the difficulty in reaching steady state suggested that the amount of catalyst being pumped into the reactor was inconsistent over the course of the reaction. The removal of **5.5** from the catalyst stock solution seemed to have improved the conversion compared to the one pump set-up however, solid formation was still observed in the catalyst stock and steady state was not achievable.
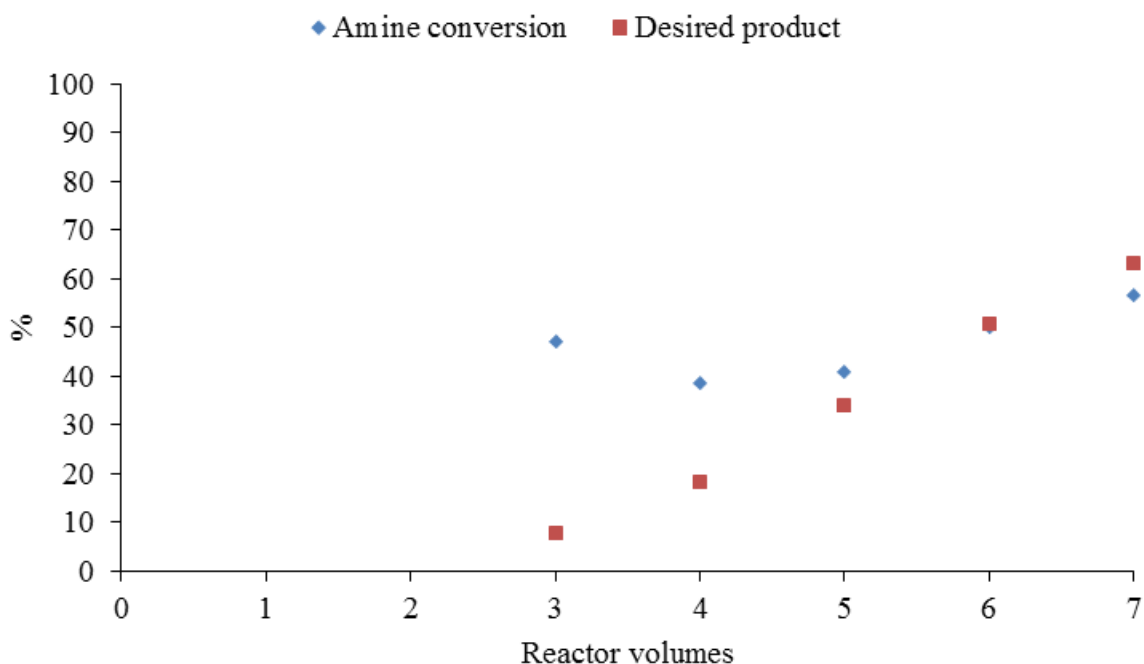
Figure 43. Continuous *N*-alkylation of *rac*-**5.1** with **5.5** using the two pump reactor set-up.

The conversion achieved under continuous flow conditions was much lower than in the microwave batch reactions. For the continuous reaction, the poor solubility of catalyst at lower temperatures meant that not all of the catalyst was able to be pumped into the reactor, leading to a lower conversion than would be expected. In the microwave reaction all of the catalyst and reagents were in the same reaction vessel and so the catalyst loading remained consistent. Also, the whole reaction solution was exposed to the high reaction temperature and so the catalyst was completely dissolved in the solution. The poor solubility of the catalyst in the continuous reaction could also be responsible for the difficulty in reaching steady state, as not all of the catalyst could be pumped into the reactor this may have led to variation in the catalyst loading between reactor volumes. To overcome this problem, the catalyst stock solution would need to be heated to a much higher temperature to ensure dissolution. This would require a heated pump head to ensure no precipitation in the pump and the catalyst solution being heated to a higher temperature

in the sand bath. Heating the solution to a higher temperature increases the risk of evaporation and may cause some reaction to occur in the stirred vessel. To prevent any reaction in the stirred vessel the reagents would need to be separated into different feeds, which would require multiple pumps. However, the homogeneity of the solution appeared to also be affected by the addition of amine to the catalyst solution, giving rise to a change from a dark brown suspension of catalyst to a clear orange solution. Therefore, the presence of the amine in the catalyst stock solution may also be required for catalyst solubility and activation and so separating the reagents into multiple feeds may also hinder the reaction.

5.2.3.4 Reaction Metrics for Optimum Microwave Conditions

Reaction metrics were calculated for the optimum microwave conditions: 180 °C, 10 min, 0.5 mol%, 1 M, 5 Eq to determine the efficiency of the process. The Process Mass Intensity (PMI)[143] was calculated as 5.4, according to Equation 4.1. The PMI of a process describes the quantity of the materials being used in a process that are present in the final product and so it is a measure of efficiency. A PMI value of 1 would indicate a process in which all or the reagents are combined in the final product and therefore no waste is produced. As the calculation includes catalysts and solvents, a process that has no associated waste is very unlikely. The PMI for this reaction using existing literature conditions developed by Saidi *et al.* (98% yield, 155 °C, 10 h, 1 mol%, 0.5 M, 3 Eq) was calculated as 10.5.[29] This comparison showed that the optimum conditions developed herein exhibited a reduction in reaction time, catalyst loading and PMI and so an increase in efficiency. When the process is more dilute, a larger amount of the reaction mixture is made up of solvent and so less of the total mass of the process is incorporated into the product. Whilst the two processes had similar values for the numerator in the PMI

equation, the denominator was 2.5-fold greater for the process developed herein, compared to the literature process, as more of the reaction mixture was incorporated into the product. (Note: these calculations did not include any work-up or purification procedures as this information was not available in the literature).

5.3 *N*-alkylation of Single Enantiomer 1-Phenylethylamine

The *N*-alkylation of single enantiomer **5.1** was then investigated for the potential of coupling to the continuous enzymatic resolution (Chapter 2) with the view to alkylating the amine enantiomer that was not derivitised in the resolution step (Scheme 85).
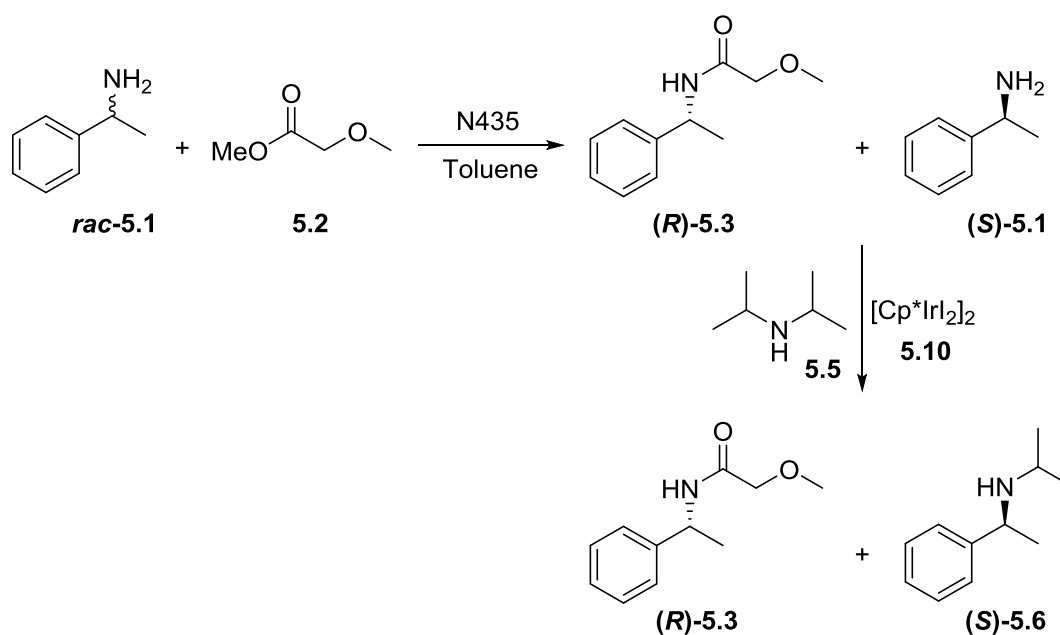
Scheme 85. Coupled resolution – *N*-alkylation reaction design.

As discussed previously, kinetic resolution has a maximum yield of 50% when only one enantiomer is desired. This means that the other 50% is waste, unless it can be recycled or used in a subsequent reaction. Coupling the kinetic resolution to an *N*-alkylation reaction

would provide the opportunity to re-use the undesired enantiomer. The reaction would produce a single enantiomer secondary amine, a higher value product than the primary amine. It is difficult to obtain single enantiomer secondary amines *via* enzymatic resolution as few enzymes have been shown to accept secondary amine substrates,[55, 72] this coupled procedure would provide a solution to not only reuse the leftover primary amine enantiomer, but also to access single enantiomer secondary amines. The aim of the following sections was to determine if the single enantiomer amine could be alkylated without racemisation, to obtain single enantiomer *N*-alkylated product and then develop a coupled process.

5.3.1 Microwave Single Enantiomer *N*-Alkylation Reactions

Initially the single enantiomer *N*-alkylation was studied to determine whether the primary amine could be *N*-alkylated without racemisation. The reactions were carried out using (*S*)-**5.1** under microwave heating, following the procedure described above in Section 5.2.3 (Scheme 86).
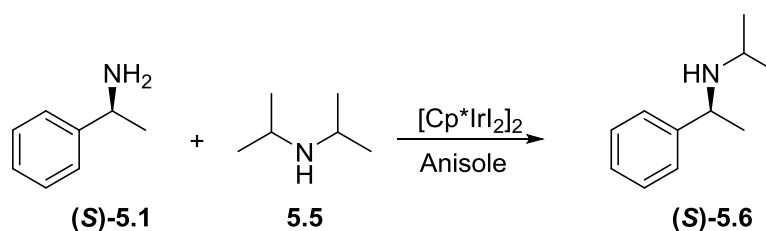
Scheme 86. [Cp*IrI$_2$]$_2$ (**5.10**) catalysed *N*-alkylation of (*S*)-**5.1**.

The reactions were first carried out at temperatures of 150, 175 and 200 °C, as higher temperatures showed higher conversion when investigating the racemic *N*-alkylation. All of these reactions were carried out at the specified temperature for 30 min, using 0.5 mol% catalyst **5.10**, 1 M (*S*)-**5.1** and 3 Eq of **5.5**. The data showed that, whilst higher conversions

were obtained at 175 and 200 °C, the desired product *ee* dropped significantly as the temperature was increased, to only 5% *ee* at 200 °C (Figure 44). The reaction at 150 °C gave reasonable desired product yield and maintained a high *ee* of 96%, and so this temperature was chosen for further development of the reaction.
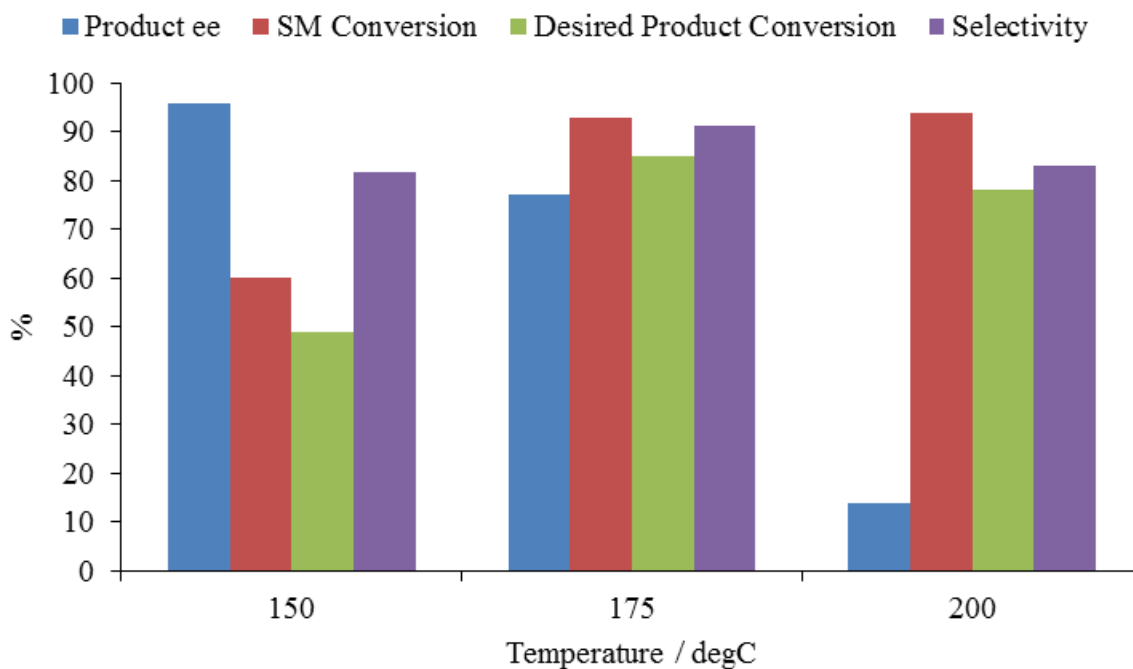
Figure 44. Temperature studies for single enantiomer *N*-alkylation microwave reactions.

Further reactions were then carried out to increase the conversion and improve the selectivity for the reaction at 150 °C (Table 14). The number of Eq of **5.5** was increased from 3 to 5 (Entry 2). As all other parameters remained constant, this did not affect the overall conversion of amine **5.1** but it did increase the selectivity for desired product by 10%. The reaction time was then increased from 30 min to 1 h, which increased the desired product yield from 53 to 92% (Entry 3). From these studies it was decided that 150 °C for 1 h and 5 Eq of **5.5** were the most appropriate conditions for the *N*-alkylation reaction

using 0.5 mol% catalyst **5.10** and 1 M (*S*)-**5.1**, to achieve high conversion and selectivity

for desired *N*-alkylated product and to maintain high product *ee*.

Table 14. Single enantiomer *N*-alkylation microwave reactions at 150 °C.[a]

Entry	Reaction time / min	Eq	Conversion of **5.1**[b] / %	Desired product **5.6** yield[b] / %	Selectivity[c] / %	Product **5.6** *ee*[d] / %
1	30	3	60	49	82	96
2	30	5	58	53	91	99
3	60	5	97	92	95	95

[a]Reaction conditions: 1 M (*S*)-**5.1**, 0.5 mol % [Cp*IrI$_2$]$_2$ **5.10**, anisole, biphenyl added as internal standard, 150 °C; [b]Determined by achiral GC analysis after calibration against internal standard; [c]Determined as (Desired product yield / Conversion of **1**)*100; [d]Determined by chiral GC as [(Area1 − Area2)/(Area1 + Area2)]*100; Eq = equivalents of **5.5**.

A reaction was carried out using these conditions for the single enantiomer *N*-alkylation in the continuous reactor, to assess the feasibility for coupling to the continuous resolution. The reactor was set-up according to the description in Section 5.2.1, using one pump. The reactor temperature was set to 150 °C and the flow rate was set to 0.047 mL min^{-1} (tRes = 60 min). GC analysis showed 20% conversion of amine **5.1** and 19% yield of desired product **5.6** (95% *ee*), giving a selectivity of 95%. Whilst the high selectivity and *ee* was encouraging, the conversion was significantly lower than that observed in the microwave reaction (97%). As in the continuous racemic *N*-alkylation reactions, some solid was observed in the reaction stock solution and so the conversion may have been lower as not all of the catalyst was able to be pumped into the reactor as discussed in Section 5.2.3.

The continuous resolution using the N435 packed reactor was repeated using the conditions from Chapter 2 (0.07 M *rac*-**5.1**, 1 Eq of methyl methoxyacetate **5.2**, 6 min tRes) at 150 °C to check the effect of the high temperature required for the *N*-alkylation step. Inconsistencies were observed under these conditions as the conversion of **5.1** varied

from 48 to 61% between 4 RV and 10 RV (Figure 45). Previous studies had shown that steady state was reached by 4 RV but in this case steady state was not reached even after 10 RV. The *ee* observed for amine **5.1** also indicated variation in the reaction as it increased from 58% after 4 RV to 78% after 10 RV. The reaction using these conditions at 60 °C gave 96% *ee* for amine **5.1**, suggesting that the high temperature was inhibiting the enzyme. When unpacking the reactor, it was observed that some of the catalyst beads had discoloured, indicating that the catalyst was being degraded by the high temperature. These observations confirmed that the coupled process would benefit from having isolated catalytic reactions as the high temperatures required for the *N*-alkylation reaction are not compatible with the enzyme.
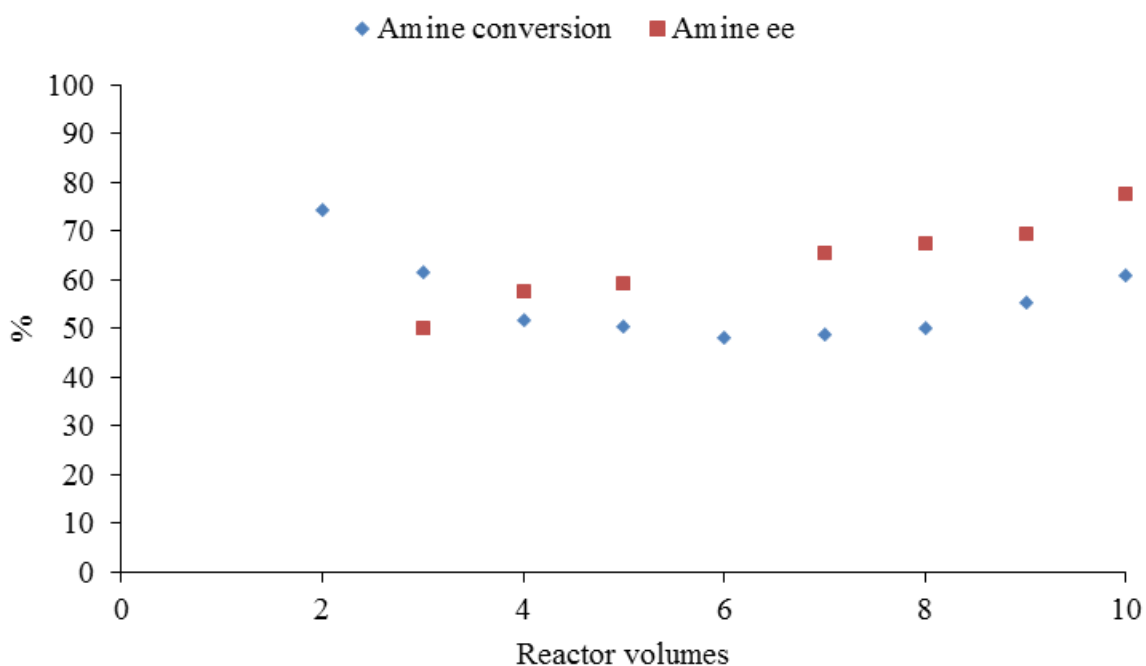
Figure 45. Conversion and *ee* of amine **5.1** for the continuous resolution at 150 °C. (Conversion determined by achiral GC, after calibration against internal standard; *ee* was determined by chiral GC).

5.3.2 Development of *N*-Alkylation – Resolution Coupled Process

5.3.2.1 Inhibition Testing

Microwave reactions were carried out to test for any inhibition caused by the coupling of the two processes (Table 15). All of the reactions were carried out using the same concentrations and equivalents of reagents and catalysts, unless stated otherwise. Firstly, a resolution reaction was carried out using conditions developed in Chapter 2: 0.07 M ***rac-5.1***, 1 Eq of methyl methoxy acetate **5.2**, 60 °C, 6 min reaction time (Entry 1). The reaction was then repeated with the addition of 5 Eq of **5.5** and 0.5 mol% catalyst **5.10** to see if the presence of the *N*-alkylation reaction components would inhibit the resolution reaction (Entry 2). This did not inhibit the reaction as the conversion was the same for both reactions. It was important to ensure that no inhibition would occur if the *N*-alkylation reaction components were pumped through the N435 packed bed to set-up a recirculation procedure. This also confirmed that no *N*-alkylation was occurring at 60 °C, so re-enforcing the requirement for two separately heated reactors. The converse reactions were then carried out to test for inhibition of the *N*-alkylation reaction in the presence of methyl methoxy acetate **5.2** (Entries 3 and 4). The enzyme was omitted from these reactions as this would remain in the packed bed reactor and so would not circulate through the alkylation reactor in the coupled process. The reaction in the presence of the ester gave a higher conversion of **5.1** than the reaction without, 73% compared to 33%. Possibly due to some favourable coordination of the ester to the catalyst that leads to enhancement of the rate. However, catalytic structures were not isolated and so no structural analysis was carried out to confirm this.

Reactions were then carried out to determine if the presence of the resolution product amide **5.3** would inhibit the *N*-alkylation reaction step. The reaction conditions in Table 15, Entry 3 were used with the addition of 1 Eq of amide **5.3**. 70% yield of desired *N*-alkylated product was achieved, again showing a higher conversion in the presence of the additive

compared to reaction without. This could again be due to coordination of the amide to the catalyst, leading to enhancement of the rate.

Table 15. Microwave reactions to test for inhibition in coupled process.[a]

Entry	Ester **5.2** Eq	Amine **5.5** Eq	Catalyst	Temperature / °C	Time / min	Conversion of **5.1**[b] / %
1	1	0	N435	60	6	14
2	1	5	N435, [Cp*IrI$_2$]$_2$	60	6	14
3	0	5	[Cp*IrI$_2$]$_2$	150	60	33[c]
4	1	5	[Cp*IrI$_2$]$_2$	150	60	73[c]

[a]Reaction conditions: 0.07 M *rac*-**5.1**, 143 mg N435, 0.5 mol % [Cp*IrI$_2$]$_2$ **5.10**, toluene, 2 mL reaction volume, biphenyl added as internal standard; [b]Determined by achiral GC analysis after calibration against internal standard; [c]Average of three runs.

5.3.2.2 Stepwise Reaction Testing

As these studies indicated that the coupling of the two reactions would not cause any inhibition, a stepwise approach to coupling the reactions under microwave heating was next investigated (Scheme 87).

First, the resolution was carried out using the same conditions as above (Table 15, Entry 1), but with a longer reaction time of 30 min to encourage a higher conversion. Next the reaction solution was transferred to a second vessel, with filtering to remove the N435, and then [Cp*IrI$_2$]$_2$ and **5.5** were added and the reaction returned to the microwave for the *N*-alkylation step. After the first step, 42% conversion of amine **5.1** was observed. However, only a further 12% conversion of amine **5.1** was observed after the second step, with only a 4% yield of desired *N*-alkylated product **5.6**. The low yield of *N*-alkylated product is particularly significant because the reagent ratios were calculated based on the concentration of amine **5.1** at the start of the resolution reaction, meaning that the catalyst

loading for the *N*-alkylation step was increased from 0.5 mol% to around 1 mol% and the

number of Eq of **5.5** was increased from 5 to 10.
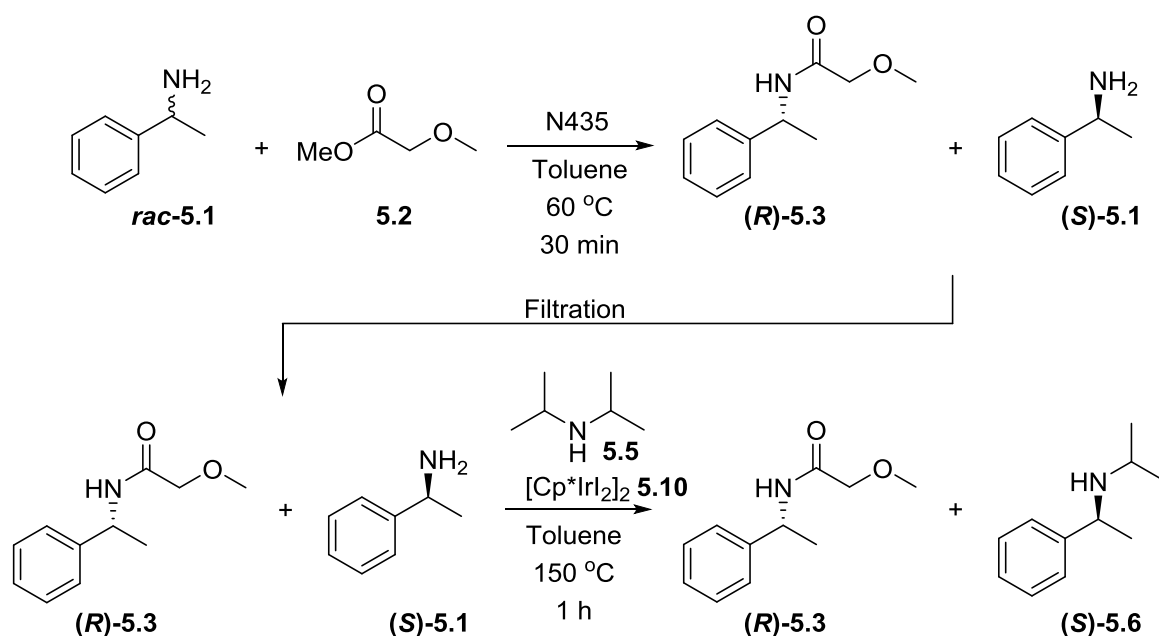
Scheme 87. Microwave coupled reaction, stepwise approach.

The inhibition testing indicated that the conversion for the *N*-alkylation step should not

have been hindered by the presence of the components from the resolution step and so this

result was unexpected. The only other difference between the inhibition testing and the

stepwise coupled reaction was the presence of N435 and so further inhibition studies were

carried out to determine if this was the cause of the low yield of the *N*-alkylated product.

For the stepwise approach N435 was filtered-off after the first step, and so this was

repeated to determine if any material was leaching off the resin and causing the inhibition

(Scheme 88). N435 and toluene were stirred for 30 min at 60 °C under microwave heating,

then the mixture was filtered and the filtrate used in the *N*-alkylation step at 150 °C for 1 h,

which gave only 6% yield of desired product **5.6**.
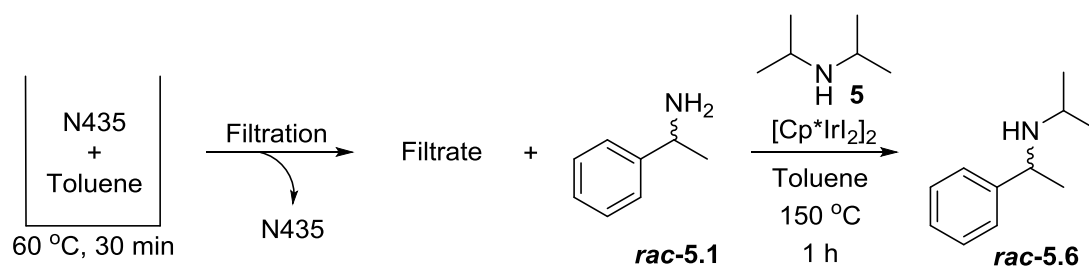
Scheme 88. Testing of resin leaching for *N*-alkylation inhibition.

A standard *N*-alkylation reaction with N435 added to the mixture gave 1% of **5.6** after 1 h. These results suggested that the low conversion observed in the stepwise coupled procedure was due to the presence of N435. As the solution was filtered to remove the solid catalyst it would appear that either enzyme was leaching off the resin or the solid support was being degraded and material was leaching into the solution, which led to inhibition of the *N*-alkylation reaction. This could be tested by using a different support for the enzyme to see if the same effect was observed or by doing imaging such as scanning electron microscopy, of the polymer support before and after the reaction to look for any degradation.

This may have resulted from the stirring within the microwave breaking down the resin. However, a stepwise coupled reaction was attempted wherein the resolution was carried out using the continuous packed bed reactor and then the eluent was collected and used in a microwave *N*-alkylation reaction (Scheme 89), for which the same effect was observed. The yield of **5.6** was only 4% in this case, which would suggest that the stirring in the microwave was not causing any further degradation of N435 compared to the packed bed reactor. This indicates that the degradation was not due to stirring as the immobilised enzyme was not exposed to any mechanical stirring whilst in the reactor.
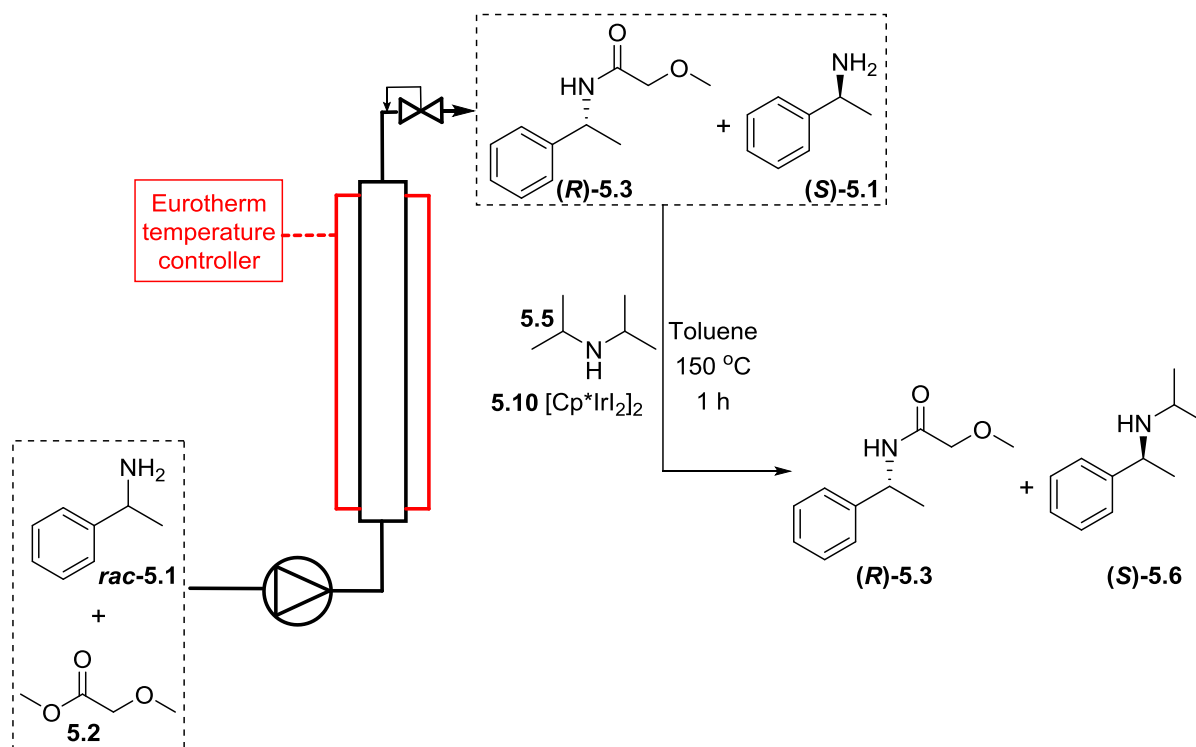
Scheme 89. Continuous resolution coupled to microwave batch *N*-alkylation, stepwise approach.

It is not currently fully understood what part of the immobilised enzyme was causing the inhibition of the *N*-alkylation step. However, a microwave experiment combining the filtrate from stirring N435 in toluene with the resolution reaction components at 60 °C for 30 min showed no production of amide **5.3** (Scheme 90). This would suggest that enzyme was not being washed off the resin in significant enough quantities for the filtrate to have catalytic activity in the resolution. This was also re-enforced by the long term operation of the enzyme under continuous flow conditions described in Chapter 2. If the enzyme was leaching from the resin, the conversion within the resolution reactor would have been expected to decrease.
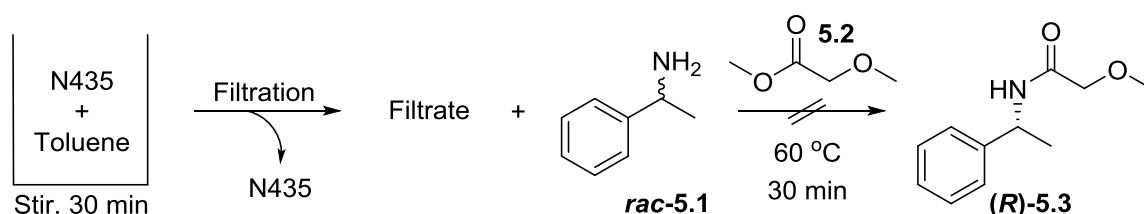
Scheme 90. Testing of enzyme leaching for resolution activity of filtrate.

5.4 Mechanistic Considerations

These investigations allowed for some further insights into the catalytic mechanism (Scheme 83) in the presence of two amines. Reactions were carried out to probe the effect of the Eq of amine **5.5** on the selectivity of the reaction for *N*-alkylation *vs.* dimer formation (Table 16). The results showed that the number of Eq of the alkylating agent had a significant effect on the selectivity of the reaction. High temperature was used to ensure full conversion of the starting material. When the Eq were increased from 1 to 3, the yield of desired product and the selectivity increased by 29%.

Table 16. Racemic *N*-alkylation testing of equivalents of **5.5**.[a]

Entry	Eq **5.5**	Conversion of **5.1**[b] / %	Desired product **5.6** yield[b] / %	Dimer yield[c] / %
1	1	100	64	36
2	3	100	93	7

[a]Reaction conditions: 1 M ***rac*-5.1**, 0.1 mol% [Cp*IrI$_2$]$_2$ **5.10**, anisole, 10 min, 220 °C, microwave heating; [b]Determined by achiral GC analysis; [c]Determined as (Conversion of **5.1** − Desired product **5.6** yield); Eq = equivalents of **5.5**.

This re-inforced that amine **5.5** first coordinates to the catalyst, followed by reaction of amine **5.1** to give the desired *N*-alkylated product **5.6**. At higher Eq, amine **5.5** out-competes amine **5.1** to coordinate to the catalyst. This is because the increase in the

number of molecules of a particular species will mean that the likelihood of that species coming into contact with the catalyst is increased and so the rate of reaction for that species will be increased. When less amine **5.5** is present, amine **5.1** is able to coordinate to the catalyst and then a second molecule of **5.1** can react to form dimers.

The retention of stereochemistry when *N*-alkylating single enantiomer amine **5.1** also gave some insight into the mechanism of the catalytic reaction. The production of *N*-alkylated amine without racemising the chiral centre suggested that amine **5.5** was coordinating to the iridium centre, rather than amine **5.1**. If amine **5.1** reacted with the iridium centre before *N*-alkylating, scrambling of the chiral centre would be expected (Scheme 91).
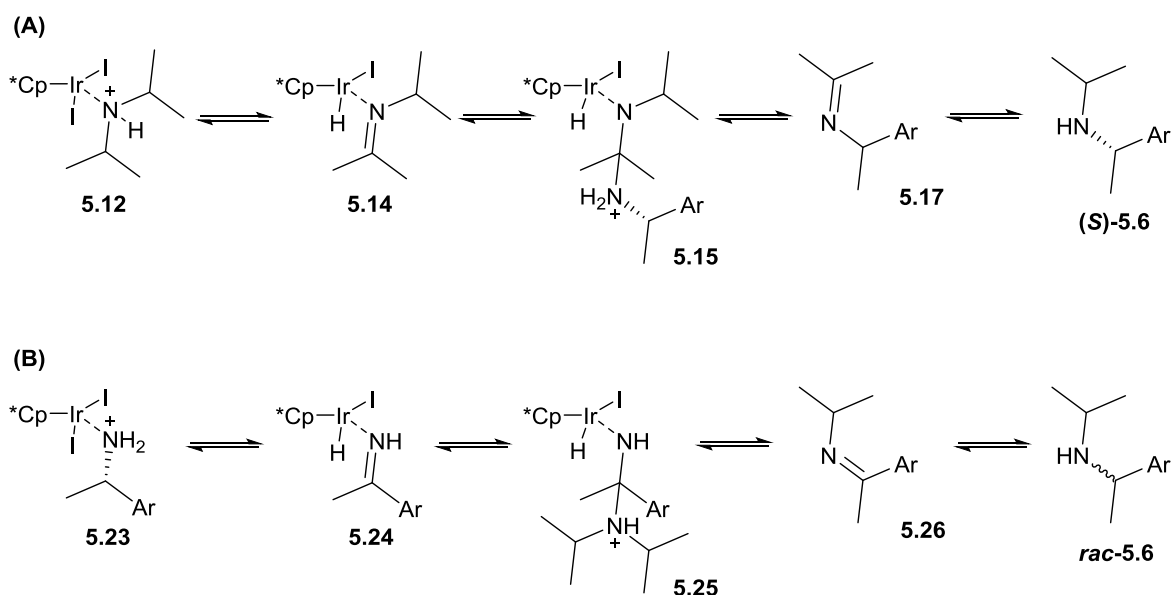
Scheme 91. Stereochemical outcome based on competition of amine coordination. (A): Amine **5.5** coordination; (B): Amine **5.1** coordination.

A reaction was carried out using 3 Eq *i*PrOH **5.27** as the alkylating agent instead of amine **5.5** (Scheme 92). Interestingly, only 1% of *N*-alkylated product **5.6** and 36% of dimers were observed. This compared to 4% of dimers for the reaction using amine **5.5**.
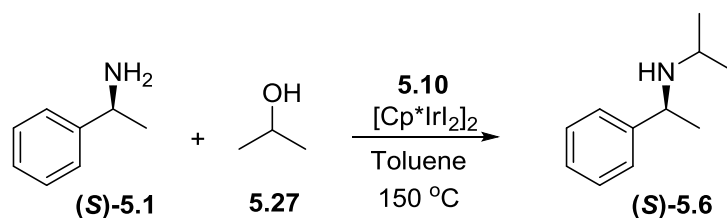
Scheme 92. *N*-alkylation reaction using *i*PrOH **5.22** as the alkylating agent.

When *i*PrOH was used, amine **5.1** was able to coordinate to the catalyst in the first step of the catalytic cycle as there was no competition from the alkylating agent. Then a second molecule of amine **5.1** could react with it in Step 3, leading to the formation of dimers **5.7** and **5.8**.

5.5 Conclusions

The iridium catalysed *N*-alkylation of **rac-5.1** *via* hydrogen borrowing methodology was investigated and experimental design was employed to screen reaction conditions with a view to optimising the reaction. High conversion and selectivity for the desired product **5.6** was achieved through the screening design under microwave batch heated conditions, in much reduced reaction times compared to literature batch studies. For the substrate studied, Saidi *et al*. reported a 98% yield of *N*-alkylated product after 10 h at 155 °C, using 1 mol% [Cp*IrI$_2$]$_2$ and 3 Eq of **5.5**.[29] The analogous process using *i*PrOH as the alkylating agent gave 91% yield of *N*-alkylated product after 10 h at 115 °C.[28] The process described herein showed a much reduced reaction time (10 min) and a reduction in the catalyst loading (0.5 mol%), leading to a reduction in the PMI. Therefore this process was a more efficient and cheaper alternative to these existing literature procedures.

The aim was to transfer the reaction from microwave batch heating to the continuous reactor to increase the throughput and for the potential to couple to sequential continuous

processes. Unfortunately, the poor solubility of the catalyst at ambient temperatures led to inconsistencies in the quantity of catalyst that was able to be pumped into the reactor, which caused variation in the conversions obtained for each RV and prevented steady state from being reached. This also led to the conversions achieved being much lower than when using microwave batch heating as not all of the desired catalyst was present in the reactor and so the catalyst loading was lower than calculated. Further work would be required to improve the catalyst solubility to be able to consistently carry out the reaction within the continuous reactor.

The *N*-alkylation of single enantiomer **5.1** was then studied under microwave heating to determine if the amine could be *N*-alkylated. After only a few further experiments, a 92% yield of the single enantiomer *N*-alkylated product **5.6** (95% *ee*) was achieved after 1 h at 150 °C. To be able to reduce the reaction time the temperature needed to be increased, which caused the *ee* to be significantly reduced and increased the formation of dimers.

It was envisaged that the single enantiomer *N*-alkylation could be coupled to the enzymatic resolution discussed in Chapter 2 as a method to utilise the underivatised enantiomer and produce single enantiomer secondary amines. For the development of the coupled process, inhibition reactions were carried out to determine if any of the components from one of the reactions would hinder the other reaction. No inhibition of the resolution reaction was observed in the presence of the *N*-alkylation reaction components. Interestingly, the addition of ester **5.2** or amide **5.3** appeared to enhance the *N*-alkylation reaction, giving ~ 40% higher conversions compared to control reaction. These studies indicated that each reaction would not be inhibited by the components from the other reaction and so coupling the two procedures should be feasible. However when the coupled process was attempted in a stepwise manner, a much lower conversion was observed for the *N*-alkylation step. Further studies indicated that this was likely due to some material leaching from the

immobilised enzyme, either from the enzyme itself or from the support. The support was a polymer of methacrylate and so perhaps some methacrylate was leaching off and inhibiting the catalyst. Further work would be required to determine the specific cause of the inhibition and whether it can be prevented.

The selectivity and retention of stereochemistry observed prompted some interesting insights into the catalytic mechanism, in terms of the order in which the two different amines coordinate to the catalyst. Amine **5.5** appeared to outcompete amine **5.1** for coordination to the iridium centre and so by increasing the Eq of **5.5** the selectivity for desired product was significantly increased, with only a few percent of dimers observed.

In summary, screening and optimisation of reaction conditions allowed for a fast and highly selective procedure to be developed for the *N*-alkylation of a primary amine. Application of this to the single enantiomer amine provided a method to single enantiomer *N*-alkylated secondary amine and a way to re-use the undesired enantiomer remaining from the enzymatic resolution. Both procedures provided high conversion and selectivity for desired product in a much shorter time frame than existing methods. There is potential for the process to be transferred into the continuous reactor to increase the throughput and to couple the reaction to the enzymatic resolution, however, further development would be required to realise this goal.

6 Conclusions

In this research, methods were sought for the combination of chemical and biological catalysts for the production of chiral amines and essential medicines. Continuous reactors and optimisation strategies were employed to increase the productivity and efficiency. Generally, by using immobilised catalysts in packed bed reactors (PBRs) the catalyst loading could be greatly increased, leading to reduced reaction times and greater productivity.

Firstly, the lipase catalysed kinetic resolution of a chiral primary amine was studied; initially in batch and then in a continuous PBR. The reaction was optimised using a one variable at a time (OVAT) approach, to give a highly selective process with reduced reaction times and higher productivity than existing literature.[92]

Secondly, the racemisation of the chiral primary amine was investigated using Ir, Ru and Pd catalysts for the potential to recycle the waste enantiomer from the resolution in a continuous DKR process. The racemisation of primary amines is known to be difficult due to the lack of appropriate catalysts and unfortunately the substrate chosen was not suitable for racemisation by the catalysts tested, due to the high reactivity of the imine intermediate which led to the formation of dimers over racemisation.

Next, the continuous lipase catalysed reaction of esters with NH_3 for the production of two essential medicines was studied. Optimisation by DoE was carried out in the continuous PBR to determine optimum operating conditions in terms of conversion. Nicotinamide, a member of the vitamin B family, was produced in 94% yield with a tRes of 60 min at 67 °C. Pyrazinamide, a treatment for TB, was produced in quantitative yield with a tRes of only 20 min at 40 °C. The ammoniolysis of a chiral amino acid ester was then investigated. However, no reaction was observed with a range of different immobilised lipases.

Finally, the Ir catalysed *N*-alkylation of a chiral primary amine was investigated; utilising a DoE screen to favour *hetero*-coupling over *homo*-coupling. Optimisation studies were carried out under microwave heated batch conditions so as to save material. A limitation of using homogeneous catalysis in flow is that it can be wasteful, without a method to efficiently recover and re-use the catalyst. The optimum conditions gave 96% conversion and 94% selectivity for the desired *hetero*-coupled product after only 10 min, which was a vastly reduced reaction time compared to existing processes. The optimised process was then transferred to the flow reactor. Unfortunately, poor catalyst solubility resulted in lower conversions and inconsistencies in the continuous set-up. It was also determined that the enantiopurity of substrate could be maintained to achieve single enantiomer *N*-alkylated product (92% yield, 95% *ee*) by minor modification of the optimised reaction conditions developed for the racemic amine, providing a method to utilise the waste enantiomer from the kinetic resolution step. However, compatibility issues arose when trying to telescope the two steps, in that the enzyme support appeared to inhibit the Ir catalyst. This is a remaining challenge to be overcome for this procedure.

The research described herein shows improved methods for chiral amine production, whilst also highlighting the challenges associated with asymmetric synthesis of amines. The studies showed how the use of continuous reactors, microwave heating and optimisation strategies can lead to lower waste, shorter reaction times and reduced energy demand, resulting in higher efficiency and productivity.

6.1   Further Work

The continuous resolution PBR was only applied to a limited number of substrates in this work and it would be useful to expand the substrate scope further. The literature shows that N435 is active for a wide range of amine and alcohol substrates and so it would be

interesting to study some more valuable, pharmaceutically relevant molecules and determine optimum methods to produce them in the lipase PBR. The secondary amines tested within this research did not show any reactivity with N435 and so a range of different immobilised lipases would need to be tested in order to increase the scope and generality of the reactor system. This would also be the case for expanding the substrate scope for the lipase catalysed ammoniolysis reactions in the PBR.

In the racemisation studies the catalyst that showed the greatest degree of racemisation *vs.* dimer formation was the Shvö catalyst, although the reaction time was long. Immobilised versions of the Ru Shvö-type catalysts could be investigated for combination with the lipase catalysed resolution in sequential PBRs. Kim *et al*. presented polymer bound versions of an Ru catalyst **6.1** for the racemisation of alcohols.[156] Their immobilisation strategy could be applied to the modified Shvö catalysts **6.2** developed by Bäckvall and co-workers that were more active for the racemisation of amines.[66] The PBR would allow higher catalyst loading per reactor volume to be achieved and so the reaction time may be reduced to give a more viable DKR system. In the catalyst screening carried out by the Bäckvall group for amine racemisation,[66] catalyst **6.3** gave full racemisation in only 19 h, with very high selectivity for the desired reaction (> 98%). It could be envisaged that this catalyst could be immobilised by polymerisation on the styrene group to create a heterogeneous catalyst (**6.4**) for use in a PBR.
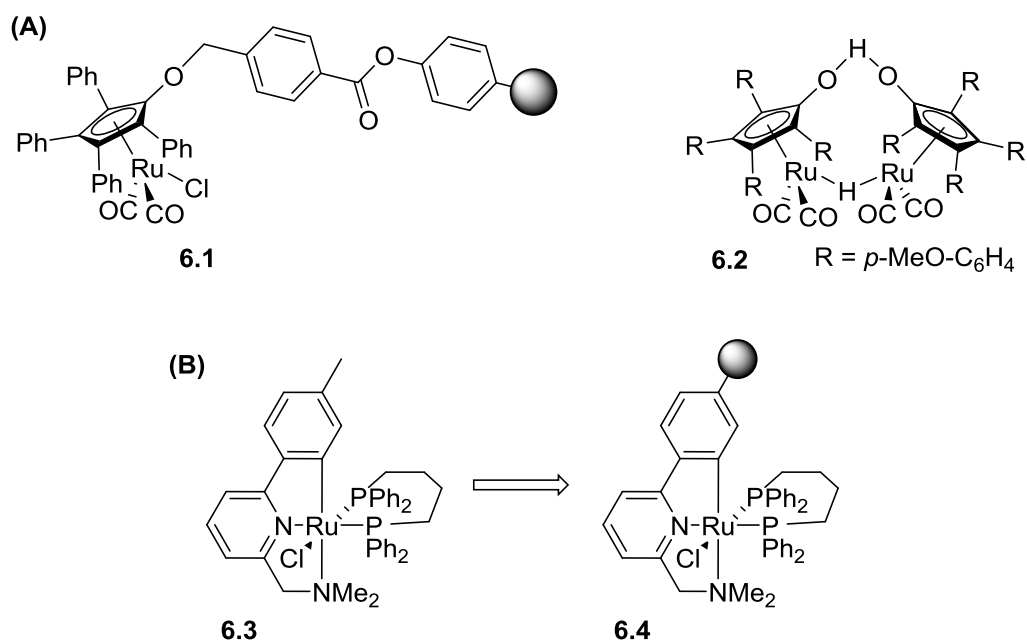
Figure 46. (A) Immobilised Ru racemisation catalyst **6.1** developed by Kim *et al.*[156] and modified Shvö catalyst **6.2** for amine racemisation developed by Bäckvall and co-workers;[66] (B) Potential heterogeneous racemisation catalyst **6.4**, based on Ru catalyst **6.3** tested by Bäckvall.[66](Grey spheres denote polymer resin).

Another route to explore further would be the heterogeneous Pd catalysed racemisation. Pd catalysts using alkaline earth supports developed by the de Vos group showed high selectivity for racemisation *vs.* dimer formation in the presence of H_2.[60] A current limitation in this work was that the current reactor set-up was unable to include gas feeds and so the Pd catalyst testing was carried out without the presence of H_2. Reactor development for the addition of gas feeds would be the next step to be able to utilise these catalysts under their optimum operating conditions, this development is currently ongoing within the research group.

However, the overriding issue with the amine racemisation is the lack of suitable catalysts. Therefore, the most valuable improvements in this area of amine racemisation would be in catalyst development, which was unfortunately beyond the remit of this project.

For the *N*-alkylation step in the continuous reactor to be developed further, the difficulties with the solubility in flow reactor need to be addressed. Lowering the concentration of the substrate appeared to reduce the amount of solid build-up in the stirred vessel and so lowering the concentration further may improve this. Whilst the DoE showed that changing the concentration had little effect on the yield and selectivity, this would reduce the productivity of the overall process and so would not be favourable. As previously discussed, increasing the temperature of the stirred vessel may increase the catalyst solubility; however, experiments would need to be carried out to determine whether any background reaction would occur between the catalyst and the substrate in the stirred vessel and would likely need a heated pump.

Further investigation into the cause of the *N*-alkylation inhibition in the presence of the immobilised lipase would also be required to determine if this can be overcome. In addition different supports for the enzyme could be tested to circumvent this. If these problems can be overcome, the coupling of the enzymatic resolution and the *N*-alkylation in the continuous system would present an opportunity to produce a single enantiomer amide from the resolution step and a single enantiomer secondary amine from the *N*-alkylation step. This would be a valuable process because there are only a few examples of lipases that can accept secondary amine substrates.[55, 72]

Alternatives to *di-iso*propylamine could also be investigated as the alkyl donor in the *N*-alkylation, which may prevent dimer formation at less harsh conditions. If the coordination of *di-iso*propylamine is inhibited by the steric bulk, then using a smaller donor such as *di*-ethylamine may ensure that only the alkyl donor coordinates to the catalyst. If the alkyl donor can completely outcompete 1-phenylethylamine for coordination to the catalyst, then this would result in only the desired *hetero*-coupled product.

Another area for development that would increase the value of the lipase PBR process is the integration of downstream processing techniques and in-line analytical techniques, to allow for more rapid analysis and determination of optimum conditions. The combination of chemo- and bio-catalysed reactions could be extended beyond DKR to combine the lipase catalysed resolution with other continuous synthetic steps for telescoped PBR processes. For example Ötvös *et al*. reported the asymmetric aldol reaction in a continuous PBR using an immobilised peptide catalyst **6.9**.[157] The optimum *ee* was only 80% and so the lipase PBR could be employed sequentially for the resolution to obtain single enantiomer product (Scheme 93).
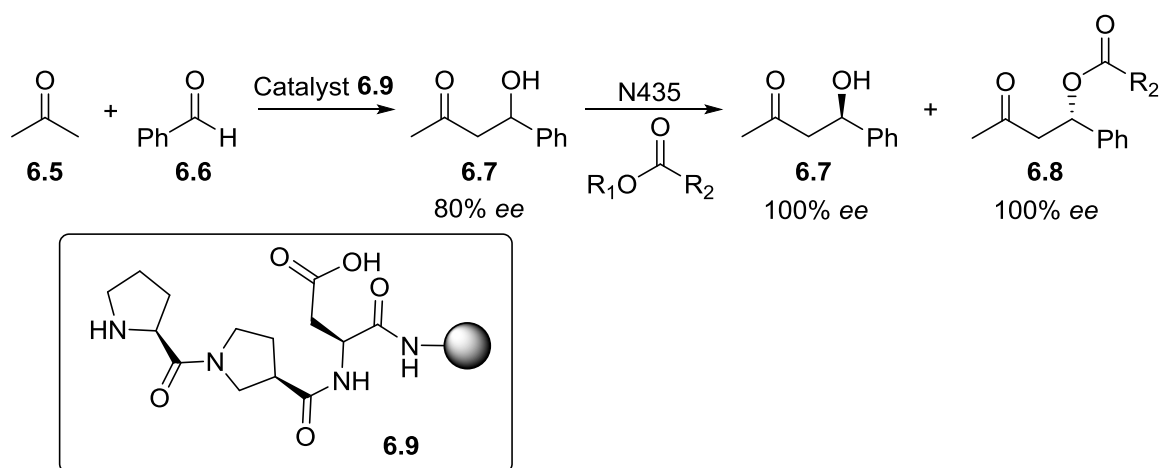
Scheme 93. Potential coupling of the lipase catalysed resolution PBR with a continuous aldol reaction in a PBR.[157]

6.2   Summary

In summary, chemical manufacturing methods must be constantly adapted and developed to achieve more efficient, cost-effective routes to target compounds. The intensification of reaction conditions achievable in flow reactors, combined with the recyclability of immobilised catalysts in PBRs, presents a viable solution to this requirement for more efficient, productive manufacturing routes. The combination of chemical and biological catalysts is a desirable concept to exploit the advantages of each catalyst type, however,

incompatibility issues means that this is not a trivial task. The work in this thesis has contributed to the development of continuous enzymatic PBRs and the use of optimisation strategies for increased productivity in the synthesis of chiral amines and essential medicines, whilst also highlighting some of the challenges associated with combining chemo- and bio-catalysis.

7 Experimental

7.1 General Experimental Methods

Unless otherwise stated, all reagents and solvents were purchased from Sigma Aldrich, Fisher Chemical, Acros Organics, Alfa Aesar, Merck or VWR International and were used without further purification. Pd/C and Pd/BaSO$_4$ catalysts were purchased from Johnson Matthey and the immobilised iridium catalyst was supplied by Yorkshire Process Technology. The activity for the Novozyme 435 batch used herein was not provided by the vendor. However an analogous product can be purchased from Sigma Aldrich with a quoted activity of $\geq$ 5000 U/g, which could be used in place of the N435 batch used. Thin layer chromatography (TLC) was carried out using silica gel 60 F$_{254}$ plates (Merck). Purifications by column chromatography were performed using silica gel, either manually or using a Biotage Isolera purification system. NMR spectra were obtained using Bruker Advance 500 at 500 MHz or using Bruker DPX 300 at 300 MHz for ^{1}H NMR and using Bruker Advance 500 at 126 MHz for ^{13}C NMR. NMR samples were recorded in CDCl$_3$ or DMSO-d^6. Chemical shifts (δ) are reported in ppm and coupling constants (J) in Hz. Multiplicities are denoted as follows: s = singlet, d = doublet, t = triplet, quart = quartet, quint = quintet, m = multiplet and br s = broad singlet. Compound multiplicities are denoted as: dd = doublet of doublets, dt = doublet of triplets *etc*. GCMS analysis was carried out on an Agilent HP-6890 instrument equipped with a HP-5973 mass selective detector and fitted with a HP-5MS column (30 m x 0.32 mm, 0.25 μm film thickness), He carrier gas. LCMS analysis was carried out on an Agilent 1290 UHPLC with Bruker HCT-Ultra detector. High resolution mass spectrometry (HRMS) was carried out on a Bruker micrOTOF with electrospray ionisation (ESI). Achiral GC analysis was carried out on an Agilent 7890B instrument fitted with a HP-5 column (30 m x 0.32 mm, 0.25 μm film thickness), H$_2$ carrier gas, FID detector. Chiral GC analysis was carried out on an Agilent HP-6890 instrument fitted with a CP-Chirasil-Dex-CB column (25 m x 0.25 mm,

0.25 μm film thickness), H_2 carrier gas, FID detector. Achiral HPLC analysis was carried out on an Agilent HP-1100 instrument fitted with a Sigma Ascentis Express C18 column (5 cm x 6.6 mm, 2.7 μm particle size) with VICI Valco 4-port sample injection (CI4W.06 manual valve, DCI4W.06 rotor, medium torque EUDA actuator, 0.06 μL injection volume). Chiral HPLC analysis was carried out on an Agilent HP-1100 instrument fitted with a Chiralpak AD column (25 cm x 4.6 mm, 10 μm particle size), 20 °C, 10 μL injection volume. All GC oven gradients and HPLC solvent gradients are described in the subsequent sections, with the corresponding analytes. Infrared (IR) analysis was carried out using a Bruker Alpha FT-IR. All microwave reactions were carried out in a CEM Discover SP Microwave Synthesizer.

7.2 Experimental Details Relating to Chapter 2

7.2.1 Chiral analysis standard method

Unless otherwise stated, all reactions were analysed by chiral GC to determine enantiomeric excess (*ee*) according to the following GC oven method: 90 °C (hold for 30 min); 40°/min to 180 °C (hold for 10 min); Inj = 300 °C; Det = 300 °C; H_2 carrier gas; 15 psi.

Enantiomeric excess was calculated from the peak areas of the two enantiomers:

$$Enantiomeric\ excess\ (\%) = \left(\frac{Area\ 1 - Area\ 2}{Area\ 1 + Area\ 2}\right) \times 100 \qquad (7.1)$$

where Area 1 is larger than Area 2.

7.2.2 Preparation of analytical standards

7.2.2.1 *N*-Acetyl-1-phenylethylamine:
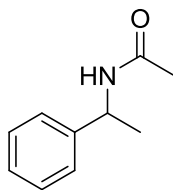
Triethylamine (1.02 g, 10.0 mmol) was added to *rac*-1-phenylethylamine (1.03 g, 8.53 mmol) in DCM (20 mL). The mixture was cooled on ice and acetic anhydride (0.94 g, 9.20 mmol) was added dropwise. The reaction was stirred at room temperature for 1.5 h. H_2O (20 mL) was then added and the layers separated. The organic phase was washed with HCl (1 M, 20 mL), dried ($MgSO_4$) and the solvent removed under vacuum to give *N*-(1-phenylethyl)acetamide as a white solid (1.16 g, 7.08 mmol, 83%). ^{1}H NMR (500 MHz, CDCl$_3$): δ 1.42 (d, *J* = 7.0 Hz, 3H, CHC*H$_3$*), 1.92 (s, 3H, C(O)C*H$_3$*), 5.07 (app quint, *J* = 7.0 Hz, 1H, C*H*CH$_3$), 5.58 (br s, 1H, N*H*), 7.19 – 7.29 (m, 5H, Ar-*H*); ^{13}C NMR (126 MHz, CDCl$_3$): δ 21.7 (*C*H$_3$), 23.5 (*C*H), 48.8 (C(O)*C*H$_3$), 126.2 (Ar*C*-H), 127.4 (Ar*C*-H), 128.7 (Ar*C*-H), 143.1 (Ar*C*), 169.0 (*C*O); *m/z* (ESI$^+$): [M+H]$^+$ 164.4; IR (solid): ν 3261, 3071, 3023, 2972, 2930, 2870, 2824, 1640, 1548, 1490, 1444 cm^{-1}; Chiral GC analysis using standard method described in Section 7.2.1: t$_R$(*N*-acetyl-[(1*R*)-1-phenylethyl]amine) = 32.1 min, t$_R$(*N*-acetyl-[(1*S*)-1-phenylethyl]amine) = 32.3 min. Data obtained was consistent with existing literature.[158]

7.2.2.2 2-Methoxy-*N*-(1-phenylethyl)acetamide:
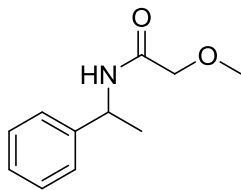
Methylmethoxy acetate (0.86g, 8.28 mmol) was added to *rac*-1-phenylethylamine (0.25 g, 2.09 mmol) in toluene (20 mL) and heated to 70 °C. After 48 h, the mixture was cooled to room temperature and HCl (1 M, 20 mL) was added. The layers were separated and the organic was dried (MgSO$_4$) and the solvent removed under vacuum to give 2-methoxy-*N*-(1-phenylethyl)acetamide as a white solid (0.046 g, 0.23 mmol, 11%). ^{1}H NMR (500 MHz, CDCl$_3$): δ 1.45 (d, $J = 7.0$ Hz, 3H, C*H$_3$*), 3.34 (s, 3H, OC*H$_3$*), 3.80 (d, $J = 15$ Hz, 1H, C*H*H), 3.85 (d, $J = 15$ Hz, 1H, CH*H*), 5.11 (app quint, $J = 7.0$ Hz, 1H, C*H*), 6.67 (br s, 1H, N*H*), 7.18 – 7.22 (m, 1H, Ar-*H*), 7.24 – 7.29 (m, 4H, Ar-*H*); ^{13}C NMR (126 MHz, CDCl$_3$): δ 21.9 (*C*H$_3$), 48.0 (*C*H), 59.1 (O*C*H$_3$), 72.0 (O*C*H$_2$), 126.2 (Ar*C*-H), 127.4 (Ar*C*-H), 128.7 (Ar*C*-H), 143.0 (Ar*C*), 168.5 (*C*O); *m/z* (ESI$^+$): [M+H]$^+$ 194.4; IR (solid): ν 3324, 3032, 2976, 2938, 2831, 2830, 1650, 1524, 1450 cm^{-1}; Chiral GC analysis using standard method described in Section 7.2.1: t_R(2-methoxy-*N*-[(*1R*)-1-phenylethyl]acetamide) = 32.7 min, t_R(2-methoxy-*N*-[(*1S*)-1-phenylethyl]acetamide) = 32.8 min. Data obtained was consistent with existing literature.[159]

7.2.2.3 *N*-[1-(4-Fluorophenyl)ethyl]-2-methoxy-acetamide
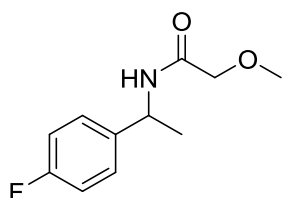
1-(4-Fluorophenyl)ethylamine (0.10 g, 0.73 mmol) was dissolved in DCM (5 mL) and the solution was cooled on ice. Methoxyacetyl chloride (0.15 g, 1.42 mmol) was then added

dropwise. After stirring for 1.5 h at room temperature, H_2O (5 mL) was added and the layers were separated. The aqueous phase was extracted with DCM (3 x 10 mL). The combined organic phases were dried ($MgSO_4$) and the solvent removed under vacuum to give a colourless oil. The crude product was purified by flash column chromatography (100% EtOAc) to give *N*-[1-(4-fluorophenyl)ethyl]-2-methoxy-acetamide as a white solid (0.096 g, 0.46 mmol, 63%). ^{1}H NMR (500 MHz, CDCl$_3$): δ 1.50 (d, *J* = 7.0 Hz, 3H, CHC*H₃*), 3.41 (s, 3H, OC*H₃*), 3.80 (d, *J* = 15 Hz, 1H, C*H*H), 3.85 (d, *J* = 15 Hz, 1H, CH*H*), 5.16 (quart, *J* = 7.0 Hz, 1H, C*H*CH₃), 6.75 (br s, 1H, N*H*), 7.01 – 7.04 (m, 2H, Ar-*H*), 7.28 – 7.31 (m, 2H, Ar-*H*); ^{13}C NMR (126 MHz, CDCl$_3$): δ 21.9 (*C*H₃), 47.5 (*C*H), 59.1 (O*C*H₃), 71.0 (*C*H₂), 115.4, 115.6 (d, Ar*C*-H), 127.8, 127.8 (d, Ar*C*-H), 138.7, 138.7 (d, Ar-*C*), 161.1, 163.0 (d, *C*F), 168.9 (*C*O); *m/z* (ESI$^+$): [M+Na]$^+$ 234.4; R$_f$ = 0.62 (100% EtOAc); IR (liquid film): ν 3409, 3305, 2978, 2934, 2828, 1737, 1655, 1500 cm^{-1}; Chiral GC oven method: 80 °C (hold for 30 min); 40°/min to 180 °C (hold for 10 min): t$_R$*N*-[1*R*-(4-fluorophenyl)ethyl]-2-methoxy-acetamide = 33.1 min, t$_R$*N*-[1*S*-(4-fluorophenyl)ethyl]-2-methoxy-acetamide = 33.2 min. Two drops of trifluoroacetic anhydride were added to samples to obtain *ee* for 1-(4-fluorophenyl)ethylamine: t$_R$1*R*-(4-fluorophenyl)ethylamine = 22.6 min, t$_R$1*S*-(4-fluorophenyl)ethylamine 23.4 min. Data obtained was consistent with existing literature.[160]

7.2.2.4 2-Methoxy-*N*-(1-methyl-3-phenylpropyl)-acetamide
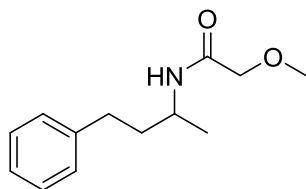
2-Amino-4-phenylbutane (0.10 g, 0.69 mmol) was dissolved in DCM (5 mL) and the solution was cooled on ice. Methoxyacetyl chloride (0.14 g, 1.31 mmol) was then added dropwise. After stirring for 2 h at room temperature, H_2O (10 mL) was added and the layers were

separated. The aqueous phase was extracted with DCM (2 x 10 mL). The combined organic phases were dried (MgSO₄) and the solvent removed under vacuum to give a colourless oil. The crude product was purified by flash column chromatography (100% EtOAc) to give 2-methoxy-N-(1-methyl-3-phenylpropyl)-acetamide as a colourless oil (0.043 g, 0.19 mmol, 28%). ^{1}H NMR (500 MHz, CDCl₃): δ 1.20 (d, J = 6.7 Hz, 3H, CHCH_3), 1.77 − 1.82 (m, 2H, CH_2CH), 2.63 − 2.67 (m, 2H, Ar-CH_2), 3.40 (s, 3H, OCH_3), 3.87 (s, 2H, COCH_2), 4.07 − 4.13 (m, 1H, CHCH₃), 6.36 (br s, 1H, NH), 7.16 − 7.19 (m, 3H, Ar-H), 7.26 − 7.29 (m , 2H, Ar-H); ^{13}C NMR (126 MHz, CDCl₃): δ 21.0 (CH₃), 32.5 (CH₂), 38.6 (CH₂), 44.6 (CH), 59.1 (OCH₃), 71.9 (OCH₂), 126.0 (ArC-H), 128.3 (ArC-H), 128.4 (ArC-H), 141.6 (Ar-C), 168.9 (CO); m/z (ESI^{+}): [M+H]$^{+}$ 222.4; R_f = 0.68 (100% EtOAc); Chiral GC oven method: 130 °C (hold for 30 min): t_R2R-methoxy-N-(1-methyl-3-phenylpropyl)-acetamide = 24.5 min, t_R2S-methoxy-N-(1-methyl-3-phenylpropyl)-acetamide = 25.2 min. Two drops of propyl chloroformate were added to samples to obtain ee for 2-amino-4-phenylbutane: t_R2R-amino-4-phenylbutane = 14.5 min, t_R2S-amino-4-phenylbutane = 14.8 min. Data obtained was consistent with existing literature.[160]

7.2.2.5 1-Phenylethyl-2-methoxyacetate
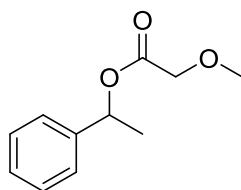
1-Phenylethanol (0.11 g, 0.93 mmol) was dissolved in DCM (5 mL). Triethylamine (0.17 g, 1.65 mmol) was added and the mixture cooled on ice. Methoxyacetyl chloride (0.18 g, 1.64 mmol) was then added dropwise and the mixture was stirred on ice for 1 h. After stirring for a further 22 h at room temperature, H₂O (5 mL) was added and the layers were separated. The aqueous phase was extracted with DCM (3 x 10 mL). The combined organic phases were

dried (MgSO$_4$) and the solvent removed under vacuum to give a yellow oil. The crude mixture was purified by column chromatography using the Biotage Isolera system (70:30 PE/EtOAc) to give 1-phenylethyl-2-methoxyacetate as a colourless oil (0.052 g, 0.27 mmol, 29%). ^{1}H NMR (500 MHz, CDCl$_3$): δ 1.50 (d, *J* = 6.6 Hz, 3H, CHC*H$_3$*), 3.37 (s, 3H, OC*H$_3$*), 3.94 (d, *J* = 15 Hz, 1H, C*H*H), 3.99 (d, *J* = 15 Hz, 1H, CH*H*), 5.93 (quart, *J* = 6.6 Hz, 1H, C*H*CH$_3$), 7.19 – 7.29 (m, 5H, Ar-*H*); ^{13}C NMR (126 MHz, CDCl$_3$): δ 22.1 (*C*H$_3$), 59.4 (*C*H), 70.0 (O*C*H$_3$), 72.9 (O*C*H$_2$), 126.2 (Ar*C*-H), 128.1 (Ar*C*-H), 128.6 (Ar*C*-H), 141.1 (Ar-*C*), 169.6 (*C*O); HRMS (ESI$^+$, *m/z*): calculated for [C$_{11}$H$_{14}$NaO$_3$]$^+$ [M+Na]$^+$ 217.0841, found 217.0840; R$_f$ = 0.39 (70:30 PE/EtOAc); IR (liquid film): ν 2984, 2934, 2828, 1751 cm^{-1}; Chiral GC analysis using standard method described in Section 7.2.1: t$_R$((1*R*)-phenylethyl-2-methoxyacetate) = 19.8 min, t$_R$((1*S*)-phenylethyl-2-methoxyacetate) = 20.5 min, t$_R$((1*R*)-phenylethanol) = 6.4 min, t$_R$((1*S*)-phenylethanol) = 6.9 min.

7.2.2.6 2-(Methoxy)-1-(4-fluorophenyl)ethyl ester
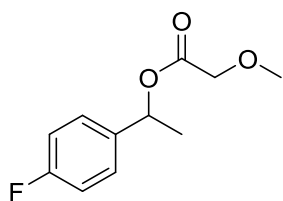
1-(4-Fluorophenyl)ethanol (1.00 g, 7.15 mmol) was dissolved in DCM (50 mL). Triethylamine (1.44 g, 14.2 mmol) was added and the mixture cooled on ice. Methoxyacetyl chloride (1.54 g, 14.2 mmol) was then added dropwise and the mixture was stirred on ice for 1 h. After stirring for a further 1 h at room temperature, H$_2$O (70 mL) was added and the layers were separated. The aqueous phase was extracted with DCM (30 mL). The combined organic phases were dried (MgSO$_4$) and the solvent removed under vacuum to give a yellow oil. The crude mixture was purified by column chromatography using the Biotage Isolera system (90:10 PE/EtOAc) to give 2-(methoxy)-1-(4-fluorophenyl)ethyl ester as a colourless

oil (0.16 g, 0.77 mmol, 11%). ^{1}H NMR (500 MHz, CDCl$_3$): δ 1.56 (d, J = 6.6 Hz, 3H, CHCH_3), 3.43 (s, 3H, OCH_3), 4.00 (d, J = 15 Hz, 1H, CHH), 4.05 (d, J = 15 Hz, 1H CHH), 5.98 (quart, J = 6.6 Hz, 1H, CHCH$_3$), 7.02 – 7.05 (m, 2H, Ar-H), 7.33 – 7.35 (m, 2H, Ar-H); ^{13}C NMR (126 MHz, CDCl$_3$): δ 22.1 (CH$_3$), 59.4 (CH), 70.0 (OCH$_3$), 72.2 (OCH$_2$), 115.3, 115.5 (d, ArC-H), 128.0, 128.1 (d, ArC-H), 136.9, 136.9 (d, ArC) 161.5, 163.4 (d, CF), 169.5 (CO); HRMS (ESI$^+$, m/z): calculated for [C$_{11}$H$_{13}$FNaO$_3$]$^+$ [M+Na]$^+$ 235.0746, found 235.0745; R$_f$ = 0.1 (90:10 PE/EtOAc); IR (liquid film): ν 2984, 2934, 2828, 1750, 1605 cm^{-1}; Chiral GC oven method: 90 °C (hold for 30 min): t$_R$(2-(Methoxy)-1R-(4-fluorophenyl)ethyl ester) = 21.5 min, t$_R$(2-(Methoxy)-1S-(4-fluorophenyl)ethyl ester) = 22.8 min, t$_R$(1R-(4-fluorophenyl)ethanol) = 7.3 min, t$_R$(1S-(4-fluorophenyl)ethanol) = 8.4 min;

7.2.2.7 4-Phenylbutan-2-yl-2-methoxyacetate
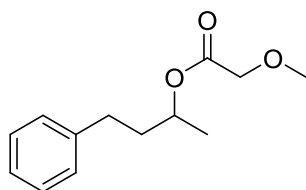
4-Phenyl-2-butanol (0.11 g, 0.71 mmol) was dissolved in DCM (5 mL). Triethylamine (0.15 g, 1.43 mmol) was added and the mixture cooled on ice. Methoxyacetyl chloride (0.14 g, 1.31 mmol) was then added dropwise and the mixture was stirred on ice for 1 h. After stirring for a further 23 h at room temperature, H$_2$O (10 mL) was added and the layers were separated. The aqueous phase was extracted with DCM (3 x 10 mL). The combined organic phases were dried (MgSO$_4$) and the solvent removed under vacuum to give a yellow oil. The crude mixture was purified by column chromatography using the Biotage Isolera system (65:35 PE/EtOAc) to give 4-phenylbutan-2-yl-2-methoxyacetate as a colourless oil (0.058 g, 0.26 mmol, 37%). ^{1}H NMR (500 MHz, CDCl$_3$): δ 1.21 (d, J = 6.3 Hz, 3H, CHCH_3), 1.73 – 1.80 (m, 1H, CHH), 1.87 – 1.94 (m, 1H, CHH), 2.52 – 2.64 (m, 2H, CH$_2$), 3.38 (s, 3H OCH_3), 3.89 (d,

$J = 17.5$ Hz, 1H, CHH), 3.93 (d, $J = 17.5$ Hz, 1H, CHH), 4.96 – 5.02 (m, 1H, CHCH$_3$), 7.09 – 7.13 (m, 3H, Ar-H), 7.19 – 7.22 (m, 2H, Ar-H); ^{13}C NMR (126 MHz, CDCl$_3$): δ 20.1 (CH$_3$), 31.8 (CH_2), 37.5 (CH_2), 59.3 (CH), 70.0 (OCH_3), 71.4 (OCH_2), 126.0 (ArC-H), 128.3 ArC-H), 128.5 (ArC-H), 141.3 (Ar-C), 170.0 (CO); m/z (ESI$^+$): [M+Na]$^+$ 245.4; R$_f$ = 0.48 (65:35 PE/EtOAc); IR (liquid film): ν 2984, 2934, 2828, 1751 cm^{-1}; Chiral GC analysis using standard method described in Section 7.2.1: t_R(R-4-phenylbutan-2-yl-2-methoxyacetate) = 32.4 min, t_R(S-4-phenylbutan-2-yl-2-methoxyacetate) = 32.5 min, t_R(R-4-phenyl-2-butanol) = 16.7 min, t_R(S-4-phenyl-2-butanol) = 17.9 min. Data obtained was consistent with existing literature.[161]

7.2.3 Novozyme 435 catalysed kinetic resolution

7.2.3.1 General procedure for Novozyme 435 catalysed kinetic resolution of *rac*-1-phenyethylamine in batch

rac-1-Phenylethylamine (0.07 M) and acyl donor (1 Eq) were added to Novozyme 435 (10 mg) in toluene (10 mL) at 60 °C. Samples were taken from the reaction every hour for chiral GC analysis. 100 μL samples were diluted to 1 mL with DCM for amide *ee*. 100 μL samples were diluted to 1 mL with DCM and 2 drops of trifluoroacetic anhydride was added for amine *ee*.

7.2.3.2 Novozyme 435 catalysed kinetic resolution of *rac*-1-phenyethylamine in continuous flow

Reactor set-up: Novozyme 435 was manually packed into a 316 stainless steel tubular reactor (1/4" OD, 1/8" ID, 3.0 mL), fitted with Supelco stainless steel frits (1/4" diameter). The packed reactor was housed within an aluminium heating block, under Eurotherm temperature control that was monitored by green K-type thermocouples inserted into the aluminium block.

The reaction solution was introduced into the reactor system using a PU-2085 dual piston pump, set to the desired flow rate. The pump was connected to the packed reactor using PTFE tubing (1/16" OD, 1/32" ID). All tee-pieces and unions used were Swagelock 316 stainless steel. Reaction samples were collected at the reactor outlet for each reactor volume, and then analysed by GC for *ee*.

The reactor volume (RV) was determined by pumping a slug of food dye in an aqueous stream through the reactor at a specified flow rate. The time between the slug entering and leaving the packed bed was then used to determine the RV according to:

$$RV\ (mL) = Flow\ rate\ (\ mL\ min^{-1}) \times Time\ spent\ in\ reactor\ (min) \quad (7.2)$$
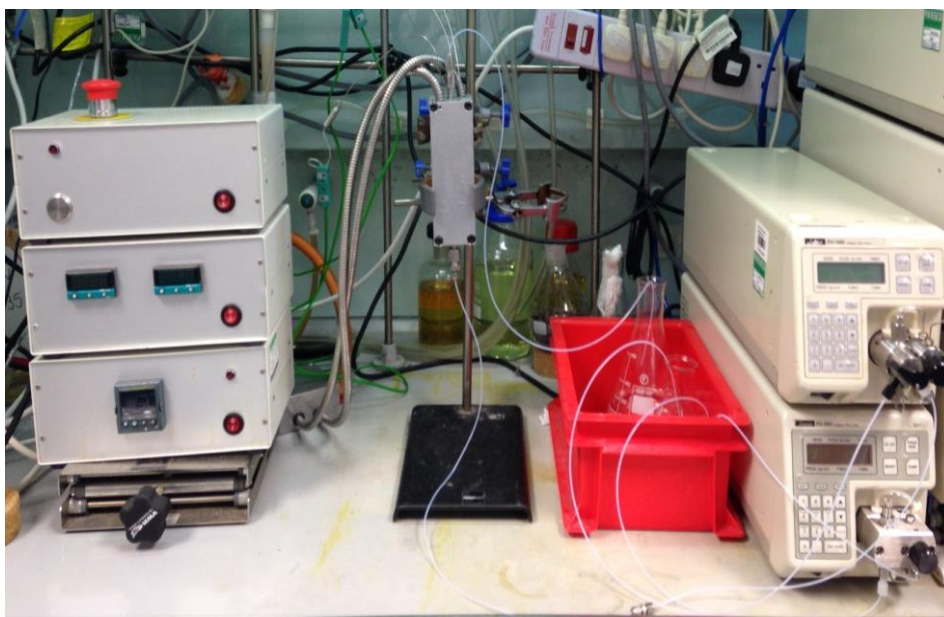
Figure 47. Continuous packed bed reactor set-up.

Table 17. Residence time screen.[a]

Entry	Flow rate / mL min^{-1}	tRes / min	Amide ee / %	Amine ee / %	Conversion / %
1	0.1	30	99	99	50
2	0.5	6	99	96	49
3	1	3	99	71	42
4	2	1.5	99	47	32

[a]Reaction conditions: 0.07 M *rac*-1-phenylethylamine, 1 eq methylmethoxy acetate, 60 °C, 3 mL reactor volume; [b]Determined by chiral GC analysis; [c]Determined by chiral GC analysis after derivatisation with trifluoroacetic anhydride; [d]Determined using Conversion = [ee_{amine} / (ee_{amine} + ee_{amide})]*100;

Table 18. Temperature screen.[a]

Entry	Temperature / °C	Amide ee^e / %	Amine ee^f / %	Conversion^g / %
1	30	100	66	40
2[b]	30	100	98	49
3[c]	30	100	75	43
4[d]	30	100	81	45
5	40	100	74	43
6	50	100	91	48
7	60	100	96	49
8	70	100	98	50
9	80	100	100	50
10	90	100	100	50
11	100	100	100	50

[a]Reaction conditions: 0.07 m *rac*-1-phenylethylamine, 1 eq methylmethoxy acetate, 3 mL reactor volume, 0.5 mL min^{-1}, tRes = 6 min; [b]tRes = 30 min; [c]Methylmethoxy acetate only pumped for 4 RV prior to reaction; [d]Solvent pumped at 60 °C for 10 RV prior to reaction; [e]Determined by chiral GC analysis; [f]Determined by chiral GC analysis after derivatisation with trifluoroacetic anhydride; [g]Determined using Conversion = [ee_{amine} / (ee_{amine} + ee_{amide})]*100;

Table 19. Concentration screen.[a]

Entry	Concentration / M	Amide ee^b / %	Amine ee^c / %	Conversion^d / %
1	0.07	99	96	49
2	0.14	99	93	48
3	0.28	99	86	46
4	0.42	99	71	41
5	0.56	99	70	41
6	0.70	99	73	42

[a]Reaction conditions: 1 eq methylmethoxy acetate, 60 °C, 3 mL reactor volume, 0.5 mL min^{-1}, tRes = 6 min; [b]Determined by chiral GC analysis; [c]Determined by chiral GC analysis after derivatisation with trifluoroacetic anhydride; [d]Determined using Conversion = [ee_{amine} / (ee_{amine} + ee_{amide})]*100;

Table 20. Catalyst recyclability testing.[a]

Time / h	Amide ee[b] / %	Amine ee[c] / %	Conversion[d] / %
1	99	91	48
2	99	98	49
3	99	98	49
4	99	96	48
6	99	97	49
7	99	97	49
23	99	95	49
24	99	95	49
25	99	95	49
27	99	97	49
28	99	97	49
29	99	96	49
30	99	94	49

[a]Reaction conditions: 0.07 m *rac*-1-phenylethylamine, 1 eq methylmethoxy acetate, 60 ℃, 3 mL reactor volume, 0.5 mL min⁻¹, tRes = 6 min; [b]Determined by chiral GC analysis; [c]Determined by chiral GC analysis after derivatisation with trifluoroacetic anhydride; [d]Determined using Conversion = [ee_{amine} / (ee_{amine} + ee_{amide})]*100;

7.2.3.3 Expanded substrate scope for Novozyme 435 catalysed kinetic resolution in continuous flow

General method: Substrate (0.14 mmol) was dissolved in toluene in 100 mL graduated flask. Methylmethoxy acetate (0.14 mmol) was dissolved in toluene in 100 mL graduated flask. The individual stock solutions were then combined in a 50:50 ratio for the reaction mixture. Novozyme 435 was packed into the stainless steel tubular reactor, which was heated to 60 °C whilst pumping toluene at 1 mL min⁻¹. Once the reactor had reached temperature and air had been purged from the system, the reaction mixture was pumped into the reactor system at 0.5 mL min⁻¹ (tRes = 6 min). Product mixture was collected at the outlet of the reactor as separate reactor volumes and analysed for *ee* of the starting material and product.

7.3 Experimental Details Relating to Chapter 3

7.3.1 GC Analysis of Components and Calibrations

Samples were analysed by GCMS according to the following GC oven method: 70 °C (hold for 1 min); 5°/min to 100 °C; 20°/min to 300 °C (hold for 1 min); Inj = 250 °C; He carrier gas; 4.76 psi; t_R(1-phenylethylamine) = 1.9 min, t_R(*N,N-di*(1-phenylethyl)amine = 12.0 and 12.2 min, t_R(*N*-(*α*-methyl)benzylidene-1-phenylethanamine = 12.9 min.

7.3.2 Preparation of analytical standards

7.3.2.1 *N*-(*α*-methyl)benzylidene-1-phenylethanamine
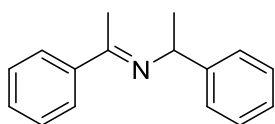
Acetophenone (0.90 g, 7.46 mmol) was added to *rac*-1-phenylethylamine (1.00 g, 8.28 mmol) in toluene (10 mL) and the mixture was heated to reflux. Concentrated H_2SO_4 (0.098 g, 0.99 mmol) was then added. After 49 h, the reaction mixture was allowed to cool to room temperature and saturated $NaHCO_{3(aq)}$ (20 mL) was added. The layers were separated and the organic phase was washed with brine (20 mL). The organic layer was dried ($MgSO_4$) and the solvent removed under vacuum to give the crude mixture as a yellow oil (0.96 g). The imine dimer was not isolated from the crude mixture, as purification by flash column chromatography returned only starting material, and was used for the synthesis of *N,N-di*(1-phenylethyl)amine without any further purification. Analysis of imine dimer in crude mixture (64% imine dimer): ^{1}H NMR (500 MHz, CDCl$_3$): δ 1.47 (d, *J* = 6.6 Hz, 3H, CHC*H₃*), 2.20 (s, 3H, CC*H₃*), 4.76 (quart, *J* = 6.6 Hz, 1H, C*H*CH₃), 7.14 − 7.90 (Ar-*H* for all components in mixture); *m/z* (ESI⁺): [M+H]⁺ 224.4;

7.3.2.2 *N,N*-di(1-phenylethyl)amine
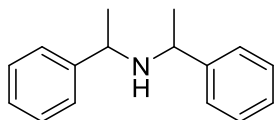
NaBH$_4$ (0.21 g, 5.45 mmol) was added to the imine crude mixture (0.50 g, 1.44 mmol imine) in MeOH (20 mL). The mixture was stirred at room temperature for 3 h. HCl (2 M) was then added to acidify and the solvent removed under reduced pressure to give an off-white solid. DCM (20 mL) and H$_2$O (20 mL) were then added and the solution basified with NaOH (1 M). The layers were separated and the aqueous phase was extracted with DCM (2 x 20 mL). The combined organics were dried (MgSO$_4$) and the solvent removed under vacuum to give a yellow oil. The crude was purified by flash column chromatography (80:20 PE/EtOAc) to give *N,N*-*di*(1-phenylethyl)amine as a pale yellow oil (0.23 g, 1.03 mmol, 72%). ^{1}H NMR (500 MHz, CDCl$_3$): δ 1.19 (d, *J* = 6.7 Hz, 3H, CHC*H$_3$*), 1.27 (d, *J* = 6.6 Hz, 3H, CHC*H$_3$*), 3.42 (quart, *J* = 6.7 Hz, 1H C*H*CH$_3$), 3.69 (quart, *J* = 6.6 Hz, 1H, C*H*CH$_3$), 7.13 − 7.27 (m, 10H, Ar-*H*); ^{13}C NMR (126 MHz, CDCl$_3$): δ 25.0 (CH3), 55.1 (CH), 126.7 (Ar*C*-H), 126.8 (Ar*C*-H), 128.4 (Ar*C*-H), 145.8 (Ar*C*); *m/z* (ESI$^+$): [M+H]$^+$ 226.4; R$_f$ = 0.21 (80:20 PE/EtOAc); IR (liquid film): ν 3082, 3061, 3025, 2960, 2924, 2863, 1602, 1491, 1450 cm^{-1}. Data obtained was consistent with existing literature.[162]

7.3.3 Iridium catalysed racemisation reactions

7.3.3.1 Racemisation of (*S*)-1-phenylethylamine using immobilised Ir-catalyst in flow

1st reactor type: (*S*)-1-Phenylethylamine in toluene was pumped, using a Harvard 11 syringe pump, through a stainless steel tubular reactor (4.0 mm ID, 25 cm, 3.1 mL) packed with immobilised Cp*Ir catalyst at the desired flow rate. The packed reactor was housed within a stainless steel heating jacket, which was placed on top of a hot-plate and heated to the desired temperature. The pump was connected to the packed reactor using PTFE tubing (1/16" OD,

1/32" ID). The product mixture was collected at the outlet of the reactor and analysed by GC to determine conversion and *ee*. The reaction mixture was transferred back into the syringes to be fed back into the reactor for re-circulation.

2nd reactor type: (*S*)-1-Phenylethylamine in toluene was pumped, using a Harvard PHD 2000 infusion syringe pump, through a stainless steel tubular reactor (1/4" OD, 1/8" ID, 3.0 mL) packed with immobilised Cp*Ir catalyst at the desired flow rate. The packed reactor was housed within an aluminium heating block, under Eurotherm temperature control that was monitored by green K-type thermocouples inserted into the aluminium block. The pump was connected to the packed reactor using PTFE tubing (1/16" OD, 1/32" ID). The product mixture was collected at the outlet of the reactor and analysed by GC to determine conversion and *ee*. The reaction mixture was transferred back into the syringes to be fed back into the reactor for re-circulation.

Table 21. Continuous racemisation of (*S*)-1-phenylethylamine, using heterogeneous Ir catalyst.[a]

Entry	Catalyst loading[c] / mol%	Temperature / °C	tRes / min	Conversion of **1**[d] / %	*ee*[e] / %
1	2.5	80	6	0	> 99
2	2.5	100	6	6	> 99
3	5	100	6	12	> 99
4[b]	2.5	110	6	1	> 99
5[b]	2.5	110	12	1	> 99
6[b]	2.5	110	30	3	> 99

[a]Reaction conditions: heterogeneous Ir catalyst, 0.07 M (*S*)-1-phenylethylamine, toluene, reactor volume = 3.1 mL; [b]Second reactor type, reactor volume = 3.0 mL; [c]Calculated relative to the entire solution flowed through the reactor over multiple cycles; [d]Determined by achiral GC analysis; [e]Determined by chiral GC analysis after derivitisation with trifluouroacetic anhydride.

7.3.3.2 Racemisation of (*S*)-1-phenylethylamine using [Cp*IrI$_2$]$_2$ in batch

(*S*)-1-Phenylethylamine (76 mg, 0.63 mmol) was added to [Cp*IrI$_2$]$_2$ (15 mg, 0.01 mmol) in toluene (10 mL). Decane (14 mg, 0.10 mmol) was added and the reaction mixture was heated to 100 °C. 100 µL samples were taken and diluted with 900 µL DCM for GCMS analysis. Two drops of trifluouracetic anhydride were added to the samples for chiral GC analysis, to determine *ee*.

Table 22. Experimental data for racemisation of (*S*)-1-phenylethylamine, using [Cp*IrI$_2$]$_2$ in batch.[a]

Time / h	Amine %[b]	Dimer %[c]	Amine *ee*[d] / %
0	100	0	99
0.5	90.5	9.5	99
1	67.5	32.5	99
1.5	58.8	41.2	99
2.5	29.6	70.4	99
3	24.3	75.7	99
4	13.3	86.7	99
5	5.6	94.4	99
6	0.4	99.6	99
7	0	100	X

[a]Reaction conditions: 0.23 M (*S*)-1-phenylethylamine, 2 mol% [Cp*IrI$_2$]$_2$ catalyst, toluene, 100 °C; [b]Determined as Amine % = (Amine area / Total area)*100; [c]Determined as Dimer % = (Dimer area / Total area)*100; [d]Determined by chiral GC analysis, after derivatisation with trifluoroacetic anhydride;

7.3.3.3 Racemisation of (*S*)-1-phenylethylamine using [Cp*IrI$_2$]$_2$ under microwave heating

General procedure: Anisole was added to [Cp*IrI$_2$]$_2$ (0.5 mol%) and biphenyl in a microwave vial and the solution stirred to dissolve the biphenyl. (*S*)-1-Phenylethylamine (1 M) was then added and the mixture heated to the desired temperature under microwave conditions for 30 min. 100 µL samples were taken before and after heating and diluted with 900 µL anisole for

achiral GC analysis, to determine conversion. Two drops of trifluoroacetic anhydride were added to the samples for chiral GC analysis, to determine *ee*.

Table 23. Racemisation microwave reactions.[a]

Entry	Temperature / °C	Amine conversion[b] / %	Amine *ee*[c] / %
1	150	34	94
2	175	74	45
3	200	85	5

[a]Reaction conditions: 1 M (*S*)-1-phenylethylamine, 0.5 mol% [Cp*IrI$_2$]$_2$, anisole, 2.5 mL total reaction volume, microwave heating, 30 min, biphenyl added as internal standard; [b]Determined by achiral GC analysis, after calibration against internal standard; [c]Determined by chiral GC analysis, after derivatisation with trifluoroacetic anhydride;

7.3.4   Ruthenium catalysed racemisation reactions

7.3.4.1 Racemisation of (*S*)-1-phenylethylamine using ruthenium Shvö catalyst in batch

 (*S*)-1-Phenylethylamine (76 mg, 0.63 mmol) was added to Shvö catalyst (28 mg, 0.03 mmol) in toluene (2.5 mL). Decane (14 mg, 0.10 mmol) was added and the reaction mixture was heated to 100 °C. 100 μL samples were taken and diluted with 900 μL DCM for GCMS analysis. Two drops of trifluoroacetic anhydride were added to the samples for chiral GC analysis, to determine *ee*.

Table 24. Experimental data for racemisation of (*S*)-1-phenylethylamine, using Shvö catalyst in batch.[a]

Time / h	Amine %[b]	Dimer %[c]	Amine *ee*[d] / %
0	100	0	100
0.5	100	0	100
1	100	0	89.6
1.5	100	0	89.6
2	100	0	94.2
3	98.4	1.6	82.5
4	97.5	2.5	82.2
5	97.1	2.9	82.2
6	94.9	5.1	80.1
23	47.7	52.3	54.3
25	42.9	57.1	-
26	41.9	58.1	47.3
27	37.1	62.9	46.9
29	34.3	65.7	43.3
46	11.3	88.7	-
47	11.4	88.6	12.0
49	10.4	89.6	6.9
51	8.0	92.0	7.4
53	5.6	94.4	2.0
72	0	100	X

[a]Reaction conditions: 0.23 M (*S*)-1-phenylethylamine, 2 mol% Shvö catalyst, toluene, 100 °C; [b]Determined as Amine % = (Amine area / Total area)*100; [c]Determined as Dimer % = (Dimer area / Total area)*100; [d]Determined by chiral GC analysis, after derivatisation with trifluoroacetic anhydride;

7.3.5 Palladium catalysed racemisation reactions

Reactions were monitored by achiral GC to determine conversion and chiral GC to determine *ee*, after derivatisation with trifluoroacetic anhydride.

7.3.5.1 Racemisation of (*S*)-1-phenylethylamine using Pd/C and Pd/BaSO₄ in batch

General procedure: Toluene (4 mL) was added to Pd/C and the mixture heated to the desired temperature. (*S*)-1-Phenylethylamine (40 mg, 0.33 mmol) and decane (146 mg, 1.0 mmol) were then added. The reaction was monitored by GC: a 300 µL sample was taken and passed through a syringe filter to remove the catalyst. 100 µL of the filtrate was taken and diluted

with 900 µL MeCN for achiral GC analysis. Two drops of trifluoroacetic anhydride were added to the samples for chiral GC analysis, to determine *ee*.

Table 25. Racemisation of (*S*)-1-phenylethylamine using Pd catalysts, under batch conditions.[a]

Entry	Catalyst type	Catalyst loading / mol%	Temperature / °C	Time / h	Amine *ee*[c] / %	Amine conversion[e] / %
1	5% Pd/C	5.7	70	24	99	16
2	5% Pd/C	6.4	100	23	99	50
3	10% Pd/C	8.5	70	23	99	10
4[b]	Pd/BaSO$_4$	3.0	70	50	99[d]	0

[a]Reaction conditions: 0.33 mmol (*S*)-1-phenylethylamine, 4.0 mL toluene, decane added as internal standard; [b]Reaction conditions: 0.35 mmol (*S*)-1-phenylethylamine, 5.0 mL toluene, 5% Pd/ BaSO$_4$ catalyst, 70 °C; [c]Determined by chiral GC after derivatisation with trifluoroacetic anhydride; [d]Determined by chiral HPLC after derivatisation with acetic anhydride; [e]Determined by achiral GC.

Entry 4: Toluene (5 mL) was added to Pd/BaSO$_4$ (10%, 3 mol%) and the mixture heated to 70 °C. (*S*)-1-Phenylethylamine (42 mg, 0.35 mmol) was then added. The reaction was monitored by chiral HPLC according to the following method: Chiralpak AD column (0.46 cm x 25 cm, 10 µm particle size), isohexane/EtOH/HNEt$_2$ 900:100:1, 1.0 mL min^{-1}, 258 nm, 20 °C, 10 µL injection volume; t$_R$(*R*-1-phenylethylamine) = 5.17 min, t$_R$(*S*-1-phenylethylamine) = 6.39 min; sample preparation: 100 µL sample was diluted with 900 µL isohexane/EtOH/HNEt$_2$ (900:100:1), and then two drops of acetic anhydride and two drops of triethylamine were added.

7.3.5.2 Racemisation of (*S*)-1-phenylethylamine using Pd/C in continuous flow

(*S*)-1-Phenylethylamine (203 mg, 1.67 mmol) and decane (73 mg, 0.51 mmol) in toluene (24 mL) was pumped, using a Jasco PU-2085 dual piston pump, through a 316 stainless steel tubular reactor (1/4" OD, 1/8" ID, 3.0 mL) manually packed with Pd/C (5%, 857 mg, 0.40

mmol Pd) at a flow rate of 0.1 mL min^{-1} (tRes = 30 min). The packed column was installed within an aluminium heating block under Eurotherm temperature control, set to 70 °C. The product mixture was collected at the exit of the column. 100 µL samples were taken and diluted with 900 µL MeCN for achiral GC analysis. Two drops of trifluoroacetic anhydride were added to the samples for chiral GC analysis, to determine *ee*. No racemisation was observed.

7.4   Experimental Details Relating to Chapter 4

7.4.1   Nicotinamide Studies

7.4.1.1 HPLC Analysis and calibrations

All reactions towards nicotinamide were analysed by achiral HPLC using the following method: H_2O (0.1% TFA)/MeCN (0.1% TFA) 95:5 to 5:95 over 7 min; then to 95:5 and hold for 2 min; 1.2 mL min^{-1}; t_R(nicotinamide) = 0.50 min, t_R(nicotinic acid) = 0.53 min, t_R(methyl nicotinate) = 1.2 min, t_R(biphenyl) = 5.9 min.

The HPLC was calibrated for the starting material and the desired product using biphenyl as internal standard to determine response factors for each component. Calibration stock solutions were made up according to:

Stock 1: 1 mmol methyl nicotinate and 0.3 mmol internal standard were dissolved in MeCN to give a 10 mL solution (0.1 M).

Stock 2: 0.3 mmol internal standard was dissolved in MeCN to give a 10 mL solution (0.03 M).

Table 26. Combination of methyl nicotinate calibration stock solutions for calibration samples.

Sample	Stock 1 volume / μL	Stock 2 volume / μL	Analyte Concentration / M	Internal Standard Concentration / M
1	1000	0	0.1	0.03
2	900	100	0.09	0.03
3	800	200	0.08	0.03
4	700	300	0.07	0.03
5	600	400	0.06	0.03
6	500	500	0.05	0.03
7	400	600	0.04	0.03
8	300	700	0.03	0.03
9	200	800	0.02	0.03
10	100	900	0.01	0.03

Stock 1: 1 mmol nicotinamide and 0.1 mmol internal standard were dissolved in MeCN to give a 10 mL solution (0.1 M).

Stock 2: 0.1 mmol internal standard was dissolved in MeCN to give a 10 mL solution (0.01 M).

Table 27. Combination of nicotinamide calibration stock solutions for calibration samples.

Sample	Stock 1 volume / μL	Stock 2 volume / μL	Analyte Concentration / M	Internal Standard Concentration / M
1	1000	0	0.1	0.01
2	900	100	0.09	0.01
3	800	200	0.08	0.01
4	700	300	0.07	0.01
5	600	400	0.06	0.01
6	500	500	0.05	0.01
7	400	600	0.04	0.01
8	300	700	0.03	0.01
9	200	800	0.02	0.01
10	100	900	0.01	0.01

$$y = 0.2907x$$
$$R^2 = 0.9997$$
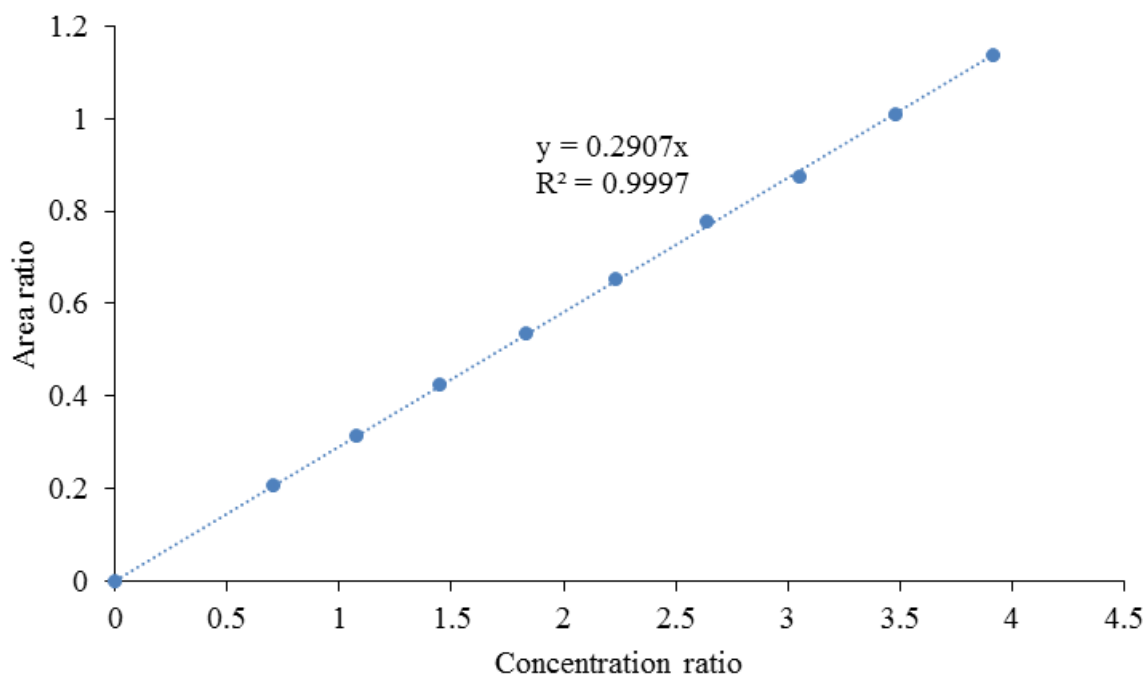
Figure 48. HPLC calibration of methyl nicotinate with biphenyl as internal standard.

$$y = 0.2912x$$
$$R^2 = 0.9997$$
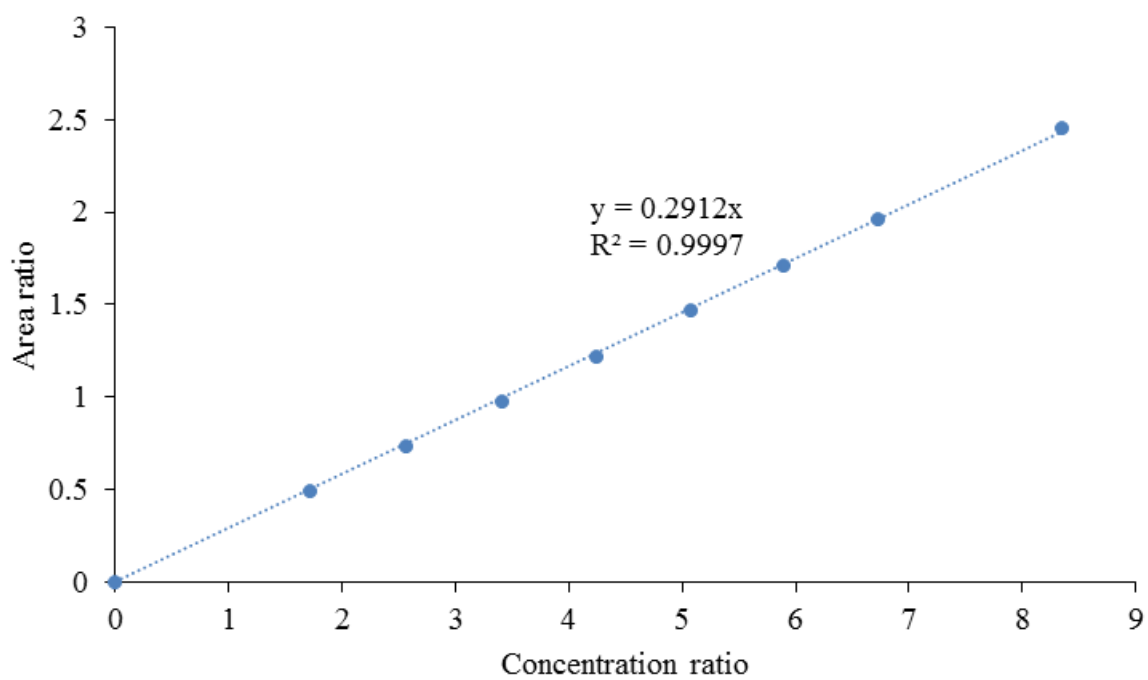
Figure 49. HPLC calibration of nicotinamide with biphenyl as internal standard.

Response factors for each of the analytes were derived from the gradient of the slope on the calibration graphs according to:

$$y = m.x \quad (7.3)$$

$$\left(\frac{Analyte\ area}{Standard\ area}\right) = R_f \times \left(\frac{Analyte\ concentration}{Standard\ concentration}\right) \quad (7.4)$$

where y is the area ratio, x is the concentration ratio and the gradient of the slope is the response factor (R_f). The response factors for methyl nicotinate and nicotinamide were determined as 0.2907 and 0.2912, respectively. The response factors were used to determine the analyte concentration from reaction samples, by rearrangement of the above equation to:

$$Analyte\ concentration = \left(\frac{Analyte\ area}{Standard\ area}\right) \times \left(\frac{Standard\ concentration}{R_f}\right) \quad (7.5)$$

when all other values are known. The conversion was then determined from the analyte concentration, as a percentage of the starting concentration:

$$Conversion\ (\%) = \left(\frac{Analyte\ concentration}{Starting\ concentration}\right) \times 100 \quad (7.6)$$

7.4.1.2 Lipase catalysed nicotinamide formation from nicotinic acid batch procedure
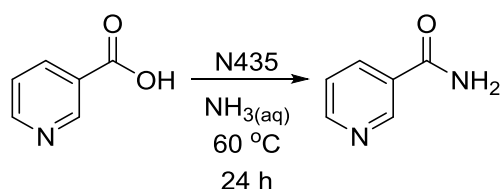
NH_3 solution (20 mL, 0.5 M in 1,4-dioxane) was added to Novozyme 435 (20 mg) and the mixture heated to 60 °C. Nicotinic acid (172 mg, 1.40 mmol) was then added. Reaction monitoring by TLC (100% EtOAc) and LCMS analysis showed no product formation. After

24 h, the reaction mixture was allowed to cool to room temperature, filtered to remove the catalyst and the solvent removed under vacuum to recover the nicotinic acid starting material.

7.4.1.3 Lipase catalysed nicotinamide formation from methyl nicotinate batch procedure
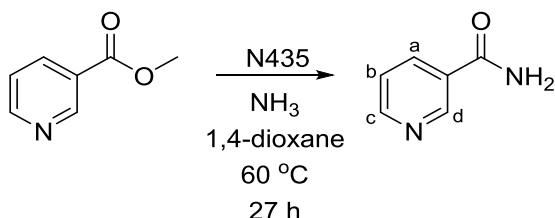
NH_3 solution (20 mL, 0.5 M in 1,4-dioxane) was added to Novozyme 435 (20 mg) and the mixture heated to 60 °C. Methyl nicotinate (192 mg, 1.40 mmol) was then added. After 27 h, the reaction mixture was allowed to cool to room temperature, the catalyst filtered off and the solvent removed under vacuum. The crude was purified by column chromatography using the Biotage Isolera system (Petroleum ether/EtOAc: 50% to 100% EtOAc, then EtOAc/MeOH: 20% MeOH) to give nicotinamide as a white solid (25 mg, 0.20 mmol, 14%). ^{1}H NMR (500 MHz, DMSO-d^6): δ 7.51 (dd, J = 8.0, 5.0 Hz, 1H, Ar-H_b), 7.60 (br s, 1H, NHH), 8.16 (br s, 1H, NHH), 8.22 (dt, J = 8.0, 2.0 Hz, 1H, Ar-H_c), 8.71 (dd, J = 5.0, 2.0 Hz, 1H, Ar-H_a), 9.04 (d, J = 2.0 Hz, 1H, Ar-H_d); ^{13}C NMR (126 MHz, DMSO-d^6): δ 123.4 (ArC-H), 129.6 (ArC-H), 135.1 (ArC-H), 148.6 (ArC-H), 151.8 (ArC), 166.4 (CO); m/z (ESI$^+$): [M+H]$^+$ 123.5; Confirmed by comparison to analytical standard.

7.4.1.4 General procedure for the continuous formation of nicotinamide

Reaction solution: 1.75 mmol methyl nicotinate and 0.1 mmol biphenyl were dissolved in NH_3 solution (0.5 M in 1,4-dioxane) to make a 25 mL stock solution.

Reactor set-up: Novozyme 435 was manually packed into a 316 stainless steel tubular reactor (1/4" OD, 1/8" ID, 2.8 mL), fitted with Supelco stainless steel frits (1/4" diameter). When the catalyst loading was varied, the reactor was packed with a mixture of Novozyme 435 and glass beads to fill the reactor tube and maintain the total reactor volume. The packed reactor was housed within an aluminium heating block, under Eurotherm temperature control that was monitored by green K-type thermocouples inserted into the aluminium block. The reaction solution was introduced into the reactor system using a PU-2085 dual piston pump, set to the desired flow rate. The pump was connected to the packed reactor using PTFE tubing (1/16" OD, 1/32" ID). All tee-pieces and unions used were Swagelock 316 stainless steel. The outlet of the reactor was connected to a back-pressure regulator (75 psi) and then fed into a collection vessel. Reaction samples were collected at the reactor outlet for each reactor volume, up to 5 RV, and then analysed by HPLC.

7.4.1.5 Scoping reactions for continuous nicotinamide formation

All scoping experiments were carried out according to the general procedure for the continuous nicotinamide formation.

Table 28. Results for scoping reactions for continuous nicotinamide formation.[a]

Reaction Level	tRes / min	Temperature / °C	Catalyst loading / g	Conversion of methyl nicotinate[c] / %
Low	20	40	0.5[b]	29
Mid	40	60	0.75[b]	78
Mid	40	60	0.75[b]	76
High	60	80	1.0	89

[a]Reaction solution = 1.75 mmol methyl nicotinate in 25 mL NH_3 solution (0.5 M in 1,4-dioxane), biphenyl added as internal standard. Reactor volume = 2.8 mL; [b]Glass beads added to fill the reactor; [c]Determined by HPLC analysis, after calibration against internal standard.

7.4.1.6 Optimisation reactions for continuous nicotinamide formation

All optimisation experiments were carried out according to the general procedure for the continuous nicotinamide formation. Experimental data for the central composite face-centred (CCF) design are given in Appendix A. Optimum conditions were determined as 60 min tRes, 67 °C and 1.0 g catalyst loading.

7.4.1.7 Reactions for testing of optimum conditions

The reaction was carried out according to the general procedure for the continuous formation of nicotinamide. The reactor was packed with Novozyme 435 (1.00 g) and heated to 67 °C. The reaction stock solution was pumped through the reactor at a flow rate of 0.047 mL min^{-1} (tRes = 60 min). Reaction samples were collected at the reactor outlet for each reactor volume, up to 5 RV, and then analysed by HPLC. 94% conversion of methyl nicotinate was observed.

7.4.1.8 Titration of NH$_3$ solutions in MeOH against standardised HCl solutions

Solution 1: 1.97 g of NaOH was dissolved in H$_2$O to give a 100 mL stock solution (0.49 M).

Solution 2: 4.2 mL of concentrated HCl was diluted with H$_2$O to give a 100 mL stock solution.

Titration of Solution 2 with Solution 1: A few drops of methyl orange indicator were added to a 10.0 mL aliquot of Solution 2. This was then titrated against standard Solution 1. The process was repeated 3 times.

Table 29. Titration of HCl Solution 2 against standard NaOH Solution 1.

Titre number	Volume of titre / L
1	0.0101
2	0.0105
3	0.0106

The concentration of Solution 2 was calculated according to the following equations:

$$Moles\ NaOH\ (mol) = Titre\ volume(L) \times Solution\ 1\ concentration(mol/L) \qquad (7.7)$$

$$Mole\ ratio\ of\ NaOH : HCl = 1 : 1 \qquad (7.8)$$

$$Concentration\ of\ Solution\ 2\ (mol/L) = \frac{Moles\ of\ HCl\ (mol)}{0.01\ (L)} \qquad (7.9)$$

The results for the 2nd and 3rd titres were combined to give an average value for the concentration of Solution 2 of 0.52 M.

Solution 3: 18 mL of 7 N NH_3 in MeOH solution was diluted with MeOH to give a 250 mL stock solution.

Titration of Solution 3 with standardised Solution 2: A few drops of bromothymol blue indicator was added to a 10.0 mL aliquot of Solution 3. This was then titrated against standardised Solution 2. The process was repeated 3 times.

Table 30. Titration of NH_3 Solution 3 against standardised HCl Solution 2.

Titre number	Volume of titre / L
1	0.0089
2	0.00885
3	0.0088

The concentration of Solution 3 was calculated according to the following equations:

$$Moles\ HCl\ (mol) = Titre\ volume(L) \times Solution\ 2\ concentration(mol/L) \qquad (7.10)$$

$$Mole\ ratio\ of\ HCl : NH_3 = 1 : 1 \qquad (7.11)$$

$$Concentration\ of\ Solution\ 3\ (mol/L) = \frac{Moles\ of\ NH_3\ (mol)}{0.01\ (L)} \qquad (7.12)$$

The results for the 2nd and 3rd titres were combined to give an average value for the concentration of Solution 2 of 0.46 M.

Solution 4: 7.96 g of NaOH was dissolved in H_2O to give a 100 mL stock solution (0.49 M).

Solution 5: 16.7 mL of concentrated HCl was diluted with H_2O to give a 100 mL stock solution.

Titration of Solution 5 with Solution 4: A few drops of methyl orange indicator was added to a 10.0 mL aliquot of Solution 5. This was then titrated against standard Solution 4. The process was repeated 3 times.

Table 31. Titration of HCl Solution 5 against standard NaOH Solution 4.

Titre number	Volume of titre / L
1	0.0104
2	0.0106
3	0.01055

The concentration of Solution 5 was calculated according to equations described above and the results for the 2nd and 3rd titres were combined to give an average value for the concentration of Solution 5 of 2.10 M.

Solution 6: 72 mL of 7 N NH_3 in MeOH solution was diluted with MeOH to give a 250 mL stock solution.

Titration of Solution 6 with standardised Solution 5: A few drops of bromothymol blue indicator was added to a 10.0 mL aliquot of Solution 6. This was then titrated against standardised Solution 5. The process was repeated 3 times.

Table 32. Titration of NH_3 Solution 6 against standardised HCl Solution 5.

Titre number	Volume of titre / L
1	0.0085
2	0.0085
3	0.0086

The concentration of Solution 6 was calculated according to equations described above and the results for the 2nd and 3rd titres were combined to give an average value for the concentration of Solution 6 of 1.79 M.

7.4.1.9 Continuous formation of nicotinamide using NH_3 solutions in methanol

All reactions were carried out according to the general procedure for the continuous formation of nicotinamide.

Reaction using 0.46 M NH_3 solution: The reaction stock solution was made-up of 1.75 mmol methyl nicotinate and 0.2 mmol biphenyl dissolved in NH_3 solution (0.46 M in MeOH) to make a 25 mL stock solution. The reactor was packed with Novozyme 435 (871 mg), fitted with a 100 psi back-pressure regulator and heated to 80 °C. The reaction stock solution was pumped through the reactor at a flow rate of 0.05 mL min^{-1} (tRes = 60 min). Reaction samples

were collected at the reactor outlet for each reactor volume, up to 5 RV, and then analysed by HPLC. No conversion was observed.

Reaction using 1.79 M NH₃ solution: The reaction stock solution was made-up of 1.75 mmol methyl nicotinate and 0.2 mmol biphenyl dissolved in NH_3 solution (1.79 M in MeOH) to make a 25 mL stock solution. The reactor was packed with Novozyme 435 (873 mg), fitted with a 100 psi back-pressure regulator and heated to 80 °C. The reaction stock solution was pumped through the reactor at a flow rate of 0.05 mL min^{-1} (tRes = 60 min). Reaction samples were collected at the reactor outlet for each reactor volume, up to 5 RV, and then analysed by HPLC. No conversion was observed.

7.4.2 Pyrazinamide Studies

7.4.2.1 HPLC Analysis and calibrations

All reactions towards pyrazinamide were analysed by achiral HPLC using the following method: H_2O (0.1% TFA)/MeCN (0.1% TFA) 99:1 hold for 2.1 min; up to 5:95 over 3.9 min, hold for 0.5 min; to 99:1 over 0.1 min and then hold for 2 min; 1.2 mL min^{-1}; t_R(pyrazinamide) = 1.6 min, t_R(pyrazine carboxylic acid) = 1.9 min, t_R(methyl pyrazine-2-carboxylate) = 3.5 min, t_R(biphenyl) = 6.2 min.

The HPLC was calibrated for methyl pyrazine-2-carboxylate and pyrazinamide using biphenyl as internal standard to determine response factors for each component. Calibration stock solutions were made up according to:

Stock 1: 1 mmol analyte was dissolved in DMSO to give a 10 mL solution (0.1 M). (Pyrazinamide was dissolved in a mixture of MeOH and DMSO).

Stock 2: 0.1 mmol internal standard was dissolved in DMSO to give a 10 mL solution (0.01 M).

Table 33. Combination of calibration stock solutions for calibration samples.

Sample	Stock 1 volume / μL	Stock 2 volume / μL	Solvent volume / μL	Analyte Concentration / M	Internal Standard Concentration / M
1	1000	100	0	0.091	0.0009
2	900	100	0	0.09	0.0009
3	800	100	100	0.08	0.001
4	700	100	200	0.07	0.001
5	600	100	300	0.06	0.001
6	500	100	400	0.05	0.001
7	400	100	500	0.04	0.001
8	300	100	600	0.03	0.001
9	200	100	700	0.02	0.001
10	100	100	800	0.01	0.001

$y = 0.2287x$
$R^2 = 0.9984$
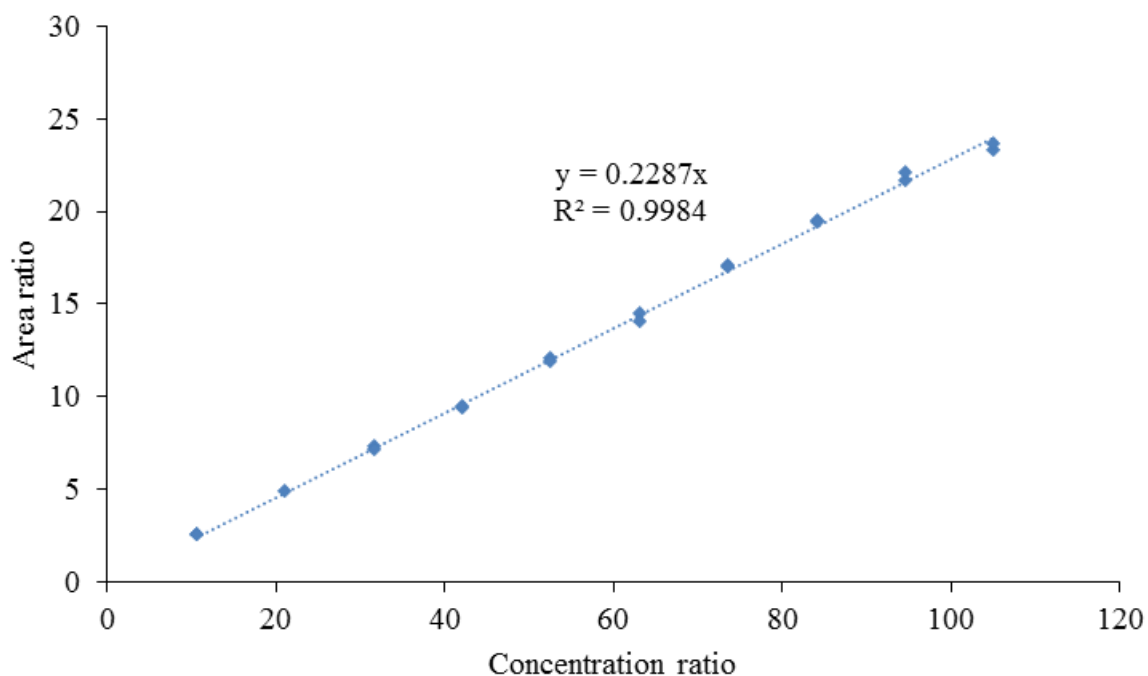
Figure 50. HPLC calibration for methyl pyrazine-2-carboxylate with biphenyl as internal standard.
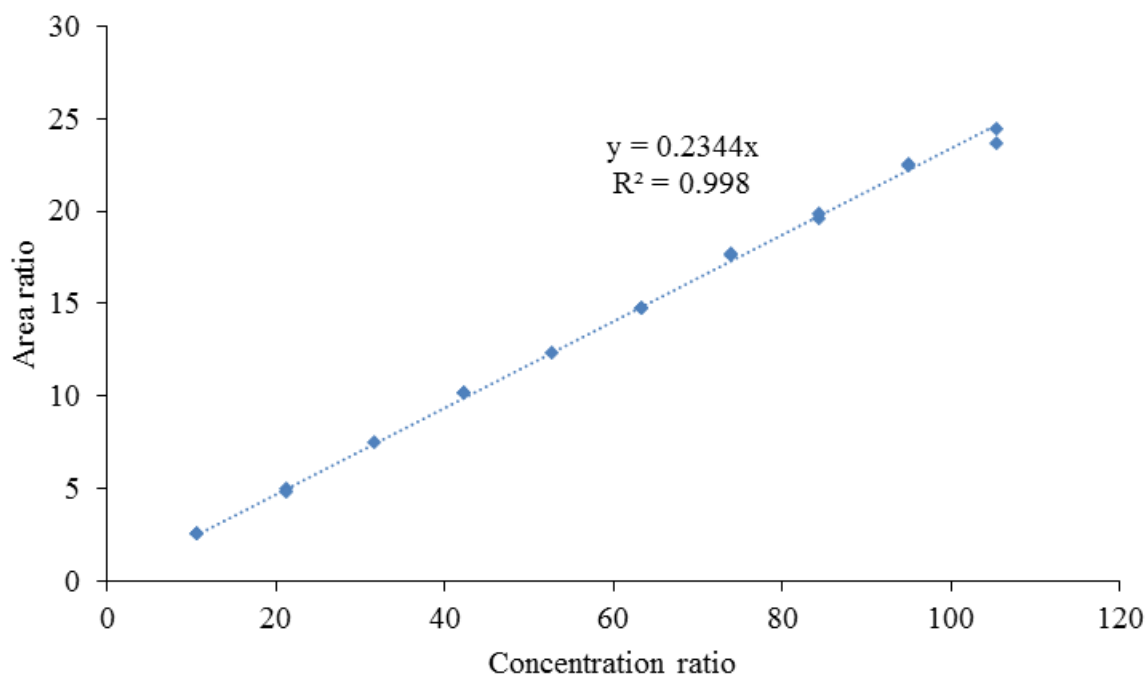
Figure 51. HPLC calibration for pyrazinamide with biphenyl as internal standard.

Response factors for each of the analytes were derived according to the method described above. The response factors for methyl pyrazine-2-carboxylate and pyrazinamide were determined as 0.2287 and 0.2344, respectively.

7.4.2.2 Methyl pyrazine-2-carboxylate synthesis
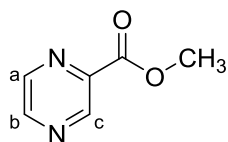
MeOH (8 mL) was added to pyrazine carboxylic acid (1.01 g, 8.13 mmol) and the mixture stirred. Concentrated H_2SO_4 (50 µL, 0.93 mmol) was then added and the reaction mixture heated to 85 °C. After 25 h, the mixture was then cooled to room temperature and the solvent removed under reduced pressure. The solid was dissolved in H_2O (10 mL) and $NaHCO_{3(aq)}$ was added to pH 8. DCM (20 mL) was added and the layers separated. The aqueous layer was

extracted with DCM (3 x 10 mL). The combined organic extracts were dried (MgSO$_4$) and the solvent removed under vacuum to give a white solid. The crude was purified using flash column chromatography (100% EtOAc) to give methyl pyrazine-2-carboxylate as a white solid (0.94 g, 6.84 mmol, 84.1%). ^{1}H NMR (500 MHz, CDCl$_3$): δ 4.06 (s, 3H, OC*H$_3$*), 8.73 (dd, *J* = 2.5, 1.5 Hz, 1H, Ar-*H$_b$*), 8.78 (d, *J* = 2.5 Hz, 1H, Ar-*H$_a$*), 9.33 (d, *J* = 1.5 Hz, 1H, Ar-*H$_c$*); ^{13}C NMR (126 MHz, CDCl$_3$): δ 53.2 (*C*H$_3$), 143.3 (Ar*C*-H), 144.4 (Ar*C*-H), 146.3 (Ar*C*-H), 147.8 (Ar*C*), 164.4 (*C*O); *m/z* (ESI$^+$): [M+H]$^+$ 139.4; IR (solid): ν 3089, 3063, 3017, 2959, 2920, 2853, 1718, 1581, 1525, 1441 cm^{-1}. Data obtained was consistent with existing literature.[163]

7.4.2.3 Lipase catalysed pyrazinamide formation batch procedure
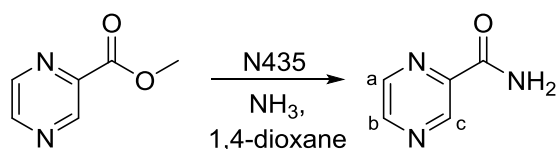
Methyl pyrazine-2-carboxylate (0.19 g, 1.34 mmol) was dissolved in NH$_3$ solution (0.5 M in 1,4-dioxane, 20 mL). The mixture was heated to 60 °C and Novozyme 435 (0.02 g) was added. After 24 h, the reaction mixture was allowed to cool to room temperature, filtered to remove the catalyst and the solvent removed under vacuum to give a white solid (0.19 g). The crude product was purified by flash column chromatography (100% EtOAc) to give pyrazinamide as a white solid (0.15 g, 1.18 mmol, 88%). ^{1}H NMR (500 MHz, DMSO-*d^6*): δ 7.87 (br s, 1H, N*H*), 8.26 (br s, 1H, N*H*), 8.73 (dd, *J* = 2.5, 1.5 Hz, 1H, Ar-*H$_b$*), 8.87 (d, *J* = 2.5 Hz, 1H, Ar-*H$_a$*), 9.20 (d, *J* = 1.5 Hz, 1H, Ar-*H$_c$*); ^{13}C NMR (126 MHz, DMSO-*d^6*): δ 143.4 (Ar*C*-H), 143.6 (Ar*C*-H), 145.1 (Ar*C*-H), 147.4 (Ar*C*), 165.0 (*C*O); *m/z* (ESI$^+$): [M+H]$^+$ 124.6; Confirmed by comparison to analytical standard.

7.4.2.4 General procedure for the continuous formation of pyrazinamide

Reaction solution: 1.75 mmol methyl pyrazine-2-carboxylate and 0.1 mmol biphenyl were dissolved in NH_3 solution (0.5 M in 1,4-dioxane) to make a 25 mL stock solution.

Reactor set-up: Novozyme 435 was manually packed into a 316 stainless steel tubular reactor (1/4" OD, 1/8" ID, 2.8 mL), fitted with Supelco stainless steel frits (1/4" diameter). When the catalyst loading was varied, the reactor was packed with a mixture of Novozyme 435 and glass beads to fill the reactor tube and maintain the total reactor volume. The packed reactor was housed within an aluminium heating block, under Eurotherm temperature control that was monitored by green K-type thermocouples inserted into the aluminium block. The reaction solution was introduced into the reactor system using a PU-2085 dual piston pump, set to the desired flow rate. The pump was connected to the packed reactor using PTFE tubing (1/16" OD, 1/32" ID). All tee-pieces and unions used were Swagelock 316 stainless steel. The outlet of the reactor was connected to a back-pressure regulator (75 psi) and then fed into a collection vessel. Reaction samples were collected at the reactor outlet for each reactor volume, up to 5 RV, and then analysed by HPLC.

Table 34. Results for the continuous formation of pyrazinamide.[a]

Entry	tRes / min	Temperature / °C	Catalyst loading / g	Ester conversion[c] / %
1	60	67	1.0	100
2	40	60	0.75[b]	100
3	20	40	0.50[b]	100
4	20	40	0.25[b]	98
5	20	40	0	1.5
6	60	80	0	10

[a]Reaction solution = 1.75 mmol methyl pyrazine-2-carboxylate in 25 mL NH_3 solution (0.5 M in 1,4-dioxane), biphenyl added as internal standard. Reactor volume = 2.8 mL; [b]Glass beads added to fill the reactor; [c]Determined by HPLC analysis, after calibration against internal standard.

7.4.2.5 Continuous formation of pyrazinamide using NH₃ solutions in methanol

The NH$_3$ in MeOH solutions (0.46 M and 1.79 M) from the nicotinamide study were used for the following reactions and all reactions were carried out according to the general according to the general procedure for the continuous formation of pyrazinamide.

Reaction using 0.46 M NH$_3$ solution: The reaction stock solution was made-up of 1.76 mmol methyl pyrazine-2-carboxylate and 0.13 mmol biphenyl dissolved in NH$_3$ solution (0.46 M in MeOH) to make a 25 mL stock solution. The reactor was packed with Novozyme 435 (500 mg) and glass beads, fitted with a 100 psi back-pressure regulator and heated to 40 °C. Methyl pyrazine-2-carboxylate was not completely soluble in the reaction stock solution and so an in-line filter was added before the pump. The reaction stock solution was pumped through the reactor at a flow rate of 0.15 mL min^{-1} (tRes = 20 min). Reaction samples were collected at the reactor outlet for each reactor volume, up to 5 RV, and then analysed by HPLC.

Reaction using 1.79 M NH$_3$ solution: The reaction stock solution was made-up of 1.80 mmol methyl pyrazine-2-carboxylate and 0.13 mmol biphenyl dissolved in NH$_3$ solution (1.79 M in MeOH) to make a 25 mL stock solution. The reactor was packed with Novozyme 435 (505 mg) and glass beads, fitted with a 100 psi back-pressure regulator and heated to 40 °C. Methyl pyrazine-2-carboxylate was not completely soluble in the reaction stock solution and so an in-line filter was added before the pump. The reaction stock solution was pumped through the reactor at a flow rate of 0.15 mL min^{-1} (tRes = 20 min). Reaction samples were collected at the reactor outlet for each reactor volume, up to 5 RV, and then analysed by HPLC.

7.4.3   *N*-Acetyl-*(D/L)*-phenylalanine studies

7.4.3.1 Analytical Methods

Samples were analysed by GCMS to monitor for product formation according to the following GC oven method: 70 °C (hold for 1 min); 5°/min to 100 °C; 20°/min to 300 °C

(hold for 1 min); Inj = 250 °C; He carrier gas; 4.76 psi; t_R(N-acetylphenylalanine methyl ester) = 12.3 min;

Samples were analysed by chiral GC to determine *ee* according to the following GC oven method: 140 °C (hold for 30 min); Inj = 300 °C; Det = 300 °C; H_2 carrier gas; 15 psi; t_R(R-N-acetyl-phenylalanine) = 17.0 min, t_R(S-N-acetyl-phenylalanine) = 17.5 min.

7.4.3.2 *N*-Acetyl-phenylalanine methyl ester synthesis
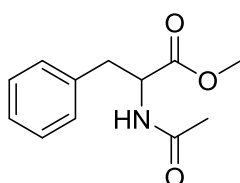
N-Acetylphenylalanine (4.97 g, 24.0 mmol) was dissolved in MeOH (125 mL). The mixture heated to reflux and then concentrated H_2SO_4 (0.15 mL, 2.87 mmol) was added. After 5 h, the mixture was allowed to cool to room temperature. $NaHCO_{3(aq)}$ (50 mL) and DCM (50 mL) were added and the layers separated. The aqueous phase was extracted with DCM (3 x 50 mL). The combined organics were dried ($MgSO_4$) and the solvent removed under vacuum to give *N*-acetylphenylalanine methyl ester as a cream coloured solid (4.04 g, 18.3 mmol, 76%).

^{1}H NMR (500 MHz, $CDCl_3$): δ 1.92 (s, 3H, OC*H₃*), 3.03 (dd, *J* = 6.0, 14.0 Hz, 1H, C*H₂*CH), 3.08 (dd, *J* = 6.0, 14.0 Hz, 1H, C*H₂*CH),3.66 (s, 3H, C(O)C*H₃*), 4.82 (dt, *J* = 60., 8.0 Hz, 1H, CH₂C*H*), 5.80 (br s, 1H, N*H*), 7.01 − 7.03 (m, 2H, Ar-*H*), 7.16 − 7.24 (m, 3H, Ar-*H*); ^{13}C NMR (126 MHz, $CDCl_3$): δ 22.2 (*C*H₂), 36.7 (*C*H), 51.8 (CO*C*H₃), 53.6 (O*C*H₃), 126.5 (Ar*C*-H), 128.2 (Ar*C*-H), 129.0 (Ar*C*-H), 137.2 (Ar*C*-H), 169.3 (Ar*C*), 172.2 (*C*O); *m/z* (ESI⁺): [M+H]⁺ 222.3; IR (solid): ν 3333, 3029, 3008, 2963, 2935, 1745, 1648, 1532, 1437 cm⁻¹; Data obtained was consistent with existing literature.[164]

7.4.3.3 Novozyme 435 catalysed ammoniolysis of *N*-acetylphenylalanine methyl ester batch procedure

NH_3 solution (10 mL, 0.5 M in 1,4-dioxane) was added to Novozyme 435 (730 mg) and the mixture heated to 67 °C. *N*-Acetylphenylalanine methyl ester (155 mg, 0.70 mmol) and biphenyl (49 mg, 0.32 mmol) were then added. After 24 h, the mixture was allowed to cool to room temperature, filtered to remove the immobilised lipase and the solvent removed under vacuum. No reaction was observed.

7.4.3.4 General procedure for batch screening of lipases for the ammoniolysis of *N*-acetylphenylalanine methyl ester

N-Acetylphenylalanine methyl ester (110 mg, 0.50 mmol) was dissolved in NH_3 solution (10 mL, 0.5 M in 1,4-dioxane). The mixture heated to 40 °C and immobilised lipase (500 mg) was added. After 24 h, the mixture was allowed to cool to room temperature, filtered to remove the immobilised lipase and the solvent removed under vacuum. ^{1}H NMR analysis was carried out to determine the presence of product.

Immobilised lipase enzymes used in batch screen:

Lipase B from *Candida Antarctica* immobilized on polyacrylic resin (Novozyme 435).

Lipase A from *Candida Antarctica* (CalA) immobilised on Immobead 150, recombinant from *Aspergillus oryzae*, 3781 U/g.

Lipase from *Candida Rugosa* immobilised on Immobead 150, 464 U/g.

Lipase from *Thermomyces Lanuginosus* (TLL) immobilised on Immobead 150, 3000 U/g.

Table 35. Results from batch screening of lipases for the ammoniolysis of *N*-acetylphenylalanine methyl ester.[a]

Entry	Enzyme	Conversion
1	N435	0
2	CalA (1892 U)	0
3	C. Rugosa (232 U)	0
4	C. Rugosa[b] (1624 U)	0
5	TLL (1502 U)	0

[a]Reaction conditions: 0.5 mmol substrate, 10 mL NH_3 solution (0.5 M in 1,4-dioxane), 500 mg catalyst, 40 °C, 24 h; [b]3.5 g catalyst used;

7.5 Experimental Details Relating to Chapter 5

7.5.1 GC Analysis of Components and Calibrations

Samples were analysed by GCMS according to the following GC oven method: 70 °C (hold for 1 min); 5°/min to 100 °C; 20°/min to 300 °C (hold for 1 min); Inj = 250 °C; He carrier gas; 4.76 psi; t_R(1-phenylethylamine) = 1.9 min, t_R(*N*-isopropyl-1-phenylethylamine) = 2.8 min, t_R(Biphenyl) = 5.5 min, t_R(2-methoxy-*N*-(1-phenylethyl)acetamide) = 8.9 min;

Samples were analysed by achiral GC according to the following GC oven method: 70 °C (hold for 1 min); 5°/min to 100 °C; 20°/min to 300 °C (hold for 1 min); Inj = 250 °C; Det = 250 °C; H_2 carrier gas; 10.8 psi; t_R(1-phenylethylamine) = 1.9 min, t_R(*N*-isopropyl-1-phenylethylamine) = 2.8 min, t_R(Biphenyl) = 5.5 min, t_R(2-methoxy-*N*-(1-phenylethyl)acetamide) = 8.9 min;

The achiral GC was calibrated for the 1-phenylethylamine, *N*-isopropyl-1-phenylethylamine and 2-methoxy-*N*-(1-phenylethyl)acetamide using biphenyl as internal standard to determine response factors for each component. Calibration stock solutions were made up according to:

Stock 1: 1 mmol analyte and 1 mmol internal standard were dissolved in toluene to give a 10 mL solution (0.1 M).

Stock 2: 1 mmol internal standard was dissolved in toluene to give a 10 mL solution (0.1 M).

Table 36. Combination of calibration stock solutions for calibration samples.

Sample	Stock 1 volume / µL	Stock 2 volume / µL	Analyte Concentration / M	Internal Standard Concentration / M
1	900	100	0.09	0.1
2	800	200	0.08	0.1
3	700	300	0.07	0.1
4	600	400	0.06	0.1
5	500	500	0.05	0.1
6	400	600	0.04	0.1
7	300	700	0.03	0.1
8	200	800	0.02	0.1
9	100	900	0.01	0.1

$y = 0.6314x$
$R^2 = 0.9995$
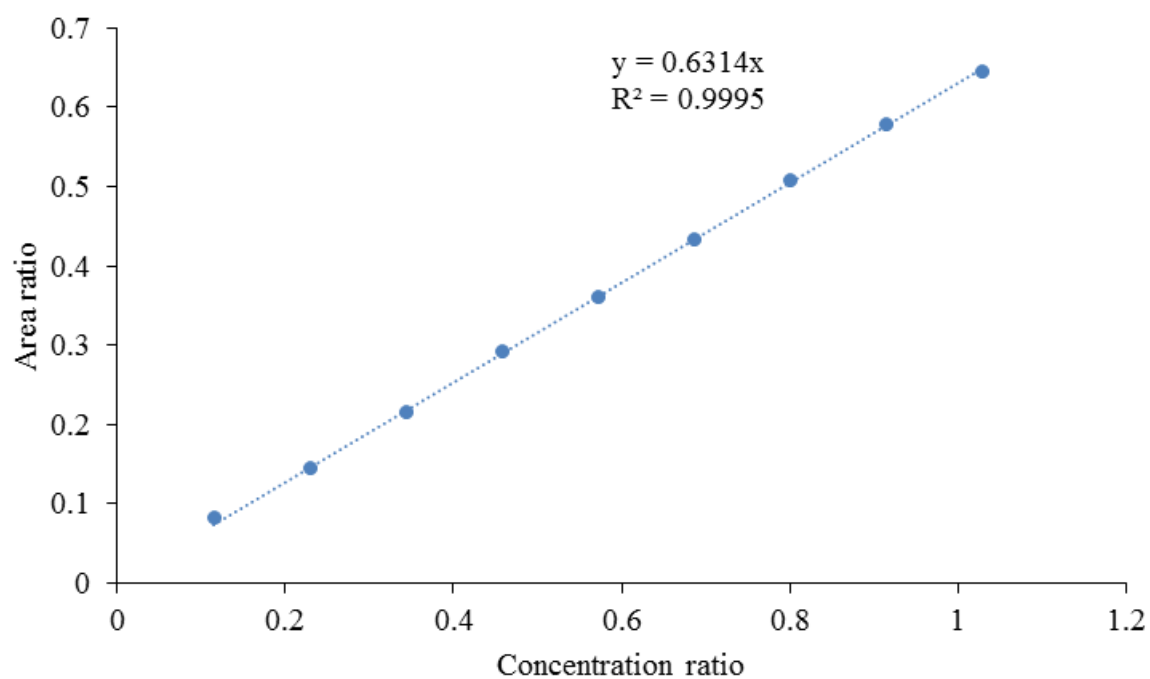
Figure 52. GC calibration of 1-phenylethylamine with biphenyl as internal standard.
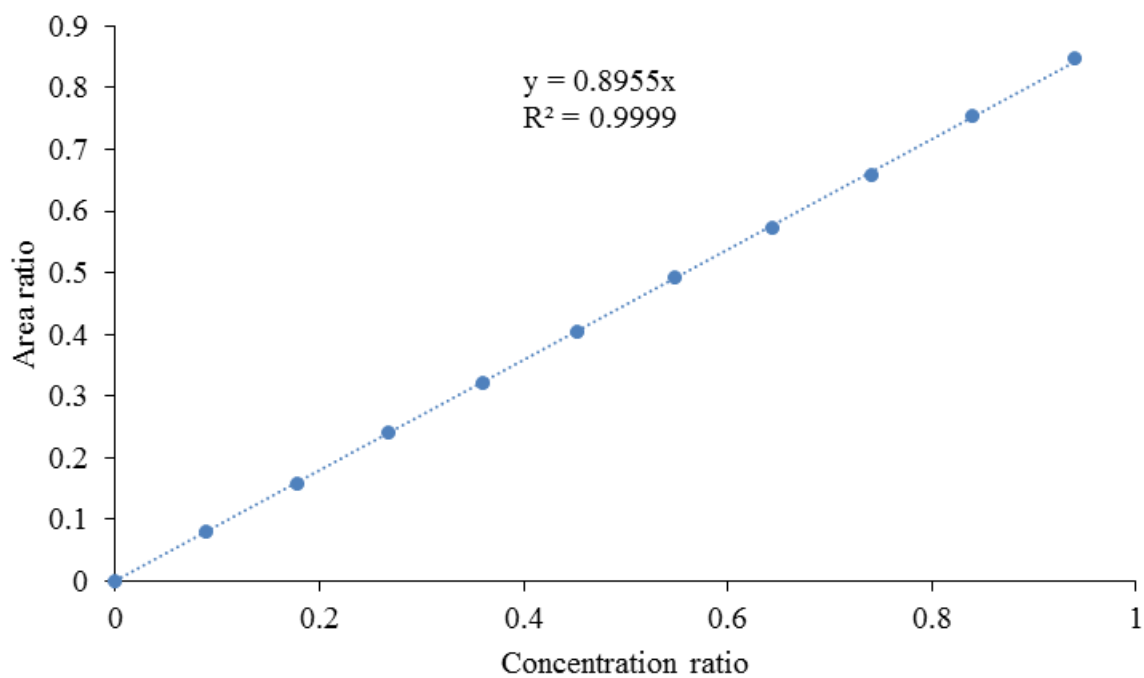
Figure 53. GC calibration of *N*-isopropyl-1-phenylethylamine with biphenyl as internal standard.
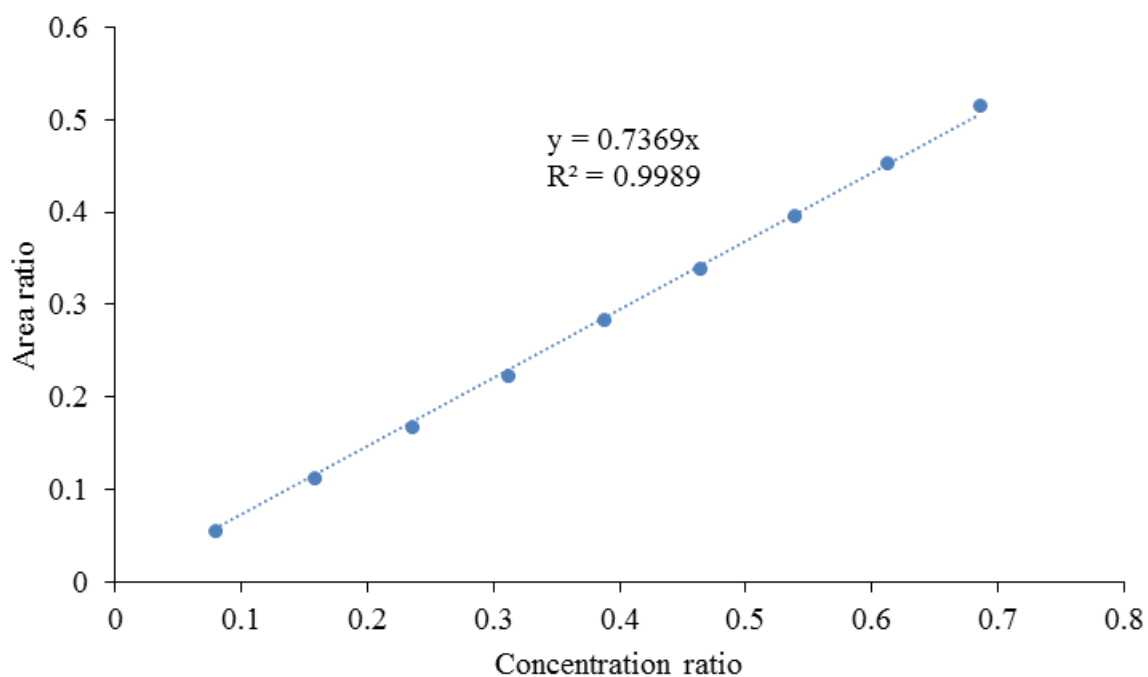
Figure 54. GC calibration of 2-methoxy-*N*-(1-phenylethyl)acetamide with biphenyl as internal standard.

Response factors for each of the analytes were derived according to the method described above. The response factors for 1-phenylethylamine, *N*-isopropyl-1-phenylethylamine and 2-methoxy-*N*-(1-phenylethyl)acetamide were determined as 0.6314, 0.8955 and 0.7369, respectively.

Samples were analysed by chiral GC to determine enantiomeric excess (*ee*) according to the following GC oven method: 80 °C (hold for 60 min); 40°/min to 180 °C (hold for 10 min); Inj = 300 °C; Det = 300 °C; H_2 carrier gas; 15 psi; t_R(2-Methoxy-*N*-[(*1R*)-1-phenylethyl]acetamide) = 62.9 min, t_R(2-Methoxy-*N*-[(*1S*)-1-phenylethyl]acetamide) = 63.0 min. Two drops of trifluoroacetic anhydride were added to samples to obtain *ee* for 1-penylethylamine and *N*-isopropyl-1-phenylethylamine: t_R((*R*)-1-phenylethylamine) = 18.3 min, t_R((*S*)-1-phenylethylamine) = 18.7 min, t_R((*R*)-*N*-isopropyl-1-phenylethylamine) = 30.5 min, t_R((*S*)-*N*-isopropyl-1-phenylethylamine) = 31.6 min.

7.5.2   Diiodo(pentamethylcyclopentadienyl)iridium(III)dimer catalyst synthesis

Acetone (45 mL) was added to [Cp*IrCl$_2$]$_2$ (1.00 g, 1.25 mmol) in a 3-necked flask fitted with thermometer and air condenser. NaI (1.90 g, 12.7 mmol) was added and the solution degassed with N_2 for 15 min. The mixture was then heated to reflux (55 – 60 ºC) under N_2. After 26 h, the mixture was allowed to cool to room temperature and DCM (50 mL) was added. The organic was washed with H_2O (3 x 50 mL) and brine (1 x 50 mL). The organic was dried (MgSO$_4$) and the solvent removed under vacuum to give a brown solid. The crude was recrystallised from DCM/PE to give a red/brown solid (1.02 g, 0.89 mmol, 71.2%). ^{1}H NMR (500 MHz, CDCl$_3$): δ 1.76 (s, 30H, Cp-C*H$_3$*); ^{13}C NMR (126 MHz, CDCl$_3$): δ 10.7 (Cp-*C*H$_3$), 88.9 (Cp*C*); Data obtained was consistent with existing literature.[57]

7.5.3 Preparation of analytical standards

7.5.3.1 *N*-Isopropyl-1-phenylethylamine
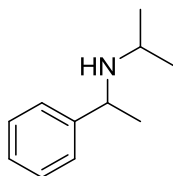
Acetone (250 mL) was added to *rac*-1-phenylethylamine (10.0 g, 82.5 mmol) and the solution heated to reflux. After 22.5 h, the reaction was allowed to cool to room temperature and the solvent removed to give a colourless oil. MeOH (220 mL) was added and the solution cooled on ice. NaBH$_4$ (6.27 g, 166 mmol) was added and the mixture stirred on ice for 1 h and for a further 2 h at room temperature. HCl (2 M) was added to acidify and the solvent removed under vacuum to give a white slurry. H$_2$O and DCM were added, the solution basified with NaOH (1 M) and extracted with DCM (3 x 50 mL). The combined organics were washed with H$_2$O (1 x 50 mL), dried (MgSO$_4$) and the solvent removed under vacuum to give the crude product as a colourless oil. The crude was purified by column chromatography using the Biotage Isolera system (EtOAc:EtOAc/Et$_3$N(5%), 80:20 to 0:100) to give *N*-isopropyl-1-phenylethylamine as a colourless liquid (3.49 g, 21.0 mmol, 25%). ^{1}H NMR (500 MHz, CDCl$_3$): δ 0.99 (d, *J* = 6.0 Hz, 3H, isopropyl-C*H₃*), 1.02 (d, *J* = 6.0 Hz, 3H, isopropyl-C*H₃*), 1.33 (d, *J* = 6.5 Hz, 3H, CHC*H₃*), 2.62 (sept, *J* = 6.0 Hz, 1H, isopropyl-C*H*), 3.88 (quart, *J* = 6.5 Hz, 1H, C*H*CH₃), 7.21 − 7.24 (m, 1H, Ar-*H*), 7.27 − 7.34 (m, 4H, Ar-*H*); ^{13}C NMR (126 MHz, CDCl$_3$): δ 22.2 (*C*H₃), 24.1 (*C*H₃), 24.9 (*C*H₃), 45.5 (*C*H), 55.1 (*C*H), 126.4 (Ar*C*-H), 126.7 (Ar*C*-H), 128.4 (Ar*C*-H), 146.1 (Ar*C*); *m/z* (ESI$^+$): [M+H]$^+$ 164.5; R$_f$ = 0.50 (100% EtOAc); IR (liquid film): ν 3062, 3025, 2960, 2926, 2865, 1602, 1492, 1465, 1451 cm^{-1}; Data obtained was consistent with existing literature.[28]

7.5.4 Heterogeneous catalyst testing

7.5.4.1 Batch Reaction

Xylene (5 mL) was added to immobilised catalyst (38 mg, 0.5 mol%, 6.28% Ir by ICP) and the mixture heated to 130 ºC. *rac*-1-Phenylethylamine (282 mg, 2.33 mmol) and *di-iso*propylamine (722 mg, 7.14 mmol) were then added. The reaction was monitored by GCMS, using the standard method, by sampling 100 µL of the reaction mixture and diluting with 900 µL MeCN. After 20 h, the reaction mixture was allowed to cool to room temperature and then filtered to remove the catalyst. H_2O (10 mL) was added and acidified with HCl (1 M). The layers were separated, the aqueous phase was basified with NaOH (1 M) and then extracted with DCM (3 x 20 mL). The combined organics were dried ($MgSO_4$) and the solvent removed under vacuum to give a yellow oil (0.24 g). ^{1}H NMR analysis of the crude mixture showed only a mixture of desired product and dimers.

Table 37. GCMS analysis of the *N*-alkylation of *rac*-1-phenylethylamine using immobilised Ir catalyst in batch.

Time / h	SM Area%	Desired product Area%	Dimers Area%
0	100	0	0
1	87	11	1.8
2	71	25	4.2
3	61	33	6.4
5	36	52	13
20	0	64	36

7.5.4.2 Continuous reaction

Reaction solution: *rac*-1-phenylethylamine (1.03 g, 8.53 mmol) and *di-iso*propylamine (2.53 g, 25.0 mmol) were dissolved in toluene (12 mL) as a single stock solution.

Reactor set-up: Heterogeneous Ir catalyst (ICP > 0.3 mmol/g) was manually packed into a 316 stainless steel tubular reactor (1/4" OD, 1/8" ID, 2.8 mL) fitted with Supelco stainless steel frits (1/4" diameter), to a loading of 4.7 mol% calculated relative to one reactor volume

(RV). The packed reactor was housed within an aluminium heating block, under Eurotherm temperature control, set to 100 °C. The stock solution was fed into the reactor using a Jasco PU-2085 dual piston pump, with a 60 min tRes, under 40 psi back pressure. The pump was connected to the packed reactor using PTFE tubing (1/16" OD, 1/32" ID). All tee-pieces and unions used were Swagelock 316 stainless steel. Reaction samples were collected at the reactor outlet for each reactor volume, and then analysed by GCMS.

Table 38. GCMS analysis of the *N*-alkylation of *rac*-1-phenylethylamine using immobilised Ir catalyst in continuous reactor.

Reactor volume	Desired product Area%
1	-
2	-
3	24
4	13
5	9
6	7
7	6

7.5.5 Homogeneous catalyst testing

7.5.5.1 General procedure for *rac*-1-phenylethylamine *N*-alkylation microwave reactions

Anisole was added to [Cp*IrI$_2$]$_2$ and biphenyl in a microwave vial and the solution stirred to dissolve the biphenyl. *rac*-1-Phenylethylamine and *di-iso*propylamine were then added and the mixture heated to the desired temperature under microwave conditions. 100 µL samples were taken before and after heating and diluted with 900 µL anisole for achiral GC analysis according to the general method to determine conversion (7.5.1).

Table 39. Racemic *N*-alkylation initial microwave reactions.[a]

Entry	Temperature / °C	Time / min	Catalyst loading / mol%	Conc of **1** / M	Eq	Amine **1**[c] / %	Desired product **6**[c] / %	Dimers[c] / %
1	100	10	0.1	0.1	1	100	0	0
2	100	30	0.2	1	3	100	0	0
3	150	10	1.0	0.5	3	28	69	3
4	200	10	1.0	0.5	3	5	84	11
5	200	30	0.5	1	3	0	89	11
6[b]	220	10	0.2	1	1	0	64	36
7[b]	220	10	0.1	1	3	0	93	7

[a]Reaction conditions: *rac*-1-phenylethylamine, *di-iso*propylamine **5**, [Cp*IrI$_2$]$_2$, toluene, biphenyl added as internal standard, total reaction volume = 2 mL; [b]Solvent = anisole; [c]Percentage composition determined by GCMS analysis; Eq = equivalents of *di-iso*propylamine.

7.5.5.2 Scoping reactions for *N*-alkylation under microwave heating

Table 40. Results from *rac*-1-phenylethylamine *N*-alkylation scoping reactions.[a]

Level	Time / min	Temp / °C	Catalyst / mol%	Conc / M	Eq	SM Conv[b] / %	Desired[b] / %	Dimers[c] / %	Selectivity[d] / %
Lower	10	180	0.3	0.5	2	79	50	29	63
Mid	20	190	0.4	0.75	3.5	93	95	-2	102
Upper	30	200	0.5	1.0	5	96	87	9	91

[a]Reaction conditions according to general procedure, total reaction volume = 5.0 mL; [b]Determined by achiral GC analysis, after calibration against internal standard; [c]Determined from: Dimers = (SM Conversion – Desired Product yield); [d]Determined from: Selectivity = (Desired Product yield/(Desired Product yield + Dimer yield))*100; Eq = equivalents of *di-iso*propylamine;

7.5.5.3 Screening reactions for *N*-alkylation under microwave heating

All reactions were carried out according to the general procedure. Experimental results for the 1st and 2nd fractional factorial Resolution V screening designs are given in Appendix B. Optimum conditions were determined as 180 °C, 10 min, 0.5 mol% catalyst loading, 1 M *rac*-1-phenylethylamine and 5 Eq of *di-iso*propylamine (96% conversion of amine, 91% desired product yield).

7.5.5.4 Continuous *N*-alkylation Procedure

Reaction solution, one pump: rac-1-Phenylethylamine (1 M or 0.5 M) and *di-iso*propylamine (5 Eq), [Cp*IrI$_2$]$_2$ (0.5 mol%), biphenyl (4.0 mmol) and anisole were combined in a stirred vessel that was heated to 40 °C in a sand bath.

Reactor set-up, one pump: The reaction solution was fed into the stainless steel tubular reactor (1/4" OD, 1/8" ID, 2.8 mL) reactor using a Jasco PU-2085 dual piston pump, with a 10 min tRes, under 100 psi back pressure. The packed reactor was housed within an aluminium heating block, under Eurotherm temperature control, set to 180 °C. The pump was connected to the packed reactor using PTFE tubing (1/16" OD, 1/32" ID), with an in-line filter fitted to the end of the tubing. All tee-pieces and unions used were Swagelock 316 stainless steel. Reaction samples were collected at the reactor outlet for each reactor volume, and then analysed by achiral GC.

Reaction solutions, two pumps: Pump A = *di-iso*propylamine (12.64 g, 125 mmol), biphenyl (299 mg, 1.94 mmol) and anisole (2.5 mL). Pump B = *rac*-1-phenylethylamine (12.13 g, 100 mmol), [Cp*IrI$_2$]$_2$ (286 mg, 0.5 mol%), biphenyl (300 mg, 1.95 mmol) and anisole (7.1 mL) combined in a stirred vessel that was heated to 40 °C in a sand bath.

Reactor set-up, two pumps: The reaction solutions were fed into the stainless steel tubular reactor (1/4" OD, 1/8" ID, 2.8 mL) reactor using Jasco PU-2085 and Jasco PU-1585 dual piston pumps, with a 10 min tRes, under 100 psi back pressure. The two feeds were combined in a tee-piece prior to entering the reactor. The packed reactor was housed within an aluminium heating block, under Eurotherm temperature control, set to 180 °C. The pump was connected to the packed reactor using PTFE tubing (1/16" OD, 1/32" ID), with an in-line filter fitted to the end of the tubing. All tee-pieces and unions used were Swagelock 316

stainless steel. Reaction samples were collected at the reactor outlet for each reactor volume, and then analysed by achiral GC.

7.5.6 Single enantiomer *N*-alkylation reactions

7.5.6.1 General procedure for (*S*)-1-phenylethylamine *N*-alkylation microwave reactions

Anisole was added to [Cp*IrI$_2$]$_2$ and biphenyl in a microwave vial and the solution stirred to dissolve the biphenyl. *(S)*-1-Phenylethylamine and *di-iso*propylamine were then added and the mixture heated to the desired temperature under microwave conditions. 100 μL samples were taken before and after heating and diluted with 900 μL toluene for GC analysis according to the general methods to determine conversion and *ee* (Section 7.5.1).

Table 41. *(S)*-1-Phenylethylamine *N*-alkylation microwave reactions.

Entry	Temperature/ °C	Reaction time / min	Eq	Amine conversion[b] / %	Desired Product[b] / %	Selectivity[c] / %	Product *ee*[d] / %
1	200	30	3	94	78	83	14
2	175	30	3	93	85	91	77
3	150	30	3	60	49	82	96
4	150	30	5	58	53	91	99
5	150	60	5	97	92	95	95

[a]Reaction conditions: 1 M (*S*)-1-phenylethylamine, 0.5 mol % [Cp*IrI$_2$]$_2$, anisole, biphenyl added as internal standard, 150 °C; [b]Determined by achiral GC analysis after calibration against internal standard; [c]Determined as (Desired product yield / Conversion of amine)*100; [d]Determined by chiral GC as [(Area1 − Area2)/(Area1 + Area2)]*100; Eq = equivalents of *di-iso*propylamine.

7.5.6.2 Inhibition microwave reactions

For the following reactions a catalyst stock solution was prepared from [Cp*IrI$_2$]$_2$ (21 mg, 0.019 mmol) in toluene (5 mL).

Microwave resolution inhibition test: Toluene (1.8 mL) was added to Novozyme 435 (145 mg) and biphenyl (78 mg, 0.51 mmol) in a microwave vial and the solution stirred to dissolve the biphenyl. *rac*-1-Phenylethylamine (18 µL, 17 mg, 0.14 mmol), methylmethoxy acetate (14 µL, 15 mg, 0.14 mmol), catalyst stock solution (100 µL) and *di-iso*propylamine (98 µL, 71 mg, 0.70 mmol) were then added and the mixture heated to 60 °C for 6 min under microwave conditions. 100 µL samples were taken before and after heating and diluted with 900 µL toluene for GC analysis according to the general method to determine conversion (Section 7.5.1). (14% amide yield).

Control reaction: Toluene (2 mL) was added to Novozyme 435 (143 mg) and biphenyl (78 mg, 0.51 mmol) in a microwave vial and the solution stirred to dissolve the biphenyl. *rac*-1-Phenylethylamine (18 µL, 17 mg, 0.14 mmol) and methylmethoxy acetate (14 µL, 15 mg, 0.14 mmol) were then added and the mixture heated to 60 °C for 6 min under microwave conditions. 100 µL samples were taken before and after heating and diluted with 900 µL toluene for GC analysis according to the general method to determine conversion (Section 7.5.1). (14% amide yield).

Microwave N-alkylation ester inhibition test: Toluene (1.8 mL) was added to catalyst stock solution (100 µL) and biphenyl (74 mg, 0.48 mmol) in a microwave vial and the solution stirred to dissolve the biphenyl. *rac*-1-Phenylethylamine (18 µL, 17 mg, 0.14 mmol), methylmethoxy acetate (14 µL, 15 mg, 0.14 mmol), and *di-iso*propylamine (98 µL, 71 mg, 0.70 mmol) were then added and the mixture heated to 150 °C for 60 min under microwave conditions. 100 µL samples were taken before and after heating and diluted with 900 µL toluene for GC analysis according to the general method to determine conversion (Section 7.5.1). (81% conversion, 76% *N*-alkylated yield).

Microwave N-alkylation amide inhibition test: Toluene (1.8 mL) was added to 2-methoxy-*N*-(1-phenylethyl)acetamide (27 mg, 0.14 mmol) and biphenyl (73 mg, 0.47 mmol) in a microwave vial and the solution stirred to dissolve the solids. *rac*-1-Phenylethylamine (18 µL, 17 mg, 0.14 mmol), catalyst stock solution (100 µL) and *di-iso*propylamine (98 µL, 71 mg, 0.70 mmol) were then added and the mixture heated to 150 °C for 60 min under microwave conditions. 100 µL samples were taken before and after heating and diluted with 900 µL toluene for GC analysis according to the general method to determine conversion (Section 7.5.1). (84% conversion, 70% *N*-alkylated yield).

Control reaction: Toluene (1.9 mL) was added to catalyst stock solution (100 µL) and biphenyl (90 mg, 0.58 mmol) in a microwave vial and the solution stirred to dissolve the biphenyl. *rac*-1-Phenylethylamine (18 µL, 17 mg, 0.14 mmol) and *di-iso*propylamine (98 µL, 71 mg, 0.70 mmol) were then added and the mixture heated to 150 °C for 60 min under microwave conditions. 100 µL samples were taken before and after heating and diluted with 900 µL toluene for GC analysis according to the general method to determine conversion (Section 7.5.1). (60% conversion, 44% *N*-alkylated yield).

7.5.6.3 Stepwise coupled procedure: microwave batch resolution with microwave batch *N*-alkylation

Step 1, Resolution: Toluene (2 mL) was added to Novozyme 435 (144 mg) and biphenyl (73 mg, 0.48 mmol) in a microwave vial and the solution stirred to dissolve the biphenyl. *rac*-1-Phenylethylamine (18 µL, 17 mg, 0.14 mmol) and methylmethoxy acetate (14 µL, 15 mg, 0.14 mmol) were then added and the mixture heated to 60 °C for 30 min under microwave conditions. 100 µL samples were taken before and after heating and diluted with 900 µL toluene for GC analysis according to the general methods to determine conversion and *ee* (Section 7.5.1). (42% conversion, 59% amine *ee*).

Step 2, N-alkylation: The product solution from Step 1 was filtered through cotton wool into a clean microwave vial. Catalyst stock solution (100 µL) and *di-iso*propylamine (98 µL, 71 mg, 0.70 mmol) were then added and the mixture heated to 150 °C for 60 min under microwave conditions. 100 µL samples were taken before and after heating and diluted with 900 µL toluene for GC analysis according to the general methods to determine conversion and *ee* (Section 7.5.1). (12% conversion, 4% *N*-alkylated yield, amine *ee* 62%).

7.5.6.4 Testing effect of Novozyme 435 on *N*-alkylation microwave reactions

Novozyme 435 filtrate added to N-alkylation, Step 1: Toluene (2 mL) was added to Novozyme 435 (144 mg) in a microwave vial and the mixture heated to 60 °C for 30 min under microwave conditions.

Step 2: The solution from Step 1 (1.5 mL) was filtered through cotton wool into a clean microwave vial and fresh toluene (0.4 mL) was added to make the total reaction volume up to 2.0 mL. Catalyst stock solution (100 µL), biphenyl (80 mg, 0.52 mmol), *rac*-1-phenylethylamine (18 µL, 17 mg, 0.14 mmol) and *di-iso*propylamine (98 µL, 71 mg, 0.70 mmol) were then added and the mixture heated to 150 °C for 60 min under microwave conditions. 100 µL samples were taken before and after heating and diluted with 900 µL toluene for GC analysis according to the general method to determine conversion (Section 7.5.1). (15% conversion, 6% *N*-alkylated yield).

Novozyme 435 added to N-alkylation: Toluene (1.9 mL) was added to catalyst stock solution (100 µL), Novozyme 435 (145 mg) and biphenyl (72 mg, 0.46 mmol) in a microwave vial. *rac*-1-Phenylethylamine (18 µL, 17 mg, 0.14 mmol) and *di-iso*propylamine (98 µL, 71 mg, 0.70 mmol) were then added and the mixture heated to 150 °C for 60 min under microwave

conditions. 100 µL samples were taken before and after heating and diluted with 900 µL toluene for GC analysis according to the general methods to determine conversion and *ee* (Section 7.5.1). (11% conversion, 1% *N*-alkylated yield).

7.5.6.5 Stepwise coupled procedure: continuous resolution with microwave batch *N*-alkylation

Step 1, Resolution: Reaction stock solution was prepared from *rac*-1-phenylethylamine (3.03 g, 25.0 mmol), methyl methoxyacetate (2.60 g, 25.0 mmol) and biphenyl (0.77 g, 5.0 mmol) dissolved in toluene, up to 25 mL. The stainless steel tubular reactor (1/4" OD, 1/8" ID, 2.8 mL) was packed with Novozyme 435 (977 mg). The reactor was primed with toluene (1 mL min^{-1}) and heated to 60 °C. Reaction stock solution was then pumped through the reactor at 0.47 mL min^{-1} (tRes = 6 min) and samples were collected for each reactor volume, up to 5 reactor volumes. 100 µL samples were taken before and after heating and diluted with 900 µL toluene for GC analysis according to the general methods to determine conversion and *ee* (Section 7.5.1).

Step 2, N-alkylation: The 5th reactor volume sample from Step 1 (2.0 mL) was added to [Cp*IrI$_2$]$_2$ (2.9 mg, 0.0026 mmol) and *di-iso*propylamine (700 µL, 505 mg, 5.0 mmol) and the mixture heated to 150 °C for 60 min under microwave conditions. 100 µL samples were taken before and after heating and diluted with 900 µL toluene for GC analysis according to the general methods to determine conversion and *ee* (Section 7.5.1).

7.5.6.6 Coupled procedure: microwave batch heating

Toluene (9.4 mL) was added to [Cp*IrI$_2$]$_2$ (1.9 mg, 0.0017 mmol) and biphenyl (387 mg, 2.51 mmol) in a microwave vial. Novozyme 435 (718 mg), *rac*-1-phenylethylamine (90 µL, 85

mg, 0.70 mmol), methyl methoxyacetate (69 µL, 73 mg, 0.70 mmol) and *di-iso*propylamine (491 µL, 355 mg, 3.50 mmol) were then added and the mixture heated to 150 °C for 60 min under microwave conditions. 100 µL samples were taken before and after heating and diluted with 900 µL toluene for GC analysis according to the general methods to determine conversion and *ee* (Section 7.5.1). (22% conversion, 1% *N*-alkylated, 18% amine *ee*, 66% amide *ee*).

7.5.6.7 Testing of filtrate for resolution activity

Step 1: Toluene (2.5 mL) was added to Novozyme 435 (144 mg) in a microwave vial and the mixture heated to 60 °C for 30 min under microwave conditions.

Step 2: The solution from Step 1 (1.8 mL) was filtered through cotton wool into a clean microwave vial and fresh toluene (0.16 mL) was added to make the total reaction volume up to 2.0 mL. *rac*-1-Phenylethylamine (18 µL, 17 mg, 0.14 mmol), methylmethoxy acetate (14 µL, 15 mg, 0.14 mmol) and biphenyl (76 mg, 0.49 mmol) were then added and the mixture heated to 60 °C for 30 min under microwave conditions. 100 µL samples were taken before and after heating and diluted with 900 µL toluene for GC analysis according to the general method to determine conversion (Section 7.5.1). No conversion was observed.

8 Appendix A

Table 42. Results from nicotinamide three-level, three variable CCF design.[a]

Experiment	Run order	tRes / min	Temperature / °C	Catalyst loading / g	Methyl nicotinate conversion[b] / %	Nicotinamide yield[b] / %
1	9	20	40	0.5	32	34
2	1	60	40	0.5	67	60
3	3	20	80	0.5	44	41
4	15	60	80	0.5	81	84
5	14	20	40	1	51	49
6	4	60	40	1	86	79
7	11	20	80	1	75	72
8	7	60	80	1	95	96
9	5	20	60	0.75	63	57
10	17	60	60	0.75	90	90
11	6	40	40	0.75	64	60
12	13	40	80	0.75	80	80
13	8	40	60	0.5	71	68
14	16	40	60	1	83	84
15	12	40	60	0.75	80	80
16	10	40	60	0.75	85	78
17	2	40	60	0.75	78	74

[a]Reaction conditions: 1.75 mmol methyl nicotinate, 25 mL NH_3 solution (0.5 M in 1,4-dioxane), biphenyl added as internal standard, catalyst = N435, reactor volume = 2.8 mL; [b]Determined by achiral HPLC analysis, after calibration against internal standard; Colour coding: green = lower limit, yellow = mid-point, red = upper limit for each variable.

9   Appendix B

Table 43. Results from first racemic *N*-alkylation screening design.[a]

Experiment	Run order	Temperature / °C	Time / min	Catalyst loading / mol%	Concentration / M	Eq	Amine conversion[b] / %	Desired product[b] / %	Dimer yield[c] / %	Selectivity[d] / %
1	11	150	10	0.1	0.1	3	0	0	0	0
2	13	150	30	0.1	0.1	1	8	3	5	38
3	6	200	10	0.1	0.1	1	34	7	27	21
4	17	200	30	0.1	0.1	3	29	10	19	34
5	15	150	10	0.5	0.1	1	0	0	0	0
6	19	150	30	0.5	0.1	3	6	0.2	5.8	3
7	8	200	10	0.5	0.1	3	77	34	43	44
8	7	200	30	0.5	0.1	1	82	58	24	71
9	4	150	10	0.1	1	1	3	0.7	2.3	23
10	1	150	30	0.1	1	3	3	1	2	33
11	2	200	10	0.1	1	3	47	38	9	81
12	18	200	30	0.1	1	1	59	46	13	78
13	9	150	10	0.5	1	3	19	11	8	58
14	10	150	30	0.5	1	1	39	30	9	77
15	5	200	10	0.5	1	1	82	63	19	77
16	14	200	30	0.5	1	3	93	87	6	94
17	12	175	20	0.3	0.55	2	62	53	9	85
18	3	175	20	0.3	0.55	2	73	62	11	85
19	16	175	20	0.3	0.55	2	80	66	14	83

[a]Reaction conditions: *rac*-1-phenylethylamine, *di-iso*propylamine, [Cp*IrI$_2$]$_2$, anisole, biphenyl added as internal standard, total reaction volume = 5.0 mL, microwave heating; [b]Determined by achiral GC analysis, after calibration against internal standard; [c]Determined as (Amine conversion – Desired product); [d]Determined as (Desired product / Amine conversion)*100; Eq = equivalents of *di-iso*propylamine; Green indicates lower limit of each variable, red indicates upper limit of each variable, yellow indicates mid-points.

Table 44. Results from second racemic *N*-alkylation screening design.[a]

Experiment	Run order	Temperature / °C	Time / min	Catalyst loading / mol%	Concentration / M	Eq	Amine conversion[b] / %	Desired product[b] / %	Dimer yield[c] / %	Selectivity[d] / %
1	15	180	10	0.3	0.5	5	73.5	67.2	6.3	91
2	11	200	10	0.3	0.5	2	90.0	86.0	4.0	96
3	4	180	30	0.3	0.5	2	91.0	79.9	11.1	88
4	8	200	30	0.3	0.5	5	96.9	90.2	6.7	93
5	14	180	10	0.5	0.5	2	87.1	79.2	7.9	91
6	9	200	10	0.5	0.5	5	92.8	82.3	10.5	89
7	5	180	30	0.5	0.5	5	96.8	90.6	6.2	94
8	13	200	30	0.5	0.5	2	92.8	78.6	14.2	85
9	16	180	10	0.3	1	2	73.8	65.5	8.3	89
10	18	200	10	0.3	1	5	96.5	90.6	6.0	94
11	7	180	30	0.3	1	5	96.9	91.4	5.4	94
12	6	200	30	0.3	1	2	92.4	78.2	14.3	85
13	19	180	10	0.5	1	5	96.2	90.6	5.6	94
14	1	200	10	0.5	1	2	91.9	79.1	12.8	86
15	2	180	30	0.5	1	2	90.5	84.9	5.6	94
16	17	200	30	0.5	1	5	97.4	90.6	6.8	93
17	10	190	20	0.4	0.75	3.5	94.8	87.4	7.4	92
18	12	190	20	0.4	0.75	3.5	95.4	88.6	6.9	93
19	3	190	20	0.4	0.75	3.5	95.1	87.8	7.3	92

[a]Reaction conditions: *rac*-1-phenylethylamine, *di-iso*propylamine, [Cp*IrI$_2$]$_2$, anisole, biphenyl added as internal standard, total reaction volume = 2.5 mL, microwave heating; [b]Determined by achiral GC analysis, after calibration against internal standard; [c]Determined as (Amine conversion – Desired product); [d]Determined as (Desired product / Amine conversion)*100; Eq = equivalents of *di-iso*propylamine; Green indicates lower limit of each variable, red indicates upper limit of each variable, yellow indicates mid-points.

10 Bibliography

1. D. Ghislieri and N. J. Turner, *Top. Catal.*, 2014, **57**, 284-300.
2. M. Breuer, K. Ditrich, T. Habicher, B. Hauer, M. Keßeler, R. Stürmer and T. Zelinski, *Angew. Chem. Int. Ed.*, 2004, **43**, 788-824.
3. P. T. Anastas and J. C. Warner, *Green Chemistry: Theory and Practice*, 1st edn., Oxford University Press, 1998.
4. P. T. Anastas and M. M. Kirchhoff, *Acc. Chem. Res.*, 2002, **35**, 686-694.
5. *Comprehensive asymmetric catalysis*, eds. E. N. Jacobsen, A. Pfaltz and H. Yamamoto, Springer-Verlag Berlin Heidelberg, 1999.
6. R. Noyori, *Chem. Soc. Rev.*, 1989, **18**, 187-208.
7. M. Kitamura, T. Ohkuma, S. Inoue, N. Sayo, H. Kumobayashi, S. Akutagawa, T. Ohta, H. Takaya and R. Noyori, *J. Am. Chem. Soc.*, 1988, **110**, 629-631.
8. T. Ohkuma, H. Ooka, S. Hashiguchi, T. Ikariya and R. Noyori, *J. Am. Chem. Soc.*, 1995, **117**, 2675-2676.
9. W. S. Knowles, *Acc. Chem. Res.*, 1983, **16**, 106-112.
10. W. S. Knowles, *J. Chem. Educ.*, 1986, **63**, 222.
11. R. Noyori, *Angew. Chem. Int. Ed.*, 2002, **41**, 2008-2022.
12. W. S. Knowles, *Angew. Chem. Int. Ed.*, 2002, **41**, 1998-2007.
13. J.-H. Xie, S.-F. Zhu and Q.-L. Zhou, *Chem. Rev.*, 2011, **111**, 1713-1760.
14. K. Huang, S. Li, M. Chang and X. Zhang, *Org. Lett.*, 2013, **15**, 484-487.
15. S. Gladiali and E. Alberico, *Chem. Soc. Rev.*, 2006, **35**, 226-236.
16. S. Hashiguchi, A. Fujii, J. Takehara, T. Ikariya and R. Noyori, *J. Am. Chem. Soc.*, 1995, **117**, 7562-7563.
17. R. Noyori and S. Hashiguchi, *Acc. Chem. Res.*, 1997, **30**, 97-102.
18. T. Ikariya and A. J. Blacker, *Acc. Chem. Res.*, 2007, **40**, 1300-1308.
19. X. Wu, X. Li, A. Zanotti-Gerosa, A. Pettman, J. Liu, A. J. Mills and J. Xiao, *Chem. Eur. J.*, 2008, **14**, 2209-2222.
20. A. J. Blacker and P. Thompson, in *Asymmetric Catalysis on Industrial Scale: Challenges, Approaches and Solutions*, eds. H.-U. Blaser and H.-J. Federsel, Wiley-VCH, 2nd edn., 2010, pp. 265-290.
21. X. Sun and A. Gavriilidis, *Org. Process. Res. Dev.*, 2008, **12**, 1218-1222.
22. M. Zanfir, X. Sun and A. Gavriilidis, *Chem. Eng. Sci.*, 2007, **62**, 741-755.
23. A. Fujii, S. Hashiguchi, N. Uematsu, T. Ikariya and R. Noyori, *J. Am. Chem. Soc.*, 1996, **118**, 2521-2522.
24. N. Uematsu, A. Fujii, S. Hashiguchi, T. Ikariya and R. Noyori, *J. Am. Chem. Soc.*, 1996, **118**, 4916-4917.
25. G. K. M. Verzijl, A. H. M. de Vries, J. G. de Vries, P. Kapitan, T. Dax, M. Helms, Z. Nazir, W. Skranc, C. Imboden, J. Stichler, R. A. Ward, S. Abele and L. Lefort, *Org. Process. Res. Dev.*, 2013, **17**, 1531-1539.
26. X. Wu, C. Wang and J. Xiao, *Platinum Metals Rev.*, 2010, **54**, 3-19.
27. X. Li, J. Blacker, I. Houson, X. Wu and J. Xiao, *Synlett*, 2006, **2006**, 1155-1160.
28. O. Saidi, A. J. Blacker, M. M. Farah, S. P. Marsden and J. M. J. Williams, *Chem. Commun.*, 2010, **46**, 1541-1543.
29. O. Saidi, A. J. Blacker, M. M. Farah, S. P. Marsden and J. M. J. Williams, *Angew. Chem. Int. Ed.*, 2009, **48**, 7375-7378.
30. K.-i. Fujita, Z. Li, N. Ozeki and R. Yamaguchi, *Tet. Lett.*, 2003, **44**, 2687-2690.
31. S. Bähn, D. Hollmann, A. Tillack and M. Beller, *Adv. Synth. Catal.*, 2008, **350**, 2099-2103.
32. Y. Zhang, C.-S. Lim, D. S. B. Sim, H.-J. Pan and Y. Zhao, *Angew. Chem. Int. Ed.*, 2014, **53**, 1399-1403.

33. F. Leipold, S. Hussain, D. Ghislieri and N. J. Turner, *ChemCatChem*, 2013, **5**, 3505-3508.

34. D. Ghislieri, A. P. Green, M. Pontini, S. C. Willies, I. Rowles, A. Frank, G. Grogan and N. J. Turner, *J. Am. Chem. Soc.*, 2013, **135**, 10863-10869.

35. N. J. Turner, *Nat. Chem. Biol.*, 2009, **5**, 567-573.

36. V. Köhler, K. R. Bailey, A. Znabet, J. Raftery, M. Helliwell and N. J. Turner, *Angew. Chem. Int. Ed.*, 2010, **49**, 2182-2184.

37. T. Li, J. Liang, A. Ambrogelly, T. Brennan, G. Gloor, G. Huisman, J. Lalonde, A. Lekhal, B. Mijts, S. Muley, L. Newman, M. Tobin, G. Wong, A. Zaks and X. Zhang, *J. Am. Chem. Soc.*, 2012, **134**, 6467-6472.

38. D. Ghislieri, D. Houghton, A. P. Green, S. C. Willies and N. J. Turner, *ACS Catal.*, 2013, **3**, 2869-2872.

39. M. J. Abrahamson, E. Vázquez-Figueroa, N. B. Woodall, J. C. Moore and A. S. Bommarius, *Angew. Chem. Int. Ed.*, 2012, **51**, 3969-3972.

40. C. K. Savile, J. M. Janey, E. C. Mundorff, J. C. Moore, S. Tam, W. R. Jarvis, J. C. Colbeck, A. Krebber, F. J. Fleitz, J. Brands, P. N. Devine, G. W. Huisman and G. J. Hughes, *Science*, 2010, **329**, 305-309.

41. M. D. Truppo, N. J. Turner and J. D. Rozzell, *Chem. Commun.*, 2009, 2127-2129.

42. L. Pasteur, *Comptes Rendus Hebdomadaires des Seances de l'Academie des Sciences*, 1853, **37**.

43. A. J. Blacker, S. Brown, B. Clique, B. Gourlay, C. E. Headley, S. Ingham, D. Ritson, T. Screen, M. J. Stirling, D. Taylor and G. Thompson, *Org. Process. Res. Dev.*, 2009, **13**, 1370-1378.

44. F. W. Reimherr, W. F. Byerley, M. F. Ward, B. J. Lebegue and P. H. Wender, *Psychopharmacology Bulletin*, 1988, **24**, 200-205.

45. A. Ghanem and H. Y. Aboul-Enein, *Chirality*, 2005, **17**, 1-15.

46. A. S. de Miranda, L. S. M. Miranda and R. O. M. A. de Souza, *Biotechnol. Adv.*, 2015, **33**, 372-393.

47. H. Kitaguchi, P. A. Fitzpatrick, J. E. Huber and A. M. Klibanov, *J. Am. Chem. Soc.*, 1989, **111**, 3094-3095.

48. E. Juaristi, J. Escalante, J. L. León-Romo and A. Reyes, *Tetrahedron: Asymm.*, 1998, **9**, 715-740.

49. E. Juaristi, J. L. León-Romo, A. Reyes and J. Escalante, *Tetrahedron: Asymm.*, 1999, **10**, 2441-2495.

50. Novozymes, *Immobilised lipase enzymes*, http://www.novozymes.com/en/solutions/pharmaceuticals/biocatalysis/immobilized-lipase-enzymes, Accessed 14th February 2017.

51. M. T. Reetz and C. Dreisbach, *CHIMIA International Journal for Chemistry*, 1994, **48**, 570-570.

52. V. Gotor-Fernández, R. Brieva and V. Gotor, *J. Mol. Catal. B*, 2006, **40**, 111-120.

53. O. Verho and J.-E. Bäckvall, *J. Am. Chem. Soc.*, 2015, **137**, 3996-4009.

54. C. E. Hoben, L. Kanupp and J.-E. Bäckvall, *Tet. Lett.*, 2008, **49**, 977-979.

55. G. F. Breen, *Tetrahedron: Asymm.*, 2004, **15**, 1427-1430.

56. O. Pàmies and J.-E. Bäckvall, *Trends Biotechnol.*, 2004, **22**, 130-135.

57. A. J. Blacker, M. J. Stirling and M. I. Page, *Org. Process. Res. Dev.*, 2007, **11**, 642-648.

58. S. Murahashi, N. Yoshimura, T. Tsumiyama and T. Kojima, *J. Am. Chem. Soc.*, 1983, **105**, 5002-5011.

59. M. T. Reetz and K. Schimossek, *CHIMIA* 1996, **50**, 668-669.

60. A. N. Parvulescu, P. A. Jacobs and D. E. De Vos, *Chem. Eur. J.*, 2007, **13**, 2034-2043.

61. A. N. Parvulescu, E. Van der Eycken, P. A. Jacobs and D. E. De Vos, *J. Catal.*, 2008, **255**, 206-212.

62. A. N. Parvulescu, P. A. Jacobs and D. E. De Vos, *Adv. Synth. Catal.*, 2008, **350**, 113-121.

63. A. L. E. Larsson, B. A. Persson and J.-E. Bäckvall, *Angewandte Chemie International Edition in English*, 1997, **36**, 1211-1212.

64. B. A. Persson, A. L. E. Larsson, M. Le Ray and J.-E. Bäckvall, *J. Am. Chem. Soc.*, 1999, **121**, 1645-1650.

65. O. Pàmies, A. H. Éll, J. S. M. Samec, N. Hermanns and J.-E. Bäckvall, *Tet. Lett.*, 2002, **43**, 4699-4702.

66. L. K. Thalén, D. Zhao, J.-B. Sortais, J. Paetzold, C. Hoben and J.-E. Bäckvall, *Chem. Eur. J.*, 2009, **15**, 3403-3410.

67. O. Verho, E. V. Johnston, E. Karlsson and J.-E. Bäckvall, *Chem. Eur. J.*, 2011, **17**, 11216-11222.

68. C. A. Denard, J. F. Hartwig and H. Zhao, *ACS Catal.*, 2013, **3**, 2856-2864.

69. K. Engström, E. V. Johnston, O. Verho, K. P. J. Gustafson, M. Shakeri, C.-W. Tai and J.-E. Bäckvall, *Angewandte Chemie (International Ed. in English)*, 2013, **52**, 14006-14010.

70. E. V. Johnston, O. Verho, M. D. Kärkäs, M. Shakeri, C.-W. Tai, P. Palmgren, K. Eriksson, S. Oscarsson and J.-E. Bäckvall, *Chem. Eur. J.*, 2012, **18**, 12202-12206.

71. L. K. Thalén and J.-E. Bäckvall, *Beilstein J. Org. chem.*, 2010, **6**, 823-829.

72. M. Stirling, J. Blacker and M. I. Page, *Tet. Lett.*, 2007, **48**, 1247-1250.

73. F. Darvas and D. György, in *Flow Chemistry, Volume 1: Fundamentals*, eds. F. Darvas, G. Dorman and V. Hessel, De Gruyter, 2014, pp. 9-58.

74. V. Hessel, D. Kralisch, N. Kockmann, T. Noël and Q. Wang, *ChemSusChem*, 2013, **6**, 746-789.

75. D. Webb and T. F. Jamison, *Chem. Sci.*, 2010, **1**, 675-680.

76. A. Adamo, P. L. Heider, N. Weeranoppanant and K. F. Jensen, *Ind. Eng. Chem. Res.*, 2013, **52**, 10802-10808.

77. D. R. Snead and T. F. Jamison, *Angew. Chem. Int. Ed.*, 2015, **54**, 983-987.

78. D. C. Fabry, E. Sugiono and M. Rueping, *React. Chem. Eng.*, 2016, **1**, 129-133.

79. N. Holmes, G. R. Akien, R. J. D. Savage, C. Stanetty, I. R. Baxendale, A. J. Blacker, B. A. Taylor, R. L. Woodward, R. E. Meadows and R. A. Bourne, *React. Chem. Eng.*, 2016, **1**, 96-100.

80. C. R. Matte, C. Bordinhão, J. K. Poppe, R. C. Rodrigues, P. F. Hertz and M. A. Z. Ayub, *J. Mol. Catal. B*, 2016, **127**, 67-75.

81. O. Levenspiel, *Chemical Reaction Engineering*, 3rd edn., John Wiley & Sons, 1999.

82. G. W. Lamb, F. A. Al Badran, J. M. J. Williams and S. T. Kolaczkowski, *Chemical Engineering Research and Design*, 2010, **88**, 1533-1540.

83. N. Zotova, F. J. Roberts, G. H. Kelsall, A. S. Jessiman, K. Hellgardt and K. K. Hii, *Green Chem.*, 2012, **14**, 226-232.

84. L. H. Andrade, W. Kroutil and T. F. Jamison, *Org. Lett.*, 2014, **16**, 6092-6095.

85. I. Itabaiana Jr, L. S. de Mariz e Miranda and R. O. M. A. de Souza, *J. Mol. Catal. B*, 2013, **85–86**, 1-9.

86. K. Frings, M. Koch and W. Hartmeier, *Enzyme and Microbial Technology*, 1999, **25**, 303-309.

87. C. Csajági, G. Szatzker, E. Rita Tőke, L. Ürge, F. Darvas and L. Poppe, *Tetrahedron: Asymm.*, 2008, **19**, 237-246.

88. C. Thomas Juliana, D. Burich Martha, T. Bandeira Pamela, R. Marques de Oliveira Alfredo and L. Piovan, *Biocatalysis*, 2017, **3**, 27.

89. A. Sánchez, F. Valero, J. Lafuente and C. Solà, *Enzyme and Microbial Technology*, 2000, **27**, 157-166.
90. J.-C. Chen and S.-W. Tsai, *Biotechnology Progress*, 2000, **16**, 986-992.
91. ThalesNano, *ThalesNano Flow Chemistry Reactors*, http://thalesnano.com/, Accessed 14th May 2017.
92. A. S. de Miranda, L. S. M. Miranda and R. O. M. A. de Souza, *Org. Biomol. Chem.*, 2013, **11**, 3332-3336.
93. C. Roengpithya, D. A. Patterson, A. G. Livingston, P. C. Taylor, J. L. Irwin and M. R. Parrett, *Chem. Commun.*, 2007, 3462-3463.
94. A. S. de Miranda, R. O. M. A. de Souza and L. S. M. Miranda, *RSC Adv.*, 2014, **4**, 13620-13625.
95. A. S. de Miranda, M. V. de M. Silva, F. C. Dias, S. P. de Souza, R. A. C. Leao and R. O. M. A. de Souza, *React. Chem. Eng.*, 2017.
96. S. Wuyts, J. Wahlen, P. A. Jacobs and D. E. De Vos, *Green Chem.*, 2007, **9**, 1104-1108.
97. WHO, *WHO Model List of Essential Medicines*, http://www.who.int/medicines/publications/essentialmedicines/en/, Accessed 23rd June 2016.
98. D. Mandala, S. Chada and P. Watts, *Org. Biomol. Chem.*, 2017, **15**, 3444-3454.
99. J. Verghese, C. Kong, D. Rivalti, E. Yu, R. Krack, J. Alcazar, J. B. Manley, D. T. McQuade, S. Ahmad, K. Belecki and F. Gupton, *Green Chem.*, 2017.
100. A. Adamo, R. L. Beingessner, M. Behnam, J. Chen, T. F. Jamison, K. F. Jensen, J.-C. M. Monbaliu, A. S. Myerson, E. M. Revalor, D. R. Snead, T. Stelzer, N. Weeranoppanant, S. Y. Wong and P. Zhang, *Science*, 2016, **352**, 61-67.
101. R. Munirathinam, J. Huskens and W. Verboom, *Adv. Synth. Catal.*, 2015, **357**, 1093-1123.
102. S. J. Fletcher and C. M. Rayner, *Tet. Lett.*, 1999, **40**, 7139-7142.
103. R. E. Gawley, *J. Org. Chem.*, 2006, **71**, 2411-2416.
104. M. Cammenberg, K. Hult and S. Park, *ChemBioChem*, 2006, **7**, 1745-1749.
105. M. C. de Zoete, F. van Rantwijk and R. A. Sheldon, *Catalysis Today*, 1994, **22**, 563-590.
106. L. Michaelis and M. L. Menten, *Biochemische Zeitschrift*, 1913, **49**, 333-369.
107. K. A. Johnson and R. S. Goody, *Biochemistry*, 2011, **50**, 8264-8269.
108. D. N. Jumbam, R. A. Skilton, A. J. Parrott, R. A. Bourne and M. Poliakoff, *J. Flow Chem.*, 2012, **2**, 24-27.
109. R. A. Sheldon, *Green Chem.*, 2007, **9**, 1273-1283.
110. M.-J. Kim, W.-H. Kim, K. Han, Y. K. Choi and J. Park, *Org. Lett.*, 2007, **9**, 1157-1159.
111. K. P. J. Gustafson, R. Lihammar, O. Verho, K. Engström and J.-E. Bäckvall, *J. Org. Chem.*, 2014, **79**, 3747-3751.
112. J. Paetzold and J. E. Bäckvall, *J. Am. Chem. Soc.*, 2005, **127**, 17620-17621.
113. A. C. Eliot and J. F. Kirsch, *Annual Review of Biochemistry*, 2004, **73**, 383-415.
114. S. J. Lucas, B. D. Crossley, A. J. Pettman, A. D. Vassileiou, T. E. O. Screen, A. J. Blacker and P. C. McGowan, *Chem. Commun.*, 2013, **49**, 5562-5564.
115. M. J. Stirling, J. M. Mwansa, G. Sweeney, A. J. Blacker and M. I. Page, *Org. Biomol. Chem.*, 2016, **14**, 7092-7098.
116. P. G. A. Winkworth and A. J. Blacker, Unpublished Results.
117. J. R. Breen, M. T. H. Kwan and A. J. Blacker, Unpublished Results.
118. J.-S. Im, S.-H. Ahn and Y.-H. Park, *Chemical Engineering Journal*, 2013, **234**, 49-56.
119. ThalesNano, *H-Cube Continuous-flow Hydrogenation Reactor*, http://thalesnano.com/h-cube, Accessed 5th April 2017.

120. M. R. Chapman, M. H. T. Kwan, G. King, K. E. Jolley, M. Hussain, S. Hussain, I. E. Salama, C. González Niño, L. A. Thompson, M. E. Bayana, A. D. Clayton, B. N. Nguyen, N. J. Turner, N. Kapur and A. J. Blacker, *Org. Process. Res. Dev.*, 2017.
121. C. Astorga, F. Rebolledo and V. Gotor, *Synthesis*, 1993, **1993**, 287-289.
122. M. A. P. J. Hacking, F. van Rantwijk and R. A. Sheldon, *J. Mol. Catal. B*, 2001, **11**, 315-321.
123. F. Björkling, H. Frykman, S. E. Godtfredsen and O. Kirk, *Tetrahedron*, 1992, **48**, 4587-4592.
124. E. G. Ankudey, H. F. Olivo and T. L. Peeples, *Green Chem.*, 2006, **8**, 923-926.
125. S. Ranganathan, T. Gärtner, L. O. Wiemann and V. Sieber, *J. Mol. Catal. B*, 2015, **114**, 72-76.
126. M. C. de Zoete, A. C. K.-v. Dalen, F. van Rantwijk and R. A. Sheldon, *J. Chem. Soc., Chem. Commun.*, 1993, 1831-1832.
127. M. C. de Zoete, A. C. Kock-van Dalen, F. van Rantwijk and R. A. Sheldon, *J. Mol. Catal. B*, 1996, **2**, 19-25.
128. M. A. P. J. Hacking, M. A. Wegman, J. Rops, F. van Rantwijk and R. A. Sheldon, *J. Mol. Catal. B*, 1998, **5**, 155-157.
129. M. A. Wegman, M. A. P. J. Hacking, J. Rops, P. Pereira, F. van Rantwijk and R. A. Sheldon, *Tetrahedron: Asymm.*, 1999, **10**, 1739-1750.
130. W. F. Slotema, G. Sandoval, D. Guieysse, A. J. J. Straathof and A. Marty, *Biotechnol. Bioeng.*, 2003, **82**, 664–669.
131. S. Luque, J. R. Álvarez and F. P. Cuperus, *J. Mol. Catal. B*, 2014, **107**, 73-78.
132. R. Chuck, *Applied Catalysis A: General*, 2005, **280**, 75-82.
133. T. Nagasawa, C. D. Mathew, J. Mauger and H. Yamada, *Applied and Environmental Microbiology*, 1988, **54**, 1766-1769.
134. *Eur. Pat.*, EP0307926 (A2), 1989.
135. *Eur. Pat.*, EP0770687 A3, 1998.
136. N. M. Shaw, K. T. Robins and A. Kiener, *Adv. Synth. Catal.*, 2003, **345**, 425–435.
137. R. K. Henderson, C. Jimenez-Gonzalez, D. J. C. Constable, S. R. Alston, G. G. A. Inglis, G. Fisher, J. Sherwood, S. P. Binks and A. D. Curzons, *Green Chem.*, 2011, **13**, 854-862.
138. M. R. Owen, C. Luscombe, Lai, S. Godbert, D. L. Crookes and D. Emiabata-Smith, *Org. Process. Res. Dev.*, 2001, **5**, 308-323.
139. G. E. P. Box, W. G. Hunter and J. S. Hunter, in *Statistics for Experimenters*, Wiley, 1st edn., 1978, pp. 510-539.
140. Umetrics, *User guide to MODDE, Version 10.1*, http://mksdataanalytics.com/sites/default/files/downloads/1/user_guide_to_modde_10.1.pdf, Accessed 2nd February 2017.
141. A. M. Klibanov, *Nature*, 2001, **409**, 241-246.
142. P. J. Halling, *Philosophical Transactions of the Royal Society of London. Series B: Biological Sciences*, 2004, **359**, 1287-1297.
143. C. Jimenez-Gonzalez, C. S. Ponder, Q. B. Broxterman and J. B. Manley, *Org. Process. Res. Dev.*, 2011, **15**, 912-917.
144. WHO, *WHO Media Centre Fact Sheet - Tuberculosis*, http://www.who.int/mediacentre/factsheets/fs104/en/, Accessed 17th February 2017.
145. S. A. Hall and P. E. Spoerri, *J. Am. Chem. Soc.*, 1940, **62**, 664-665.
146. A. S. Suresh, P. Baburajan and M. Ahmed, *Tet. Lett.*, 2015, **56**, 4864-4867.
147. U. S. D. o. H. a. H. S. F. a. D. Administration, 2015.
148. R. J. Ingham, C. Battilocchio, J. M. Hawkins and S. V. Ley, *Beilstein J. Org. chem.*, 2014, **10**, 641-652.

149. P. López-Serrano, M. A. Wegman, F. van Rantwijk and R. A. Sheldon, *Tetrahedron: Asymm.*, 2001, **12**, 235-240.
150. L. H. Andrade, B. A. Sousa and T. F. Jamison, *J. Flow Chem.*, 2016, **6**, 67-72.
151. V. Hessel, S. Hardt and H. Löwe, in *Chemical Micro Process Engineering: Fundamentals, Modelling and Reactions*, Wiley-VCH, 10th edn., 2004.
152. G. E. P. Box and J. S. Hunter, *Technometrics*, 2000, **42**, 28-47.
153. G. E. P. Box and J. S. Hunter, *Technometrics* 1961, **3**, 449-458.
154. G. E. P. Box and D. W. Behnken, *Technometrics*, 1960, **2**, 455-475.
155. T. N. Glasnov and C. O. Kappe, *Chem. Eur. J.*, 2011, **17**, 11956-11968.
156. N. Kim, S.-B. Ko, M. S. Kwon, M.-J. Kim and J. Park, *Org. Lett.*, 2005, **7**, 4523-4526.
157. S. B. Ötvös, I. M. Mándity and F. Fülöp, *J. Catal.*, 2012, **295**, 179-185.
158. M. J. Burk, Y. M. Wang and J. R. Lee, *J. Am. Chem. Soc.*, 1996, **118**, 5142-5143.
159. L. K. Thalén, C. Roesch and J.-E. Bäckvall, *Organic Syntheses*, 2012, **89**, 255-266.
160. M. Päiviö, P. Perkiö and L. T. Kanerva, *Tetrahedron: Asymm.*, 2012, **23**, 230-236.
161. A. Chighine, S. Crosignani, M.-C. Arnal, M. Bradley and B. Linclau, *J. Org. Chem.*, 2009, **74**, 4753-4762.
162. N. Mistry and S. P. Fletcher, *Adv. Synth. Catal.*, 2016, **358**, 2489-2496.
163. C. B. P. Ligiero, L. C. Visentin, R. Giacomini, C. A. L. Filgueiras and P. C. M. L. Miranda, *Tet. Lett.*, 2009, **50**, 4030-4032.
164. J. E. Taylor, M. D. Jones, J. M. J. Williams and S. D. Bull, *J. Org. Chem.*, 2012, **77**, 2808-2818.